



The
University
Of
Sheffield.

Characterisation of Antibiotic Resistance in *Clostridium difficile*

BY

YASIR ADIL JABBAR ALABDALI

**A thesis submitted in part fulfilment for the degree of
Doctor of Philosophy.**

**Department of Molecular Biology and Biotechnology,
University of Sheffield.**

November 2017

Declaration

I, Yasir Adil Jabbar Alabdali, confirm that the presented work in this thesis is my own work, except acknowledgment or references that were written. I totally agree that the library of Sheffield university may copy or give this thesis for researchers request.

Signature by

Yasir Adil Jabbar Alabdali

Abstract

Clostridium difficile is a Gram-positive, obligate anaerobe and an opportunistic pathogen that causes antibiotic associated diarrhoea. The incidence of *C. difficile* infection (CDI) increased dramatically in the early years of this century, an epidemic caused by the previously rare ribotype 027. In addition to causing large hospital outbreaks this lineage was also associated with seemingly more severe disease. Ribotype 027 strains have been reported to produce more spores and more toxin, perhaps going some way to explaining the efficient transmission and poor clinical outcome.

We sought to understand the peptidoglycan biosynthetic pathways active in both vegetative cells and during sporulation, in order to identify proteins playing a role in resistance to cell wall targeting antibiotics. A total of 11 genes predicted to encode penicillin-binding proteins (PBPs) were identified in the genome of R20291, the UK prototypic ribotype 027 strain. Two putative PBPs were taken forward for further study: one class B PBP, SpoVD, required for both sporulation and cephalosporin resistance, and one class C PBP, Cwp20, that contributes to cephalosporin resistance.

A $\Delta spoVD$ mutant showed two strong phenotypes: a sporulation defect and cephalosporin sensitivity. In addition, an interaction between SpoVD and SpoVE that appears to be crucial in both sporulation and cephalosporin resistance was demonstrated. A $\Delta cwp20$ mutant had a clear defect in cephalosporin resistance. Disruption of *cwp20* in a strain that completely lacked the S-layer provided further evidence for a role cephalosporin resistance. Cwp20 was determined to be a class A β -lactamase.

The third part of this thesis is devoted to identification of genes that are responsible for ceftazidime, cefoxitin and ciprofloxacin resistance. A total of 6,000 transposon mutants were screened for resistance to each antibiotic. Three genes with defects in resistance to these antibiotics were chosen for detailed analysis. SpoVE, a membrane protein and putative lipid II flippase, was found to be involved in both cefoxitin and ceftazidime resistance. A *CD0398* mutant was found to have a defect under ceftazidime selection. Complementation restored ceftazidime resistance and *CD0399*

was identified as a class A β -lactamase. A CD0622 mutant was found to have a defect under ciprofloxacin selection and CD0622 was demonstrated to act as an efflux pump.

Dedicated To

My Father: ADIL JABBAR ALABDALI

My Mother: KEFAA FADHIL

My Daughter: FATIMA YASIR ADIL

Acknowledgements

First and foremost, I am very grateful to thank my supervisor Dr Robert Fagan for his massive support throughout the entire project of my PhD. I would like to emphasise my gratitude to him for learning me to be self-dependant and patient to get a good result.

I would like to thank my sponsor the higher committee for education development in Iraq (HCED) for funding over the last four years. I would like to acknowledge Dr. Aimee Shen (Tufts University) for sending three plasmids with antibodies.

I would to thank my colleagues are in the laboratory, Joe Kirk, Peter Oatley, Nadia J Fernandes and Oishik Banerji for their help in different ways and many aspects of my project. I would also like to thanks my the best friends Murtakab Alhejjaj and Adnan Al-mousawi in Sheffield as for the last four years , they were the only friends that support and encourage me. Thanks you so much for all these nice memories.

Finally, huge thanks for all my family, especially my Mother, Father and my daughter Fatima for their unconditional support and love throughout my study in the UK and in my life generally.

List of Abbreviations

Abbreviations	Full name
ACE	allele-coupled exchange
ATC	anhydrotetracycline
BHI	brain heart infusion
CDAD	<i>C. difficile</i> -associated disease
CDDM	<i>C. difficile</i> defined medium
CDI	<i>C. difficile</i> infection
CFU	colony-forming unit
CWB	domain cell wall binding
CWP	cell wall protein
DMSO	Dimethylformamide
DNA	deoxyribonucleic acid
DPA	dipicolinic acid
EDTA	Ethylenediaminetetracetic acid
FC	5-fluorocysteine
FOA	5-fluoroorotic acid
FU	5-fluorouracil
HMW SLP	high molecular weight S-layer protein
HRP	Horseshoe peroxidase
IEP	intron-encoded protein
IPTG	isopropyl β -D-1-thiogalactopyranoside
ITR	inverted terminal repeat
LB	Luria-Bertani
LMW SLP	low molecular weight S-layer protein
MAL	muramic- δ -lactam
MW	molecular weight
NAG	N-acetylglucosamine
NAM	N-acetylmuramic acid
OD	optical density
ORF	open reading frame
PBP	penicillin-binding protein
PBS	phosphate-buffered saline
PCR	polymerase chain reaction
PG	peptidoglycan
pH	hydrogen potential
PLG	phase lock gel
PMC	pseudomembrane colitis
RAM	retrotransposition-activated marker
RBS	ribosome binding site
RNA	ribonucleic acid
SDS-PAGE	Sodium dodecylsulphate-polyacrylamide gel electrophoresis
TEM	transmission electron microscopy
WT	wild-type
X-Gal	5-bromo-4-chloro-3-indolyl- β -D-galactopyranoside

Contents

1. Chapter 1 Introduction	2
1.1. <i>Clostridium difficile</i>	2
1.2 <i>C. difficile</i> epidemiology	2
1.2.1 Hospital-acquired infection.....	3
1.2.2 Community-acquired infection	6
1.3 Transmission of <i>C. difficile</i>	6
1.4 <i>C. difficile</i> pathogenesis.....	7
1.5 <i>C. difficile</i> toxins	9
1.6 The <i>C. difficile</i> S-layer	12
1.7 Antibiotic resistance in <i>C. difficile</i>	13
1.7.1 Treatment	16
1.7.2 Standard therapy	16
1.8 The cell wall and peptidoglycan structure	17
1.8.1 Classification of PBPs	21
1.9 β -lactam antibiotics	23
1.10 Mode of action	24
1.11 Mechanisms of resistance	24
1.12 Sporulation	28
1.12.1 Entry into sporulation	30
1.13 Spore morphogenesis	34
1.13.1 Spore core	34
1.13.2 Spore cortex	36
1.13.3 Spore coat	36
1.13.4 The exosporium.....	41
1.14 Overview of genetic manipulation of studying <i>C. difficile</i>	42
1.14.1 Clostridial vector systems	42
1.14.2 Genomic mutations in <i>C. difficile</i>	43
1.14.2.1 ClosTron insertional mutagenesis.....	43
1.14.2.2 Homologous recombination techniques	43
1.14.2.3 Transposon mutagenesis and sequencing.....	48
1.15 Project aims.....	49
2. Chapter 2 Materials and Methods	50
2.1. Bacterial strains and growth conditions	51
2.2 DNA manipulation.....	58
2.2.1 Extraction of gDNA from <i>C. difficile</i>	58
2.2.2 Crude DNA extraction	59
2.2.3 Polymerase chain reaction (PCR)	59
2.2.4 Agarose gel electrophoresis.....	60
2.2.5 DNA purification	60
2.2.6 Restriction endonuclease digestion of DNA	61
2.2.7 Plasmid purification	61
2.2.8 DNA Ligation.....	61
2.3.1 DNA cloning	62
2.3.2 Cloning after restriction enzymes digestion	62
2.3.3 Cloning by inverse PCR.....	62

2.3.4 Gibson assembly	62
2.4 Production of Chemically-competent <i>E. coli</i>	63
2.4.1 Transformation	63
2.5 Plasmid transfer into <i>C. difficile</i>	64
2.6 Homologous recombination	65
2.7 Complementation and restoration of the <i>pyrE</i> gene in R20291	67
2.7.1 Restoration of the <i>pyrE</i> gene in mutant strains.....	67
2.7.2 Mutant strain complementation	67
2.8 ClosTron insertional mutagenesis.....	68
2.9 Southern blotting	68
2.10 Determination of antibiotic minimum inhibitory concentrations	69
2.11 Proteins labelling with Bocillin-FL	70
2.12 β -lactamases assay	70
2.12.1 Active site titration.....	71
2.13 Phenotypic assays	71
2.13.1 Sporulation efficiency	71
2.13.2. Spore chemical resistance assay.....	72
2.14. Expression and purification of recombinant proteins	72
2.14.1 Growth and protein expression	72
2.14.2 Protein solubility	72
2.14.3 Protein purification	73
2.14.4 Dialysis of purified proteins	73
2.14.5 Protein concentration determination.....	74
2.14.6 Mass spectrometry	74
2.14.7 Protein-Protein interactions	74
2.14.8 β -Galactosidase activity assay.....	76
2.15 Protein characterisation.....	77
2.15.1 S-layer extraction	77
2.15.2 Membrane fractionation.....	77
2.15.3 SDS-PAGE and Coomassie staining	78
2.15.4 Semi-dry transfer	78
2.15.5 Western blotting	78
2.16 Microscopy.....	79
2.16.1 Phase contrast and fluorescence microscopy	79
2.16.2 Transmission electron microscopy (TEM)	79
2.17 Transposon mutagenesis	79
2.17.1 Mutagenesis.....	79
2.17.2 Identification of transposon insertion sites	80
2.18 Bioinformatics	80
3. Chapter 3.....	82
3.1. Introduction	82
3.1.1 SpoVD.....	82
3.2 Results	87
3.2.1 Bioinformatic analysis of PBPs in <i>C. difficile</i>	87
3.2.2 Deletion of the <i>spoVD</i> gene	88
3.2.3 Complementation of the <i>spoVD</i> mutant and restoration of the <i>pyrE</i> gene	90
3.2.4 Southern blot confirmation of knockout and complementation of <i>spoVD</i>	92

3.3 Determination of antibiotic MIC	94
3.4 Sporulation of R20291, R20291 Δ <i>spoVD</i> and R20291 Δ <i>spoVD pyrE::spoVD</i>	95
3.4.1 Characterisation of spore resistance to environmental stresses	98
3.4.2 Characterisation of spore morphology	100
3.5 Expression and localisation SpoVD	102
3.6 The impact of <i>spoVD</i> mutant on the expression of sporulation associated genes and localisation of promoter activity	105
3.7 The impact of <i>spoVD</i> mutant on toxin production	114
3.8 Function analysis of SpoVD domains	116
3.9 Interaction between SpoVD and SpoVE	123
3.10 SpoVD is a Class B PBP	132
3.11 Discussion	136
4. Chapter 4	142
4.1 Introduction	143
4.1.1 Cwp20	143
4.2: Results	147
4.2.1 Deletion of the <i>cwp20</i> gene	147
4.2.2 Complementation of the <i>cwp20</i> mutant and restoration of the <i>pyrE</i> gene.....	149
4.2.3 Southern blot confirmation of knockout and complementation <i>cwp20</i>	151
4.3 Determination of antibiotic MICs	153
4.4 Functional analysis of the β -lactamase domain in Cwp20.....	154
4.5 Cwp20 β -lactamase activity	156
4.6 The role of the S-layer in cephalosporin resistance.....	165
4.7 Determination of antibiotic MICs	167
4.8 Discussion.....	169
5. Chapter 5	170
5.1 Introduction	171
5.1.1 Transposon mutagenesis	171
5.2 Results	172
5.2.1 Construction of transposon mutants in <i>C. difficile</i> R20291 and screening for ceftazidime, cefoxitin and ciprofloxacin resistance.....	172
5.3 Identification of the transposon site.....	172
5.4 Phenotypic analysis.....	178
5.4.1 Deletion of <i>CD0622</i>	178
5.4.2 Determination of antibiotic MICs	180
5.4.3 Synergistic between ciprofloxacin and reserpine in <i>C. difficile</i> R20291	181
5.5 CD0399	183
5.5.1 Functional analysis of the CD0399 β -lactamase domain.....	185
5.5.2 CD0399 β -lactamases activity	187
5.6 Discussion.....	198
6. Chapter 6	200
6.1 Final Discussion	201
7. References	205

List of Figures

Figure 1.1: CDI mortality rates in England and Wales from 2002 to 2012	4
Figure 1.2: The steps of the infection with <i>C. difficile</i>	5
Figure 1.3: The pathogenicity of <i>C. difficile</i>	8
Figure 1.4: Toxins produced by <i>C. difficile</i>	10
Figure 1.5: The 29 proteins constituting the cell wall protein family of <i>C. difficile</i>	14
Figure 1.6: The architecture of peptidoglycan	19
Figure 1.7: The cytoplasmic steps of peptidoglycan biosynthesis	20
Figure 1.8: Types of penicillin-binding proteins	22
Figure 1.9: Generalised structures of β -lactam antibiotics	25
Figure 1.10: The mechanism of β -lactam binding with the PBP active site serine	26
Figure 1.11: Schematic diagram of sporulation and germination in <i>B. subtilis</i>	29
Figure 1.12: Schematic diagram of sporulation regulation in <i>B. subtilis</i> and <i>C. difficile</i>	33
Figure 1.13: Spore structural layers.....	35
Figure 1.14: The <i>B. subtilis</i> cortex peptidoglycan structure	37
Figure 1.15: Schematic diagram of coat assembly in <i>B. subtilis</i> and <i>C. difficile</i>	40
Figure 1.16: Schematic diagram of Clostron insertional mutagenesis	45
Figure 1.17: Homologous recombination using <i>pyrE</i> system	47
Figure 3.1: . The position of <i>spoVD</i> on the chromosome of <i>B. subtilis</i> and <i>C. difficile</i> ..	85
Figure 3.2: Structural model of SpoVD (residues 59-656)	86
Figure 3.3: Deletion of <i>spoVD</i> using homologous recombination.....	89
Figure 3.4: Complementation of <i>spoVD</i> and restoration of the <i>pyrE</i> gene.....	91
Figures 3.5: Southern blot confirmation of <i>spoVD</i> knockout and complementation	93
Figure 3.6: Sporulation efficiency of R20291 wild type, R20291 Δ <i>spoVD</i> and R20291 Δ <i>spoVD pyrE::spoVD</i> strains	96
Figure 3.7: Phase contrast microscopy of sporulation assay	97
Figure 3.8: Characterisation of spore resistance to environmental stresses.....	99
Figure 3.9: Phase contrast and TEM of <i>C. difficile</i> R20291	101
Figure 3.10: Subcellular localisation of SpoVD in <i>C. difficile</i> R20291.....	103
Figure 3.11: The expression of <i>sspA</i> , <i>sipL</i> and <i>spoVT</i> genes in R20291 Δ <i>spoVD</i>	106
Figure 3.12: Subcellular localisation of SspA, SipL and SpoVT expression in R20291 Δ <i>spoVD</i>	112
Figure 3.13: Western blot analyses of proteins known to be involved in sporulation .	113
Figure 3.14: TcdB toxin production	115
Figure 3.15: Functional analysis of SpoVD domains	119
Figure 3.16: Sporulation requires both transpeptidase and PBP dimer domains	120
Figure 3.17: TEM analysis of <i>C. difficile</i> R20291 Δ <i>spoVD</i> + <i>spoVD</i> (the full-length and truncated <i>spoVD</i>) strain ultrasections.....	122
Figure 3.18: β -galactosidase assays showing the interaction between SpoVD and SpoVE	125
Figure 3.18: The interaction between SpoVD and SpoVE.....	128
Figure 3.19: The interaction between SpoVD and SpoVE.....	131
Figure 3.20: Purification of SpoVD and SpoVDS311A.....	133
Figure 3.21: Bocillin-FL labelling of SpoVD and SpoVDS311A	135
Figure 4.1: General characteristics of Cwp20.....	146
Figure 4.2: Deletion of <i>cwp20</i> using homologous recombination	148
Figure 4.3: Complementation of <i>cwp20</i> and restoration of the <i>pyrE</i> gene.....	150

Figure 4.4: Southern blot confirmation of <i>cwp20</i> knockout and complementation..	152
Figure 4.5: Purification of Cwp20 and Cwp20S116A	155
Figure 4.6: β -lactamase activity	159
Figure 4.7: Kinetic enzyme analysis of Cwp20 and TEM with nitrocefin and clavulanic acid	161
Figure 4.8: Bocillin-FL labelling of Cwp20, Cwp20S116A, TEM and SpoVD.....	163
Figure 4.9: Analysis of electrospray ionization mass spectrometry	164
Figure 4.10: Knockout of <i>cwp20</i> using CloStron.....	166
Figure 5.1: Transposon insertion sites	175
Figure 5.2: Deletion of <i>CD0622</i> using homologous recombination	179
Figure 5.3: General characteristics of CD0399	184
Figure 5.4: Purification of CD0399 and CD0399S120A	186
Figure 5.5: β -lactamase activity	189
Figure 5.6: Analysis of electrospray ionization mass spectrometry	191
Figure 5.7: Kinetic analysis of CD0399, CD0399S108 and TEM with nitrocefin and clavulanic acid	194
Figure 5.8: Bocillin-FL labelling of CD0399, CD0399S102A, TEM and SpoVD.....	196
Figure 5.9: Ceftazidime blocks bocillin-FL labelling	197

List of Tables

Table 2.1.1: Media	51
Table 2.1.2: <i>C. difficile</i> defined medium CDDM.....	52
Table 2.1.3: Supplements	53
Table 2.1.4: Bacterial strains.....	54
Table 3.1: Identification of genes encoding PBPs in <i>C. difficile</i> R20291.....	87
Table 3.3: Minimum inhibitory concentrations against the wild type R20291 and <i>spoVD</i> mutant and complementation strains ($\mu\text{g/ml}$)	94
Table 3.4: Minimum inhibitory concentrations against the wild type R20291 and truncation <i>spoVD</i> constructs strains ($\mu\text{g/ml}$)	118
Table 4.1: Minimum inhibitory concentrations against the wild type R20291 and <i>cwp20</i> mutants and complementation strains ($\mu\text{g/ml}$)	153
Table 4.2: Kinetic parameters of TEM, Cwp20 and Cwp20S116A.....	160
Table 4.3: Minimum inhibitory concentrations of the wild type R20291 and <i>cwp20</i> mutants and complementation strains ($\mu\text{g/ml}$)	168
Table 5.1: MICs of transposon mutants ($\mu\text{g/ml}$)	173
Table 5.2: Minimum inhibitory concentrations of the wild type R20291 and deletion and insertional mutant strains ($\mu\text{g/ml}$)	177
Table 5.3: Minimum inhibitory concentrations against the wild type R20291 and <i>CD0622</i> mutants and complementation strains ($\mu\text{g/ml}$)	180
Table 5.4: Minimum inhibitory concentrations of ciprofloxacin in the presence and absence of reserpine ($\mu\text{g/ml}$)	182
Table 5.5: Kinetic parameters of TEM, CD0399, CD0399S108A and CD0399S102A	193

Chapter One

Introduction

1. Introduction

1.1. *Clostridium difficile*

In 1861, Louis Pasteur identified the first bacteria which were capable of growing without oxygen, and he introduced the term anaerobic bacteria (Bahl *et al.*, 2001). The Clostridia are Gram-positive bacilli that form spores and are obligate anaerobes (Cato *et al.*, 1986).

Clostridium difficile was identified in the 1930's by Hall and O'Toole (Hall and O'Toole, 1935). In 1974, Tedesco reported patients with pseudomembranous colitis (PMC) when they were treated with clindamycin (Tedesco *et al.*, 1974), and in 1978, *C. difficile* was identified as the primary agent causing PMC. Anatomical studies revealed that the pseudomembranous lesions are composed of fibrin, mucin and inflammatory cells within the mucosal epithelium of infected patients (Sumner and Tedesco, 1975; Price and Davies, 1977). *C. difficile* toxins were found in 95% of patients with PMC, and their presence was also linked to *C. difficile* antibiotic-associated diarrhoea (AAD) (Jarvis, 2001). In addition to PMC, infection with *C. difficile* was associated with critical complications, including toxic-megacolon, and ileus disease following antibiotic treatment (Bartlett, 2002).

1.2 *C. difficile* epidemiology

C. difficile infection (CDI) has been a common complication of using antibiotics for nearly 40 years. Mortality due to CDI increased rapidly in England and Wales between 2004 and 2007, from 2,238 (23.3 per million population) to 8,324 (82.9 per million population) respectively. However, since 2007, CDI mortality in England and Wales has fallen dramatically to 2,053 (19.6 deaths per million population) and 1,646 (15.3 per million population) in 2011 and 2012 respectively. The increase in CDI was associated with the emergence of a previously rare ribotype 027 or BI/NAP1 strain (Creagh, 2008). In 2003, in North America and many European countries, this ribotype 027 strain was reported as the virulent strain causing the increase in CDI cases (He *et al.*, 2013). Ribotype 027 was first detected in the UK in Stoke Mandeville hospital in June 2005. The strain was toxinotype III with the ability to produce a third, binary toxin (composed of CdtA and CdtB), and was also found to be resistant to fluoroquinolones

(Kuijper *et al.*, 2005; Health Protection Agency, 2005). This ribotype has now spread worldwide. At the peak of the outbreak in 2007 *C. difficile* was responsible for more than 5 times as many deaths as MRSA in England and Wales (8,324 and 1,517 deaths respectively) (www.statistics.gov.uk) (Figure 1.1).

Ribotype 027 strains were found to be resistant to newer fluoroquinolones such as gatifloxacin and moxifloxacin but were susceptible to lincosamide, macrolide, and streptogramin B, as they lacked an *ermB* gene (Kuijper *et al.*, 2006). *In vitro* studies have shown that ribotype 027 can produce significantly more toxin A and toxin B than a control strain (16 and 23 times more respectively) (Kuijper *et al.*, 2006). Also, this ribotype has shown increased production of spores compared with a ribotype that was not associated with CDI outbreaks (Owens, 2007). The cost of CDI in the USA is estimated to be \$4.8 billion per year, including the burden of long-term treatment of patients outside the hospital (Depestel and Aronoff, 2013; He *et al.*, 2013).

1.2.1 Hospital-acquired infection

C. difficile mostly infects elderly people and hospitalised patients following disruption of the intestinal microbiota by treatment with broad-spectrum antibiotics (McFarland, 2008). This disruption allows *C. difficile* to colonise and proliferate in the gut. Many antibiotics are associated with CDI, but some present higher risk, such as cephalosporins, clindamycin and fluoroquinolones (Johnson *et al.*, 1999, Pepin *et al.*, 2005). Clindamycin and cephalosporin use in particular has been linked to CDI for many decades. Many *C. difficile* strains are entirely resistant to both clindamycin and cephalosporin antibiotics (Johnson *et al.*, 1999). Fluoroquinolones have been implicated in triggering CDI more recently, particularly with ribotype 027 strains that are more resistant strains to these antibiotics (Pepin *et al.*, 2005). The primary risk factor for CDI is long-term hospitalisation. However, many different factors can increase risk of CDI, including contamination of the local environment with spores, an extended period of antibiotic exposure, poor hygiene among hospital workers and intestinal tract susceptibility among elderly people who have a weak immune system (Figure 1.2) (Rupnik *et al.*, 2009).

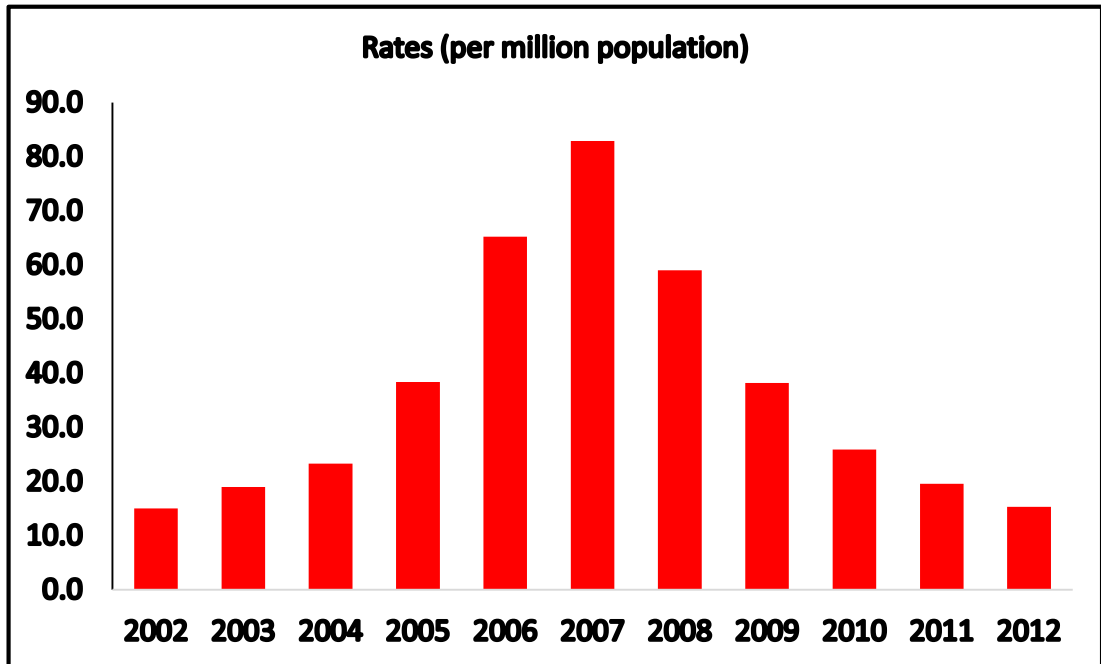


Figure 1.1: CDI mortality rates in England and Wales from 2002 to 2012. (Office for National Statistics, 22 August 2013; http://www.ons.gov.uk/ons/dcp171778_323989.pdf).

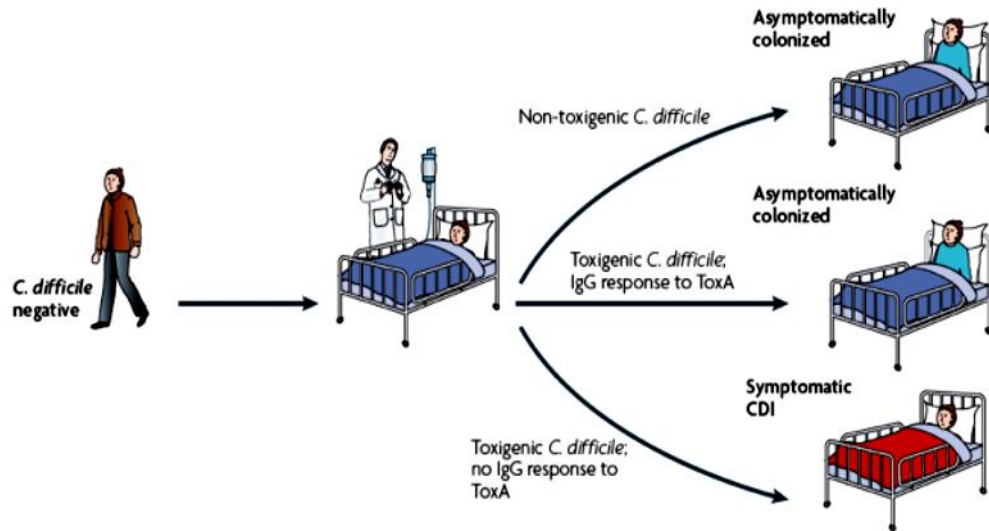


Figure 1.2: The steps of infection with *C. difficile*. *C. difficile* infection starts by formation of spores that are transferred via contact with the hospital environment or health care workers. After treatment with antibiotics, CDI with a toxigenic strain can lead to a rise in serum IgG against toxin A (TcdA), resulting in asymptomatic carriage. If no IgG response is elicited the result is symptomatic CDI. In contrast, acquisition of a non-toxicogenic strain will also result in asymptomatic carriage. Reproduced with permission (Rupnik *et al.*, 2009).

1.2.2 Community-acquired infection

C. difficile is thought to be a commensal bacterium in 1-3% of the healthy adult and 40-60% of the neonatal population (McFarland *et al.*, 2000; Kuipers and Surawicz, 2008). However, community-acquired infection has been observed, albeit with a lower rate than in hospitalised patients. In the USA community-acquired CDI rates have increased to 7.7 per 100,000 persons and interestingly, 35% of community-acquired cases do not have antibiotic exposure in the 42 days prior to detection of CDI (Hirschhorn *et al.*, 1994). In recent years, there has also been a significant increase in CDI in children and pregnant women without contact with the hospital environment or treatment with broad-spectrum antibiotics (Kim *et al.*, 2008; Roupael *et al.*, 2008). Genome sequencing of *C. difficile* isolates showed significant diversity, pointing to the existence of a substantial reservoir, perhaps from asymptomatic carriers (Eyre *et al.*, 2013).

1.3 Transmission of *C. difficile*

One of the most important factors in the transmission of *C. difficile* is the spore (Deakin *et al.*, 2012). Endospores are produced in many bacteria species that belong to the *Bacillus* and *Clostridium* genera. Endospores can survive in many unsuitable conditions, and resist extreme physical and chemical treatments, including heat and oxygen exposure, alcohol and many disinfectant treatments (Setlow, 2006; Setlow, 2007). This makes eradication of spores more difficult, and allows persistence in the environment for a long time. It has been reported that the spores can remain viable for up to 70 days in hospital rooms, enhancing the ability to transfer from patients infected with CDI to other people (Dubberke and Wertheimer, 2009; Dubberke *et al.*, 2007).

Spore contamination from asymptomatic carriers has a potential role in transferring epidemic and non-epidemic *C. difficile* strains (Riggs *et al.*, 2007). Reducing spore contamination on equipment and workers is critical to prevent *C. difficile* spreading (Gerding *et al.*, 2008). In the human gut, which is a suitable anaerobic environment, the spores germinate to produce vegetative cells. Toxin production and secretion then leads to diarrhoea in susceptible individuals further spread of spores. The

spores of *C. difficile* have been shown to be highly infectious and are sufficient to cause CDI in animal models after treatment with an antibiotic (Lawley *et al.*, 2009b).

In 2012, it was determined that Spo0A plays an essential role in sporulation, persistence and transmission (Deakin *et al.*, 2012). Deletion of *spo0A* results in loss of persistence despite *C. difficile* still causing intestinal disease. This demonstrated the important role of the master regulator Spo0A in the sporulation process, transmission and persistence of *C. difficile*. Spo0A is a transcriptional regulator and is required for initial sporulation steps.

1.4 *C. difficile* pathogenesis

To understand the mechanisms of *C. difficile* pathogenicity, one must consider several factors that are involved in *C. difficile* infection. One of the major issues is the disruption of the normal flora in the human gut. *C. difficile* spores are introduced by ingestion, forming vegetative cells and then multiplying, following germination. Subsequently, *C. difficile* start to colonise by adhering to the mucus layer and enterocytes or intestinal absorptive cells, with the aid of flagella and surface proteins (Figure 1.3) (Janoir *et al.*, 2007).

The next phase of pathogenicity is toxin production (Vaishnavi *et al.*, 2010). *C. difficile* has two large toxins, TcdA and TcdB, and both of them cause damage of the colonic mucosa after *C. difficile* colonisation (Deneve *et al.*, 2009). Both toxins glucosylate small Rho proteins causing disorganisation of the cell cytoskeleton (Dupuy *et al.*, 2008; Vaishnavi, 2010). CDI generally first presents as self-limiting diarrhea before progressing to more severe symptoms such as fever, severe diarrhoea, leukocytosis and abdominal pain.

CDI disease is typically characterised by formation of inflammatory lesions, known as pseudomembranes, in the colon. The pseudomembranes can progress to more severe manifestations such as sepsis or toxic megacolon. These events have been reported to cause significant mortality and morbidity (Rupnik *et al.*, 2009).

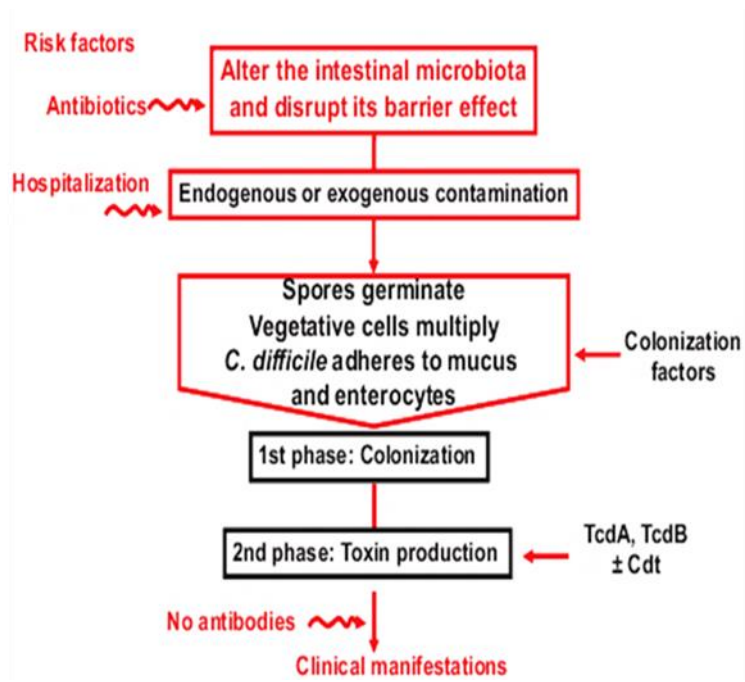


Figure 1.3: The pathogenicity of *C. difficile*. The basic steps of the infection mechanisms of *C. difficile*. Reproduced with permission (Deneve *et al.*, 2009).

1.5 *C. difficile* toxins

C. difficile produces two main toxins, TcdA and TcdB (Figure 1.4). TcdA is an enterotoxin and TcdB is cytotoxic, however both of the toxins have cytotoxic activity. This activity leads to actin cytoskeleton disruption and loss of tight junctions, which can progress to destroy the intestinal epithelium, decreasing the transepithelial resistance and accumulation of fluid (Thelestam and Chaves-Olarte, 2000; Rupnik and Just, 2006; Riegler *et al.*, 1995). The importance of TcdA and TcdB toxins in *C. difficile* pathogenicity has been studied extensively. Using a knockout strain it was demonstrated that toxin A does not play a significant role in *C. difficile* pathogenicity, with mutants retaining the ability to cause disease in hamsters, whereas a toxin B mutant was virulent in the same model (Lyras *et al.*, 2009). However, these conclusions have been challenged, with a second study suggesting that both TcdA and TcdB have important roles for *C. difficile* in hamster infection (Kuehne *et al.*, 2010).

TcdA and TcdB are members of the large clostridial toxin (LCT) family, which includes *Clostridium sordellii* lethal toxin (Tcsl) and hemorrhagic toxin (TcsH), *C. novyi* alpha-toxin (TcnA), and *Clostridium perfringens* Tcpl (types B and C) (von Eichel-Streiber *et al.*, 1996; Amimoto *et al.*, 2007). The LCTs are single-chain toxins with three main domains: an N-terminal catalytic domain, a central translocation domain and a C-terminal binding domain (von Eichel-Streiber *et al.*, 1996). The N-terminal domains of both toxin A and B are glucosyl transferases that are responsible for glucosylation and inactivation of small GTPase proteins such as Rho, Rac or Cdc42. These modifications lead to changes in the cellular cytoskeleton. The active site of the glucosyltransferase domain is a D-X-D motif (Reinert *et al.*, 2005). This motif, along with a distal tryptophan residue, is responsible for binding to glucose, and a mutation in this motif leads to loss of the glucosyltransferase activity (Teichert *et al.*, 2006). The C-terminal (receptor-binding domain) contains polypeptide repeats, named the combined repetitive oligopeptides (CROPs). These CROPs are homologous to carbohydrate and choline binding proteins (Just and Gerhard, 2004). This domain is thought to be responsible for binding of the toxin to a cell surface receptor (Genth *et al.*, 2008). It has been shown that the receptor-binding domain of TcdA binds to many types of oligosaccharides, including alpha-Gal- (1,3), beta-Gal-(1,4) and beta-GlcNAc (Greco *et al.*, 2006).

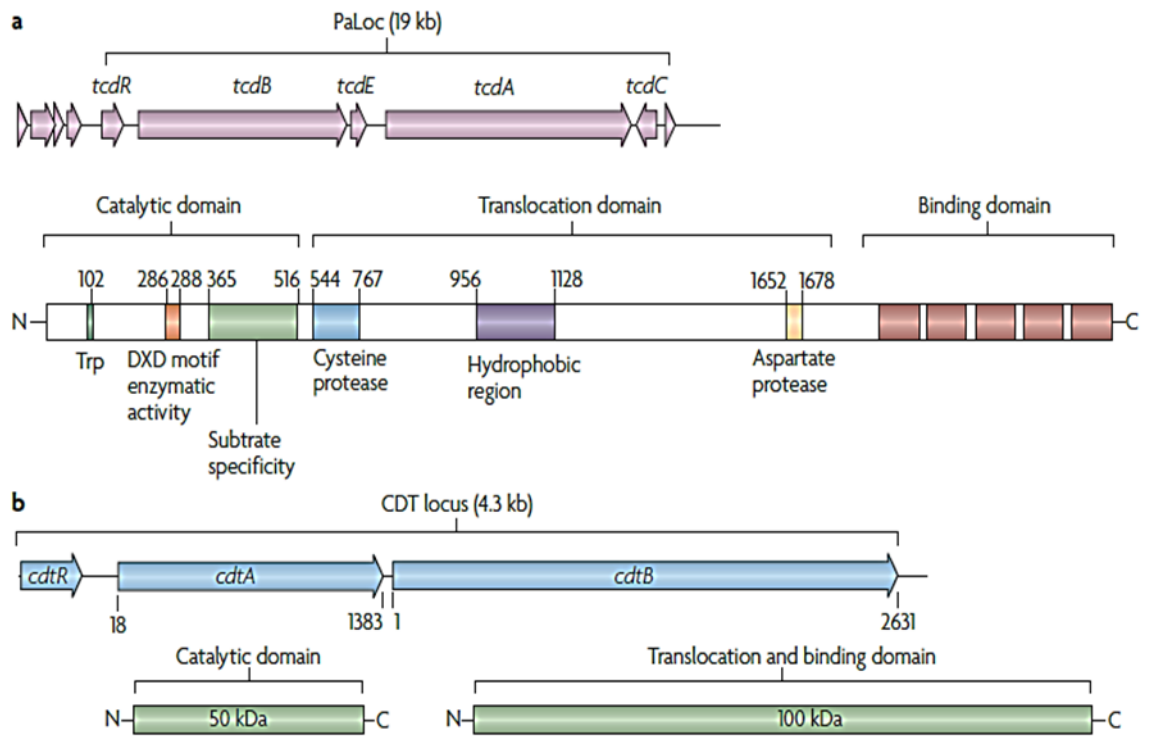


Figure 1.4: Toxins produced by *C. difficile*. **A:** The PaLoc contains five genes involved in toxin expression, *tcdR*, *tcdB*, *tcdE*, *tcdA* and *tcdC*. TcdA and TcdB are highly similar single-chain toxins. The functional domains and motifs of TcdB are shown in the schematic below. **B:** The binary toxin CDT locus is encoded in a different region of the chromosome containing three genes: *cdtA*, *cdtB*, and *cdtR*. CdtR is involved in regulation of both *cdtA* and *cdtB*. CdtA has ADP-ribosylating activity, while CdtB is the binding and translocation module. Adapted with permission from Rupnik *et al.* (2009).

The middle translocation domain contains a hydrophobic putative transmembrane region, which may play a role in translocation of the catalytic domain in the cell cytosol (Just and Gerhard, 2004). The translocation domain also contains a cysteine protease motif, responsible for auto-proteolytic release of the catalytic domain (Egerer *et al.*, 2007) (Figure 1.4).

Following binding to the cell surface receptor, the toxin is taken up into an endosome. Acidification of the endosome causes a conformational change in the translocation domain that facilitates formation of a pore by the hydrophobic region (transmembrane domain) (Giesemann *et al.*, 2006). Once the glucosyltransferase domain enters the cell cytosol, the toxin is cleaved by the cysteine protease (Egerer *et al.*, 2007), in response to activation by inositol hexakisphosphate (InsP6), a regulator of many processes in eukaryotic cells (Reineke *et al.*, 2007). The catalytic domain is then able to inactivate GTPase proteins, leading to disorganisation of the cellular cytoskeleton (Aktories and Just, 2005; Just and Gerhard, 2004).

In *C. difficile* both toxins TcdA and TcdB are expressed from a single locus, the PaLoc, that includes an additional three genes: *tcdR*, *tcdE* and *tcdC* (Figure 1.4-A). TcdR is a sigma factor that is required for transcription of both toxin genes (Mani and Dupuy, 2001). TcdC is responsible for the negative regulation of both toxins; it is thought to be an anti-sigma factor that sequesters TcdR (Matamouros *et al.*, 2007). *tcdC* is highly expressed in mid-log phase, which leads to decreased expression of both toxins (Carter *et al.*, 2011, Hundsberger *et al.*, 1997, Saujet *et al.*, 2011). TcdE is predicted to be a holin-like protein that is responsible for toxin secretion (Govind and Dupuy, 2008). Although the PaLoc is found in all toxigenic *C. difficile* strains, it is replaced by 115 kb of non-coding DNA in non-toxigenic strains (Rupnik, 2008). The toxins are secreted typically in late log and stationary phase. This production is dependent on environmental factors such as amino acids, glucose concentration and biotin, as well as the temperature and the presence of antibiotics (Hundsberger *et al.*, 1997; Dupuy *et al.*, 2008; Saxton *et al.*, 2009). Another factor that is involved in toxin regulation is CodY, which can repress toxin production in the presence of some amino acids such as proline and cysteine (Dineen *et al.*, 2010).

Some *C. difficile* strains produce a third, binary toxin, composed of CdtA and CdtB. This toxin is unrelated to TcdA and TcdB. CdtA ADP-ribosylates actin in the host, while CdtB acts to translocate CdtA (Figure 1.4-B) (Stubbs *et al.*, 2000). The binary toxin is encoded away from the PaLoc in a locus named Cdtloc. Expression of both CtdA and CtdB is controlled by CdtR (Carter *et al.*, 2007). Interestingly, epidemic variants of *C. difficile* can produce TcdA, TcdB and the binary toxin (Hundsberger *et al.*, 1997; Stubbs *et al.*, 2000). The role of the binary toxin in CDI is still not fully understood. However, the binary toxin has cytotoxic effects on Vero cell and has been shown to have enterotoxin activity in rabbit model assays (Perelle *et al.*, 1997). More recent studies have shown that severe diarrhoea is associated with binary toxin secretion (Bacci *et al.*, 2011, Barbut *et al.*, 2005) and that binary toxin can modulate the epithelial layer increasing *C. difficile* colonisation in the gut (Schwan *et al.*, 2009).

1.6 The *C. difficile* S-layer

C. difficile has a surface layer (S-layer), a two-dimensional proteinaceous crystalline array that coats the entire cell. The S-layer plays important roles in interactions with the host. Furthermore, this layer provides important and perhaps essential functions to the cell, such as acting as a permeability barrier (Fagan and Fairweather, 2014).

The S-layer of *C. difficile* has two major proteins (S-layer proteins, SLPs) that are formed through the cleavage of the SlpA precursor protein by Cwp84, an S-layer associated cysteine protease. Cleavage of SlpA leads to the formation of two proteins, the low molecular weight (LMW) and the cell wall-binding domain (CWB2) containing high molecular weight (HMW) SLPs. The HMW and LMW SLPs interact to form a heterodimeric complex (Fagan *et al.*, 2009) that then assembles as a 2-dimensional array to cover the whole cell. SlpA has been shown to adhere to gut epithelial cells *ex vivo*, which may help in colonisation of the gut (Calabi and Fairweather, 2002). Recently, it has been shown that a spontaneous mutation in *slpA* did not effect persistence of *C. difficile* in the hamster gut. In addition, this mutant had major defects in sporulation and toxin production. The *slpA* mutant was also sensitive to two main components of innate immunity, lysozyme and LL-37 (Kirk *et al.*, 2017). Another S-layer protein (Cwp2), has

also been implicated in virulence (Bradshaw *et al.*, 2017). Mutation of *cwp2* led to loss of adherence to the colonic Caco-2 cells *in vitro*. In addition, this mutant had increased toxin production but no effect on sporulation.

There are a further 28 cell wall proteins (CWPs), which are scattered throughout the *C. difficile* S-layer. These proteins have three conserved CWB2 motifs (Pfam 04122), and are anchored to the cell wall via an interaction between the CWB2 motifs and the anionic polymer PSII (Willing *et al.*, 2015). This is a new mechanism for protein anchoring to the cell wall in Gram-positive bacteria. Moreover, each protein has a separate passenger domain which provides function to the proteins (Figure 1.5) (Fagan *et al.*, 2011; Emerson and Fairweather, 2009). The functions of some CWPs have been studied. Cwp66 has been implicated in adherence to the gut epithelium and is probably involved in colonisation (Waligora *et al.*, 2001). CwpV has been shown to play a pivotal role in cell auto-aggregation, which is important in bacterial infection and cell clumping (Emerson *et al.*, 2009). Evidence also suggests that S-layer associated cell wall proteins are among the most important factors in the maintenance of cell envelope integrity. Cwp84 has protease activity for cleaving SlpA into the HMW and LMW SLPs and, mutagenesis leads to formation of an abnormal S-layer (de la Riva *et al.*, 2011; Kirby *et al.*, 2009; Fagan and Fairweather, 2014). Cwp22 has L,D-transpeptidase activity, and is involved in formation of peptidoglycan (Peltier *et al.*, 2011).

1.7 Antibiotic resistance in *C. difficile*

The disruption of gut microflora and a reduction of bacterial diversity, induced by heavy usage of antibiotics, is a prerequisite for the development of CDI. Subsequently, the dysbiotic microbiota provides only weak colonisation resistance against *C. difficile* and CDI can develop (Knecht *et al.*, 2014). CDI is fatal in about 10-20% of cases of antibiotic-associated diarrhoea (AAD) and colitis (Shaughnessy *et al.*, 2013). Clindamycin, cephalosporins and the penicillins are most frequently associated with hospital-acquired *C. difficile*-associated diarrhoea (Thomas *et al.*, 2003).

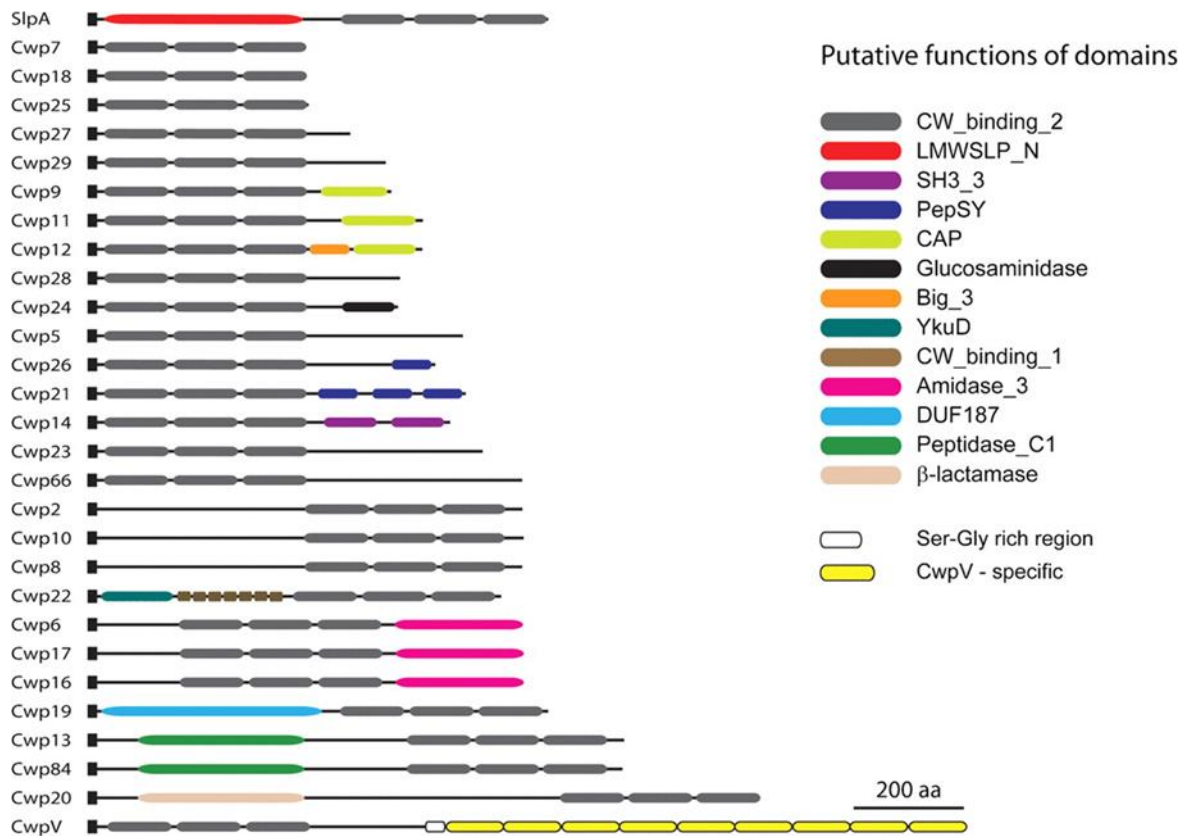


Figure 1.5: The 29 proteins constituting the cell wall protein family of *C. difficile*. Notable members of this family include: the major S-layer protein SlpA, which forms the majority of the S-layer, Cwp84, the protease responsible for cleavage of SlpA into the LMW and HMW SLPs, Cwp66, an adhesin which may be involved in colonisation of the gut and CwpV, a phase variable surface protein that promotes auto-aggregation. All proteins contain a predicted N-terminal secretion signal, shown in black. Reproduced with permission from Fagan *et al.*, (2011).

A recent publication indicated that third-generation cephalosporins and clindamycin are still the most commonly associated antibiotics in nosocomial *C. difficile* (Slimings and Riley, 2013).

The genome of *C. difficile* strain 630 has been analysed, showing several genes that may be involved in cephalosporin resistance (Spigaglia, 2016). In 2005, the fluoroquinolones, such as moxifloxacin, ciprofloxacin, gatifloxacin and levofloxacin, were linked to the development of CDI in European hospitals for the first time (Spigaglia *et al.*, 2008). 83 moxifloxacin-resistant isolates were analysed to identify the mechanism of resistance. Overall, the isolates showed a conserved mutation in the gyrase subunit GyrA (Thr82Ile) and four different substitutions in GyrB (Asp426Asn, Asp426Val, Arg447Lys and Ser416Ala). These point mutations confer resistance against fluoroquinolones including moxifloxacin, ciprofloxacin and gatifloxacin.

CDI incidence has increased due to emergence of a new highly virulent epidemic strains such as ribotype 027 strain R20291. This strain is resistant to many traditional drugs and causes increased mortality and recurrence (Pepin *et al.*, 2005; McDonald *et al.*, 2005; Goorhuis *et al.*, 2007; Clements *et al.*, 2010). In addition, increased CDI in European hospitals has also been associated with the emergence of another virulent lineage, ribotype 078 (Bauer *et al.*, 2011). *C. difficile* strains show significant differences in the patterns of antibiotic resistance, perhaps due to differences in the geographical location and local policies in drug prescribing (Spigaglia, 2016). From over 30 studies published from 2012 to 2015, the rates of resistance to cephalosporin was 55%, while 47% were resistant to erythromycin and fluoroquinolones. Resistance to the second generation of cephalosporin (cefoxitin) was observed in 79% of isolates, compared with 38% to the third generation of cephalosporins (ceftriaxone and cefotaxime). Similarly, resistance to the second generation fluoroquinolone ciprofloxacin was seen in 99% of cases, while the third generation fluoroquinolones moxifloxacin and gatifloxacin had significantly lower rates of resistance at only 34% (Spigaglia, 2016). This may explain how CDI develops in patients treated with these antibiotics. The most common *C. difficile* isolates are from ribotype 027 in Poland and Israel (Adler *et al.*, 2015; Freeman *et al.*, 2015; Lachowicz *et al.*, 2015) and ribotype 078 in Europe and the USA (Varshney *et al.*, 2014; Freeman *et al.*, 2015). These ribotypes are multi-drug resistant (MDR). Indeed, a

2005 European survey found that 55% of *C. difficile* isolates were MDR (Spigaglia *et al.*, 2011). Likewise, 13 studies published between 2012 and 2015 identified MDR *C. difficile* isolates with resistance to clindamycin, fluoroquinolones, erythromycin and cephalosporins (Spigaglia, 2016). Interestingly, these MDR strains include previously rare ribotypes such as ribotype 176, a relative of ribotype 027. This new ribotype 176 strains, isolated in Poland and the Czech Republic, also showed erythromycin, moxifloxacin, ciprofloxacin and rifampin resistance (Obuch-Woszczatynski *et al.*, 2014; Krutova *et al.*, 2015). In Italy, MDR strains belonging to ribotype 356, related to ribotype 018, have also been identified (Spigaglia *et al.*, 2016; Spigaglia *et al.*, 2010).

1.7.1 Treatment

The severity and frequency of the CDI has increased over the last two decades. This has been associated with emergence of hypervirulent *C. difficile* ribotype 027 strains. Even though CDI has become more frequent and severe, most patients respond to traditional antibiotic treatment. However, limitations in drug development have become a more urgent issue in the last decade, highlighting the need to develop new methods to combat *C. difficile*.

1.7.2 Standard therapy

The most effective treatment for *C. difficile* infection is a combination of metronidazole and vancomycin (Bauer *et al.*, 2009; Cohen *et al.*, 2010). *C. difficile*-associated disease (CDAD) has been treated with vancomycin and metronidazole for nearly 25 years. However, 20% of patients develop recurrent infection. This leads to increased incidence of severe complications such as toxic megacolon and sepsis (McFarland, 2005).

However, a reduction in metronidazole efficacy against some ribotypes (including 027, 106, and 001) has been observed, albeit without clinical resistance (Brazier *et al.*, 2008). A 2002 study described screening of 415 *C. difficile* strains isolated

between 1993 and 2000 for metronidazole and vancomycin resistance. The rate of resistance to metronidazole was 6.3% (MIC 16 µg/ml), while for the vancomycin the overall rate of resistances was 3.1% (Pelaez *et al.*, 2002). A decrease in the efficacy of vancomycin against *C. difficile* ribotype 027 isolates was also observed in 2007 (Pepin *et al.*, 2007). Interestingly, the highest resistance for the combination of metronidazole and vancomycin occurred in patients who were also infected with HIV (Pelaez *et al.*, 2002). It seems that an effective treatment for severe CDI is not currently available, while the resistance to many common antibiotics has risen over the years.

A new antibiotic has recently been used to successfully treat *C. difficile* infection. This antibiotic, called fidaxomicin, is a macrocyclic that has been shown to be an effective treatment for *C. difficile* less adverse effects on the normal flora of the human gut (Louie *et al.*, 2011). In a comparison study with oral vancomycin, fidaxomicin showed similar activity, including a similar rate of recurrent infection or CDI complications. The FDA confirmed that fidaxomicin is the best antibiotic treatment for CDAD (Mullane *et al.*, 2011). However, this antibiotic is not in common use as it is significantly more expensive than both vancomycin and metronidazole (Mullane, 2014).

1.8 The cell wall and peptidoglycan structure

Peptidoglycan is the major conserved component of the bacterial cell wall, which protects and stabilises cell from lysis due to high osmotic pressure (Silhavy *et al.*, 2010; Mascher *et al.*, 2006; de Pedro *et al.*, 2002). The peptidoglycan gives the cell rigidity and determines the shape (Gan *et al.*, 2008). Furthermore, the cell wall provides protection against stress conditions, and is also involved in communication with the environment. The cell wall also has an essential role in bacterial pathogenesis, facilitating bacterial invasion, evasion of the immune system and providing an anchor point for virulence factors such as adhesins (Silhavy *et al.*, 2010). Peptidoglycan consists of a polymerised disaccharide backbone of N-acetylglucosamine and N-acetylmuramic acid (Figure 1.6) (Vollmer *et al.*, 2008), cross-linked with short peptide stems, most commonly L-alanine, D-glutamate, meso-2,6-diaminopimelic acid (or L-lysine) and two D-alanines. Cross-linking between peptide stems normally occurs between the amino group of the

diamino acid at position 3 and the carboxyl group of D-Ala at position 4 (Varma and Young, 2004; Priyadarshini *et al.*, 2006; Vollmer *et al.*, 2008). However, recent analysis of *C. difficile* peptidoglycan revealed a high proportion of unusual 3-3 cross-links, generated by an L, D-transpeptidation process (Peltier *et al.*, 2011). Moreover, 96% of the N-acetylglucosamine was found to be de-acetylated in the *C. difficile* glycan structure, which provides resistance against lysozyme.

The transpeptidase or carboxypeptidase activities of Penicillin-Binding Proteins (PBPs) are required for peptidoglycan synthesis (Goffin and Ghuysen, 1998; Sauvage *et al.*, 2008). Transpeptidase activity is dependent on a conserved SXXK motif that includes the active site serine for catalytic activity. In addition, class A and C β -lactamases also share this conserved SXXK motif and active site serine (Matagne *et al.*, 1999; Zapun *et al.*, 2008). The active site serine works by attacking the carbonyl group of D-Ala, forming an ester linkage that causes release of the last D-Ala of the donor peptide by transpeptidation (Zapun *et al.*, 2008). This leads to formation of a covalent complex, the acyl-enzyme intermediate. This complex is hydrolysed by a DD-carboxypeptidase.

Biosynthesis of peptidoglycan is a complex process, requiring 20 chemical reactions to produce the glycan chain. This process starts in the cytoplasm, and includes synthesis of nucleotide precursors and lipid-linked intermediates in the inner leaflet of the membrane, followed by polymerisation on the outer side of the membrane. Cytoplasmic synthesis involves three main steps: production of UDP-N-acetylglucosamine from fructose 6-phosphate, synthesis of UDP-N-acetylmuramic acid, and sequential addition of amino acids to UDP-N-acetylmuramic acid to generate N-acetylmuramyl-pentapeptide (Figure 1.7) (Bouhss *et al.*, 2008; Kotnik *et al.*, 2007; Barreteau *et al.*, 2008).

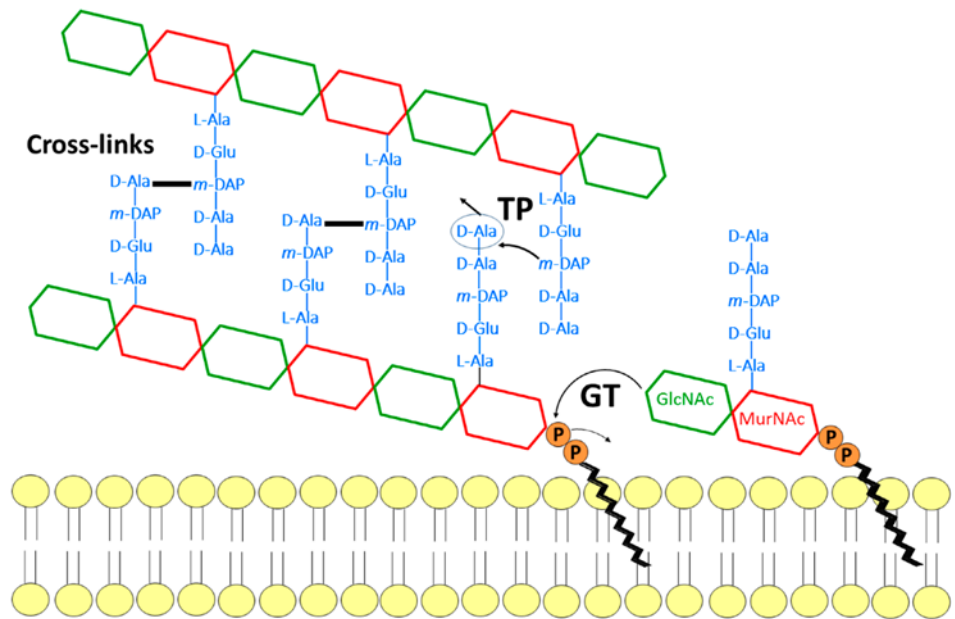


Figure 1.6: The architecture of peptidoglycan. The peptidoglycan consists of two aminosugars, N-acetylglucosamine (GlcNAc) and N-acetylmuramic acid (MurNAc), which are linked with a pentapeptide, L-alanine, D-glutamic acid, L-lysine (or meso-diaminopimelic acid) and two D-alanines. Reproduced with permission from Sauvage and Terrak, (2016).

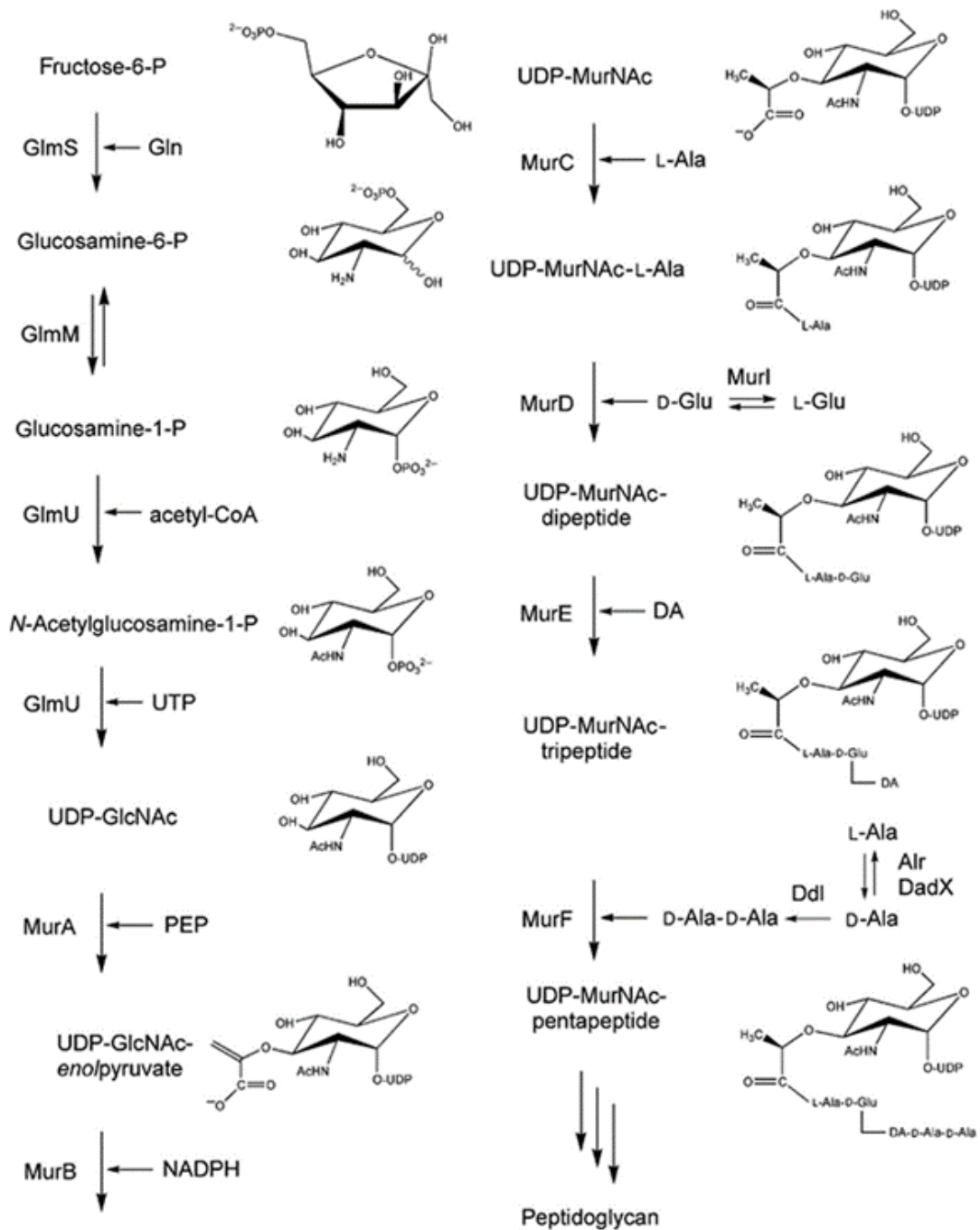


Figure 1.7: The cytoplasmic steps of peptidoglycan biosynthesis. DA, diamino acid (generally meso-A2pm or L-Lys). Reproduced with permission from Barreteau *et al.*, (2008).

1.8.1 Classification of PBPs

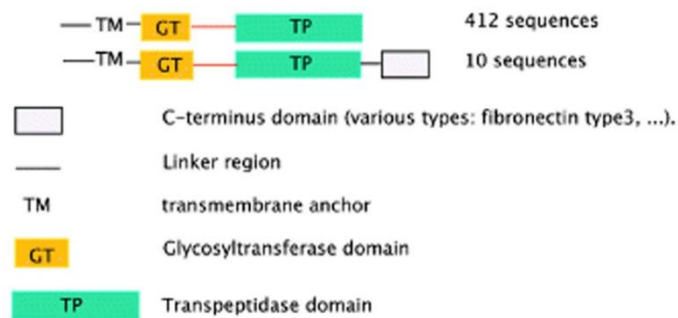
PBPs can be classed in two subgroups: high molecular mass (HMM) and low molecular mass (LMM) enzymes. The HMM PBPs further divide into three main types, class A, class B and class C, according to their functional glycosyltransferase (GT) and transpeptidase (TP) domains (Sauvage *et al.*, 2008). Some HMM PBPs are bifunctional enzymes and have both transpeptidase and glycosyltransferase domains (Llinas *et al.*, 2005; Silvaggi *et al.*, 2005). In contrast, the LMM are all monofunctional D,D-transpeptidases (Meberg *et al.*, 2004; Nelson and Young, 2001).

Class A PBPs have both GT and TP domains connected to a short C-terminal sequence. The C-terminal sequence is linked by a fibronectin type 3 domain, which is considered a structural element. The GT and TP domains are essential in bacterial metabolism and cell wall synthesis. Moreover, another group of class A PBPs are the monofunctional GT enzymes (MGTs), which have a different GT domain linked to a transmembrane anchor. These proteins play a significant role in the bacterial cell cycle (Figure 1.8) (Wang *et al.*, 2001).

Class B PBPs subdivide into four main groups, but are all monofunctional with only TP activity, and are anchored to the membrane via an N-terminal transmembrane domain. The simplest class B subgroup is typified by *E. coli* PBP3 (Figure 1.8). Two of the other class B subgroups also contain one or two C-terminal copies of the PASTA (penicillin-binding protein and serine/threonine kinase associated domain). Although there is no known biochemical function for the PASTA domain, it is thought to play a role in β -lactam binding (Yeats *et al.*, 2002). The last subgroup contains a further NTF2 (nuclear transport factor 2) domain with no known function (Macheboeuf *et al.*, 2006) (Figure 1.8). This domain has also been observed in crystal structures of both PBP2a and PBP5fm from *Staphylococci* and *Enterococci* respectively, but without clear function (Lim and Strynadka, 2002; Sauvage *et al.*, 2002).

1-

Class A enzymes

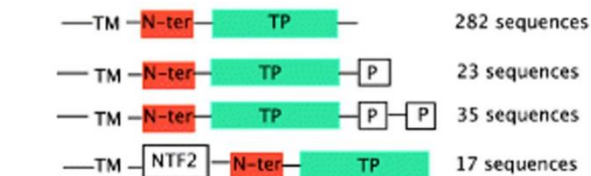


(b) Mono Glycosyltransferases



2-

Class B enzymes



N-ter N-terminus domain ranging in size from 60 (*Deinococcus radiodurans*) to 400 residues (*Clostridium tetani*) depending on the size of the regions shown in light blue in fig. 3.

P PASTA domain

NTF2 Nuclear transport Factor 2-like domain

3-

DD-carboxypeptidases

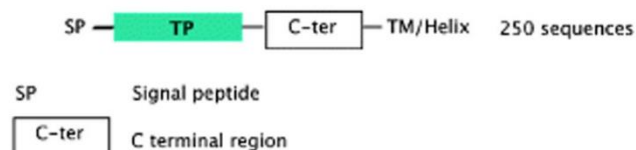


Figure 1.8: Types of penicillin-binding proteins. The PBP types represented in this diagram are based on analysis of 213 eubacterial genomes (Macheboeuf *et al.*, (2006). Most PBPs anchor to the membrane via a transmembrane helix (TM), or an amphipathic helix. Reproduced with permission from Macheboeuf *et al.*, (2006).

Class C PBPs have two catalytic activities, D,D-carboxypeptidase and D,D-endopeptidase. D,D-carboxypeptidases remove the last D-alanine in mucopeptides by attacking the C-terminal of the terminal D-Ala-D-Ala dipeptide, while the DD-endopeptidases hydrolyse the remaining linkage of peptide bridges from glycan strands (Sauvage *et al.*, 2008). Class C PBPs have a signal peptide and TP domain linked to the transmembrane anchor, located in the C-terminal (Figure 1.8) (Macheboeuf *et al.*, 2006).

1.9 β -lactam antibiotics

Penicillin was discovered by Alexander Fleming in 1928 when he observed growth inhibition of *Staphylococcus* colonies by *Penicillium notatum* fungus (Abraham, 1991). Fleming identified the compound that caused the growth inhibition and named it penicillin. However, it was not until 1940 that penicillin was first used in patients who had infections with *Streptococci* (Fleming, 1929). The discovery of penicillin was the first step to developing a large family of β -lactam antibiotics. For his discovery, Fleming received the Nobel Prize in Physiology or Medicine in 1945.

Dorothy Hodgkin determined the chemical structure of penicillin using X-ray crystallography, demonstrating that the antibiotic contained a four-membered heterocyclic ring integrated with a five-membered thiazolidine ring (Crowfoot *et al.*, 1949). In 1939, Howard Walter Florey recruited Ernst Chain to determine the biological and chemical properties of the substance (Ligon, 2004). As a result, in 1940 they reported using penicillin to treat infection in mice, rats, and cats (Abraham and Chain, 1940). The next year they used penicillin in 10 cases of human infection with *S. aureus* (Abraham *et al.*, 1941). In 1941, Florey recruited Heatley to mass produce penicillin and to treat 100 patients. They collaborated with Peoria, at the Department of Agriculture of the Northern Regional Research Laboratory, Illinois, to develop methods for mass production (Henderson, 1997). As a result, they succeeded in identifying a novel species of *Penicillium*, *P. chrysogenum*, which was able to produce a higher amount of penicillin than *P. notatum*. Eventually, penicillin was used in the UK and the USA in late 1942 and 1943 in several clinical cases (Fleming, 1943; Rammelkamp and Keefer, 1943).

Following the discovery of penicillin, many related antibiotics were produced by modification of the chemical structure. These antibiotics contain the same β -lactam ring but a different acyl side group (Crowfoot *et al.*, 1949). All of these compounds are grouped within the wider family of β -lactam antibiotics (Figure 1.9A). Another class of β -lactam antibiotics are the cephalosporins, which were discovered and isolated from *Cephalosporium salmosynnematum* (Roberts, 1952). These antibiotics contain a β -lactam ring integrated with a six-membered dihydrothiazine ring, with side groups (R1 and R2) fused either side of the cephalosporin nucleus (Walsh, 2003). (Figure 1.9B). Cephalosporin has been used to treat many diseases due to much higher efficacy against both Gram-positive and Gram-negative bacteria in comparison with other β -lactam antibiotics (Brotzu, 1948; Burton and Abraham, 1951).

1.10 Mode of action

The β -lactam antibiotics typically work as pseudosubstrates of the transpeptidase PBPs, also called DD-transpeptidases, leading to killing of the cell by weakening of the cell wall during growth (Matagne *et al.*, 1999). The β -lactam antibiotics mimic the dipeptide D-Ala–D-Ala and bind to the active site serine of PBPs; the β -lactam ring opens and forms a new covalent acyl–enzyme complex. This stable acyl–enzyme inhibits PBP-mediated crosslinking and eventually makes the cell wall unable to resist osmotic forces causing lysis (Goffin and Ghuysen, 2002) (Oliva *et al.*, 2003; Beadle *et al.*, 2001) (Figure 1.10). However, the actual mode of action of β -lactam antibiotics is not entirely understood (Bayles, 2000).

1.11 Mechanisms of resistance

Three distinct mechanisms can result in resistance to β -lactam antibiotics.

Firstly, the concentration of antimicrobial inside the cell can be reduced by the action of efflux pumps or changes in porins that affect permeability to prevent antimicrobial entering the cell. Secondly, the antibiotic can be degraded by the action of β -lactamases that hydrolyse β -lactam ring.

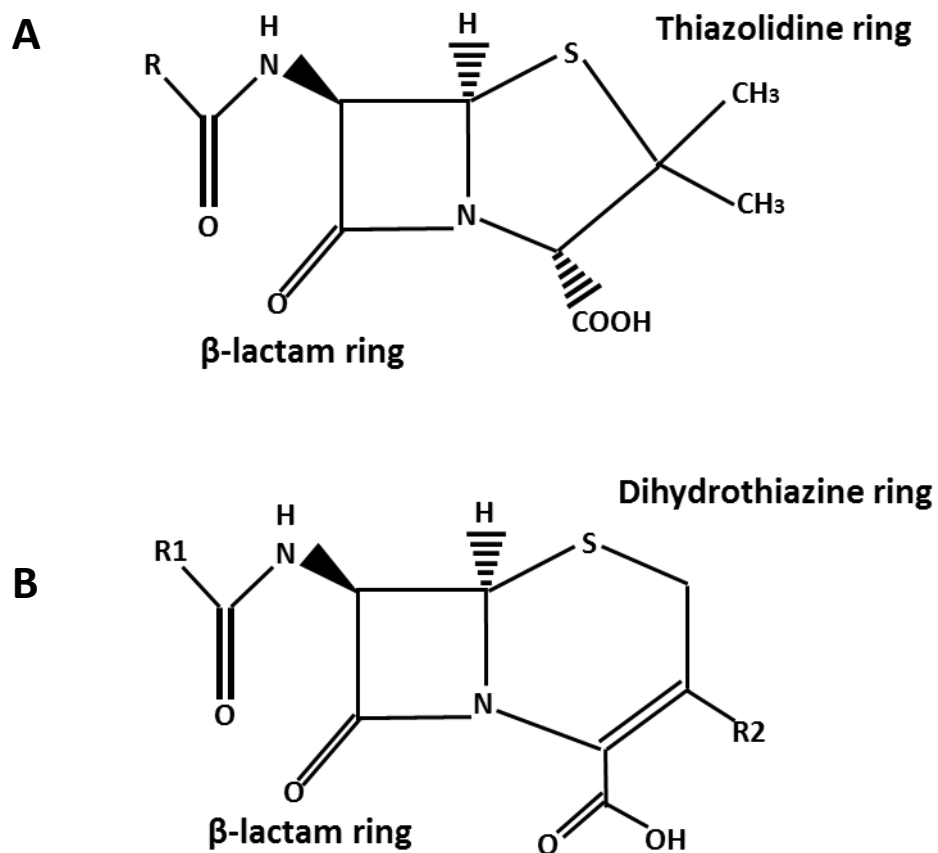


Figure 1.9: Generalised structures of β -lactam antibiotics. **A:** The structure of the penicillin core, 6-aminopenicillanic acid (6-APA). The acyl side group (R) is the site of modification of the different types of β -lactam antibiotics. **B:** The structure of the cephalosporin core, 7-aminocephalosporanic acid (7-ACA). Substitution at α -aminoacidic R1 or R2 side chain yields different cephalosporin antibiotics.

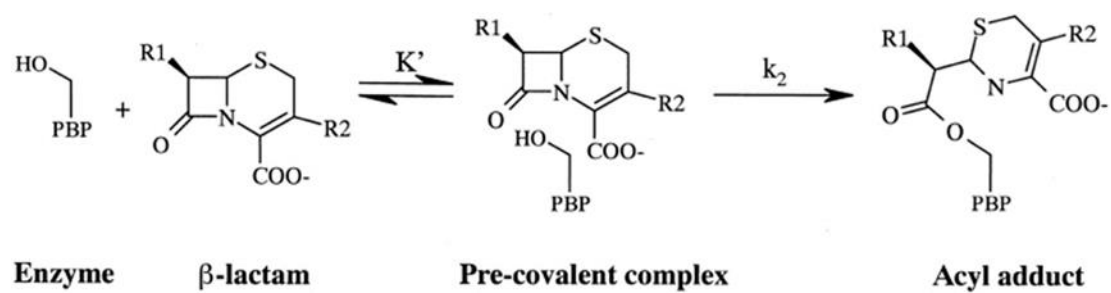


Figure 1.10: The mechanism of β -lactam binding with the PBP active site serine. A stable acyl-enzyme complex can prevent peptidoglycan cross-linking. Reproduced with permission from Beadle *et al.*, (2001).

Thirdly, changes in PBP structure can create β -lactam-insensitive enzymes for cell wall transpeptidation (Walsh, 2000; Wilke *et al.*, 2005; Harbottle *et al.*, 2006; Spigaglia, 2016).

1. One of the most important mechanisms for resistance to antibiotics are multidrug efflux pumps, these are found in almost all bacterial species and are normally chromosomally encoded, often on mobile genetic elements (Blanco *et al.*, 2016). This mechanism was first described in *E. coli* tetracycline resistance (McMurry *et al.*, 1980). In general, there are five main groups of efflux transporters: the adenosine triphosphate (ATP) binding cassette (ABC) transporters (Lubelski *et al.*, 2007), the resistance nodulation division (RND) group (Tseng *et al.*, 1999), the major facilitator group (MFG) (Law *et al.*, 2008), the small multidrug resistance (SMR) group (Chung and Saier, 2001) and the multidrug and toxic compound extrusion (MATE) group (Kuroda and Tsuchiya, 2009). Efflux pumps are characterised based on protein sequence similarity, the specificity of binding with substrate and diffusion into the inner membrane. The ABC transporters use ATP as their energy source, while the other groups rely on the proton motive force (Nikaido, 2011). These transporters are present in both Gram-positive and Gram-negative bacteria, except the RND group, which is specific for Gram-negatives, and the MFS family, which is more relevant for Gram-positive bacteria (Nikaido, 2011).
2. β -lactamase enzymes are able to attack the β -lactam rings of monobactams, carbapenems and penicillins, leading to antibiotic hydrolysis and inactivation of the drug (Bush and Bradford, 2016). β -lactamases have been identified in many different pathogens, leading to the introduction of β -lactamase inhibitors or extended-spectrum β -lactam antibiotics to combat this resistance mechanism (Bradford, 2001). Introduction of the extended-spectrum β -lactams was followed by the emergence of Extended-Spectrum Beta-Lactamases (ESBLs) in parallel with increasing cephalosporin resistance (e.g. to ceftazidime and cefotaxime) (Knothe *et al.*, 1983; Paterson and Bonomo, 2005). β -lactamases are classified based on protein sequence or enzyme function. In the Ambler scheme, β -lactamases were classified into four different classes (A, B, C and D), using

amino acid sequence (Ambler, 1980). A later classification scheme divided the β -lactamases into three main groups: the serine β -lactamase group (Ambler class A and D), the cephalosporinases group (Ambler class C) and the metallo β -lactamases group (Ambler class B). These groups are further divided into many different subclasses. In general, β -lactamase class A, C and D are dependent on binding to a critical serine residue, leading to antibiotic hydrolysis, while class B β -lactamases require a divalent zinc co-factor for the hydrolysis process (Bush *et al.*, 1995; Bush and Jacoby, 2009). Over 890 unique amino acid sequences for β -lactamases were identified in 2009 and are available on BLAST (Bush and Jacoby, 2009).

3. A change in the structure of a class B PBP can also lead to resistance. For example, PBP2x in penicillin-resistant *Streptococcus pneumoniae* (PRSP) (Chesnel *et al.*, 2003; Dessen *et al.*, 2001), PBP2a in methicillin-resistant *S. aureus* (MRSA) (Lim and Strynadka, 2002), PBP5 in *Enterococcus faecium* (Sauvage *et al.*, 2002) and PBP1b from *S. pneumoniae* (Macheboeuf *et al.*, 2005). These PBPs contain mutations that lead to alterations of the antibiotic target, reducing the affinity of antibiotic binding (Fernandes *et al.*, 2013).

Interestingly, analysis of the *C. difficile* 630 genome has identified several genes that may be involved in β -lactam resistance by two main mechanisms: β -lactamase enzyme secretion and target site modification of PBPs (Spigaglia, 2016).

1.12 Sporulation

The sporulation endospore formation process was first described by Robert Koch (Koch, 1876) and Ferdinand Cohn (Cohn, 1877). The fundamental principle of sporulation depends on tight temporal and spatial control of gene expression. Most of the core genes involved are conserved in both *Bacillus* and *Clostridium* species (Paredes *et al.*, 2005). In *B. subtilis* the sporulation process has been studied extensively, underpinning our knowledge of the molecular basis of this process and becoming a useful tool for research dealing with the importance of sporulation (Figure 1.11) (Sonenshein, 2000).

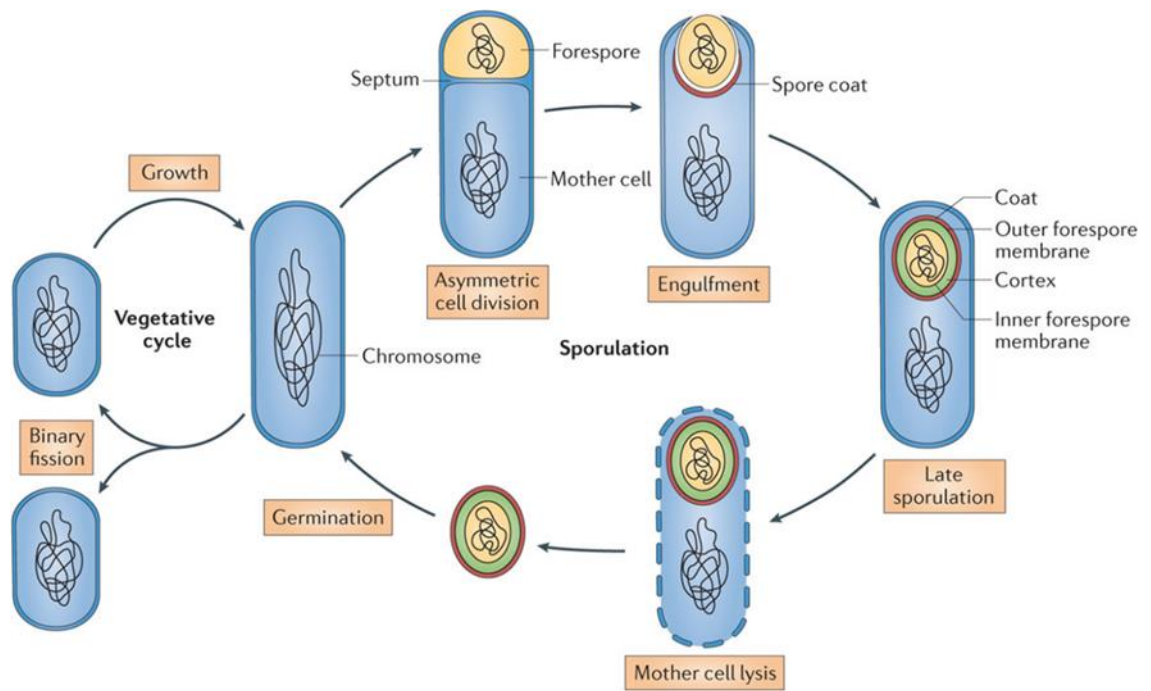


Figure 1.11: Schematic diagram of sporulation and germination in *B. subtilis*. In response to stress, *B. subtilis* can undergo asymmetric cell division to form two compartments, a smaller forespore and larger mother cell. The forespore is eventually engulfed to form a cell-within-a-cell structure. Specific gene expression, in response to a sigma factor cascade, plays a significant role in this process. There are 4 core sigma factors involved: σE and σK in the mother cell compartment, and σF and σG in the forespore. At the end of the process, once spore maturation completes, the mother cell lyses, releasing the mature endospore to the external environment. This spore can persist for a long time in the environment without effects on viability. Under the appropriate conditions, the spores germinate and outgrow to form a vegetative cell. Reproduced with permission from McKenney *et al.*, (2013).

1.12.1 Entry into sporulation

Spo0A phosphorylation is the initiating step in the sporulation process. Spo0A is the master transcriptional regulator with an essential role in bacterial adaptation during environmental changes. The *spo0A* gene is expressed from two different promoters: P_v during vegetative growth, dependent on σ A and P_s during sporulation, individually activated by σ H, encoded by *spo0H* (Siranosian and Grossman, 1994). The level of Spo0A phosphorylation is critical; low level phosphorylation leads to biofilm formation, while high level phosphorylation leads to spore formation (Gonzalez-Pastor *et al.*, 2003, Hamon and Lazazzera, 2001; Fujita and Losick, 2005). In both *Bacillus* and *Clostridium* species, Spo0A phosphorylation is carried out by several orphan histidine kinases (Higgins and Dworkin, 2012; Steiner *et al.*, 2011). In *C. difficile* 630 there are five orphan histidine kinases (CD1492, CD1352, CD1949, CD1579 and CD2492) which may be involved in Spo0A activation (Underwood *et al.*, 2009). A *CD2492* mutant displayed a reduction in spore formation of 3.5 fold compared to the wild type, while inactivation of *spo0A* entirely abolished spore formation (Underwood *et al.*, 2009). Despite the identification of candidate histidine kinases, Spo0A phosphorylation in *C. difficile* is still poorly understood. The absence of both Spo0F and Spo0B proteins, which are involved in transferring the phosphate group to Spo0A in *B. subtilis*, suggests that the phosphate group is directly transferred to Spo0A by the histidine kinases in *C. difficile*. This has been previously observed in *Clostridium acetobutylicum* (Steiner *et al.*, 2011) and direct phosphorylation by CD1579 has been observed in *C. difficile* (Underwood *et al.*, 2009). In contrast, *B. subtilis* Spo0A phosphorylation has been studied extensively, and involves several orphan histidine kinases (KinA-E). These respond to external signals, leading to eventual transfer of phosphate to Spo0A directly or by Spo0F and Spo0B (Jiang *et al.*, 2000; Burbulys *et al.*, 1991). The kinase activity is repressed by two main regulatory factors, Kipl and Sda. These proteins can bind to KinA and prevent the initial phosphorylation. Another mechanism of Spo0A regulation are the protein aspartate phosphatases (RapA, RapB, RapE and RapH). These proteins can dephosphorylate Spo0F, leading to a reduction of Spo0A phosphorylation levels (Perego *et al.*, 1994).

Spo0A phosphorylation is induced by either environmental cues or nutrition limitation (Schaeffer *et al.*, 1965). These cues also include changes in GTP concentration,

the first indicator of nutrient depletion in media. CodY has been identified as a GTP-binding protein and a central repressor of many genes in stationary phase. Once the concentration of GTP drops in response to nutrient depletion, CodY activity decreases and target genes are derepressed, allowing the initiation of sporulation (Handke *et al.*, 2008, Ratnayake-Lecamwasam *et al.*, 2001). Another factor that has an effect on the spore formation is cell to cell communication. This mechanism involves three main proteins, PhrA, PhrC and PhrE (Phr signaling peptides) (Pottathil and Lazazzera, 2003). These proteins inhibit Rap phosphatase activity, leading to initiation of the sporulation process.

Finally, a number of DNA replication proteins allow replication of DNA and inhibit the sporulation process. These proteins include DisA, Sda and SirA. DisA is responsible for the cyclic di-adenosine monophosphate (c-di-AMP) synthesis and monitors chromosome integrity during the sporulation process (Bejerano-Sagie *et al.*, 2006). Sda is involved in the inhibition of the sporulation while cellular replication is active (Burkholder *et al.*, 2001). Lastly, SirA prevents new DNA replication during the sporulation process (Rahn-Lee *et al.*, 2009, Wagner *et al.*, 2009).

Following Spo0A phosphorylation, the *abrB* gene is repressed. This gene encodes a negative regulator of some genes in stationary phase during the sporulation process (Perego *et al.*, 1988). This step leads to activation of *spoIIA*, *spoIIE* and *spoIIG* transcription. Activation of this locus is considered an important trigger of asymmetric cell division, which includes nucleoid remodelling (Ben-Yehuda *et al.*, 2003) and localisation of the cytoskeleton, including the tubulin homologue FtsZ, to the cell pole. During the formation of the septum, approximately one third of the genetic material is transferred to the forespore, while the remaining is then transferred by the SpoIIIE protein (DNA translocase) (Wu and Errington, 1994).

Following DNA translocation and cell division, the engulfment mechanism starts. There are three main steps in engulfment. The first step involves the DPM machinery, which comprises three main proteins (SpoIID, SpoIIP and SpoIIM) that hydrolyse the peptidoglycan between the mother cell and forespore (Chastanet and Losick, 2007). This action leads to invagination of the mother cell membrane around the forespore. The second step is membrane force movement; fusing of the mother cell membrane at the

cellular pole behind the forespore, releasing the forespore compartment into the cytosol (Meyer *et al.*, 2010). Lastly, the interaction between SpoIIQ and SpoIIAH leads to formation of a channel between the two compartments, called the feeding tube. This complex facilitates membrane movement between the two compartments (Fimlaid *et al.*, 2015; Broder and Pogliano, 2006).

The sporulation pathway is controlled by four principal sigma factors, σ_F , σ_E , σ_K and σ_G . These sigma factors are conserved in both *B. subtilis* and *C. difficile* (de Hoon *et al.*, 2010). In both species two sigma factors (σ_F and σ_G) are active in the forespore compartment, and two (σ_E and σ_K) are active in the mother cell compartment (Pereira *et al.*, 2013). However, recent analysis has shown that the sporulation process in *C. difficile* lacks the criss-cross communication between the compartment-specific sigma factors that is observed in *B. subtilis* (Figure 1.12) (Fimlaid *et al.*, 2013; Pereira *et al.*, 2013; Saujet *et al.*, 2013). In both species, σ_F activates σ_G . However, in *C. difficile*, σ_E is not needed to activate σ_G , σ_G is not required to activate σ_K and proteolytic activation is dispensable for σ_K (Fimlaid *et al.*, 2013; Pereira *et al.*, 2013; Saujet *et al.*, 2013; Haraldsen and Sonenshein, 2003). Moreover, the morphological cues for the activation of the sigma factors in *C. difficile* do not appear to be the same as found in *B. subtilis*, because engulfment does not require σ_G activation in *C. difficile* (Fimlaid *et al.*, 2013; Pereira *et al.*, 2013).

Another difference between *C. difficile* and *B. subtilis* is the number of genes that are regulated by the four sigma factors. RNA sequencing and microarray analysis identified more than 200 genes that are governed by the four sigma factors during the sporulation process in *C. difficile*: σ_F regulates 25 genes (compared with 47 in *B. subtilis*); σ_E regulates 97 (282 in *B. subtilis*); σ_K regulates 56 (147 in *B. subtilis*), and σ_G controls 50 (104 in *B. subtilis*) (Fimlaid *et al.*, 2013; Saujet *et al.*, 2013). Notably, the regulation pathway during the sporulation process is likely to be different within the *Clostridium* spp. For instance, in *C. perfringens* and *C. acetobutylicum* σ_K seems to appear early to activate σ_F (Al-Hinai *et al.*, 2014; Harry *et al.*, 2009), whereas the earliest σ factor in both *B. subtilis* and *C. difficile* is σ_F (Fimlaid *et al.*, 2013; Pereira *et al.*, 2013; Saujet *et al.*, 2013; de Hoon *et al.*, 2010).

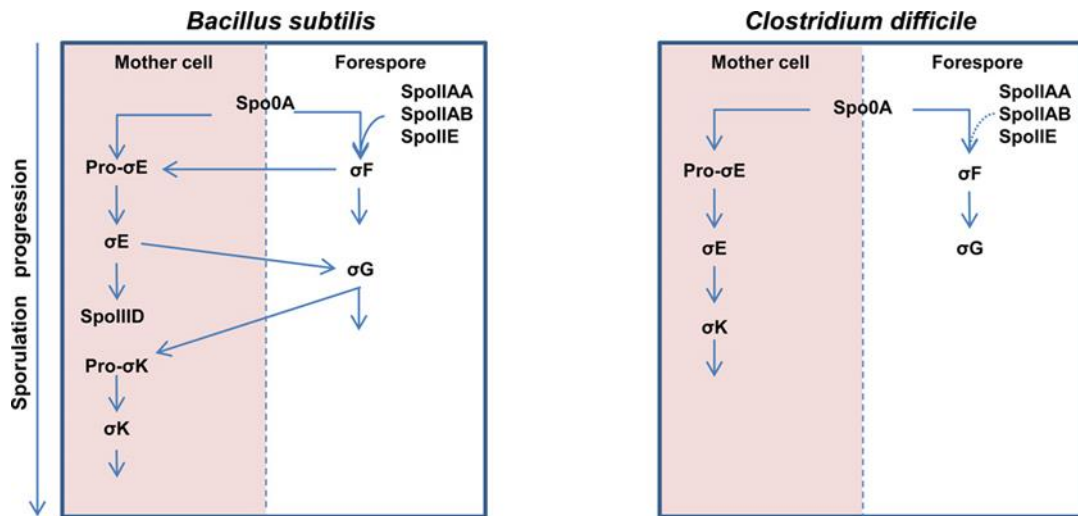


Figure 1.12: Schematic diagram of sporulation regulation in *B. subtilis* and *C. difficile*. *B. subtilis* sporulation is regulated by criss-cross mechanisms, which includes two sigma factors specific for the mother cell (σE and σK) and two sigma factors in the forespore (σF and σG). σF is activated after formation of cell septum. This activation leads to expression of genes that are responsible for cleavage of proteins that inhibit pro- σE , in turn leading to activation of σE . σE then activates σG post-translationally in the forespore. Activation of σG induces genes that in turn activate σK proteolytically in the mother cell. Active σE is also required for activation σK . In *C. difficile* σF is required for activation of σG , and proteolytic activation of σE at least partially. σE then activates σK , but σK activation does not involve proteolytic digestion unlike in *B. subtilis* and *C. perfringens*. Importantly, σE is not necessary for activation of σG . Reproduced with permission from Paredes-Sabja *et al.*, (2014).

Furthermore, in *C. acetobutylicum*, σ K seems to appear in two different stages of the sporulation process, an entirely unique pattern in comparison with other sporulating bacteria (Al-Hinai *et al.*, 2014). These studies have shown the significant diversity in regulation of the σ factors during the sporulation process of both *Clostridium* and *Bacilli* species (Paredes-Sabja *et al.*, 2014).

1.13 Spore morphogenesis

Upon completion of forespore engulfment, the sigma factors regulating sporulation change dramatically, both σ F and σ E are repressed, while σ G becomes active in the forespore and σ K becomes active in the mother cell. The resulting gene expression completes spore morphogenesis. The mature spore has several important structural layers: the core, which contains the genetic material, the core is then surrounded by an inner membrane that protects the DNA from chemical agents due to its low permeability for small molecules. Surrounding this is a layer of peptidoglycan called primordial germ cell wall. This becomes the cell wall of the new vegetative cell following germination. The cortex, consisting of altered peptidoglycan with NAM residues cyclised to form muramic- δ -lactam (MAL) with no amino acid side chain, then surrounds the germ cell wall. The cortex is in turn surrounded by an outer membrane that is derived from the mother cell during engulfment and, lastly, the protective and proteinaceous coat layer forms the outmost layer. In *C. difficile* the existence of an additional exosporium layer has been proposed (Figure 1.13) (McKenney *et al.* 2013; Reineke *et al.*, 2013; Paredes-Sabja *et al.*, 2014).

1.13.1 Spore core

Following forespore engulfment, modifications occur for the protection of the genetic material inside the forespore compartment. In addition to chromosomal DNA, ribosomes and tRNAs, the core also contains many spore-specific enzymes. These proteins are required for the metabolism pathway, followed by dormancy phase. In this process, water is replaced by dipicolinic acid (DPA); water forms only 25-50% of forespore dry weight (Murrell, 1967).

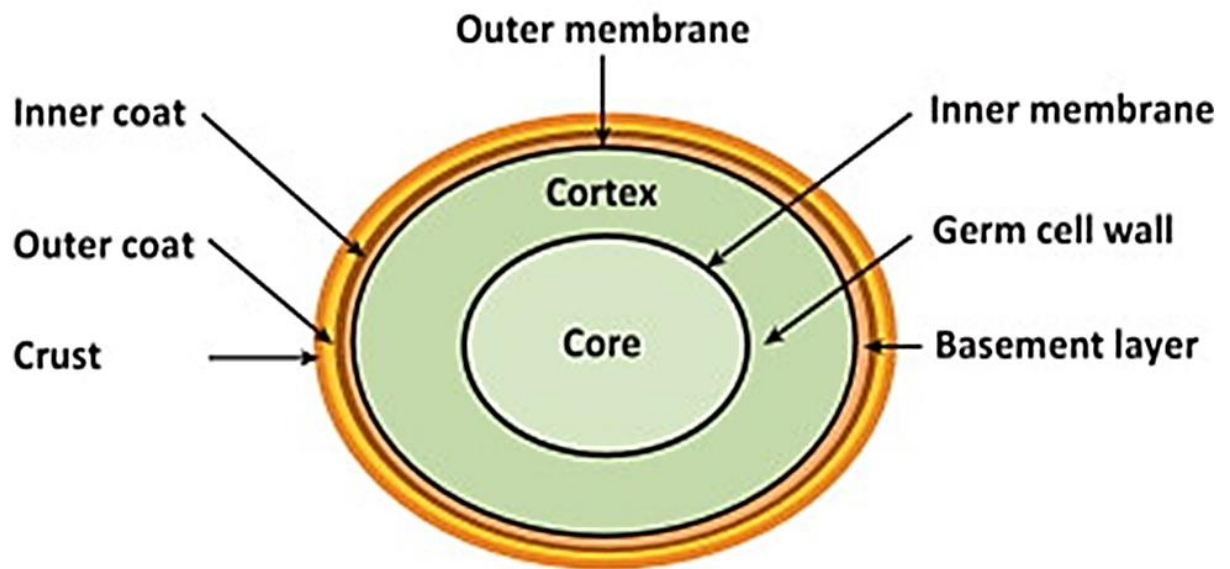


Figure 1.13: Spore structural layers. The inner compartment, the core, contains the DNA, RNA and all necessary enzymes. These elements are very important for spore resilience. The core is dehydrated and contains a high concentration of Ca^{2+} -DPA and the DNA is saturated with α/β -type small acid-soluble proteins (SASPs) that protect the spore from UV radiation and heat. The core is then surrounded by an inner membrane that protects the DNA from chemical agents due to its low permeability for small molecules. The primordial cell wall surrounds the inner membrane, followed by the cortex layer. The cortex consists the peptidoglycan that contains muramic- δ -lactam (MAL). The MAL residues allow specific identification of the cortex by cortex-lytic enzymes (CLEs), allowing hydrolysis of the cortex without damage to the primordial cell wall. The final coat layer contains about 80 proteins that are specific for the spore. These proteins provide protection from lytic enzymes and chemical agents. The coat layer is subdivided into a basal layer, inner coat, outer coat and crust. In *C. difficile* the coat is surrounded by an extra layer called exosporium. Reproduced with permission from Reineke *et al.*, (2013).

The mother cell produces DPA which is transferred to the forespore compartment where the DPA chelates with calcium at a ratio of 1:1 (Driks, 2002). The low water content is compensated for by the DPA making up 20% of dry weight (Setlow, 1994). This content contributes to the spore's resistance to desiccation, wet heat and H₂O₂ (Setlow, 2006). The DNA in the core is also saturated with α/β -type small acid-soluble proteins (SASPs). These proteins form 5-10% of the total core (Driks, 2002). SASP transcription is dependent on σ G (Cabrera-Hernandez and Setlow, 2000). The SASPs protect the DNA from damage like UV radiation, dehydration, heat, and toxic chemicals including hydrogen peroxide, formaldehyde and nitrous acid (Setlow, 2007).

1.13.2 Spore cortex

The spore is surrounded by two membranes, an inner and outer lipid bilayer. These membranes are separated by two types of peptidoglycans. The inner layer is called the germ cell wall. The germ cell wall is derived from the wall of the sporulating cell and is similar in structure. During germination, the germ cell wall provides the wall for the new vegetative cell (Tipper and Linnett, 1976).

Outside of the primordial wall is a thicker layer of the peptidoglycan called the cortex. In the cortex peptidoglycan about half of the NAM residues are cyclised muramic- δ -lactam (MAL) with no amino acid side chain (Warth and Strominger, 1969; Warth and Strominger, 1972) (Figure 1.14). These residues allow cortex hydrolysis during the germination process, while the primordial cell wall remains intact (Makino and Moriyama, 2002). In *B. subtilis*, the MAL residues are formed by an N-acetylmuramoyl-L-alanine amidase encoded by *cwID*, disruption of which results in spores that are defective in germination (Popham *et al.*, 1996, Sekiguchi *et al.*, 1995).

1.13.3 Spore coat

A proteinaceous coat surrounds the cortex layer, and is comprised of three separate layers: an amorphous basal layer, a lamellar inner coat and an electron-dense, striated outer coat (McKenney *et al.*, 2013). Recently, an additional crust layer has been characterised in *B. subtilis* (McKenney *et al.*, 2010).

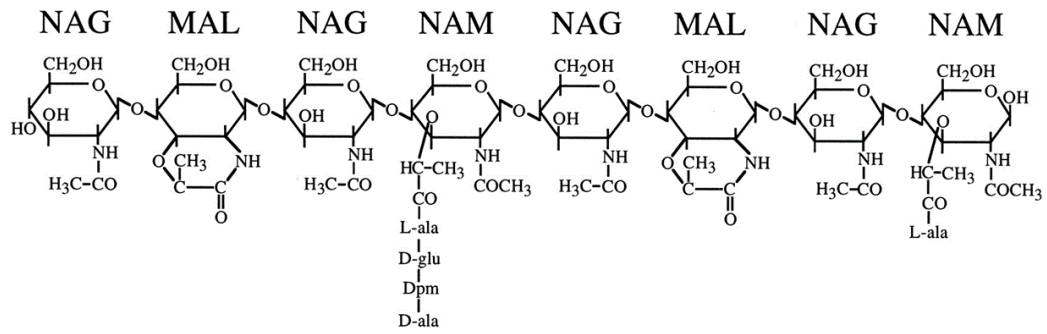


Figure 1.14 The *B. subtilis* cortex peptidoglycan structure. Muramic- δ -lactam (MAL) replaces approx. 50% of N-acetylmuramic acid (NAM) residues in the peptidoglycan. Pentapeptides on the remaining N-acetylmuramic acid (NAM) residues cross-link the peptidoglycan. Reproduced with permission from Popham *et al.* (1996).

The coat layers contain approximately 80 proteins that are synthesised by the mother cell, and subsequently transferred to the forespore compartment, targeted to the outer surface of the spore. Spore coats vary significantly between bacterial species. For example, only half of the *B. subtilis* protein coat proteins are conserved in other *Bacillus* species. In *Clostridium* species, there are very few identifiable protein coat orthologues (Henriques and Moran, 2007, Permpoonpattana *et al.*, 2011).

The major function of the protein coat is to protect the genetic material from environmental conditions by blocking access to the spore core. Moreover, these protein coats provide protection for spore inner layers from oxidising agents.

One of the most important coat components that is responsible for the spore protection from hydrogen peroxide is CotA, which is a copper-dependent laccase (Riesenman and Nicholson, 2000). CotA participates in spore resistance against UV radiation by providing a pigment that is structurally identical to melanin (Hullo *et al.*, 2001, Riesenman and Nicholson, 2000). Another protein coat component that provides protection against lysozyme and glycan-hydrolysing enzymes is CotE. CotE also confers protection against predators such as bacteriovores, nematodes such as *Caenorhabditis elegans* and protozoan such as *Tetrahymena thermophile* (Klobutcher *et al.*, 2006, Laaberki and Dworkin, 2008). Finally, the coat layer plays an important role in germination by responding to germinants such as sugars, peptidoglycan fragments, ions and amino acids.

C. difficile spores must germinate in order to initiate CDI (Howerton *et al.*, 2013). In *Clostridium* spp. and *Bacillus* spp., germination is normally started by triggering of a protease-like proteins, leading to release of calcium dipicolinic acid (DPA) from the spore core. This leads to degradation of the peptidoglycan of the cortex layer, allowing core hydration and followed by resumption of metabolism processes in the core (Paredes-Sabja *et al.*, 2011). In general, *C. difficile* spores respond to bile salts in the small intestine, such as cholate, taurocholate, deoxycholate and glycocholate, or amino acid such as L-glycine. These chemicals act as germinants (Howerton *et al.*, 2011; Sorg and Sonenshein, 2008). In *C. difficile*, it has been demonstrated that CspC is a serine protease, responsible for the bile salt response, and leading to release of dipicolinic acid

(DPA) from the spore core in response to taurocholate and glycine. In addition, a point mutation in *cspC* leads to spore germination in response to chenodeoxycholate, which is normally an inhibitor of germination (Adams *et al.*, 2013; Francis *et al.*, 2013; Sorg and Sonenshein, 2009). In *C. difficile*, the mechanism of spore germination is similar to spore germination in *C. perfringens*, which requires Csps and SleC for cortex hydrolysis (Adams *et al.*, 2013; Burns *et al.*, 2010; Francis *et al.*, 2013; Paredes-Sabja *et al.*, 2009a, Paredes-Sabja *et al.*, 2009b). In *C. difficile*, CspB is responsible for processing pro-SleC into active SleC and the latter causes cortex degradation (Adams *et al.*, 2013; Gutelius *et al.*, 2014). Although germination in *C. difficile* has been studied (Adams *et al.*, 2013; Francis *et al.*, 2013; Burns *et al.*, 2010), the details of cortex hydrolysis remain unclear (Paredes-Sabja *et al.*, 2014). For instance, in *C. perfringens* and *B. subtilis*, SpoVA is responsible for regulation of Ca–DPA release, while its role in *C. difficile* is still to be elucidated (Paredes-Sabja *et al.*, 2014).

In *B. subtilis*, coat assembly is coordinated by morphogenetic proteins such as SpoVM, CotE, SafA, SpoVID, and SpoIVA. These proteins interact with other coat proteins to form three necessary modules; for example, SafA interacts with proteins that are involved in inner coat assembly, while CotE interacts with proteins that participate in outer coat assembly. The third module involves cooperation between SatA and CotE and the basal layer protein SpoIVA, which is considered the first protein in coat assembly. A final extra module is governed by CotX, CotY and CotZ. These proteins have been recently determined to be assembled in the crust layer (McKenney *et al.*, 2010) (Figure 1.15).

In *C. difficile*, SpoIVA and SpoVM homologues have been identified (Galperin *et al.*, 2012). Furthermore, the SpoIVA protein has been shown to be localised in the forespore compartment as in *B. subtilis* (Putnam *et al.*, 2013). Despite the fact that there are some similarities between the coat proteins in *C. difficile* and *B. subtilis*, the SpoVID, SafA, and CotE proteins do not have homologues in *C. difficile*. This finding indicates that coat proteins are divergent (Henriques and Moran, 2007; Galperin *et al.*, 2012). Indeed, a protein (SipL, CD3567) that interacts with the SpoIVA protein via a LysM domain, has recently been identified in *C. difficile*.

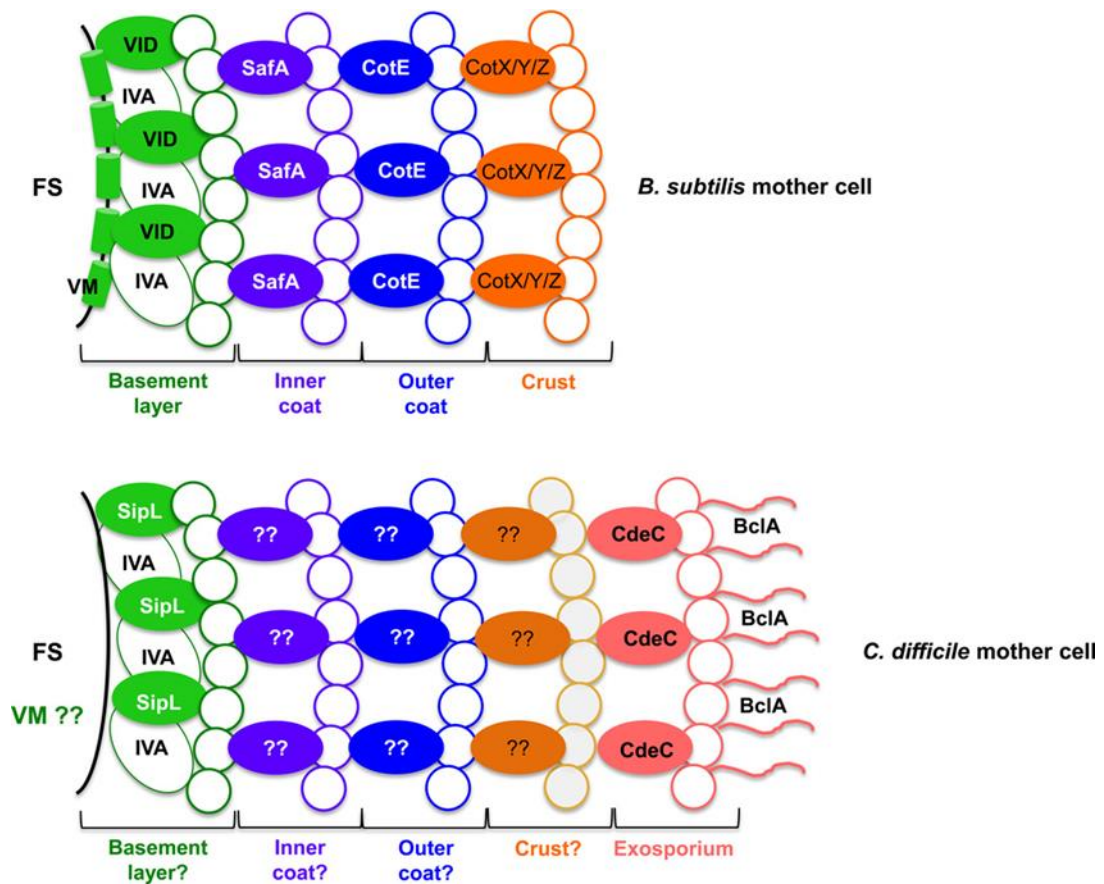


Figure 1.15: Schematic diagram of coat assembly in *B. subtilis* and *C. difficile*. In *B. subtilis* SpoIVA and SpoVID localise to the basement layer of the coat structure, while in *C. difficile* SipL and SpoIVA localise there. SpoVM in *B. subtilis* localises to the outer membrane, while in *C. difficile* it is unclear if SpoVM localises to the membrane (VM??). The proteins that are responsible for both the inner and outer coat layers are also uncharacterised in *C. difficile* (indicated by ??). While, in *B. subtilis* both SafA and CotE are the main constituents of the inner and outer coat. It is also unclear whether *C. difficile* has crust layer or not (indicated by ??). In *C. difficile* the exosporium proteins are CdeC, BclA1, BclA2 and BclA3. CdeC is located on the inner face of the exosporium, while BclA1, BclA2 and BclA3 are on the outermost exosporium layer. Abbreviations: VID, SpoVID; VM, SpoVM; IVA, SpoIVA; FS, forespore and (??), unidentified proteins. Reproduced with permission from Paredes-Sabja *et al.*, (2014).

This interaction is essential for driving coat assembly. Additionally, SipL helps to transfer the coat protein from the proximal cap of the mother cell to complete encasement (Figure 1.15) (Putnam *et al.*, 2013; McKenney *et al.*, 2013; Wang *et al.*, 2009). The coat assembly also undergoes extensive post-translational modification, including cross-linkage and glycosylation. All of these processes play a significant role in spore coat assembly (McKenney *et al.*, 2013).

1.13.4 The exosporium

In *C. difficile* the spore is surrounded by a further glycoprotein layer known as the exosporium (Figure 1.15). The exosporium layer is divergent between species (Panessa-Warren *et al.*, 2007) and provides resistance against chemical agents and enhances adhesion to host tissues by providing a hydrophobic surface.

The exosporium is also the first contact with the immune system, mediating the first interaction between the host and the pathogen. The exosporium structure has been studied extensively in *B. anthrax*, showing a paracrystalline basal layer, surrounded by a hair-like nap that is formed by the collagen-like glycoprotein BclA. In *C. difficile* 630 there are three *bclA* homologues, *bclA1* (CD0332), *bclA2* (CD3230), and *bclA3* (CD3349). These genes encode the three main proteins of the *C. difficile* exosporium (Henriques and Moran, 2007; Lawley *et al.*, 2009). The hairy nap structure in *C. difficile* is different in shape than that of *B. anthracis*, appearing scruffier and disorganised (Figure 1.15) (Lawley *et al.*, 2009; Barra-Carrasco *et al.*, 2013).

The BclA1, BclA2 and BclA3 proteins have three functional domains, N terminal domain, collagen domain and C terminal domain (Sebahia *et al.*, 2006; Pizarro-Guajardo *et al.*, 2014). Recently, the BclA proteins in *C. difficile* have been shown to be expressed in the mother cell compartment under σ_K (Fimlaid *et al.*, 2013; Saujet *et al.*, 2013).

However, the actual role of the BclAs is still unclear. Studies on the *C. difficile* exosporium have found another unique exosporium cysteine-rich protein called CdeC (CD1067) (Barra-Carrasco *et al.*, 2013). A *cdeC* deletion caused significant reduction in

the assembly of both the coat layer and exosporium. The *cdeC* mutant also showed differences in the content of both inner and outer coat layers. For example, the inner layer was thicker, while the outer layer was thinner in comparison with wild type (Barra-Carrasco *et al.*, 2013). This finding suggests that CdeC works as an anchor protein, which interfaces between both the coat layer and the exosporium (Figure 1.15) (Paredes-Sabja *et al.*, 2014). Moreover, the *cdeC* mutant was also shown to have a higher water content in the core than the wild type, and spores were sensitive to both heat and ethanol treatments. This indicates that CdeC could have a significant role in the early stage of spore formation (Barra-Carrasco *et al.*, 2013; Paredes-Sabja *et al.*, 2014).

1.14 Overview of genetic manipulation of studying *C. difficile*

Our understanding of CDI has been hindered by the lack of appropriate methods for the genetic manipulation of *C. difficile*. Effective genetic tools are pivotal for the identification of genes that are responsible for pathogenesis and colonization. Until recently few methods were available for the manipulation of the *C. difficile* chromosome. At a minimum a genetic manipulation toolbox must allow transfer of DNA (normally plasmid) into the bacterium and manipulation of the genome (for example using homologous recombination).

1.14.1 Clostridial vector systems

The first method used to deliver DNA into *C. difficile* was filter mating, which can be used to facilitate transfer of conjugative transposons from a *B. subtilis* donor to *C. difficile* (Mullany *et al.*, 1991). Although this method successfully transferred heterologous DNA, the transfer frequency was very low (10^{-8} per donor) (Mullany *et al.*, 1994). More recently, *E. coli* has been used as a donor to transfer plasmid DNA to *C. difficile* via conjugation. This method depends completely on shuttle vectors, such as pMTL960, which have a *C. difficile* replicon (pCD6), an *E. coli* origin and an origin of transfer (*oriT*) (Purdy *et al.* 2002). The *catP* gene from *C. perfringens* was added as a selectable marker. CatP confers chloramphenicol resistance in *E. coli* and thiamphenicol resistance in *C. difficile*. The native promoter from the *cwp2* gene has been well

characterised and has been used successfully for over-expressing proteins in *C. difficile* (Dembek *et al.*, 2012, Emerson *et al.*, 2009, Reynolds *et al.*, 2011; de la Riva *et al.*, 2011). More recently, a tetracycline-inducible promoter has been introduced (Fagan and Fairweather, 2011). This promoter has also been used to knock down gene expression using antisense RNA (Fagan and Fairweather, 2011). Finally, removal of the transcriptional terminator downstream of *tetR* allows conditional disruption of plasmid replication and rapid loss of plasmid after 13 generations of bacterial growth (Dembek *et al.*, 2015).

1.14.2 Genomic mutations in *C. difficile*

1.14.2.1 Clostron insertional mutagenesis

Clostron was the first technique for creation of stable mutants within targeted genes in Clostridial genomes (Heap *et al.*, 2007). The system is based on insertion of a group II intron into the target gene using a mechanism in which the intron RNA is reverse transcribed directly into the target site. Group II intron mobility was firstly identified by Mohr *et al.* (2000). The group II intron element was found in the *Lactococcus lactis ltrB* gene. Changing the intron sequence altered the insertion target and provided a method to disrupt any gene of interest. The group II intron was modified through addition of a retrotransposition-activated marker (RAM), an antibiotic resistance marker with inserted group I intron. Following transcription of the group II intron, the selectable RAM marker is restored by group I intron splicing (Figure 1.16). In 2010, the system was updated (Heap *et al.*, 2010) to become a milestone in molecular studies of *C. difficile* and used in many types of studies related to the genetic manipulation of *C. difficile* (de la Riva *et al.*, 2011, Deakin *et al.*, 2012, Emerson *et al.*, 2009, Kirby *et al.*, 2009, Reynolds *et al.*, 2011).

1.14.2.2 Homologous recombination techniques

Despite the fact that the Clostron system provides a reliable, reproducible and fast method to disrupt a targeted gene, insertional mutants can have polar effects. Multiple insertions have also been reported in some cases, which can make screening

of potential mutants time consuming. Lack of additional selectable markers also creates difficulty in disruption of multiple genes.

In order to overcome all of these problems homologous recombination was developed. The first attempts using single crossover integration of plasmids were unstable and frequently reverted to wild type (O'Connor *et al.*, 2006). In 2012, two robust methods were successfully used to create double crossover mutants in *C. difficile*. The first method depends on the *codA* gene from *E. coli*. *codA* encodes cytosine deaminase that converts the innocuous 5-fluorocytosine (FC) into highly toxic 5-fluorouracil (FU). The 5-fluorouracil (FU) toxicity occurs via uracil phosphoribosyltransferase, which inhibits thymidylate synthase, an essential enzyme in DNA nucleotide synthesis. Moreover, FU causes misincorporation of fluorinated nucleotide into both DNA and RNA (Heidelberger *et al.*, 1983; Longley *et al.*, 2003).

The plasmid carrying *codA* and 500 bp down and upstream of the targeted gene is conjugated into *C. difficile*. The transconjugant colonies become thiamphenicol resistance. The origin of replication of pMTL-SC7215 is pBP1 from *Clostridium botulinum*. This replicon has been used successfully for homologous recombination in both *C. difficile* R20291 and 630. This replicon is unstable in *C. difficile*, allowing rapid plasmid loss due to segregational instability into daughter cells (Cartman and Minton, 2010).

First crossover is confirmed by colony PCR and the double crossover is selected for on minimal medium supplemented with FC. Colony PCR is then typically used for screening to differentiate between the wild type and stable double crossover mutant. This system has been successfully applied in *C. difficile* R20291 to correct a point mutation in the *tcdC* gene, allowing confirmation of the role of *tcdC* in toxin regulation (Cartman *et al.*, 2012).

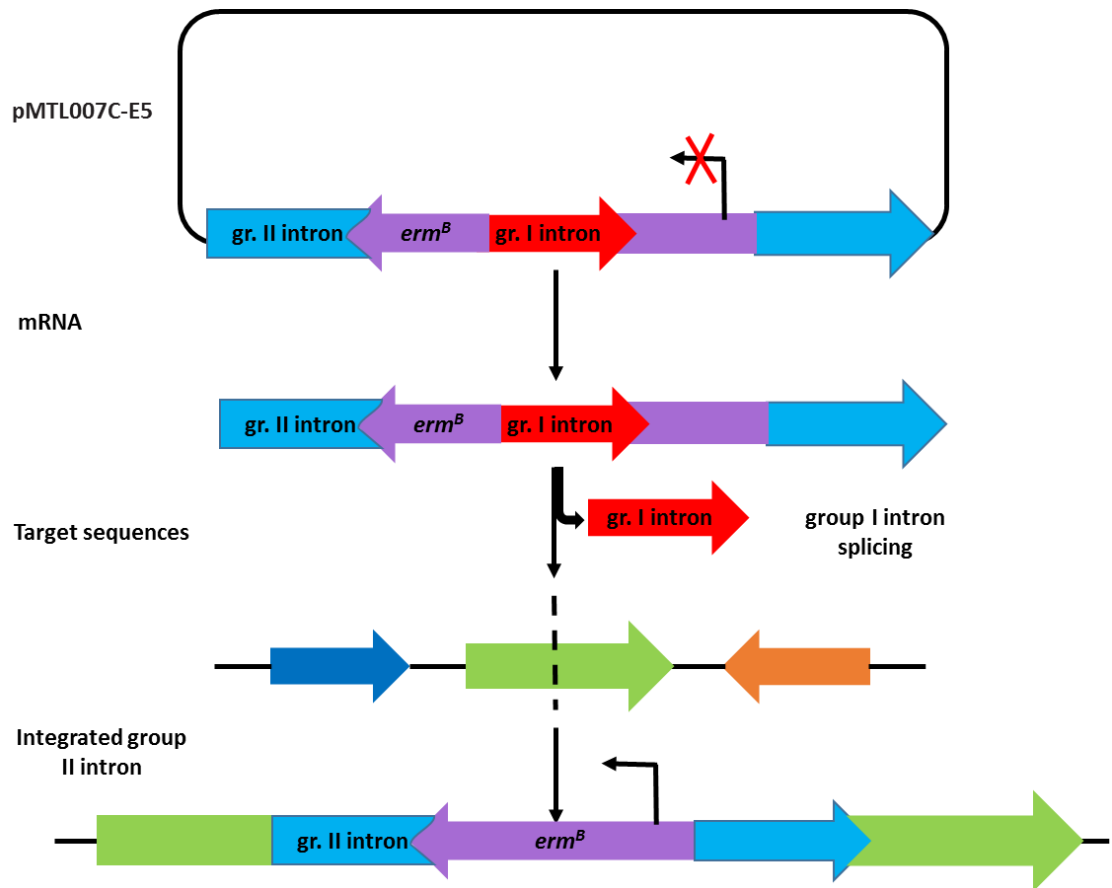


Figure 1.16. Schematic diagram of Clostron insertional mutagenesis. The plasmid pMTL007C-E5, carrying the group II intron, is conjugated into *C. difficile*. After the transcription the group I intron is spliced activating the *ermB* cassette and the group II intron then integrates into the targeted gene, leading to disruption of the gene expression. The RAM marker encodes erythromycin and lincomycin resistance.

The second system relies on a different selectable marker, *pyrE*. *pyrE* encodes orotate phosphoribosyltransferase, which is responsible for pyrimidine biosynthesis and can be used as both a positive and negative selectable marker. PyrE is necessary for growth in the absence of exogenous uracil and PyrE can also convert 5-fluoro-orotate (FOA) to 5-fluoro-uracil, which is toxic for the cell. The toxicity is caused by misincorporation of the fluorinated nucleotide into both DNA and RNA. Hence, FOA can be used for selection of plasmid loss. As with the CodA system above, non-native plasmid replicons are used to aid selection of recombinants. Despite the flexibility of *pyrE* as a selectable marker there is one major drawback, mutagenesis requires a strain background in which the native *pyrE* gene has already been deleted.

Following successful modification of the chromosome the *pyrE* gene must be restored to wild type to return uracil prototrophy. However, this can be achieved at the same time as delivering additional DNA into the chromosome, for example when complementing a mutant (Figure 1.17).

The *pyrE* system has been successfully used to deliver 40 kb of lambda DNA into the *C. acetobutlicum* genome (Heap *et al.*, 2012). Recently, this system has also been used by Ng *et al.* (2013) to put new DNA anywhere into the chromosome of *C. difficile* strains R20291 and 630 with a pre-existing deletion in the *pyrE* gene. These systems are now the gold standard for genetic manipulation in *C. difficile*.

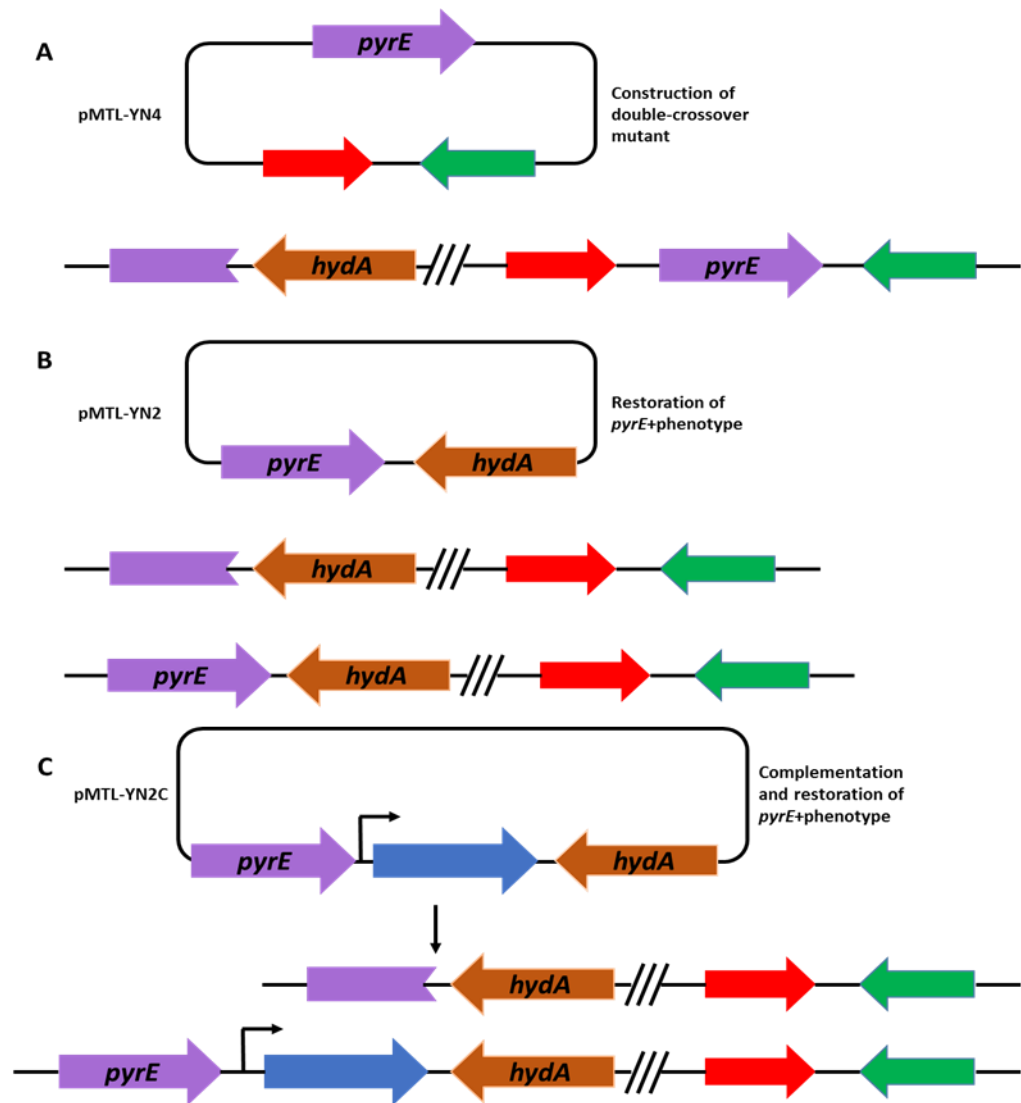


Figure 1.17: Homologous recombination using *pyrE* system. **A:** A pMTL-YN4-based plasmid carrying fragments homologous to both down and upstream of the targeted gene (red and green) and a copy of *pyrE* (purple) on the same plasmid. This plasmid conjugated into *C. difficile* R20291 Δ *pyrE*. Subsequently, the single crossover is selected by growing the transconjugant colonies onto BHI supplemented with thiamphenicol. These colonies were cultured on a minimal medium supplemented with FOA for double crossover selection. **B:** The created mutant was restored the uracil prototrophy by delivering pMTL-YN2 plasmid, which has a *pyrE* WT copy and then selects for double crossover. **C:** The complementation strain is constructed by cloning the whole WT gene, including the promoter region, into pMTL-YN2C. This constructed plasmid is conjugated into the mutant strain followed by selection for the second crossover. pMTL-YN2C allows insertion of DNA in the *pyrE* locus at the same time as restoration of the wild type *pyrE* gene.

1.14.2.3 Transposon mutagenesis and sequencing

Transposons have become a useful tool in the 'molecular toolbox' since the 1950s (McClintock, 1950). Transposons can allow genetic manipulation of virtually any gene in an organism (Kidwell and Lisch, 2001, Alekshun and Levy, 2007).

The biggest advantage of transposon mutagenesis is the ability to create large numbers of random insertional mutants, which enables the researcher to determine the phenotype associated with a particular gene. With high-throughput sequencing or tagged transposon and marker rescue methods, it is possible to identify the transposon insertion site and create comprehensive libraries of insertional mutants. This allows analysis of phenotype- genotype relationships (Hensel *et al.*, 1995). These techniques have been successfully used to study virulence in pathogenic organisms such as *Staphylococcus aureus* (Mei *et al.*, 1997), *Streptococcus agalactiae* (Jones *et al.*, 2000), *Salmonella enterica* Typhimurium (Hensel *et al.*, 1995), *Streptococcus pneumoniae* (Polissi *et al.*, 1998) and *Listeria monocytogenes* (Autret *et al.*, 2001). This technique can also be used to differentiate essential and non-essential genes by studying patterns of transposon insertion (Barquist *et al.*, 2013).

The first Clostridial transposon mutagenesis system was developed for *C. perfringens* (Vidal *et al.*, 2009, Lanckriet *et al.*, 2009). However, this system relied on transformation, so cannot be applied to *C. difficile*. In 2010 a mariner transposon mutagenesis system was developed for *C. difficile* using 'pseudo-suicide' vectors that are segregationally unstable (Cartman and Minton, 2010). The utility of this system was still limited by the efficiency of conjugation however, as the transposition process was not controlled. In 2015, a transposon system was developed that allowed control of both transposition timing and plasmid loss (Dembek *et al.*, 2015). The *Himar1* transposase was cloned downstream of the inducible Ptet promoter and the *tetR* gene was orientated such that transcriptional readthrough would affect plasmid replication from the pCD6 origin (Fagan and Fairweather, 2011). This system was combined with TraDIS to identify transposon insertion sites (Dembek *et al.*, 2015). This system was used to create 70,000 unique mutants in *C. difficile* R20291 and then to identify all essential genes and those required for sporulation (Dembek *et al.*, 2015).

1.15 Project aims

Antibiotic resistance plays a pivotal role in *Clostridium difficile* epidemiology and allows emergence of new *C. difficile* strains that are more virulent. While, the genetic basis of antibiotic resistance has been extensively studied in *C. difficile*, there is still a lot we do not know.

Three complementary types of mutagenesis were used in this project to identify genes involved in antibiotic resistance. Firstly, identified genes encoding penicillin-binding proteins were deleted using homologues recombination to understand the impact on resistance to cell wall-targeting antibiotics. Secondly, Clostron mutagenesis was used to disrupt a gene encoding a specific cell wall protein to understand the role and the mechanism of that protein. Lastly, transposon insertional mutagenesis was used to identify more gene subsets that are involved in resistance to cephalosporin and fluoroquinolone antibiotics.

The major aims of this project were:

1. Investigation of the role of SpoVD in both sporulation and cephalosporin resistance.
2. Expression, interaction and domain analysis for SpoVD.
3. Purification, cloning and analysis of SpoVD enzymatic activity.
4. Investigation of the role of Cwp20 in cephalosporin resistance.
5. Purification, cloning, demonstration of Cwp20 as class A β -lactamase.
6. Identification of additional genes contributing to cephalosporin and fluoroquinolone resistance in *C. difficile* R20291.

Chapter Two

Materials and Methods

2. Materials and Methods

2.1. Bacterial strains and growth conditions

C. difficile strains were cultured on brain-heart infusion (BHI) agar (Oxoid), BHIS agar (BHI agar supplemented with 0.1% L-cysteine and 0.5% BD Bacto Yeast Extract) and Brazier's CCEY Agar supplemented with egg yolk emulsion (Oxoid) and defibrinated horse blood (Oxoid) (Table 2.1.1) or *C. difficile* Defined Medium (CDDM), supplemented with 5-fluorocytosine (FC) or 5-fluoro-orotate (FOA) when required (Table 2.1.2) (Karasawa *et al.*, 1995). The BHIS was also supplemented with 0.1% sodium taurocholate for bacterial sporulation assay (Table 2.1.3). The BHI agar or TY broth were supplemented with uracil (5 µg/ml) for growth of *C. difficile* R20291Δ*pyrE* (Table 2.1.3).

C. difficile strains were also grown in BHI broth (Oxoid), BHIS broth or TY broth, supplemented with appropriate antibiotics when required: thiamphenicol (15 µg/ml), cycloserine (250 µg/ml) and lincomycin (20 µg/ml) (Table 2.1.3). All liquid cultures were inoculated after pre-reduction in the anaerobic cabinet (Don Whitley Scientific) at 37°C, in an atmosphere of 10% CO₂, 10% H₂ and 80% N₂.

2.1.1 Media

Media	Ingredients (per liter)	(per liter)
LB Broth	Merck LB broth	25 g
LB Agar	Merck LB Agar	37 g
BHIS agar	BHI agar	37 g
	Yeast extract	5 g
	L-cysteine	1 g
TY Broth	Tryptone	20 g
	Yeast extract	30 g
Brazier's CCEY Agar	Bioconnections CCEY Agar	48 g
	Egg yolk emulsion	40 ml
	Defibrinated Horse blood	10 ml

Table 2.1.2 *C. difficile* defined medium CDDM

Ingredients	Stock concentration (mg/ml)	Final concentration (mg/ml)
Amino acids (5X)		
Casamino Acids	50	10
L-Tryptophan	2.5	0.5
L-Cysteine	2.5	0.5
Salts (10X)		
Na ₂ HPO ₄	50	5
NaHCO ₃	50	5
KH ₂ PO ₄	9	0.9
NaCl	9	0.9
Glucose (20X)		
D-Glucose	200	10
Trace salts (50X)		
(NH ₄) ₂ SO ₄	2.0	0.04
CaCl ₂ · 2H ₂ O	1.3	0.026
MgCl ₂ · 6H ₂ O	1.0	0.02
MnCl ₂ · 4H ₂ O	0.5	0.01
CoCl ₂ · 6H ₂ O	0.05	0.01
Iron (100X)		
FeSO ₄ · 7H ₂ O	0.4	0.004
Vitamins (100X)		
D-Biotin	0.1	0.001
Calcium-D-pantothenate	0.1	0.001
Pyridoxine	0.1	0.001

2.1.3 Supplements

Supplements	Final concentration
Sodium taurocholate	0.1%
5-fluorocytosine (FC)	0.05 mg/ml
5-fluoro-orotate (FOA)	2 mg/ml
Uracil	5 µg/ml
Antibiotics	Final concentrations
Chloramphenicol	15 µg/ml
Thiamphenicol	15 µg/ml
Cycloserine	250 µg/ml
Kanamycin	50 µg/ml
Ampicillin	100 µg/ml
Lincomycin	20 µg/ml
Erythromycin	500 µg/ml

E. coli strains were grown on LB agar (Merck) and LB broth overnight at 37°C for routine work. Overnight express instant TB medium (Merck), supplemented with 1% (v/v) glycerol, was used to induce protein expression. The cultures were supplemented with appropriate antibiotics: chloramphenicol (15 µg/ml), kanamycin (50 µg/ml), ampicillin (100 µg/ml) and erythromycin (500 µg/ml) (Table 2.1.3).

E. coli NEB5α New England Biolabs (NEB) was used for all cloning procedures. *E. coli* CA434 was used as a donor strain to deliver all plasmid constructs into *C. difficile* by conjugation. *E. coli* Rosetta (Novagen) was used for recombinant protein production. Cultures were normally grown at 37°C with agitation (250 rpm). All strains were frozen in 18.5% Glycerol/LB broth for future work. Strain details are provided in table 2.1.4.

2.1.4 Bacterial strains

<i>C. difficile</i> strains	Details	Source
R20291	Hyper-virulent, epidemic <i>C. difficile</i> strain isolated in UK between 2004–2005, ribotype 027.	Stoke Mandeville United Kingdom
R20291 Δ <i>pyrE</i>	Uracil auxotroph of R20291. Deletion in <i>pyrE</i> gene allowing for genetic manipulation (Allele-Coupled recombination).	(Ng <i>et al.</i> , 2013)
630	The first genomic sequence strain of <i>C. difficile</i> , ribotype 012.	(Sebahia <i>et al.</i> , 2006)
Liv22	Isolated from a human in Liverpool in 2009, ribotype 106.	Brendan Wren
M120	Isolated from a human in UK in 2007, ribotype 078.	Brendan Wren
CDKK-959	Nontoxic strain isolated from asymptomatic carrier in 2008, ribotype 053.	Kieran Kelly
R7404	Isolated from a human in UK in 2003, toxin A-B+, ribotype 017.	S. Ward
Ox247	Toxic strain isolated in UK in 2007, ribotype 005.	Neil Fairweather
TL178	Toxic strain isolated in UK, ribotype 002.	Neil Fairweather
R20291 <i>s/pA</i>	R20291 strain with a spontaneous mutation in <i>s/pA</i> , a bp insertion after nucleotide 282, creating a stop codon. This mutant is resistant to diffocin (Av-D291.2).	(Kirk, <i>et al.</i> , 2016)

R20291 Δ <i>spoVD</i>	R20291 with the entire <i>spoVD</i> gene deleted, except the first and last three codons.	This study
R20291 Δ <i>spoVD</i> <i>pyrE::spoVD</i>	R20291 Δ <i>spoVD</i> complemented by inserting the wild type gene under the native promoter in the <i>pyrE</i> gene locus.	This study
R20291 Δ <i>cwp20</i>	R20291 with the entire <i>cwp20</i> gene deleted, except the first and last three codons.	This study
R20291 Δ <i>cwp20</i> <i>pyrE::cwp20</i>	R20291 Δ <i>cwp20</i> complemented by inserting the wild type gene under the native promoter in the <i>pyrE</i> gene locus.	This study
R20291 <i>slpA</i> <i>cwp20::ermB</i>	Knockout of <i>cwp20</i> in R20291 <i>slpA</i> strain by insertion of a group II intron using Clostron.	This study
R20291 <i>slpA cwp20::ermB</i> / pYAA046	Complementation of R20291 <i>slpA cwp20::ermB</i> by delivering the whole <i>cwp20</i> gene under the constitutive promoter P _{<i>cwp2</i>} (pYAA046).	This study
R20291 <i>CD0398::Tn</i>	Knockout of <i>CD0398</i> by insertion of a mariner-based transposon.	This study
R20291 <i>CD0398::Tn</i> / pYAA074	Complementation of the R20291 <i>CD0398::Tn</i> by delivering the whole <i>CD0399</i> gene under the constitutive promoter P _{<i>cwp2</i>} (pYAA074).	This study
R20291 <i>CD0622::Tn</i>	Knockout of <i>CD0622</i> by insertion of a mariner-based transposon.	This study

R20291 Δ CD0622	R20291 with the entire <i>CD0622</i> gene deleted, except the first and last three codon.	This study
R20291 Δ CD0622/ pYAA072	Complementation of R20291 Δ CD0622 by delivering the whole <i>CD0622</i> gene under the constitutive promoter P_{cwp2} (pYAA072).	This study
R20291 <i>snap-spoVD</i>	Snap tag-encoding DNA was added to 5' end of <i>spoVD</i> in the native locus using homologous recombination.	This study
R20291 <i>nsnap-spoVD</i>	nSnap tag-encoding DNA was added to 5' end of <i>spoVD</i> in the native locus using homologous recombination.	This study
<i>E. coli</i> strains	Details	Source
CA434	<i>E. coli</i> HB101 strain used in conjugation for delivery of plasmids into <i>C. difficile</i> , contains conjugative plasmid R702.	Neil Fairweather
NEB5 α	Commercial <i>E. coli</i> K12 strain used for initial transformation. Genotype: <i>fhuA2</i> Δ (<i>argF-lacZ</i>)U169 <i>phoA glnV44</i> Φ 80 Δ (<i>lacZ</i>)M15 <i>gyrA96 recA1 relA1 endA1 thi-1 hsdR17</i>	New England Biolabs
Rosetta	<i>E. coli</i> Rosetta (Novagen) used to express recombinant proteins. Genotype: F ⁻ <i>ompT hsdS_B</i> (<i>r_B⁻ m_B⁻</i>) <i>gal dcm</i> (DE3) pLacIRARE (Cam ^R).	Novagen
DHM1	<i>E. coli</i> adenylate cyclase deficient (<i>cyo</i>) mutant used in the two hybrid assay.	(Karimova <i>et al.</i> , 2000)

2.2 DNA manipulation

2.2.1 Extraction of gDNA from *C. difficile*

A 5 ml *C. difficile* culture was grown overnight in TY broth. Cultures were centrifuged for 10 min at 4,000 x *g* and the bacterial pellets were frozen. Frozen pellets were thawed, resuspended in lysis buffer (200 mM NaCl, 50 mM EDTA, 20 mM tris-HCl pH 8.0), and incubated with bacteriophage endolysin (1 h at 37°C). The bacteriophage endolysin has been identified as an effective protein against 30 different strains of *C. difficile* including the virulent ribotype 027 strain R20291 (Mayer *et al.*, 2008). The bacteriophage endolysin was purified from *E. coli* strain Rosetta carrying plasmid pHAS042 (Peltier *et al.*, 2015), encoding His tag-CD27L (bacteriophage endolysin). The bacteriophage endolysin hydrolyses bacterial peptidoglycan, leading to cell wall disruption (Fischetti, 2005; Loessner, 2005). Following endolysin treatment the *C. difficile* sample was then treated with 20 mg/ml pronase (Sigma Aldrich) (1 h at 55°C), followed by 10% N-lauroylsarcosine (1 h at 37°C) and finally 0.25 mg/ml RNase (Sigma Aldrich) (1 h at 37°C).

The suspension was transferred to a 1.5 ml heavy phase lock gel (PLG) tube (Scientific Laboratory Supplies). An equal volume of Phenol: Chloroform: Isoamyl alcohol ratio 25:24:1 was added and the mixture centrifuged at 13,000 x *g* for 2 min, taking supernatant, this step was repeated twice. An equal volume of Chloroform: Isoamyl alcohol ratio 24:1 was then added and the mixture centrifuged at 13,000 x *g* for 2 min. The supernatant was transferred to a microfuge tube and DNA precipitated by adding 1 volume of ice-cold isopropanol and incubation overnight at -20°C. DNA was harvested by centrifuging the sample at 15,000 x *g* for 15 min. The pellet was washed with an equal volume of 70% ethanol and centrifuged at 15,000 x *g* for 10 min at 4°C. Ethanol was removed by air-drying the pellet for 5-10 min. The pellet was resuspended in 50 µl nuclease-free water. Quantity and quality of gDNA were checked by NanoDrop and agarose gel electrophoresis.

2.2.2 Crude DNA extraction

Chelex 100 resin (Bio-Rad) was used to extract crude gDNA. Chelex was resuspended in 100 μ l nuclease-free water (50 mg/ml), mixed with a single colony, boiled at 100°C for 10 min and centrifuged at 20,000 x *g* for 10 min. Supernatants were transferred to a new microfuge tube for analysis and screening.

2.2.3 Polymerase chain reaction (PCR)

Colony PCR and routine screening PCR were done using *Taq* polymerase master mix (2x): 100 mM tris, 500 mM KCl, 0.1% gelatin, 0.1% tween20, 20 mM MgCl₂ pH:9.0, 0.2% cresol red, 10 mM dNTPs, 2 mg/ml *Taq*. *Taq* polymerase lacks proofreading activity (3' to 5' exonuclease activity), but accuracy was not necessary for screening. PCR was done in 20 μ l reactions adding 0.1 μ M forward and reverse primers. A PCR programme of the *Taq* polymerase was normally set:

Steps	Temperature	Time	Number Cycles
Initial denaturation	94°C	3 min	1
Denaturation	94°C	30 sec	34
Annealing	58°C	30 sec	
Extension	72°C	1 min per kb	
Final extension	72°C	10 min	1
Hold	12°C	∞	

PCR for amplification of gDNA for cloning or inverse PCR using plasmids as the template, as performed using 2xPhusion high-fidelity PCR master mix (NEB), following the manufacturer's protocol. Briefly, PCR reaction was performed in 50 μ l including 25 μ l Master Mix 0.5 μ M forward, reverse primers and 5% DMSO. PCR programme for Phusion normally consisted of:

Steps	Temperature	Time	Number Cycles
Initial denaturation	98°C	3 min	1
Denaturation	98°C	30 sec	32
Annealing	56°C	30 sec	
Extension	72°C	20-30 sec per kb	
Final extension	72°C	10 min	1
Hold	12°C	∞	

Primers were synthesised by Eurofins (listed in Appendix A1, Table A1).

2.2.4 Agarose gel electrophoresis

Agarose [0.7 - 1% (w/v)] (Invitrogen) in 1 x TAE (40 mM tris acetate, 2 mM Na₂EDTA pH 8.3) was heated to 100°C until the agarose powder was dissolved. SybrSafe (Invitrogen) DNA stain was added at a concentration of 1:100,000, while ethidium bromide was added at a final concentration of 1 µg/ml when the agarose was sufficiently cool. The gel was poured into a gel tray and, once solidified, 1 x TAE was added. DNA samples were prepared by adding 10x DNA loading dye (25 mM tris, 0.125% (w/v) bromophenol blue, 30% (v/v) glycerol, pH 7.6). Electrophoresis was carried out at 130 V for 30 min in 1x TAE buffer. The DNA samples were visualised on a UV transilluminator at 312 nm, and the images recorded on a Bio-Rad documentation system.

2.2.5 DNA purification

PCR products and digests were cleaned up using the GeneJET PCR Purification Kit (Thermo Scientific), following the manufacturer's protocol. Briefly, a 1:1 volume of binding buffer was added and transferred to a DNA-binding column, followed by centrifugation at 10,000 x g for 1 min. The column was washed by adding 700 µl of wash buffer and centrifugation at 10,000 x g for 1 min. Next, the column was centrifuged again at 10,000 x g for 1 min to remove residual wash buffer. The column was placed in a new 1.5 ml microfuge tube and DNA was eluted by adding 20 µl of nuclease-free water. For extraction of DNA from agarose gels, the band was excised and weighed a 1:1 volume of binding buffer and 10 µl of 3 M sodium acetate, pH 5.2 was added. Then the mixture

was incubated at 55°C for 10 min to dissolve the gel, followed by cleaned up steps as described above.

2.2.6 Restriction endonuclease digestion of DNA

Restriction digests were normally carried out using enzymes supplied by New England Biolabs (NEB), following the manufacturer's instructions. Briefly, 1-2 µg of purified DNA was routinely digested by 10-20 U of the restriction enzyme in a suitable NEB buffer, the reaction was incubated at 37°C for 2 h. Double digestions were carried out using the recommended buffer for both restrictions enzymes or in a buffer that allows 100% activity for both restrictions enzymes. Otherwise, the reactions were carried out sequentially.

2.2.7 Plasmid purification

Plasmid DNA was routinely extracted from *E. coli* using QIAprep Spin Miniprep Kit (Qiagen), following the manufacturer's instructions. Briefly, 5 ml of overnight culture was centrifuged at 4,000 x *g* for 10 min and the bacterial pellets were re-suspended in 250 µl buffer P1. Next, buffer P2 was added (250 µl), and the sample was incubated for 5 min after gentle mixing 350 µl buffer N3 was then added to the sample, mixed gently and centrifuged at 20,000 x *g* for 5 min. The supernatant was transferred to a QIAprep column and centrifuged at 20,000 x *g* for 1 min. The column was then washed twice with 500 µl wash buffer. Next, the column was centrifuged again at 10,000 x *g* for 1 min. The column was placed in a new 1.5 ml microfuge tube and plasmid DNA was finally eluted by adding 60 µl of nuclease-free water and centrifugation at 20,000 x *g* for 1 min. The plasmids generated in this project are listed in Appendix A, Table A2.

2.2.8 DNA Ligation

DNA ligation was carried out using T4 DNA Ligase (NEB) or Quick Stick ligase (Bioline), following the manufacturer's protocols. Briefly, 25 ng of plasmid DNA was mixed with a three-fold molar excess of insert (PCR product), and either 1 µl 10x buffer and 0.5 µl T4 Ligase or 2.5 µl of 4x quick stick buffer and 0.5 µl Quick-Stick Ligase. Reactions were made up to a final volume of 10 µl by adding nuclease-free water. Reactions were incubated for 2 h or 15 min at room temperature respectively.

2.3.1 DNA cloning

Cloning work was carried out using three different methods to construct new plasmids.

2.3.2 Cloning after restriction enzymes digestion

Firstly, primers were designed to amplify a gene of interest, adding restriction sites sequences. Subsequently, the PCR reaction was performed with these primers. Once the PCR product was obtained, both the plasmid DNA and the PCR product were digested with appropriate restriction enzymes. The digestion was carried out at 37°C for 2 h as described in 2.2.6. Next, both the digestions were cleaned up using the GeneJET PCR Purification Kit (Thermo scientific) as described in 2.2.5, followed by ligation using Quick-Stick Ligase (Bioline) or T4 DNA Ligase (NEB) as described in 2.4.8. The ligation product (2 µl) was transformed into competent NEB 5-alpha *E. coli* (NEB), as described in 2.4.1.

2.3.3 Cloning by inverse PCR

In order to delete or add DNA sequences to an existent plasmid, inverse PCR was used using divergent primers flanking the area of interest and the plasmid was linearized using Phusion PCR. The template was digested by adding 20 U *DpnI* (NEB) and incubating at 37°C for 2 h. Then the product was purified and eluted in 20 µl of nuclease-free water as described in 2.2.5. Next, the DNA fragment was phosphorylated using T4 polynucleotide kinase (NEB) at 37°C for 30 min; the reaction included 20 µl eluted DNA product, 3 µl PNK buffer (10x stock), 3 µl of ATP (10 mM) and 1 µl PNK enzyme. The reaction was completed to a final volume of 30 µl by adding nuclease-free water. After 30 min the DNA was again purified and eluted in 20 µl nuclease-free water as described in 2.2.5. Next the concentration was measured using a nanodrop and 50 ng of the eluted product was ligated using Quick Stick ligase (Bioline) for 15 min or the T4 ligase for 2 h at room temperature as described 2.2.8. The ligation product (2 µl) was transformed into competent NEB 5-alpha *E. coli* (NEB), as described in 2.4.1.

2.3.4 Gibson assembly

Gibson assembly was used as the quickest way to clone 2 to 6 fragments of DNA in one reaction without adding extra DNA such as the restriction site sequences.

NEbuilder (<http://nebuilder.neb.com>) was used to design primers, adding complementary overhangs to join DNA fragment to each other and the plasmid. The plasmid to be cloned into was linearized using inverse PCR with divergent primers (Appendix A1, Table A1). Next, the template of the linearized plasmid was digested with 20 U *DpnI* (NEB) incubated at 37°C for 2 h. Subsequently, PCR products were purified and eluted in 20 µl of nuclease-free water as described in 2.2.5. These PCR products were used in Gibson Assembly reactions (NEB), following the manufacturer's protocol. Briefly, 25 ng of plasmid DNA was mixed with a three-fold molar excess of each insert, 5 µl of HiFi DNA Assembly Master Mix, and the reaction was brought to a final volume of 10 µl with nuclease-free water. Next, the sample was incubated at 50°C for 30 min, followed by transformation of 4 µl of the assembled product into competent NEB 5-alpha *E. coli* (NEB), as described 2.4.1. SOEing PCR (Ho *et al.*, 1989) was also used to join PCR products for use in some cloning experiments. SOEing PCR products were also purified and eluted in 20 µl of nuclease-free water as described in 2.2.5.

2.4 Production of Chemically-competent *E. coli*

E. coli CA434 or Top10 was cultured overnight in LB broth at 37°C. Next day, the culture OD was measured, sub-cultured in 250 ml LB broth to an OD_{600nm} of 0.01 and grown at 37°C to an approximate OD_{600nm} of 0.6. The culture was then centrifuged at 4,000 x *g* for 10 min at 4°C. The pellet was resuspended in 5 ml ice-cold 100 mM CaCl₂ and incubated on ice for 15 min. The cells were harvested at 4,000 x *g* for 10 min at 4°C, and re-suspended in ice-cold 1 ml CaCl₂, 15% glycerol (v/v) and incubated on ice for 2 h. After 2 h, the bacterial suspensions were aliquoted (50 µl) in chilled microfuge tubes and frozen at -80°C. For production of competent *E. coli* DHMI, the bacteria were first grown on LB agar supplemented with X-Gal/IPTG overnight at 37 °C to avoid blue colonies A single white colony was picked for culturing overnight. DHMI commonly displays problematic reversion of the *cyaA* mutation. Competent cell were then prepared as before.

2.4.1 Transformation

Transformation was normally carried out using commercial NEB 5-alpha competent *E. coli* (NEB), following the manufacturer's protocol. Briefly, 2-4 µl of ligated

DNA was transferred to 25 µl aliquots of chemically competent cell and incubated on ice for 30 min. After 30 min the cells were heat-shocked at 42°C for 30 sec and followed by incubation on ice for 5 min. 0.5 ml of pre-warmed SOC broth was then added and incubated at 37°C for 1 h. After 1 h incubation the sample was spread on LB agar supplemented with the suitable antibiotic. These steps were carried out similarly with homemade competent cells such as Top10, CA434 and DHM1 cells.

2.5 Plasmid transfer into *C. difficile*

The conjugation process between *C. difficile* and *E. coli* CA434 was carried out in two different ways:

Firstly, plasmids were delivered into *C. difficile* by conjugation from *E. coli* CA434 as described previously (Cartman and Minton, 2010) with some modifications. Briefly, *C. difficile* (5 ml TY broth), and CA434 (10 ml LB broth with 15 µg/ml chloramphenicol) were grown overnight. The following day, the OD_{600nm} was measured for both *C. difficile* and CA434. Subcultures were set up to an OD_{600nm} of 0.05 in 10 ml pre-reduced TY broth for the *C. difficile*, and to an OD_{600nm} of 0.01 in 10 ml LB broth with 15 µg/ml chloramphenicol for CA434. After 3 h incubation at 37°C (approx. OD₆₀₀ of 0.5 for *C. difficile* and 0.1 for *E. coli*), the *E. coli* were harvested at 4,000 × *g* for 2 min. The supernatant was discarded and the pellet was resuspended in PBS buffer and centrifuged at 4,000 × *g* for 2 min, this step was repeated. The CA434 pellet was transferred to an anaerobic cabinet and resuspended gently in 400 µl *C. difficile*. The mixture was spotted (20 µl spots) onto pre-reduced Brazier's (CCEY) or BHI agar. The plates were incubated overnight in anaerobic conditions at 37°C. After 24 h of incubation, the spots were harvested with 1 ml reduced TY Broth. This suspension was spread onto several BHI agar plates containing 15 µg/ml thiamphenicol and 250 µg/ml cycloserine and incubated overnight.

Secondly, plasmids were delivered into *C. difficile* from *E. coli* CA434 as described recently (Kirk and Fagan, 2016). Briefly, overnight cultures of *C. difficile* (5 ml TY broth) and *E. coli* CA434 (5 ml LB broth supplement with 15 µg/ml chloramphenicol) were prepared. The following day, 200 µl of the overnight *C. difficile* culture was heated at

50°C for 15 min and then cooled to 37°C for 2 min. 1 ml of the *E. coli* CA434 culture was harvested at 4,000 × *g* for 2 min. The pellet of CA434 was transferred to an anaerobic cabinet and resuspended gently in 200 µl *C. difficile* that had been heated. The mixture was spotted (20 µl spots) onto pre-reduced BHI. The plates were incubated overnight in anaerobic conditions at 37°C. After, 24 h incubation, the spots were harvested in 1 ml reduced TY broth. This suspension was spread onto several BHI agar plates containing 15 µg/ml thiamphenicol and 250 µg/ml cycloserine and incubated overnight.

2.6 Homologous recombination

Homologous recombination was carried out to delete genes of interest in *C. difficile* using two different systems.

Firstly, in order to generate allele coupled exchange (ACE) mutants. *C. difficile* R20291Δ*pyrE* was used as the host strain as previously described (Ng *et al.*, 2013). Briefly, 650 bp downstream and upstream of the targeted gene was amplified and cloned into pMTL-YN4 using SOEing PCR and restriction ligation as described in 2.3.2 and 2.3.4. The primers were designed using NEbuilder (<http://nebuilder.neb.com>) and *Bam*HI and *Sac*I restriction sites were added to the external primers. The plasmids were introduced into *C. difficile* R20291Δ*pyrE* as described in 2.5. A single *C. difficile* transconjugant was re-streaked twice on BHI agar supplemented with 5 µg/ml uracil, 15 µg/ml thiamphenicol and 250 µg/ml cycloserine. The transconjugant colonies grow slowly due to segregational instability of the origin of replication. Recombination with the chromosome overcomes the segregational instability and results in faster-growing colonies. Colonies that displayed faster growth were restreaked twice to purity on BHI supplemented with 5 µg/ml uracil, 15 µg/ml thiamphenicol and 250 µg/ml cycloserine. Crossover between plasmid and chromosome was confirmed using PCR with two different primers, one of them annealed to the chromosome and the second annealed to the plasmid. Subsequently, to isolate double crossovers, single crossover colonies were re-streaked on *C. difficile* minimal medium (CDDM) supplemented with 2 mg/ml 5-fluoroorotic acid (FOA) and 5 µg/ml uracil to select for plasmid loss. After 48 h incubation at 37°C, colonies were replica plated on non-selective BHI agar and BHI agar

supplemented 15 µg/ml thiamphenicol to confirm the plasmid loss (thiamphenicol sensitivity), and screened using PCR with two chromosomal primers to distinguish double-crossover mutants from wild-type R20291. PCR products were sequenced to confirm the mutant genotype. The mutant strain was frozen for future work in 18.5% Glycerol/TY broth at -80. Note, these mutants also have a deletion in the *pyrE* gene. See section 2.7.1.

Secondly, the CodA system was also used to create mutants and to insert SNAP or nSNAP tag sequences in-frame under the native promoter of the targeted gene. *C. difficile* R20291 was used as the parental strain for deletion of target gene as previously described (Cartman *et al.*, 2012). Briefly, for gene deletions, 1200 bp downstream and upstream of the targeted gene was amplified and cloned into pMTL-SC7215 using Gibson Assembly as described in 2.3.4. For insertion of SNAP or nSNAP the coding sequence of the tag was included between 1200 bp homology arms. The plasmids were introduced into *C. difficile* R20291 as described in 2.5. A single *C. difficile* transconjugant was re-streaked twice on BHI agar supplemented with 15 µg/ml thiamphenicol and 250 µg/ml cycloserine. The transconjugant colonies grow slowly due to segregational instability of the origin of replication (the same principle as the *pyrE* system). Colonies displaying faster growth were restreaked twice to purity on BHI supplemented with 15 µg/ml thiamphenicol and 250 µg/ml cycloserine. Crossover between plasmid and chromosome was confirmed using PCR with two different primers, one annealing on the chromosome and the second annealing on the plasmid. Single crossover colonies were restreaked on non-selective BHI agar incubated at 37°C for 24 h to allow plasmid loss. All growth was then harvested in 1 ml pre-reduced TY broth, diluted 10⁻¹ to 10⁻⁶, and spread onto *C. difficile* minimal media (CDMM) supplemented with 50 µg/ml FC to select for plasmid loss. After, 96 h incubation at 37°C, the colonies were replica plated on non-selective BHI agar and BHI agar supplemented 15 µg/ml thiamphenicol to confirm plasmid loss (thiamphenicol sensitivity), and screened by using PCR with two chromosomal primers to distinguish double-crossover mutants from wild-type R20291. PCR products were sequenced to confirm the mutant genotype. The mutant strain was frozen for future work in 18.5% Glycerol/TY broth at -80.

2.7 Complementation and restoration of the *pyrE* gene in R20291

2.7.1 Restoration of the *pyrE* gene in mutant strains

To restore the *pyrE*⁺ phenotype in the mutant strains, the pMTL-YN2 plasmid was delivered to the mutant strains as described in 2.5. Transconjugant colonies were re-streaked twice to purity onto BHI-supplemented with 15 µg/ml thiamphenicol, 250 µg/ml cycloserine and 5 µg/ml uracil. Then re-streaked on BHI-supplemented with thiamphenicol alone to identify pyrimidine prototrophs. Subsequently, large colonies (putative prototrophs) were re-streaked onto CDMM agar to ensure the plasmid loss and then selected for uracil prototrophy, which indicated the successful allele recombination. *pyrE* gene restoration was confirmed by PCR screening using two primers (RF295 and RF297) that flank the *pyrE* gene locus. PCR products were sequenced to confirm *pyrE* restoration in the mutant strains. The mutant strains were frozen for future work in 18.5% Glycerol/TY broth at -80.

2.7.2 Mutant strain complementation

The *spoVD* gene and its native promoter was amplified by PCR using primers RF323 and RF324 and cloned between *SacI* and *BamHI* in pMTL-YN2C. The *cwp20* gene and its native promoter was amplified by PCR using primers RF298 and RF299 and cloned between *EcoRI* and *BamHI* in pMTL-YN2C.

Plasmids were conjugated into R20291Δ*spoVD* or R20291Δ*cwp20* as described in 2.5. Transconjugant colonies were re-streaked twice to purity onto BHI-supplemented with 15 µg/ml thiamphenicol, 250 µg/ml cycloserine and 5 µg/ml uracil. Then re-streaked on BHI-supplemented with thiamphenicol alone to identify pyrimidine prototrophs. Subsequently, large colony (putative prototrophs) were re-streaked onto CDMM agar to ensure the plasmid loss and then selected for uracil prototrophy, which indicated the successful allele recombination. *pyrE* gene restoration and gene complementation were confirmed by PCR screening using two primers (RF295 and RF297) that flank the *pyrE* gene locus to distinguish between the wild type and complementation strains. PCR products were sent for Sanger sequencing to confirm the complementation genotype. The complementation strains were frozen for future work in 18.5% Glycerol/TY broth at -80.

2.8 Clostron insertional mutagenesis

The Clostron system was used to knock out *cwp20* in R20291*slpA*. The intron target site in *cwp20* was identified using the Perutka algorithm <http://www.clostron.com>. (Heap *et al.*, 2007). The retargeted plasmid was synthesised by DNA 2.0. This plasmid was transformed into *E. coli* CA434 as described in 2.4, and then transferred into R20291*slpA* by conjugation as described in 2.5. Transconjugant colonies were restreaked twice onto BHI supplemented with cycloserine (250 µg/ml) and thiamphenicol (15 µg/ml). Intron insertion was selected on BHI supplemented with lincomycin (20 µg/ml). Colony PCR was used to screen mutants using: (1) primers flanking the *erm^R* cassette, (2) primers flanking the *cwp20* gene, (3) two primers that annealed to the *cwp20* gene and the intron insertion.

2.9 Southern blotting

1.2 µg of gDNA was digested with *BsrGI* for 1 h at 37°C in a total volume of 30 µl and then separated on a 1% agarose gel at 100 V. The gel was incubated in denaturing buffer (1.5 M NaCl, 0.5 M NaOH) for 30 min to denature the DNA, then rinsed with water. Subsequently, the DNA was neutralised by incubation in neutralising buffer (1.5 M NaCl, 1 M tris-HCl, pH 7.4) for 15 min, twice, then rinsed with water. Next, DNA was transferred by capillary blotting to Biodyne B nylon membrane using the following stack:

1-Two pieces of Whatman 3 MM filter paper were soaked in 20x SSC buffer (3 M NaCl, 300 mM sodium citrate, pH 7.0) and placed in a plastic tray pre- immersed in 20x SSC buffer.

2-The gel was placed on top and covered by a piece of Biodyne B nylon membrane.

3- Another two pieces of Whatman 3 MM filter paper pre-soaked in 20x SSC buffer (3 M NaCl, 300 mM sodium citrate, pH 7.0) were added.

4- A 5 cm stack of tissue paper and a 750 g weight was placed on top and the stack left to transfer overnight at room temperature.

The following day, the stack was disassembled and the membrane was dried, then cross-linked for 30 sec using a UV Stratalinker [UV 312 nm at 70 mJ cm⁻² (Stratagene)]. Subsequently, the membrane was incubated with 10 ml pre-warmed hybridization buffer containing a probe, a PCR product labelled using the AlkPhos Direct

Labelling and Detection System (Pierce) according to the manufacturer's instructions. The labelled probe was complementary to the promoter region of targeted genes. The membrane was then incubated with mixing overnight at 42°C for hybridization. The following day, the membrane was washed twice (2 M urea, 0.1% SDS, 150 mM NaCl, 0.2% blocking reagent, 1 mM MgCl₂, 50 mM Na₂HPO₄) for 10 min at 55°C. The labelled DNA was visualised following addition of ECL solution (Clarity of Western ECL Blotting Substrates), and incubation for 5 min at room temperature, then imaging on a ChemiDoc MP System (Bio-Rad).

2.10 Determination of antibiotic minimum inhibitory concentrations [MICs]

Antibiotic MICs were determined in two different ways:

Firstly, MICs were determined as described previously (Stabler *et al.*, 2009) using Etest strips (Biomérieux, Marcy'l'Etoile, France). *C. difficile* was cultured overnight in 5 ml pre-reduced TY broth. The following day, a subculture was grown to an OD_{600nm} of approx. 0.5 in 10 ml pre-reduced TY and spread onto pre-reduced Brazier's CCEY agar plates (Bioconnections) supplemented with egg yolk emulsion (Oxoid) and defibrinated horse blood (Oxoid), using a sterile cotton swab. The plates were then dried for 20 to 30 min. Etest strips were placed onto the plates and incubated in the anaerobic cabinet at 37°C for 48 h. The MICs of antibiotics were determined following the manufacturer's instructions.

Secondly, MICs were determined using the agar dilution method from the laboratory standard institute guidelines [Clinical and laboratory standard institute, 2012]. Briefly, agar plates were prepared with a range of different concentrations of each antibiotic (2 µg/ml to 1024 µg/ml) using BHI supplemented with defibrinated horse blood (Oxoid) or Brazier's CCEY agar plates (Bioconnections) supplemented with egg yolk emulsion (Oxoid) and defibrinated horse blood (Oxoid). The plates were dried at room temperature for 2 h and then pre-reduced in the anaerobic cabinet workstation for 2 h. 100 µl of each *C. difficile* strain at an OD_{600nm} of 0.5 was spread onto the plates using a plastic spreader. The plates were incubated for 48 h in the anaerobic cabinet

workstation at (37°C). The MICs were determined by reading the lowest concentration on which the bacteria did not grow.

2.11 Protein labelling with Bocillin-FL

Purified proteins were used for labelling with fluorescent Bocillin FL as described previously by (Zhao *et al.*, 1999). Reaction mixtures contained 0.5 µg of protein, 50 µM Bocillin-FC in a reaction volume of 20 µl in PBS buffer. Reaction mixtures were incubated at 37°C for 30 min and denatured with 20 µl 2x SDS loading buffer (see section 2.15.3) at 100°C for 5 min (Laemmli, 1970). Next, 15 µl of each sample was loaded on a 10-12% polyacrylamide gel and separated. After electrophoresis the gels were rinsed immediately with MilliQ water and labelled proteins were visualized using imaging on a ChemiDoc MP System (Bio-Rad) (excitation at 494 nm and emission at 521 nm, Cy3 filter). Subsequently, the gel was stained with coomassie brilliant blue, to visualize protein loading.

2.12 β-lactamases assay

β-lactamase activity was tested using nitrocefin chromogenic substrate as described previously (O'Callaghan *et al.*, 1972). Nitrocefin stock solution at 1 mM was made in PBS. Reaction mixtures contained 1.7 µM of purified protein, 100 µM nitrocefin in a reaction volume of 100 µl in PBS buffer. Reactions were carried out in triplicate. The change of the absorbance was measured immediately at 490 nm using a Microplate reader (VICTOR X3 Multilabel Plate Reader- Pekin Elmer).

In order to identify the β-lactamases class, each purified protein was tested in the presence of clavulanic acid or EDTA. Proteins were incubated with inhibitors at different concentrations (0.01 mM to 20 mM) at 37°C for 30 min and nitrocefin was then added to the reaction at 100 µM in 100 µl. The change of the absorbance was measured immediately at 490 nm using a Microplate reader (VICTOR X3 Multilabel Plate Reader- Pekin Elmer).

2.12.1 Active site titration

The acylation assay was carried out as previously described (Bauvois *et al.*, 2005). Briefly, ceftazidime was used as an inhibitor for protein binding. 1 μ M protein was preincubated with ceftazidime at one, two and three-fold excess, for 2 h at 37°C to complete the acylation process, followed by addition of Bocillin-FL at (50 μ M) and incubation for 30 min at 37°C. The samples were mixed with 20 μ l 2x SDS loading buffer and heated at 100°C for 5 min (Laemmli, 1970). Next, 15 μ l of each sample was loaded on a 10-12% polyacrylamide gel and separated. After electrophoresis the gels were rinsed immediately with MilliQ water and labelled proteins were visualized using imaging on a ChemiDoc MP System (Bio-Rad) (excitation at 494 nm and emission at 521 nm, Cy3 filter). Subsequently, the gel was stained with coomassie brilliant blue, to visualize protein loading.

2.13 Phenotypic assays

2.13.1 Sporulation efficiency

Overnight cultures of *C. difficile* R20291 were diluted in BHI broth to an OD_{600nm} of 0.01 and incubated for 8 h, followed by dilution of the culture in BHI broth to an OD_{600nm} of 0.0001 and incubation overnight. This allowed to obtain cultures in stationary phase with no spores (T=0). This culture was then incubated for 5 days in the anaerobic cabinet at 37°C. 10-fold serial dilutions were made and 10 μ l drops were spotted onto BHIS agar supplemented with 0.1% sodium taurocholate (total cell counts). While, for total spore counts, the culture was incubated at 65°C for 30 min, followed by dilution and spotting 10 μ l drops onto BHIS agar supplemented with 0.1% sodium taurocholate. This killed the vegetative cells and left the spores to germinate. After 24 h incubation at 37°C, the number of total cells (CFUs) and spores (CFUs) in the culture were enumerated. The assay was completed in triplicate. The whole experiment was monitored via phase-contrast microscopy to visualise spore maturation. At each time point 250 μ l of culture was taken and centrifuged at 8,000 x *g* for 1 min. The pellet was washed with 1 ml PBS, centrifuged again at 8,000 x *g* for 1 min and then re-suspend in 500 μ l fresh 3.7% paraformaldehyde (PFA) in PBS. Subsequently, the sample was incubated for 30 min at room temperature on a rotating wheel. After 30 min the sample was centrifuged at

8,000 x *g* for 1 min and re-suspended in 500 µl of MilliQ water and centrifuged at 8,000 x *g* for 1 min, this was repeated three times. Then the sample was re-suspended in 500 µl of MilliQ water and 5-20 µl was dried on a glass slide, followed by a drop of 80% (v/v) glycerol and covered by a cover slip. The samples were imaged under phase contrast using the Nikon Brightfield system. Images were recorded and visualised using Fiji – ImageJ.

2.13.2. Spore chemical resistance assay

C. difficile sporulating cultures at 120 h were re-suspended in 70% EtOH, or lysozyme solution (250 µg/ml), to an OD_{600nm} of 0.1 and incubated at 37°C for 30 min. Subsequently, 10-fold serial dilutions were made and 10 µl drops were spotted onto BHIS agar supplemented with 0.1% sodium taurocholate. The number of the colonies were counted after 24 h incubation in the anaerobic cabinet at 37°C. Furthermore, the *C. difficile* culture at 120 h was incubated at 55°C, a lower temperature than the normal 65°C, for 30 min. 10-fold serial dilutions were made and 10 µl drops were spotted onto BHIS agar supplemented with 0.1% sodium taurocholate. Both assays were carried out in triplicate of three biological repeats. The number of the colonies were counted after 24 h of incubation.

2.14. Expression and purification of recombinant proteins

2.14.1 Growth and protein expression

E. coli strain Rosetta was used to over express genes of interest. Bacteria were grown in 200 ml of overnight express instant TB broth (Merck) at 37°C for 24 h with agitation (250 rpm). After 24 h the OD_{600nm} was checked and the culture was harvested at 4,000 x *g* for 15 min at 4°C and frozen at -20°C.

2.14.2 Protein solubility

Protein solubility was checked by harvesting 1 ml of un-induced (LB broth) and induced (overnight instant TB broth) cultures harboring the plasmid encoding the gene of interest. Cultures were supplemented with 50 µg/ml kanamycin or 100 µg/ml ampicillin and 1% glycerol (v/v). Pellets were re-suspended to an OD_{600nm} of 20 in 0.3 M NaCl, 0.05 M tris-HCl pH: 8.00, 0.02 M imidazole, containing: 1/10 BugBuster (Novagen)

(100 µl BugBuster for 1 ml cultures), 1/100 DNAase (10 µl 4 mg/ml DNAase for 1 ml culture) and 1/100 lysozyme (10 µl 50 mg/ml lysozyme for 1 ml culture). The mixture was incubated at room temperature for 30 min. The lysate was centrifuged at 20,000 x *g* for 2 min to separate the soluble and insoluble protein fractions. 40 µl of soluble fraction was mixed with 40 µl 2x SDS loading buffer (Laemmli, 1970), while the insoluble material was re-suspended to an OD_{600nm} of 10 in 1x SDS loading buffer including 10% SDS for resolubilization of the inclusion bodies. Subsequently, 15 µl of each fraction was loaded on a 10-12% SDS polyacrylamide gel and separated. After electrophoresis the gel was stained with coomassie brilliant blue. Protein solubility was confirmed by comparing the soluble and insoluble fractions of the overnight expression with the LB broth sample.

2.14.3 Protein purification

Frozen pellets of *E. coli* expressing the target gene were thawed in binding buffer (0.3 M NaCl, 0.05 M tris-HCl pH: 8.00, 0.02 M imidazole), containing: 1/10 BugBuster (100 µl BugBuster for 1 ml cultures), 1/100 DNAase (10 µl 4 mg/ml DNAase for 1 ml culture) and 1/100 lysozyme (10 µl 50 mg/ml lysozyme for 1 ml culture). The mixture was incubated at room temperature for 30 min. The lysate was centrifuged at 20,000 x *g* for 2 min. The supernatant containing the soluble protein was taken. Following filtration (0.22 µm), the soluble fraction was run on a HisTrap HP 1 ml column. The protein was eluted against a gradient to 0.3 M NaCl, 0.05 M tris-HCl, pH: 8.00, 0.5 M imidazole. 10 µl from each fraction was loaded on 10-12% SDS-PAGE and the gel was stained with coomassie brilliant blue. The gel was scanned using an Epson Perfection V750 Pro scanner using SilverFast software.

2.14.4 Dialysis of purified proteins

All proteins were dialysed using Slide-A-Lyzer dialysis cassettes (Thermo Scientific) (10,000 MWCO). Cassettes contained 3 ml of purified protein and were equilibrated against 2 l pre-chilled 25 mM tris-HCl pH:8, 50 mM NaCl for 6 h at 4°C. Three changes of the buffer were performed. The resulting sample was concentrated using an Amicon Centrifugal spin column with an appropriate MWCO (10,000-50,000). Then the concentrated protein was aliquoted in 200 µl and frozen at -20°C.

2.14.5 Protein concentration determination

The Bradford assay (Bradford,1976) was used to measure concentration of soluble protein. The Bio-Rad reagent (Biorad Inc, USA) was used in this assay. 200 µl of Bio-Rad Reagent, 800 µl of MilliQ water and 20 µl of soluble protein were mixed in a 1 ml cuvette. Next, the absorbance was measured at OD₅₉₅ nm and the concentration was determined using the following formula: OD₅₉₅ X 15/ volume of protein (µl) = mg protein. Otherwise, the 280 nm was used to estimate the protein concentration.

2.14.6 Mass spectrometry

Mass spectrometry was carried out by Dr Adelina Acosta Martin in the Biological Mass Spectrometry Facility (BioMics), University of Sheffield. Analysis was performed on an Agilent Technologies 6530 Accurate-Mass Q-TOF LC/MS instrument. Single MS spectra (between 1,000 to 90,000 m/z) were performed at a rate of 1 Hz. Calibration was carried out using protonated ionization spectroscopy between 400 to 2200 m/z. The spectra were applied on the positive mode including the parameter set: gas temperature: 350°C, capillary: 6.764 µA, TOF vac: 2.52E-07 torr, drying gas: 11.01 liter/min and nebulizer gas: 45 psi. The charge/mass was deconvoluted using Agilent MassHunter Qualitative Analysis B.06.00 software. Charge deconvolution showed the precise protein mass, which was matched also with analysis of MS-Product (<http://prospector.ucsf.edu/>).

2.14.7 Protein-Protein interactions

Protein-protein interaction studies were carried out in two different ways:

Firstly, Bacterial two hybrid (BACTH) was carried out to study the SpoVD-SpoVE interaction as described previously (Karimova *et al.*, 1998). Briefly, the *spoVD* gene was cloned in frame with T18 at either the N or C terminus, using *Bam*HI and *Sac*I restriction sites in pUT18 or pUT18C, whereas the *spoVE* gene was cloned in frame with T25 at either the N or C terminus using *Bam*HI and *Kpn*I restriction sites in pKT25 or pKNT25. The plasmids were transformed individually and in pairs into *E. coli* DHM1. The empty vectors were also transformed individually as negative controls. pUT18-zip and pKT25-zip were co-transformed as positive controls for the complementation. Those plasmids

express both the T18 and T25 fragments fused to leucine zipper motifs that interact with high affinity (Karimova *et al.*, 1998). Subsequently, the transformed strains were cultured on LB agar supplemented with the chromogenic substrate X-Gal (5-bromo-4-chloro-3-indolyl-B-D-galactopyranoside, 40 µg/ml), IPTG (Isopropyl β-D-1-thiogalactopyranoside, 0.5 mM) and kanamycin (50 µg/ml) or ampicillin (100 µg/ml) and the plates were incubated at 30°C.

The BACTH assay is based on the catalytic activity of the CyaA protein of *Bordetella pertussis*, which has two domains (T18 and T25) allowing synthesis of cAMP. cAMP binds to the CAP protein, which is a catabolite activator. The complex (cAMP/CAP) is responsible for regulation of transcription of many genes, including *lac* and *mal*, that are responsible for lactose and maltose utilisation. Therefore, the bacteria are able to utilize the sugars (lactose or maltose) as sole carbon source (Karimova *et al.*, 1998). In addition, the cAMP/CAP complex is able to control expression of the *lacZ* gene that encodes β-galactosidase, which can hydrolyse X-Gal. Once the β-galactosidase hydrolyses X-Gal the *E. coli* colonies become blue (Ullmann and Danchin, 1983; Miller, 1992).

Secondly, we performed split-SNAP experiments to demonstrate the interaction between the SpoVD and SpoVE proteins in *C. difficile*. The SNAP tag is a 20 kDa protein, (O6-alkylguanine-DNA alkyltransferase hAGT) (Keppler *et al.*, 2003). The split SNAP tag works in a similar way to the CyaA T18 and T25 domains, with physical co-localization of the two halves necessary for SNAP function (Mie *et al.*, 2012). nSNAP, which includes residues between 1-91, was fused to *spoVD* under the native promoter by homologous recombination (*codA* system) as described in 2.6. The resulting strain was designated R20291 *nsnap-spoVD*. Subsequently, cSNAP was cloned, which includes residues 92-182 into pRPF144 under the control of the constitutive P_{cwp2} promoter, yielding pAMBL008 and pAMBL009 plasmids. These plasmids were used to clone the *spoVE* gene in frame with cSNAP at either the N or C terminus using *BamHI* and *XhoI* or *SacI* and *XhoI* restriction sites. The resulting plasmids were pYAA054 and pYAA055 respectively. These plasmids were conjugated into strain R20291 *nsnap-spoVD*. The resulting strains were R20291 *nsnap-spoVD+csnap-spoVE* and R20291 *nsnap-spoVD+spoVE-csnap*. The empty plasmid, carrying *csnap* expressed under the control of constitutive promoter P_{cwp2} was

also conjugated into the strain R20291 *nsnap-spoVD* as a negative control. The resulting strain was R20291 *nsnap-spoVD+csnap*.

Subsequently, the strains were grown in pre-reduced TY and sampled at different time points: in exponential phase, after 24 h and 48 h. 1 ml of each sample was labelled with TMR-Star (NEB) at 37°C for 1 h at a final concentration of 250 nM. Next, the samples were centrifuged and washed twice with PBS, and then re-suspended in 0.5 ml 3.7% formaldehyde in PBS and mixed for 30 min at room temperature. Subsequently, the sample was centrifuged at 8,000 x *g* for 1 min and washed three times with MilliQ water, and re-suspended in 0.5 ml MilliQ water. 5-20 μ l was dried on a glass slide, followed by a drop of 80% (v/v) glycerol and a cover slip. The cells were imaged by fluorescence microscopy (Red TX filter) using the Nikon Brightfield system. Images were recorded and visualised using Fiji – ImageJ.

2.14.8 β -Galactosidase activity assay

In order to measure the efficiency of two hybrid complementation (T18-*spoVD*-T25-*spoVE*), β -galactosidase was quantified. 4-methylumbelliferyl β -D-galactopyranoside (MUG), (Sigma) was used as a substrate to measure the hydrolysis activity. Briefly, cultures at 30°C of *E. coli* DHMI harboring the plasmids expressing T18-*spoVD* and T25-*spoVE* and the controls were sub-cultured to an OD_{600nm} of 0.01 and grown at 37°C to an OD_{600nm} of 0.6. The cultures were then induced with 0.5 mM IPTG and incubated at 30°C for 3 h. 1 ml of each culture was centrifuged at 20,000 x *g* for 1 min, and the pellets were frozen at -20°C. Next day, the pellets were thawed and re-suspended in 0.5 ml ABT buffer (60 mM K₂HPO₄, 40 mM KHPO₄, 100 mM NaCl pH: 7, 1% Triton X-100), 50 μ l chloroform and 25 μ l 1% SDS was added and the sample was incubated at 28°C for 5 min. Subsequently, the samples were centrifuged at 20,000 x *g* for 10 min to remove the cell debris. Next, the reaction mixture (100 μ l supernatant, 80 μ l ABT buffer and 20 μ l of 0.4 mg/ml MUG substrate) was placed in a black 96-well plate and incubated in the dark for 1 h at 25°C. After 1 h incubation three different controls were added to the 96-well plate:

1- The background control was performed by adding 180 μ l ABT buffer to 20 μ l of the MUG substrate (0.4 mg/ml).

2-A serial dilution (total volume 200 μ l) from 10^{-2} to 10^{-7} was made from a stock (20 μ M) of the standard solution (4-methylumbilliferone, Sigma).

3- A negative control was performed by adding 200 μ l of the ABT buffer.

Next, the plate was placed in a microplate fluorescence reader (VICTOR X3 Multilabel Plate Reader- Pekin Elmer) and analysed using an excitation wavelength of 336 nm and an emission wavelength of 445 nm. β -galactosidase enzyme activity was normalised to OD_{600nm}. The experiment was carried out in triplicate of three biological repeats. The assay was performed with all plasmid combinations of *spoVD* and *spoVE* genes, with empty vectors as negative control, and the pUT18-*zip* and pKT25-*zip* plasmids as positive controls.

2.15 Protein characterisation

2.15.1 S-layer extraction

S-layer proteins were extracted using low pH glycine incubation as described (Wright *et al.*, 2005). Briefly, 5-50 ml of mid-log cultures of *C. difficile* (OD_{600nm} of 0.5-0.8) were centrifuged at 4,000 x *g*, for 10 min at 4°C. The pellet was re-suspended in 0.5-1 ml PBS, then centrifuged at 20,000 x *g* for 2 min and re-suspended to an OD_{600nm} of 20 in 0.2 M glycine pH 2.2. The sample was incubated at room temperature for 10 min. Once the incubation time finished the culture was centrifuged at 20,000 x *g* for 2 min and the supernatant was retained. The pH was adjusted to 7- 8 by adding 2 M tris-HCl.

2.15.2 Membrane fractionation

C. difficile cultures (overnight or mid-log) were harvested by centrifugation at 4,000 x *g*, 10 min, 4°C and then frozen at -20°C. Next day, the frozen pellet was resuspended to an OD_{600nm} of 20 by adding PBS and bacteriophage endolysin 1/10 and incubated at 37°C for 1 h. The lysate was centrifuged at 20,000 x *g* for 10 min at 4°C. The soluble fraction, which contains the cytoplasmic soluble proteins, was collected and mixed with an equal volume of 2 x Laemmli sample buffer. The insoluble fraction which contains all the membrane proteins, was re-suspended in PBS containing 1% SDS to an OD_{600nm} of 20 and then a small volume was mixed with the same volume of 2 x Laemmli sample buffer (Laemmli, 1970).

2.15.3 SDS-PAGE and Coomassie staining

Polyacrylamide gels were used to analyse protein samples in the presence of SDS. The gel was prepared using 30% acrylamide/bis-acrylamide, ratio 19:1 (5% crosslinker), according to standard protocols. The final percentage of polyacrylamide used was decided depending on the protein size. Protein samples were normally mixed with 2x Laemmli loading buffer (Laemmli, 1970), and then loaded on the gel. Electrophoresis was carried out using a vertical Mini Protean III apparatus (Bio-Rad) for 1 h at a constant voltage (180 V), until the dye front reached the gel bottom. The gel was stained routinely with coomassie brilliant blue at room temperature for 2 h [2.5% (w/v) coomassie brilliant blue R-250, 45% methanol (v/v), 10% acetic acid (v/v)], followed by overnight de-staining [45% methanol (v/v), 10% acetic acid (v/v)]. The gel was scanned using an Epson Perfection V750 Pro scanner with SilverFast software.

2.15.4 Semi-dry transfer

PVDF membrane was used for transfer of proteins for Western immunoblotting. The stack was assembled by putting two pieces of Whatman 3 MM filter paper soaked briefly in Anode buffer I (300 mM tris-HCl in 10% methanol, pH 10.4) followed by one Whatman paper soaked in Anode buffer II (25 mM tris-HCl in 10% methanol, pH 9.4), followed by PVDF membrane (wet in methanol, washed in water for 2 min, and then soaked in Anode buffer II for 5 min). Followed by the protein gel, equilibrated in Cathode buffer (40 mM glycine, 25 mM tris-HCl in 10% methanol, pH 9.4) for 10 min. The stack was completed by putting 3 pieces of Whatman paper soaked in Cathode buffer. The transfer to the membrane was carried out for 15 min at 15 V. The membrane was stained for 2 min using 0.1% ponceau S (w/v) in 5% acetic acid and then destained using tap water and dried.

2.15.5 Western blotting

The membrane was incubated with primary antibody overnight at 4°C in 3% skimmed milk in PBS. Next day, the membrane was washed with PBS and incubated for 1 h at room temperature with the secondary antibody HRP-conjugated in 3% skimmed milk in PBS, followed by five PBS washes. The membrane was visualised following addition of ECL solution (Clarity of Western ECL Blotting Substrate), and incubating for 5

min at room temperature, then imaging on a ChemiDoc MP System (Bio-Rad). Primary and secondary antibodies are listed in the Appendix A1, Table A3.

2.16 Microscopy

2.16.1 Phase contrast and fluorescence microscopy

Samples were harvested at 8,000 x *g* for 1 min, washed with PBS twice, re-suspended in 0.5 ml of 3.7% formaldehyde in PBS and mixed for 30 min at room temperature. Subsequently, the sample was centrifuged at 8,000 x *g* for 1 min, washed three times with MilliQ water, and re-suspended in 0.5 ml MilliQ water.

For fluorescence microscopy, samples were incubated with TMR-Star (NEB), as substrate for the SNAP tag, at 37°C for 1 h at a final concentration of 250 nM, centrifuged and washed twice with PBS. Then re-suspended in 0.5 ml of 3.7% formaldehyde in PBS and mixed for 30 min at room temperature. Subsequently, the sample was centrifuged at 8,000 x *g* for 1 min, washed three times with MilliQ water, and re-suspended in 0.5 ml MilliQ water. Fixed sample (5-20 µl) was dried on a glass slide, followed by a drop of 80% (v/v) glycerol and a cover slip. The samples were imaged using the Nikon Brightfield system.

2.16.2 Transmission electron microscopy (TEM)

Transmission electron microscopy was carried out by Dr Chris Hill. Briefly, overnight cultures in 5 ml pre-reduced TY were harvested at 4,000 x *g* for 10 min, washed with PBS twice, re-suspended in 0.5 ml of 3.7% formaldehyde in PBS and mixed for 30 min at room temperature. Subsequently, the sample was centrifuged at 8,000 x *g* for 1 min and washed three times with MilliQ water. The sample was re-suspended in 0.5 ml MilliQ water and sent to the EM service for sectioning. Imaging was done using a 120-kV FEI Spirit BioTWIN transmission electron microscope.

2.17 Transposon mutagenesis

2.17.1 Mutagenesis

Plasmid pRPF215 was delivered into *C. difficile* R20219 as described in section 2.5. A pure transconjugant colony was inoculated in 5 ml pre-reduced TY broth

supplemented with 15 µg/ml thiamphenicol and incubated at 37°C for 24 h. Next, this culture was sub-cultured and grown to OD_{600nm} of 0.3, and 100 µl of the culture was spread out on pre-reduced BHI agar supplemented with 20 µg/ml lincomycin and 100 ng/ml anhydrotetracycline (ATC) to induce transposition. After overnight incubation colonies were patched on non-selective BHI agar and BHI agar plates supplemented with 100 µg/ml cefoxitin, ceftazidime or ciprofloxacin. The following day, the colonies that did not grow on antibiotic plates were isolated and frozen for future work in 18.5% Glycerol/TY broth at -80.

2.17.2 Identification of transposon insertion sites

To identify the transposon insertion sites, genomic DNA was extracted from each transposon mutant and digested with *EcoRV* and *HindIII*. *EcoRV* cuts the genomic DNA 1,916 times, while *HindIII* cuts by 4,332 times. The digestion was ligated with pBluescript plasmid cut with the same restriction enzymes. Ligation was carried out using T4 ligase as described in 2.4.9. The resulting ligation mixture was transformed into *E. coli* (NEB) as described in 2.4, and the sample was cultured on LB agar supplemented with 500 µg/ml erythromycin. This was allowed cloning of the DNA fragment containing the transposon, a method called marker rescue. Clones were sequenced using two primers reading out from the transposon (RF524 and RF747), and the sequence was aligned to the R20291 genome using Geneious 7.2.1 (Biomatters).

2.18 Bioinformatics

Geneious 7.1.2 (Biomatters) was used in routine visualisation and alignment of DNA and protein sequences, including analysis of sequencing results and cloning *in silico*.

Softberry BPROM was used for promoter predication (<http://www.softberry.com>). Gibson Assembly cloning was designed using NEBuilder (<http://nebuilder.neb.com/>). Arnold terminator was used for identification of Rho-independent transcription terminators

Protein parameters, including molecular weight, transmembrane helices and isoelectric points, were predicted using the ExPASy website (<http://www.expasy.ch/tools>) and (<http://www.cbs.dtu.dk/services/TMHMM/>).

For secreted proteins, signal peptides were predicted with
(<http://www.cbs.dtu.dk/services/SignalP/>) or LipoP
(<http://www.cbs.dtu.dk/services/LipoP/>).

Chapter Three

3.1 Introduction

3.1.1: SpoVD

In *B. subtilis*, *spoVD* is located in an operon with *murE*, *muaY* and *spoVE* (Yanouri *et al.*, 1993; Figure 3.1). While in *C. difficile* *spoVD* is positioned with almost the same genes as in *B. subtilis* (Figure 3.1). In *B. subtilis*, *spoVD* transcription is dependent on SigE and is downregulated by SpoIIID (Zhang *et al.*, 1997; Daniel and Errington, 1993). In *C. difficile*, *spoVD* transcription is dependent on an unknown sigma factor.

In *B. subtilis* SpoVD is a class B PBP high molecular weight (HMW) and is essential for synthesis of the spore cortex (Bukowska-Faniband, 2015). SpoVD interacts with SpoVE, a membrane protein (lipid II flippase), and this interaction is crucial for cortex assembly (Fay *et al.*, 2010). A *spoVD* mutant produces a heat sensitive spores, completely lacking the cortex layer (Bukowska-Faniband and Hederstedt, 2013). In addition, a *spoVD* mutant accumulated peptidoglycan in the mother cell cytoplasm (Vasudevan *et al.*, 2007). The protein function is still not fully understood, but presumably, the catalytic activity of the transpeptidase domain in SpoVD is responsible for the formation of the glycan strands of the cortex layer (Liu *et al.*, 2010). In *B. subtilis*, a point mutation in the active site serine (Ser294 to Ala) of the transpeptidase domain has been used to demonstrate the acyl-enzyme complex formation and also resulted in production of heat sensitive spores, lacking the cortex layer (Bukowska-Faniband and Hederstedt, 2013).

In *C. difficile* R20291, SpoVD (73.271 kDa) has 660 amino acid residues, sharing 40% identity with SpoVD from *B. subtilis* 168, and containing three functional domains and an N-terminal membrane-spanning domain. The N-terminal transmembrane domain (residues 12-33) is predicted to be an α -helix, binding SpoVD with the cell membrane, (<http://www.cbs.dtu.dk/services/TMHMM/>) (Finn *et al.*, 2014). The three predicted functional domains are PBP dimer (residues 54-204), transpeptidase domain (residues 244-573) and a PASTA domain (residues 598-659) (<http://pfam.xfam.org/>) (Figure 3.2). SpoVD has no published structural data, but all of the predicted domains have been modelled based on the crystal structure of Pbp2x from *S. pneumoniae* (identity 33%) (Figure 3.2).

In *Bacillus subtilis*, PBP4b plays an important role in glycan synthesis. PBP4b has conserved cysteine residues in the transpeptidase domain and is present with SpoVD in the forespore (Wei *et al.*, 2004). The only difference between SpoVD and other PBPs is the PASTA domain. However, the PASTA domain is non-essential for cortex synthesis (Bukowska-Faniband and Hederstedt, 2015).

The most important domains of the PBPs are glycosyltransferase (GT) and transpeptidase (TP). Both domains have essential activities for synthesis of the glycan strands and are targeted by β -lactam antibiotics such as cephalosporin and penicillin (Sauvage and Terrak, 2016). However, the bacteria have developed many mechanisms to combat and resist the β -lactam antibiotics which lead to prolonged illnesses (Zapun *et al.*, 2008).

In this chapter, a *spoVD* mutant was created in *C. difficile* strain R20291 using the *pyrE* system as homologous recombination process. The function of SpoVD was demonstrated, involved in both sporulation and cephalosporin resistance. SpoVD expression in exponential phase was shown, localizing to the mother cell compartment, while in stationary phase it is localised to the forespore compartment. The impact of $\Delta spoVD$ on some sporulation genes was determined, including toxin production. In addition, the interaction between SpoVD and SpoVE was determined and it was shown that the PASTA domain deletion was also non-essential for spore cortex assembly as in *Bacillus subtilis*. Lastly, the Ser311 was identified as the active site serine, which is responsible for the catalytic activity of the transpeptidase domain, and this point mutation revealed the same effect on sporulation and cephalosporin resistance, as the mutant $\Delta spoVD$.

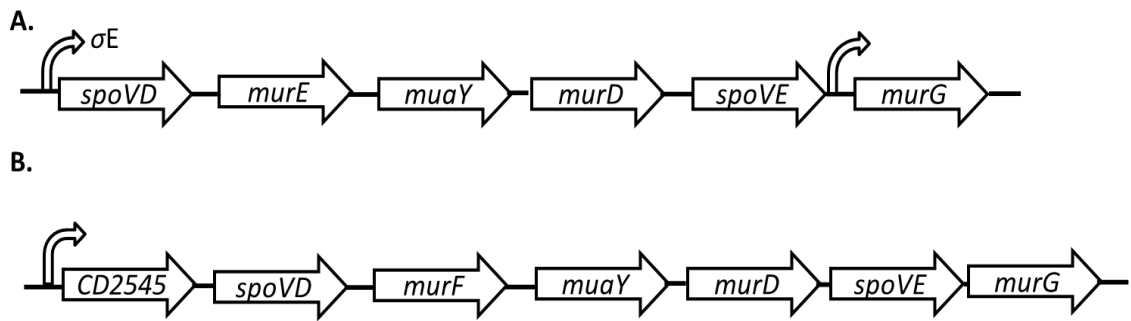


Figure 3.1. The position of *spoVD* on the chromosome of *B. subtilis* and *C. difficile*. **A:** The operon region of *spoVD* in *B. subtilis* strain 168. *spoVD* is the first gene of the five gene operon. The operon is transcribed from the SigE dependent promoter. The *murG* gene has its own promoter. The *spoVE* gene is transcribed with *spoVD* in the same operon. SpoVE is a membrane protein (lipid II flippase) **B:** The operon region of *spoVD* in *C. difficile* strains (R20291 and 630). *spoVD* is the second gene of the seven gene operon. The operon is transcribed from an unknown sigma factor dependent promoter. The *spoVE* gene is transcribed in the same operon as *spoVD*. SpoVE is a membrane protein (lipid II flippase). Unlike in *B. subtilis* 168, *murG* is in the *spoVD* operon in *C. difficile*. The same operon also includes the uncharacterised gene (CD2545) in *C. difficile*.

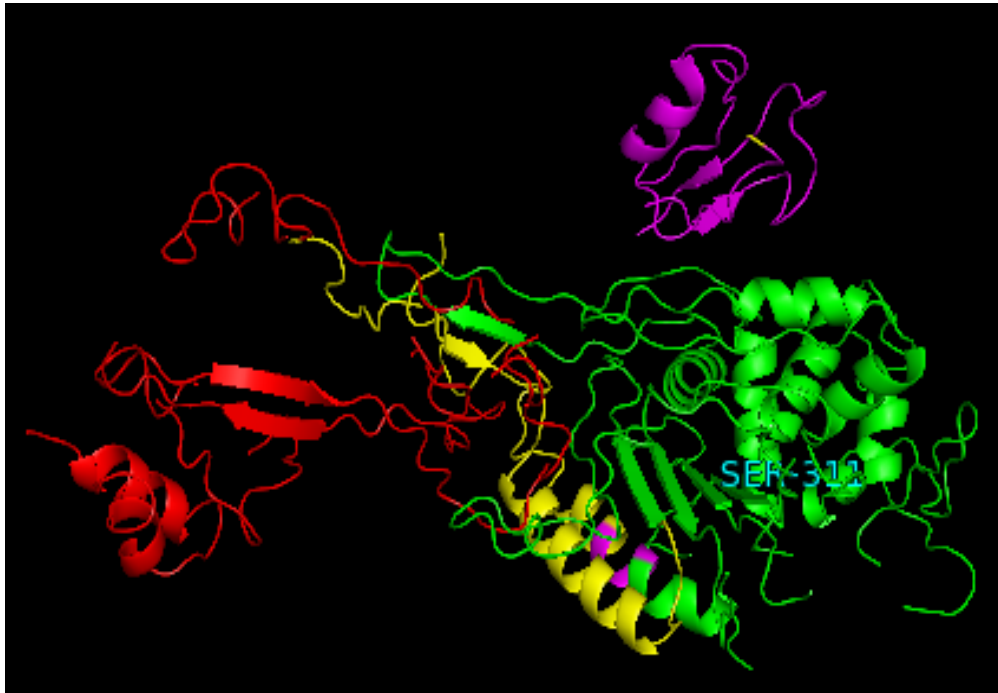


Figure 3.2. Structural model of SpoVD (residues 59-656). The PBP dimer domain is shown in red, the transpeptidase is indicated in green and the PASTA domain in purple. The active-site serine residue S311 is shown in blue. The model details of SpoVD are also presented in Liu *et al.*, (2010).

3.2: Results:

3.2.1 Bioinformatic analysis of PBPs in *C. difficile*

The first step in this project was the identification of every single gene encoding for the different classes PBPs in *C. difficile* R20291. A BLAST search was performed against the R20291 genome sequence using PBP protein sequences of *Bacillus subtilis* 168 (Sauvage *et al.*, 2008), followed by alignment of the R20291 genes with their *Bacillus subtilis* 168 homologues (Table 3.1).

Table 3.1. Identification of genes encoding PBPs in *C. difficile* R20291

Types of PBP	<i>C. difficile</i> R20291 (027)	Essential and nonessential genes	<i>Bacillus</i> <i>subtilis</i> 168	Percentage Identity
Class A	0712	Essential	<i>ponA</i>	29%
	2283	Nonessential	<i>pbpF</i>	35%
Class B	0985	Essential	<i>yrrR</i>	30%
	2544- <i>spoVD</i>	Nonessential	<i>spoVD</i>	40%
	1067	Nonessential	<i>pbpH</i>	25%
Class C	1318- <i>cwp20</i>	Nonessential	<i>pbpE</i>	25%
	3056	Nonessential	<i>pbpX</i>	24%
	2390	Nonessential	<i>dacC</i>	32%
	0441	Nonessential	<i>dacB</i>	31%
	2048	Nonessential	<i>dacA</i>	29%
	1131	Nonessential	<i>dacF</i>	44%

3.2.2 Deletion of the *spoVD* gene

A *spoVD* mutant was constructed in *C. difficile* R20291 Δ *pyrE* using a recently developed homologous recombination system (Ng *et al.*, 2013). This system uses the *pyrE* gene as both a positive and a negative selectable marker. *pyrE* encodes orotate phosphoribosyltransferase, involved in pyrimidine biosynthesis, that can be used to select for cells carrying the plasmid when grown on minimal media lacking uracil. However, it can also convert 5-fluoro-orotate (FOA) to 5-fluoro-uracil which is toxic for the cell. Hence, FOA can be used for the negative selection of the plasmid. The plasmid pMTL-YN4, carrying *pyrE*, was used to construct plasmid (pYAA024) with allele exchange cassettes having approximately 650 bp of homology to the chromosomal sequence both up- and downstream of the gene to be deleted (Figure 3.3A). This plasmid (pYAA024) was digested with *Bam*HI and *Sac*I to confirm the successful cloning of 1,300 bp insert into pMTL-YN4 (Figure 3.3C).

Plasmids were introduced into *C. difficile* R20291 as described in methods. *C. difficile* transconjugants grew slowly due to segregational instability of the origin of replication (pBP1 of *Clostridium botulinum*) on plasmid pMTL-YN4. Recombination with the chromosome overcomes the segregational instability and results in faster-growing colonies. The first crossover was confirmed by PCR using a primer specific for the chromosome (RF220) and another on the plasmid pYAA024 (RF143), PCR showed the expected product of 1,424 bp (Figure 3.3D). Double crossovers were then selected for using FOA and the successful deletion of *spoVD* was confirmed by PCR using the primers flanking the *spoVD* gene (RF212 and RF213). PCR gave the expected product of 329 bp for the mutant strain (Figure 3.3E). Following deletion, only 18 bp of the gene remained (Figure 3.3B).

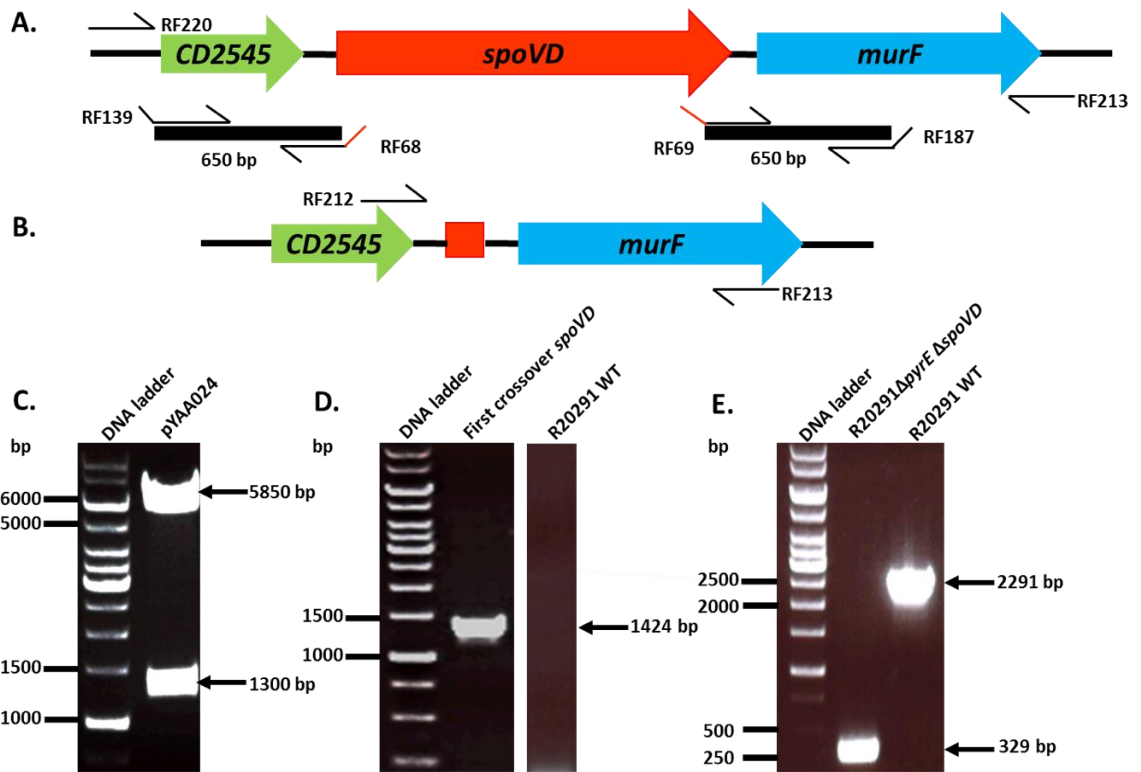


Figure 3.3: Deletion of *spoVD* using homologous recombination. **A:** Schematic diagram showing the primer design to delete the *spoVD* gene. Both internal primers have a short overlap of complementary sequence to the downstream and upstream region of the gene, whereas the external primers have *Bam*HI and *Sac*I restriction sites. PCR products were joined by SOEing PCR and the resulting product was cloned between *Bam*HI and *Sac*I in pMTL-YN4, yielding pYAA024. **B:** Schematic diagram showing the primer design to demonstrate deletion of *spoVD* gene. Following deletion, only 18 bp of the gene remain (shown in red). **C:** Agarose gel of double digestion using *Bam*HI and *Sac*I, confirming the successful cloning of 650 bp downstream and upstream of the *spoVD* gene (1,300 bp) into pMTL-YN4 (5,850 bp). **D:** PCR to demonstrate the first crossover, using a primer specific for the chromosome (RF220) and another on the plasmid pYAA024 (RF143). The PCR amplified a 1,424 bp PCR product as predicted. This confirmed recombination of the plasmid into the chromosome. Wild type R20291Δ*pyrE* was included as negative control. **E:** PCR to confirm successful deletion of *spoVD*, using primers flanking the *spoVD* gene (RF212 and RF213). PCR amplified the predicted 329 bp from the mutant, whereas the wild type R20291Δ*pyrE* gave the predicted 2,291 bp product.

3.2.3 Complementation of the *spoVD* mutant and restoration of the *pyrE* gene

The *spoVD* deletion was created in R20291 Δ *pyrE*, as a result this mutant strain has two mutations (Δ *pyrE* and Δ *spoVD*). In order to restore the *pyrE*⁺ phenotype, the pMTL-YN2 plasmid, which contains the WT *pyrE* gene was delivered to the mutant strains. Transconjugant colonies were re-streaked onto CDMM agar without uracil to select for uracil prototrophy, which indicated the successful allele recombination (R20291 Δ *spoVD*) (Figure 3.4A). The restored *pyrE* gene was confirmed by colony PCR using the two primers (RF295/RF297), which anneal in the *pyrE* locus. PCR showed the expected product of 2,000 bp for both the mutant and the wildtype strains (Figure 3.4D). Sanger sequencing was used to confirm the PCR product.

In order to complement the R20291 Δ *spoVD* mutant, it was necessary to clone *spoVD* along with upstream gene, *CD2545*. *spoVD* is the second gene in an operon with *CD2545*. The complementation was carried out by cloning both *spoVD* and *CD2545* along with the ribosome binding site (RBS) and 282 bp of the putative promoter into pMTL-YN2C using *SacI* and *Bam*HI sites. This was predicted as a promoter region of *CD2545* using BPROM (SoftBerry). The resulting clone, pYAA027, was digested by *Bam*HI and *SacI* to confirm the successful cloning of a 2,674 bp insert into pMTL-YN2C (6,924 bp) (Figure 3.4C). This plasmid was then delivered into the Δ *spoVD* mutant strain by conjugation. pMTL-YN2C allows insertion of DNA in the *pyrE* locus at the same time as restoration of the wild type *pyrE* gene.

The entire gene was cloned downstream of the restored *pyrE* gene locus. The complementation and restoration were confirmed by PCR screening using the two primers (RF295/RF297), which annealed to the *pyrE* locus. PCR showed the expected product of 4,977 bp for the complementation strain R20291 Δ *spoVD pyrE::spoVD*, while the wildtype and the R20291 Δ *spoVD* showed the expected product of 2,000 bp (Figure 3.4D). PCR products were sent for Sanger sequencing to confirm the sequence of the complementation and *pyrE* restoration.

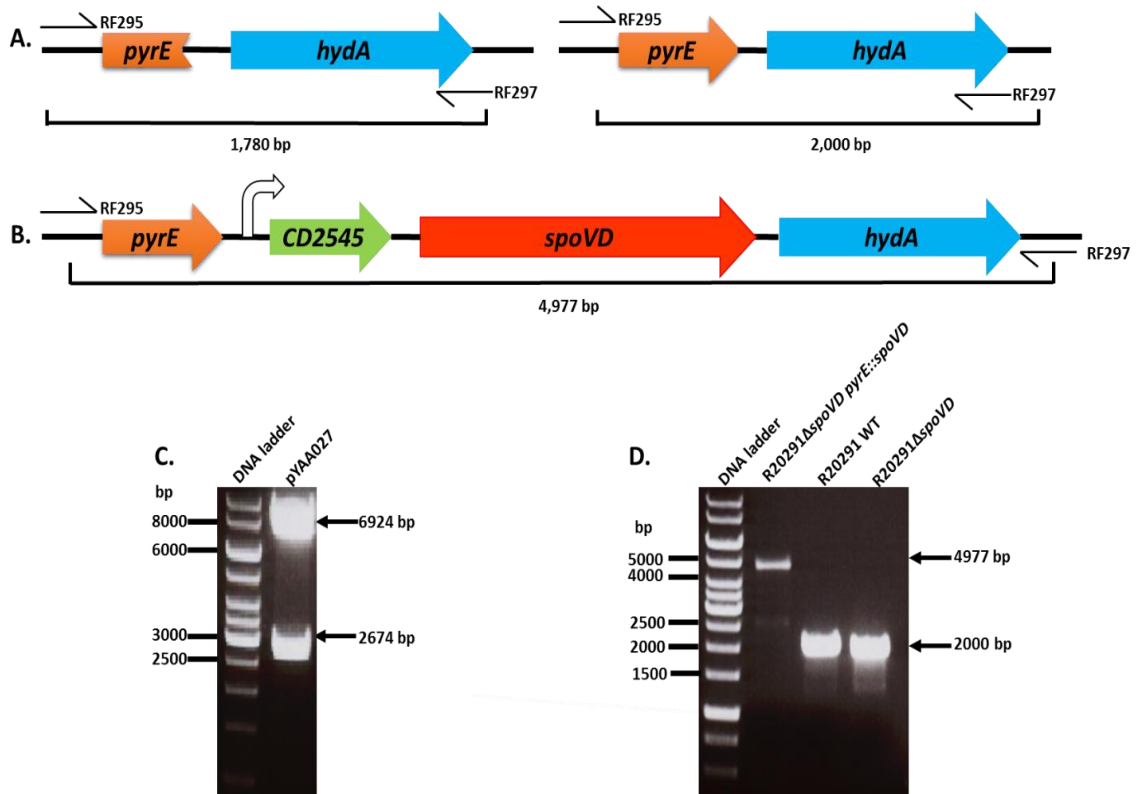
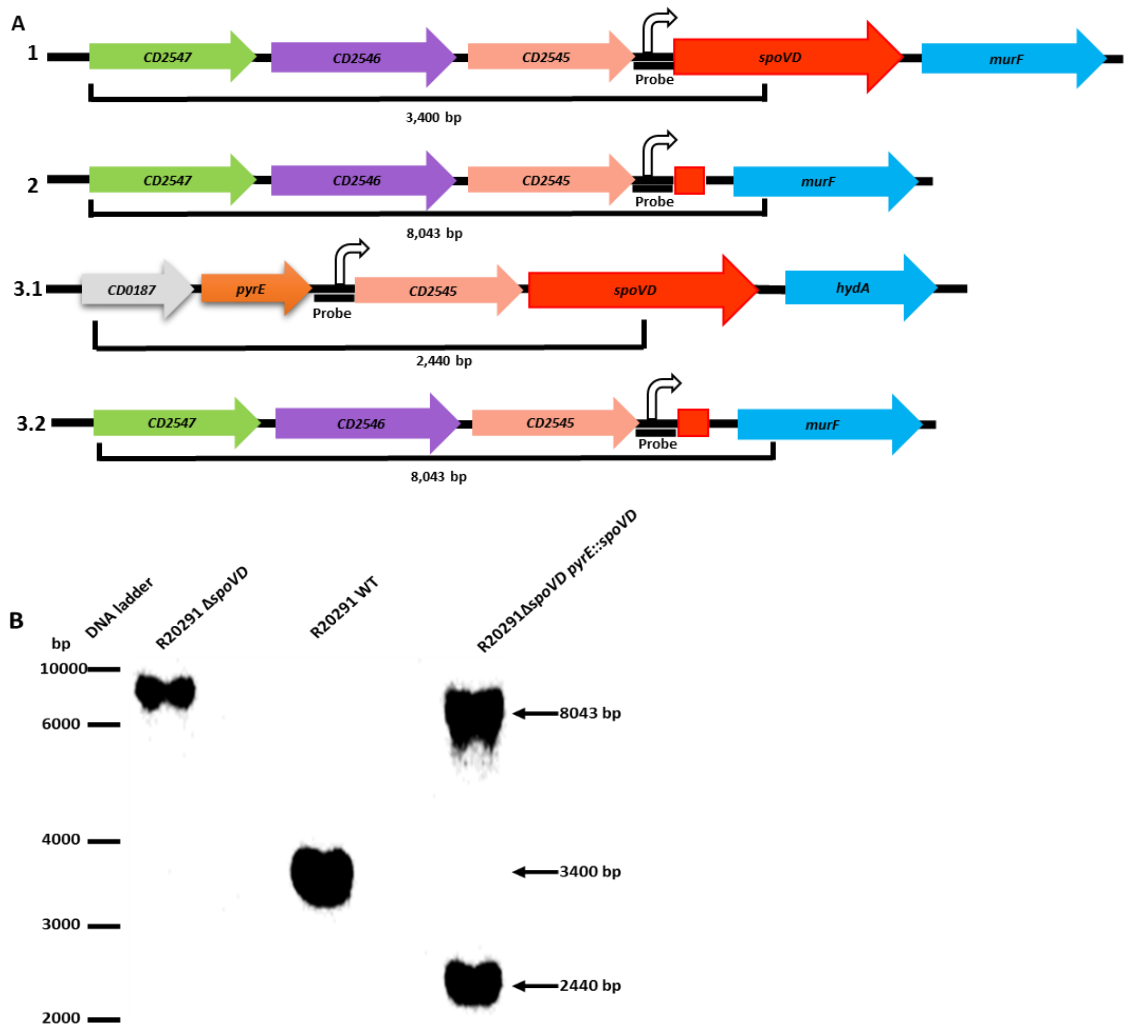


Figure 3.4: Complementation of *spoVD* and restoration of the *pyrE* gene. **A:** Schematic diagram showing the R20291Δ*pyrE* locus and the primer design for PCR screening before and after restoring *pyrE* in the *spoVD* mutant. Using these primers R20291Δ*pyrE* would give a product of 1,780 bp, increasing to 2,000 bp upon restoration of the *pyrE* gene. **B:** Schematic diagram showing the primer design for screening of insertion of *spoVD* into the *pyrE* locus. **C:** Agarose gel of double digestion using *Bam*HI and *Sac*I for plasmid pYAA027. This confirmed the successful cloning of 2,674 bp, including *spoVD* along with upstream gene, *CD2545*, the ribosome binding site (RBS) of *spoVD* and the 282 bp of putative promoter into pMTL-YN2C (6,924 bp). **D:** PCR to demonstrate the complementation *spoVD* and restoration of the *pyrE* gene using a primer flanking the *pyrE* gene locus (RF295, RF297). PCR amplified the predicted 4,977 bp product from the complementation strain, whereas the wild type R20291 gave the predicted 2,000 bp PCR product. Also, pMTL-YN2 was conjugated into the *spoVD* mutant to fix the *pyrE* gene. The PCR screen gave the expected product of 2,000 bp as the wild type, confirming the restoration of the *pyrE* gene.

3.2.4 Southern blot confirmation of knockout and complementation of *spoVD*

In order to confirm the mutant and complementation, the gDNA of the three strains, wildtype, *spoVD* mutant and complemented, were extracted, followed by digestion using two restriction enzymes *BsrGI* and *XmnI*. A 200 bp fragment covering the promoter region of *CD2545* gene was amplified by PCR and used as probe for DNA detection in a Southern blot. The probe annealed to fragments of the expected sizes: 3,400 bp in wildtype, 8,043 bp in the mutant. The probe identified two fragments in the complementation strain, the *spoVD* deletion 8,043 bp and the *CD2545/spoVD* cassette in the *pyrE* gene locus 2,440 bp (Figure 3.5).



Figures 3.5: Southern blot confirmation of *spoVD* knockout and complementation. **A:** Schematic diagram shows the genomic DNA of **(1)** the wildtype, **(2)** R2921 Δ *spoVD* and **(3.1 and 3.2)** R20291 Δ *spoVD pyrE::spoVD*. Below each is an indication of the PCD2545 fragment size following *BsrGI* and *XmnI* digestion. **B:** The gDNA of each strain was digested with *BsrGI* and *XmnI*, separated on a 1% agarose gel and transferred to a Biotodyne B nylon membrane. The membrane was blotted with a labelled probe specific for the *CD2545* promoter. The probe is illustrated with the thick black line in panel **A**. The probe visualised the difference between the wild type (3,400 bp) and the mutant strain (8,043 bp). The complementation strain showed two bands, suggesting the successful insertion of the *CD2545/spoVD* cassette into the *pyrE* gene locus (2,440 bp), along with the mutant locus (8,043 bp).

3.3 Determination of antibiotic MICs

In order to determine the MIC of cephalosporins and ciprofloxacin, the agar dilution method was used following the laboratory standard institute guidelines [Clinical and laboratory standard institute, 2012]. MICs were read after 48 h incubation at 37°C for the three strains (wildtype, $\Delta spoVD$ mutant and complemented). The *C. difficile* R20291 wild type showed the highest MIC for cefoxitin and cetazidime (128 $\mu\text{g/ml}$ and 256 $\mu\text{g/ml}$ respectively), whereas the *spoVD* mutant strain showed the lowest MICs for cefoxitin and cetazidime (32 $\mu\text{g/ml}$, 64 $\mu\text{g/ml}$ respectively). Mutation of *spoVD* had no effect on ciprofloxacin resistance as expected. Subsequently, the complemented strain was tested to determine if the wild type MICs were restored. The MIC of cetazidime, cefoxitin were restored (128 $\mu\text{g/ml}$, 256 $\mu\text{g/ml}$ respectively) (Table 3.3).

Table 3.3. Minimum inhibitory concentrations against the wild type R20291 and *spoVD* mutant and complementation strains ($\mu\text{g/ml}$).

Strains	Cefoxitin	Cetazidime	Ciprofloxacin
R20291 Wild Type	128	256	512
R20291 $\Delta spoVD$	32	64	512
R20291 $\Delta spoVD$ <i>pyrE::spoVD</i>	128	256	512

3.4 Sporulation of R20291, R20291 Δ spoVD and R20291 Δ spoVD pyrE::spoVD

A *spoVD* mutation in *B. subtilis* has a significant effect on sporulation efficiency via an important role in spore cortex assembly. Sporulation assays were used to reveal the sporulation efficiency of R20291 wild type, R20291 Δ spoVD and R20291 Δ spoVD pyrE::spoVD. *C. difficile* sporulation is normally induced during the stationary phase due to starvation. The sporulation efficiency was measured by counting the number of colony forming units (CFU) over 5 days incubation in an anaerobic cabinet at 37°C. To count spores, the culture was heated at 65°C for 30 min to kill the vegetative cells and allow spores to survive. This demonstrated the efficiency and the dynamics of sporulation (Dembek, 2014). Unlike the wild type, the Δ spoVD mutant did not make heat resistant spores. The complemented strain completely restored the sporulation efficiency to wild type levels (Figure 3.6).

The whole assay was monitored at each time point using phase contrast microscopy. The Δ spoVD strain showed phase dark spores in contrast to wild type and complementation strains which showed phase bright spores (Figure 3.7). These results are identical to those shown in a *B. subtilis* *spoVD* knockout which forms heat sensitive spores completely lacking the cortex layer (Bukowska-Faniband and Hederstedt, 2013). The rationale of this observation is that the catalytic activity of the transpeptidase domain is required for synthesis of the cortex and this layer makes the spores heat-resistant (Bukowska-Faniband and Hederstedt, 2013).

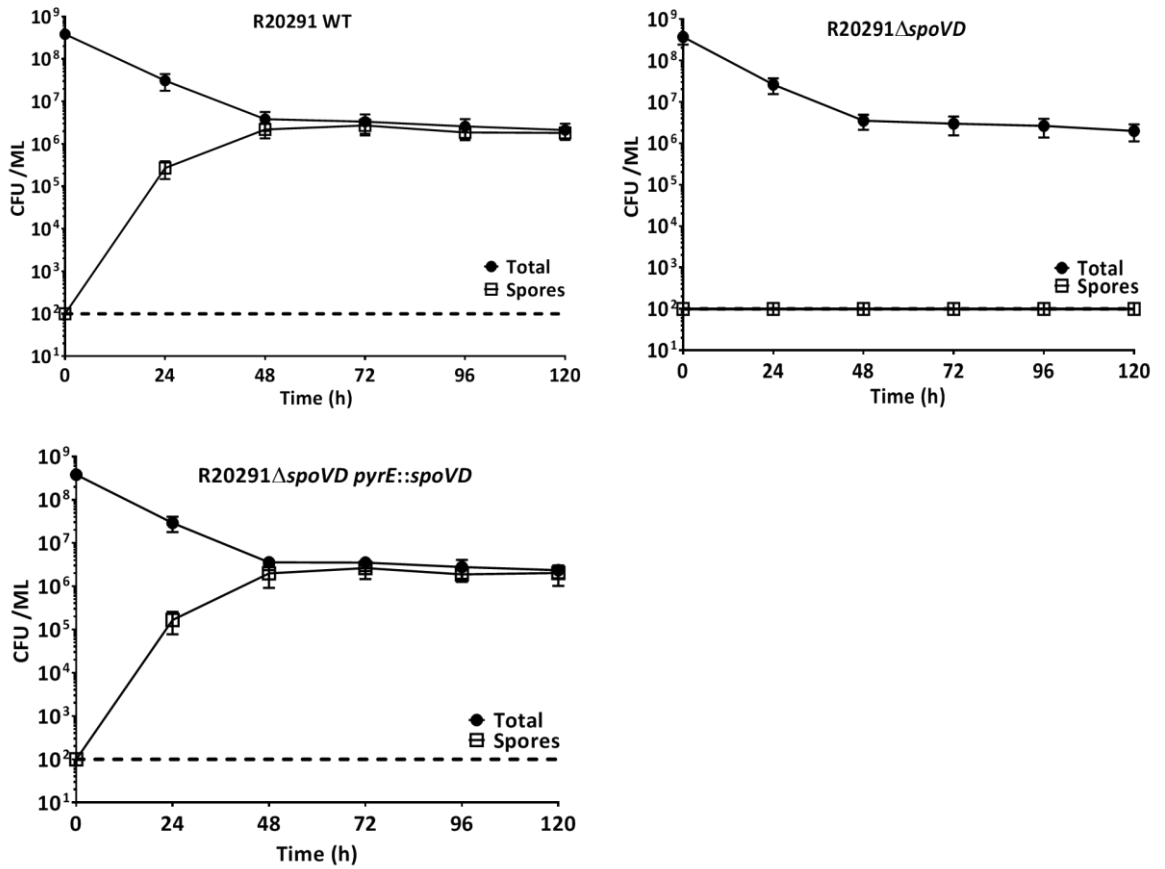


Figure 3.6: Sporulation efficiency of R20291 wild type, R20291ΔspoVD and R20291ΔspoVD *pyrE::spoVD* strains. The bacterial cultures were incubated anaerobically at 37°C for 5 days in BHI-S broth. Total bacterial and spore numbers were counted every 24 h by CFUs (total) or CFUs (spores) after treatment at 65°C for 30 min. The assay was completed in triplicate. Standard deviations are represented by black error bars. The dotted line represents the limit of detection.

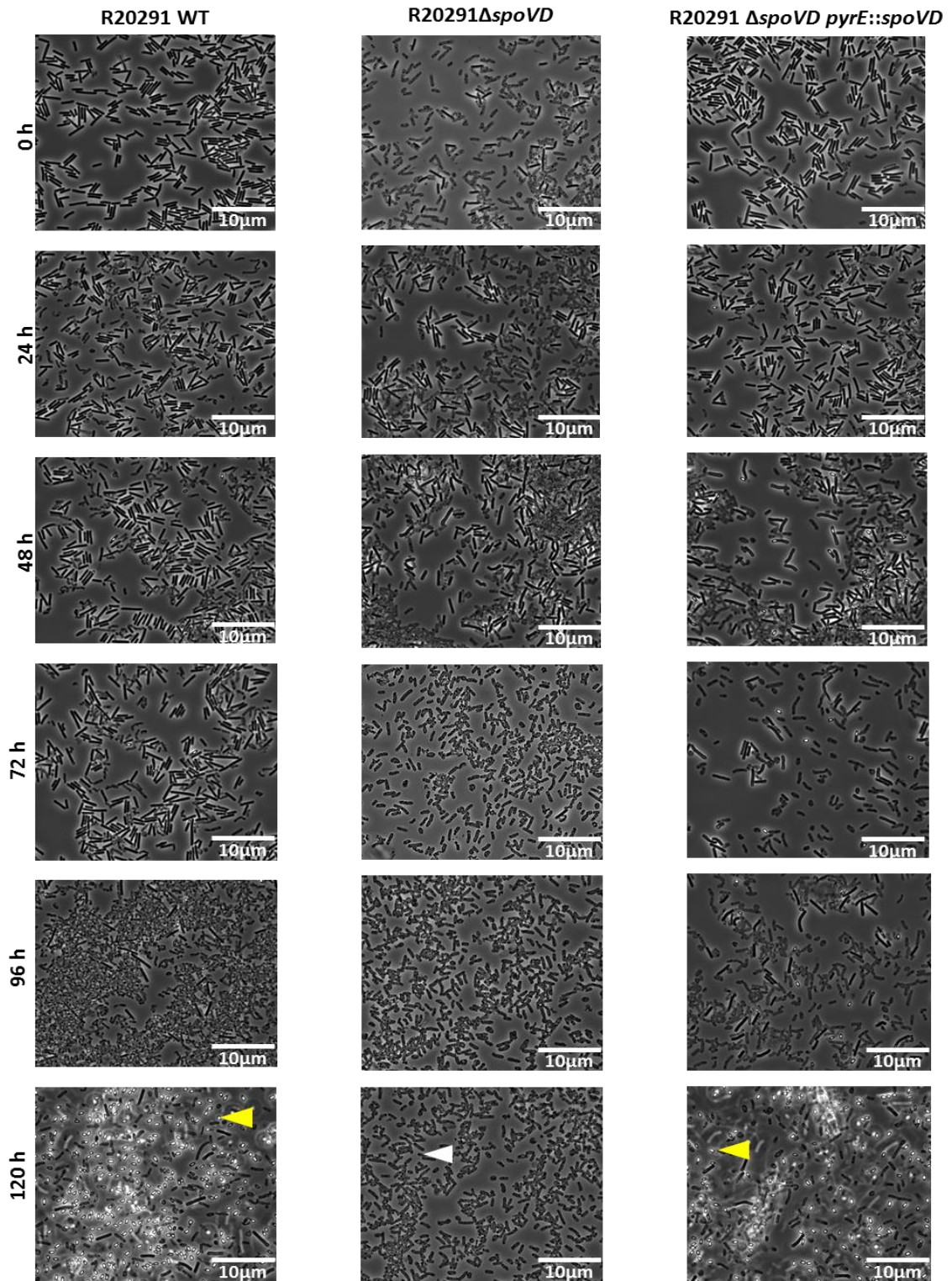


Figure 3.7. Phase contrast microscopy of sporulation assay. The sporulation efficiency of wild type *C. difficile* R20291, R20291 Δ spoVD and R20291 Δ spoVD pyrE::spoVD were monitored. Each sample was harvested at the indicated time point. The samples were fixed using 3.7% formaldehyde and dried onto glass slides, yellow arrowhead shows a representative phase bright spore, while white arrowhead shows a representative phase dark spore. The assay was done in triplicate from three biological replicates.

3.4.1 Characterisation of spore resistance to environmental stresses

C. difficile spores are multi-layered structures. These layers allow the spores to resist many different physical conditions such as pH, pressure and enzymatic action, as well as chemical agents such as ethanol (Setlow, 2006). Also, *C. difficile* spores are able to tolerate incubation at 60-80°C for 10-30 min without effect on subsequent out-growth (Burns *et al.*, 2010a). We tested the tolerance to three different conditions using sporulating cultures at 120 h of the sporulation assay. Microscopy showed that the mutant produced immature phase-dark spores and the sporulation assay showed that these spores were heat sensitive. We were unable to purify *spoVD* mutant spores (data not shown). These results were identical to those shown in *spoIVA* and *sipL* knockouts, which lack the protein coat (Putnam *et al.*, 2013). The cultures of wild type, mutant and complementation were incubated at 55°C for 30 min. The cultures were also treated with 70% ethanol and 250 µg/ml lysozyme. We did not see a significant change in spore viability for the wild type and complementation strains in any condition. However, the *spoVD* mutant was as sensitive to 55°C and 70% ethanol as the original 65°C incubation, whereas it was as resistant to lysozyme as the wild type and complemented strains (Figure 3.8). Lysozyme treatment of *C. difficile* 630 spores does not normally have a significant impact on spore viability (Dembek, 2014).

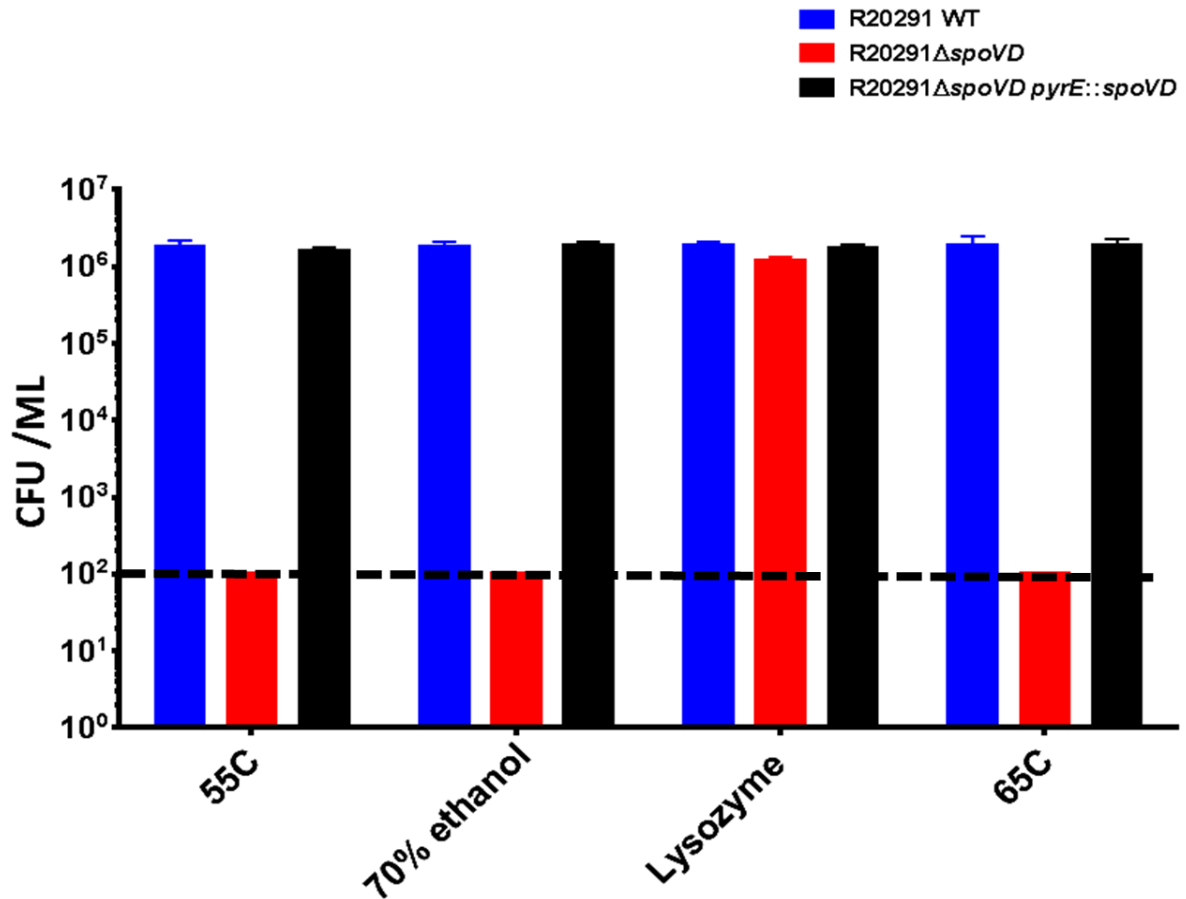


Figure 3.8: Characterisation of spore resistance to environmental stresses. Sporulating cultures of R20291, R20291 Δ spoVD and R20291 Δ spoVD *pyrE::spoVD* strains at 120 h were resuspended to OD_{600nm} 0.1 using 70% ethanol or 250 μ g/ml lysozyme. The cultures were incubated also at the lower temperature of 55°C, compared with the original 65°C treatment. Cultures were incubated on BHIS-agar plates with 0.1% sodium taurocholate to enumerate spores. Shown are means of triplicate with standard deviations represented by error bars. The dotted line represents the limit of detection.

3.4.2 Characterisation of spore morphology

A *spoVD* mutation in *B. subtilis* results in spores lacking the cortex layer. To analyse the impact of a similar mutation in *C. difficile*, we examined spores using transmission electron microscopy (TEM). Firstly, we performed optimisation for the broth type and incubation time. As a result, TY broth was identified as the best media to produce sporulating cells at a 24 h incubation time at 37°C (Figure 3.9). Subsequently, we performed TEM to analyse the sporulating cell ultrasections. The wild type and the complementation strains have the typical spore structure observed for other Gram-positive species. The typical spores contained the central core surrounded by a thick cortex layer and coat. Typical *Bacillus* spores have the same layers with an additional outside layer that is called the exosporium (Permpoonpattana *et al.*, 2011). However, the *spoVD* mutant showed a spore apparently lacking the cortex layer, consistent with heat sensitivity (Figure 3.9). This was identical to the *spoVD* mutant phenotype in *B. subtilis*, which proves that the *spoVD* knockout leads to a lack of cortex layer in the spore (Bukowska-Faniband and Hederstedt, 2013).

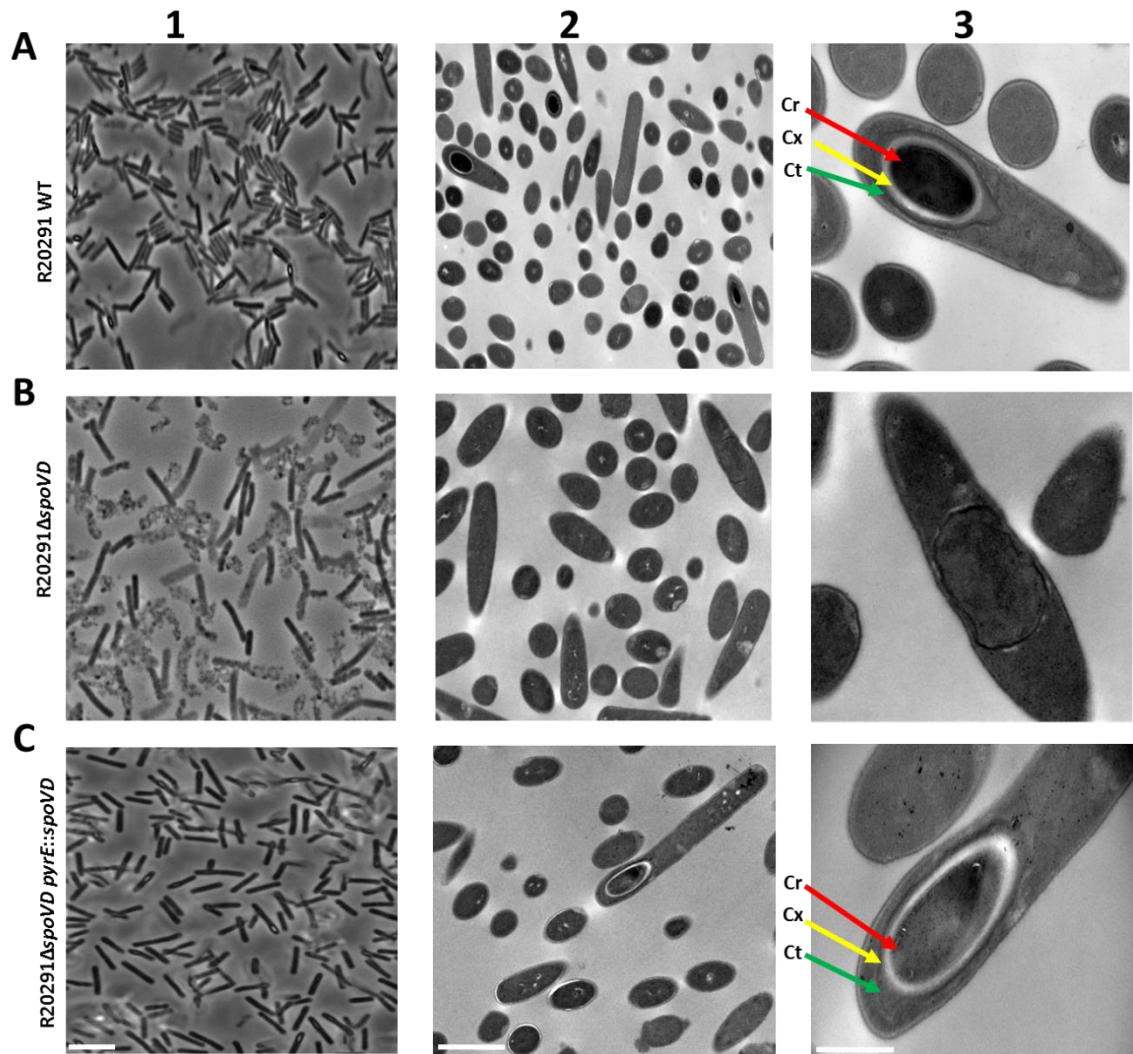


Figure 3.9: Phase contrast and TEM of *C. difficile* R20291. **A:** wild type R20291, **B:** R20291ΔspoVD, **C:** R20291ΔspoVD pyrE::spoVD, visualized by using **(1):** Phase contrast microscopy (scale bar 10 μm). **(2):** TEM (scale bar is 1 μm). **(3):** TEM (scale bar is 200 μm). Phase contrast shows a mixed sporulating population at 24 h. TEM shows three structural layers in developing spores, core (Cr), cortex (Cx) and coat (Ct) for both the wildtype and complemented strains. No cortex is visible for R20291ΔspoVD.

3.5 Expression and localisation of SpoVD

In *B. subtilis*, SpoVD localises in the cell membrane, appearing in the second hour of the sporulation process. The protein is detectable in the mother cell and then localises to the forespore membrane (Bukowska-Faniband and Hederstedt, 2015). *spoVD* transcription is dependent on the SigE factor in *B. subtilis* and is negatively controlled by SpoIIID (Daniel *et al.*, 1994; Zhang *et al.*, 1997).

To analyse the localisation of SpoVD in *C. difficile*, the Clip tag was fused to the N-terminal or C-terminus of SpoVD, with expression under the control of the constitutive promoter P_{cwp2} . Subsequently, these plasmids were conjugated into R20291 Δ *spoVD*. The resulting strains were R20291 Δ *spoVD*+*clip-spoVD* and R20291 Δ *spoVD*+*spoVD-clip*. Sporulation was tested and compared to wild type and complemented strains. The results showed that the sporulation efficiency of R20291 Δ *spoVD*+*spoVD-clip* was reduced to approx. 20%, while the R20291 Δ *spoVD*+*clip-spoVD* sporulated with 80% efficiency, similar to R20291. This suggested that *spoVD-clip* was only partially functional (Figure 3.10C).

Building upon these results, Snap tag encoding DNA was added to the 5' end on *spoVD* in the native locus using homologous recombination CodA (Figure 3.10A). The resulting strain was R20291 *snap-spoVD*. The fusion insertion was confirmed by PCR using primers flanking the *spoVD* gene (RF213, RF326; Figure 3.10A). The PCR screen showed the expected product of 3,050 bp for R20291 *snap-spoVD*, while the wild type R20291 showed the predicted product of 2,500 bp (Figure 3.10B). TMR-Star was used as a substrate to label the cells, and visualise the localisation of Snap-SpoVD during the mid-log phase after 3 h growth, in stationary phase at 24 h and late stationary phase at 48 h. Our results showed that there is clearly SpoVD expression in mid-log phase, which was localised to the mother cell in the early stages of the sporulation process. In contrast, in the stationary phase at 24 h and late stationary phase at 48 h, Snap-SpoVD seems to be localised to the forespore membrane (Figure 3.10E). Snap-SpoVD expression was confirmed by fluorescent SDS-PAGE after treating the culture with TMR-Star at each time point, showing the expected product of 92.6 kDa, the correct size of Snap-SpoVD (Figure 3.10D).

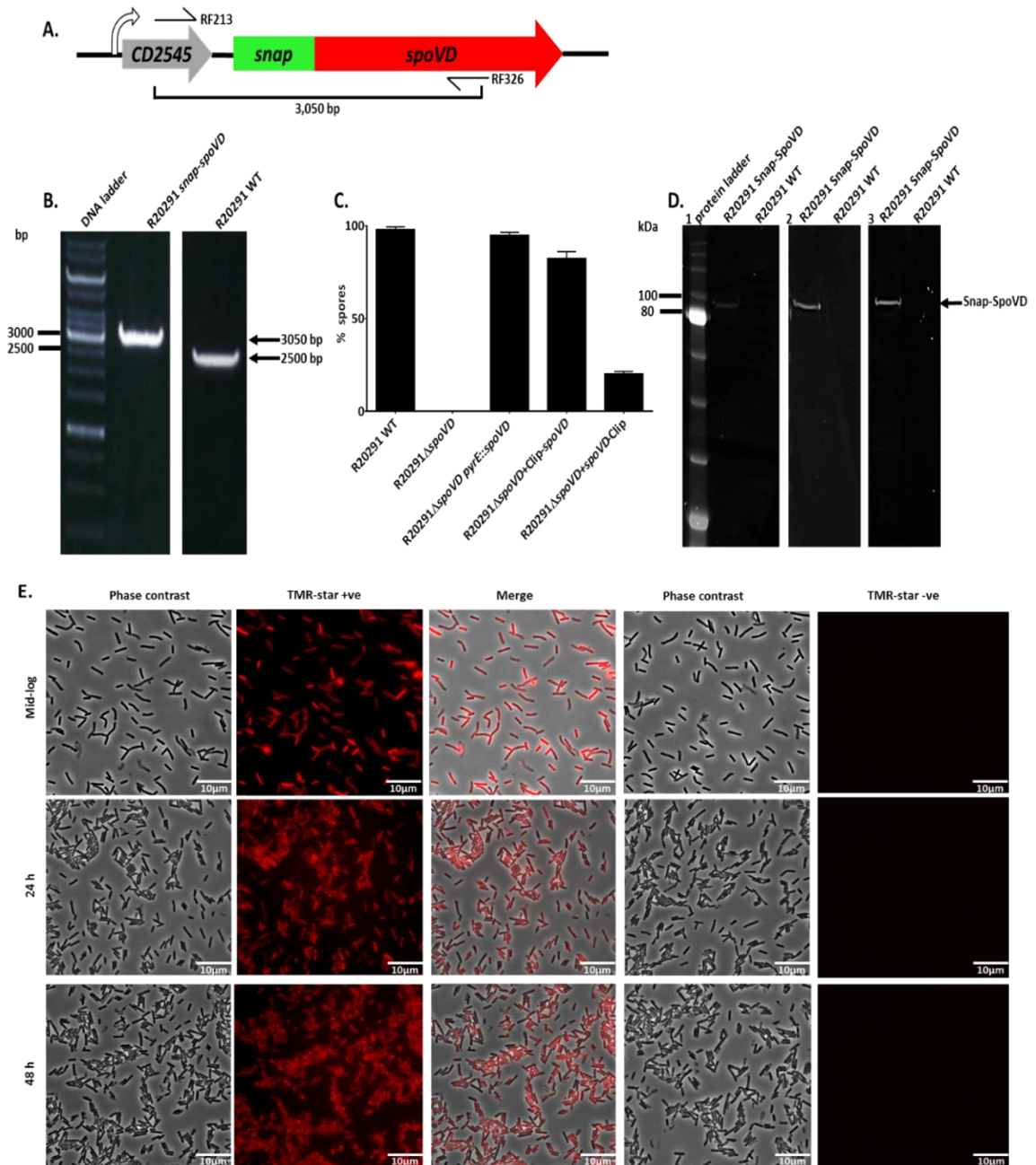


Figure 3.10: Subcellular localisation of SpoVD in *C. difficile* R20291. **A:** Schematic diagram showing the primer design for screening of R20291 *snap-spoVD*. **B:** Agarose gel showing PCR screen confirming successful insertion of DNA encoding the Snap tag fused to the chromosomal *spoVD* gene, using primers flanking the *spoVD* gene (RF213 and RF326). PCR showing the expected product of 3,050 bp for R20291 *snap-spoVD*, whereas the wild type R20291 gave the predicted 2,500 bp product. **C:** Sporulation efficiency of R20291, R20291 Δ *spoVD*, R20291 Δ *spoVD pyrE::spoVD*, R20291 Δ *spoVD+clip-spoVD* and R20291 Δ *spoVD+spoVD-clip*. Stationary phase cultures were incubated anaerobically at 37°C for 5 days in BHI-S. Total bacterial and spore counts were enumerated every 24 h by CFUs (total) or CFUs (spores) after

treatment at heat at 65°C for 30 min. The assay was completed in triplicate. Standard deviations are represented by black error bars. The percentages of spores at 120 h were calculated by dividing the number (CFUs) of the spores by the total number (CFUs) of the bacterial growth. This assay showed that the N-terminal Clip-SpoVD is more functional than SpoVD-Clip to restore sporulation. **D:** SDS-PAGE analysis of R20291 and R20291 *snap-spoVD* lysates, visualised using Snap TMR-star by fluorescence imaging, using a Cy3 filter **(1):** exponential phase, **(2):** 24 h and **(3):** 48 h. The fluorescent Snap-SpoVD is visible at approximately 92.6 kDa, the wild type was used as a negative control. **E:** R20291 *snap-spoVD* at mid-log, 24 h and 48 h in TY broth, visualised using phase-contrast and fluorescence microscopy. Each culture was labelled using TMR-star substrate 250 nM for 1 h, then fixed with 3.7% formaldehyde and dried onto glass slides. The fluorescence microscopy shows the availability of Snap-SpoVD in exponential phase, localising to the mother cell in the early stages of the sporulation process. In stationary phase at 24 h and late stationary phase at 48 h, Snap-SpoVD was localised to the forespore membrane. Unlabelled cultures were included as negative controls. Scale bar represents 10 µm.

3.6 The impact of the *spoVD* mutant on the expression of sporulation associated genes and localisation of promoter activity

The expression and the localisation of Spo0A, SspA, SpoIVA, SipL, Gpr and SpoVT was analysed to reveal the effect of the *spoVD* mutant on their localisation and expression. To identify the affect on these genes and highlight the role of *spoVD* during the sporulation process, Western blot analysis was used to distinguish expression levels and fluorescence microscopy to visualise the localisation of promoter activity in wild type, mutant and complemented strains.

We received three plasmids encoding Snap fusions to the *sspA*, *sipL* and *spoVT* native promoter regions from Dr. Aimee Shen (Tufts University). These plasmids were delivered to R20291 wild type, mutant and complemented strains, followed by fluorescence SDS-PAGE (Figure 3.11B). Each showed the expected product of 20 kDa, the correct size of Snap. The expression of each gene appeared lower in the mutant and complemented strains compared to the wild type strain (Figure 3.11A).

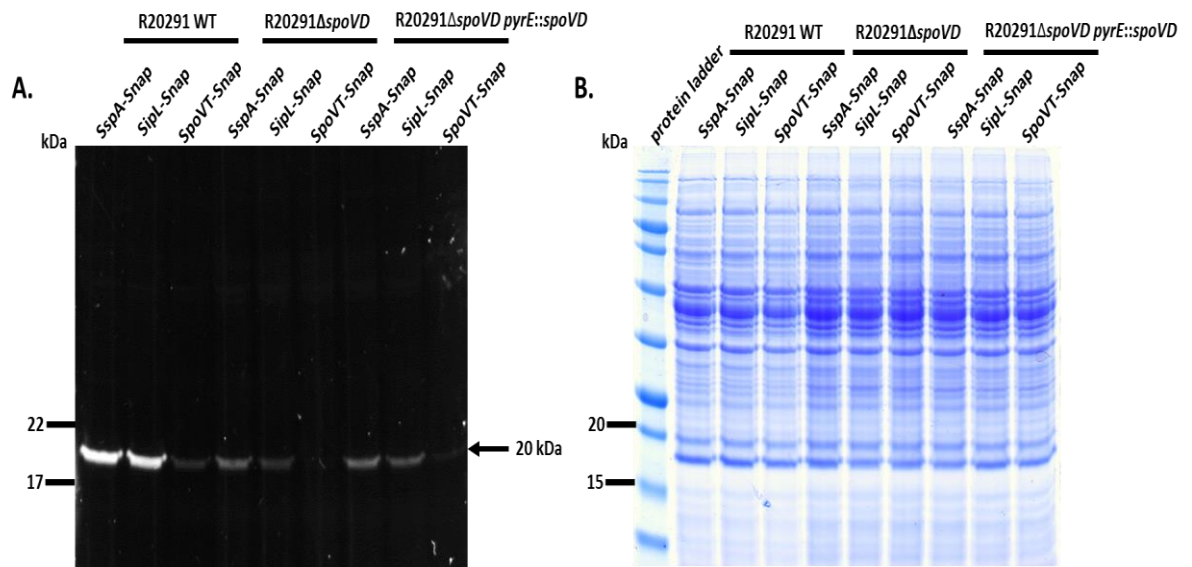


Figure 3.11: The expression of *sspA*, *sipl* and *spoVT* genes in R20291ΔspoVD. **A:** SDS-PAGE analysis of R20291, R20291ΔspoVD and R20291ΔspoVD *pyrE::spoVD* lysates, visualised using Snap TMR-star by fluorescence imaging, using a Cy3 filter, in stationary phase at 24 h. The fluorescent Snap is visible at approximately 20 kDa. **B:** SDS-PAGE analysis of the whole cell lysates. The stained gel was used as control for protein loading. Each sample was resuspended to OD_{600nm} 10 on the SDS-PAGE gel.

To analyse localisation, 24 h TY cultures were labelled with the TMR-Star substrate and visualised by fluorescence microscopy. The time was optimised to obtain sporulating cells (as described in 3.4.2). The fluorescent microscopy data showed that SspA expression localises to the spore core in all three strains as expected (Figure 3.12A).

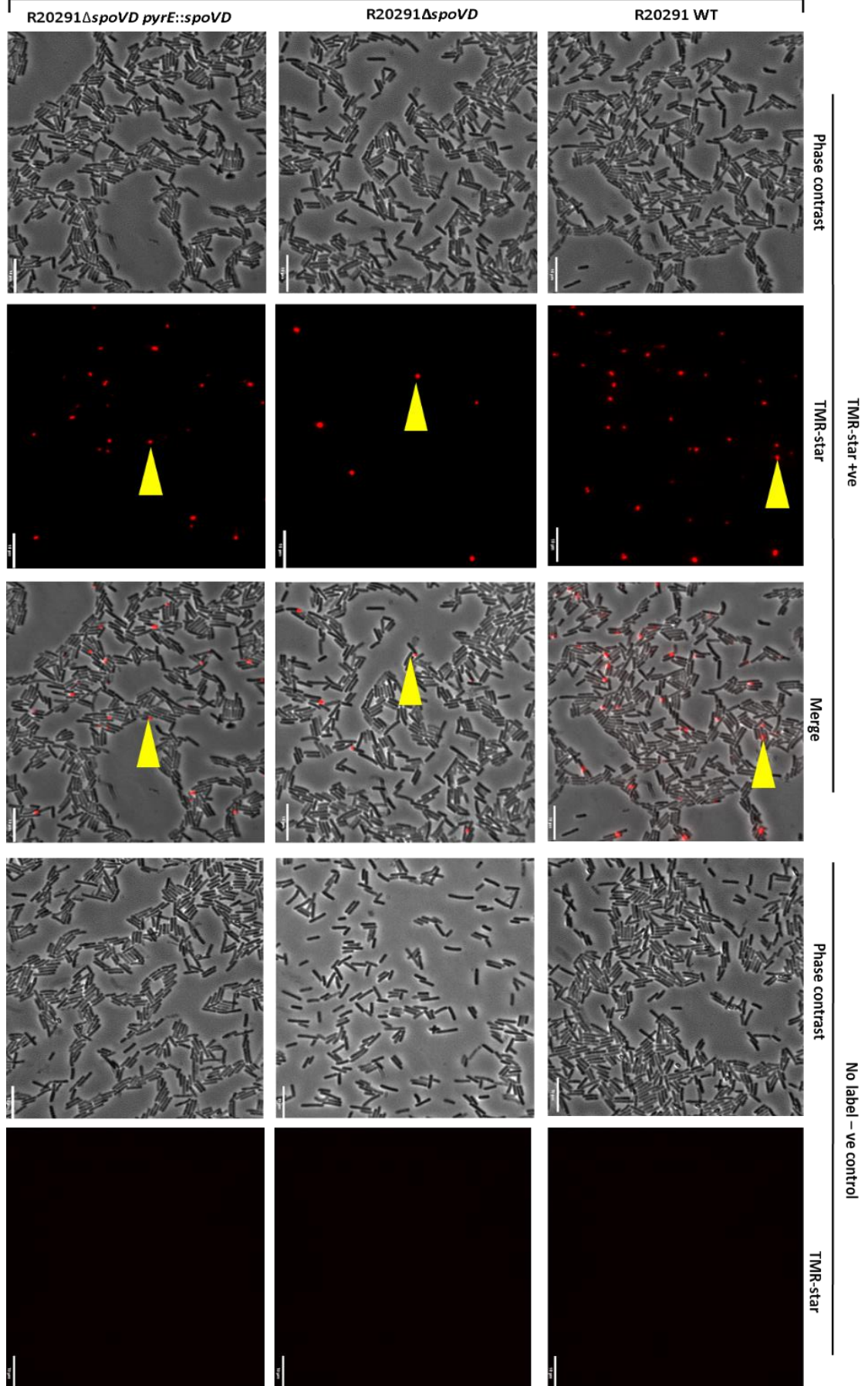
The expression of SpoVT was also tested in the *spoVD* mutant by Western blot (Figure 3.13). SpoVT was expressed at lower levels in $\Delta spoVD$ than the wildtype and complemented strains. Densitometry was performed to measure the relative intensities of each band. The mutant showed a relative intensity of 12 ± 1 , whereas the wildtype and complemented strains showed 47 ± 1 and 41 ± 1 respectively (Figure 3.13C). Furthermore, *spoVT* promoter activity was mislocalized and the specific forespore localization observed in the wild type and complemented strains was lost (Figure 3.12B).

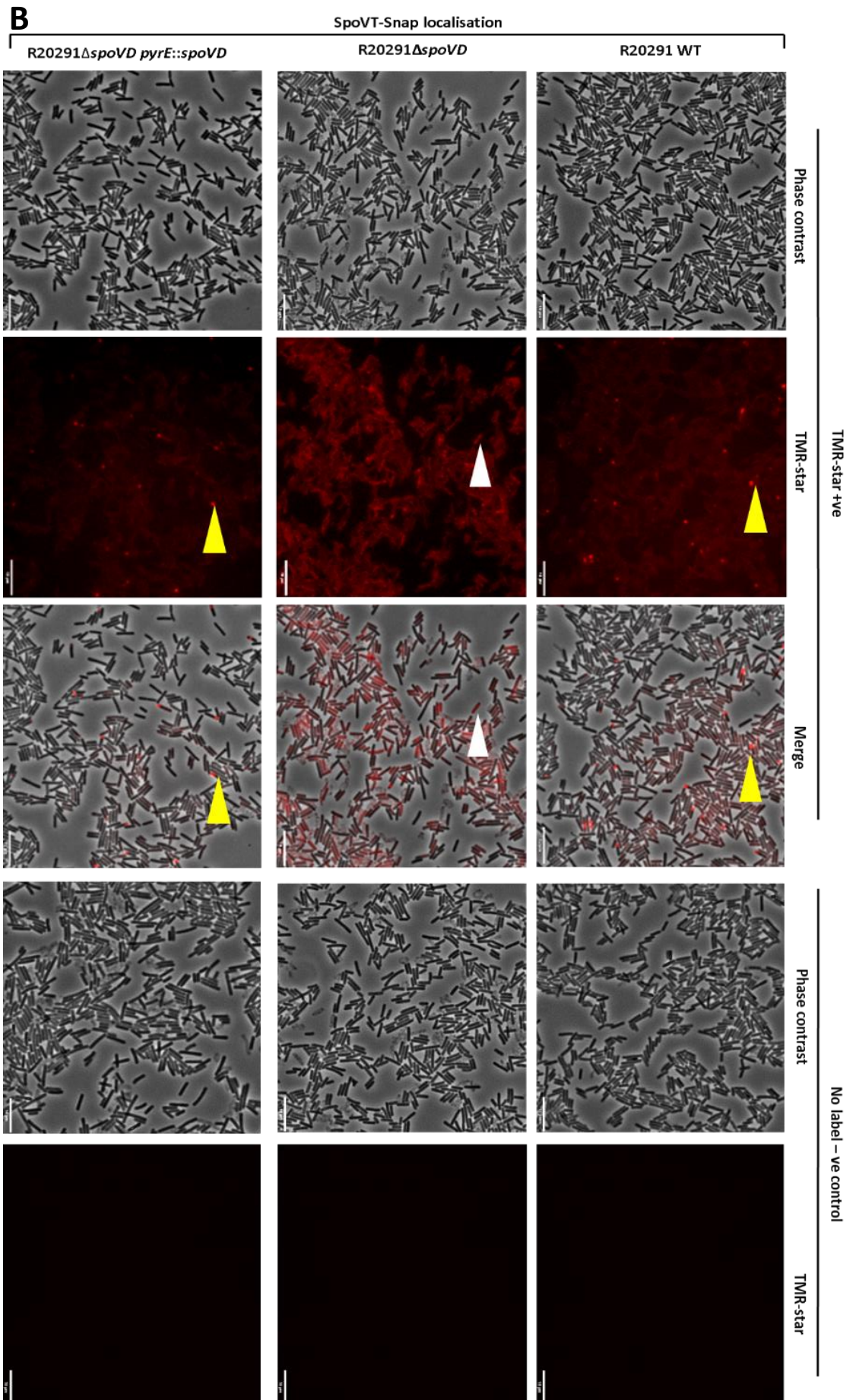
Gpr expression was analysed by Western blot using antibody raised against Gpr of *C. difficile*. Western blot analysis of three biological repeats showed that Gpr also has slightly lower expression in $\Delta spoVD$ in contrast with wildtype and complemented strains, although this does not appear to be significant by densitometry (Figure 3.13). The average intensity of the mutant was 32 ± 2 , while the wildtype and complemented strains both have an average intensity 34 ± 1 (Figure 3.13C).

The expression levels of two coat proteins SipL and SpoIVA were also tested in the three strains. Western blot analysis of three biological repeats showed a large decrease in SipL expression in $\Delta spoVD$ in contrast with wildtype and complemented strains (Figure 3.13). The average intensity of the mutant was 4 ± 4 , while the wildtype and complemented strains were 58 ± 2 and 38 ± 1 respectively (Figure 3.13C). *sipL* promoter activity in the mutant strain also mislocalized and the specific mother cell localization observed in the wildtype and complemented strains was lost (Figure 3.12C). In contrast to SipL, SpoIVA was overexpressed in the mutant strain (Figure 3.13). The average intensity of the mutant was 39 ± 4 , while the wildtype and complemented strains were 29 ± 2 and 32 ± 2 respectively (Figure 3.13A).

Finally, the expression level of the master regulator Spo0A was also examined in the three strains. Western blot analysis of three biological repeats showed slightly higher

expression levels in $\Delta spoVD$ than wildtype and complemented strains (Figure 3.13). The average intensity of the mutant was 36 ± 5 , while the wildtype and complemented strains were 32 ± 3 and 32 ± 2 respectively (Figure 3.13C).

A**SspA-Snap localisation**



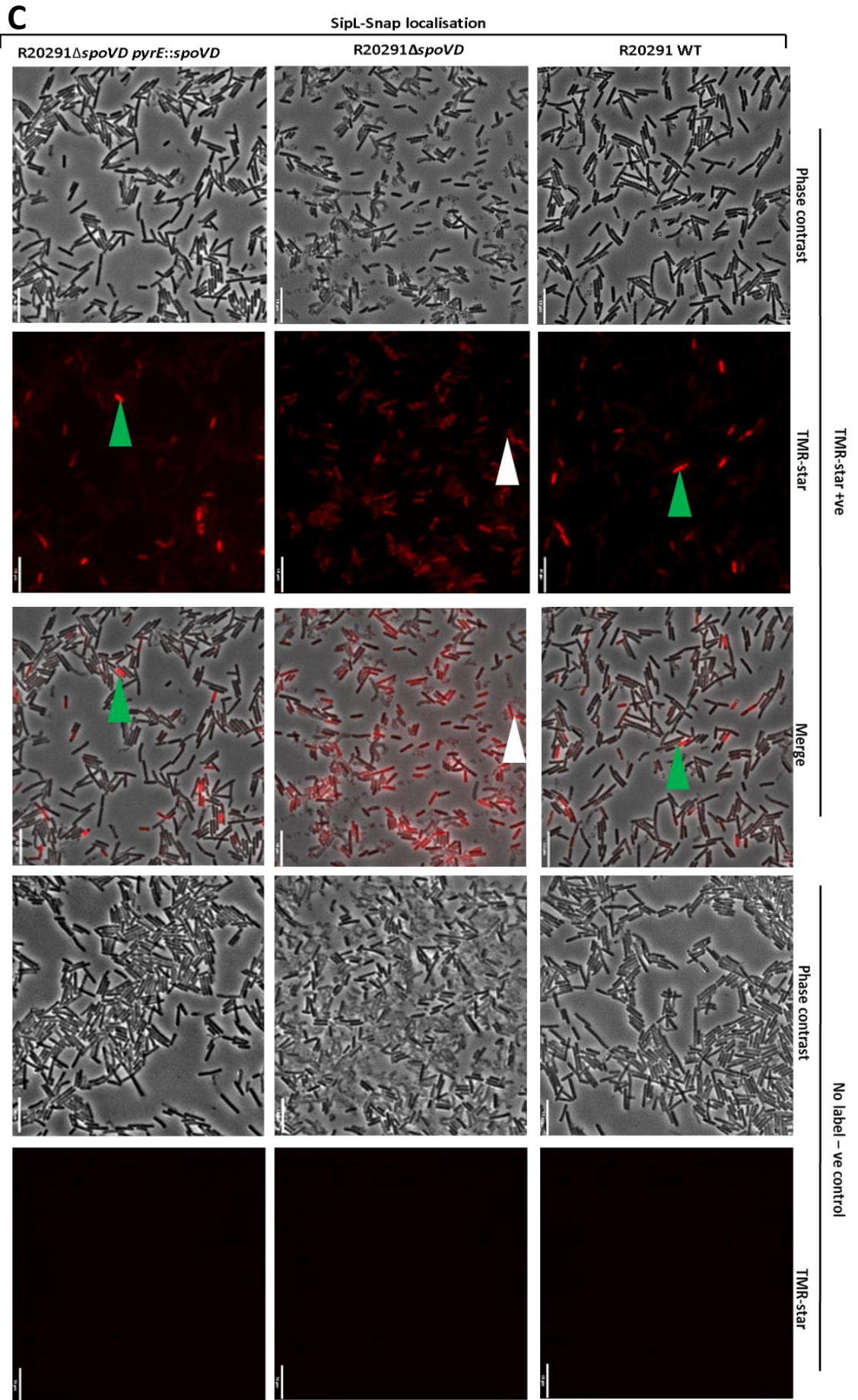


Figure 3.12: Subcellular localisation of SspA, SipL and SpoVT expression in R20291 Δ *spoVD*. Plasmids carrying *PsspA-snap* (A), *PspoVT-snap* (B) or *PsipL-snap* (C) were conjugated into the three strains. Following the conjugation, the strains were grown at 37°C in using TY broth for 24 h. 1 ml of each was labelled with 250 nM TMR-star for 1 h at 37°C, fixed with 3.7% formaldehyde and dried onto glass slides. Fluorescent microscopy showed that *sspA* promoter activity is localised to the forespores in the three strains, the yellow arrowheads show a representative localisation of Snap in the forespore region. *spoVT* promoter activity is also localised to the forespore compartment in the wildtype and complemented strains, yellow arrowheads show a representative localisation of Snap in the forespore region, while the *spoVD* mutant showed mislocalization of the *spoVT* promoter activity, with expression throughout the cell, white arrowhead shows representative mislocalization. *sipL* promoter activity is detectable in the mother cell compartment of the wildtype and complemented strains, green arrowhead shows representative localisation of Snap in mother cell compartment, while the *spoVD* mutant showed mislocalization of *sipL* promoter activity, with expression throughout the cell, white arrowhead shows a representative the mislocalization of Snap. Unlabelled cultures were included as negative controls. Scale bar represents 10 μ m.

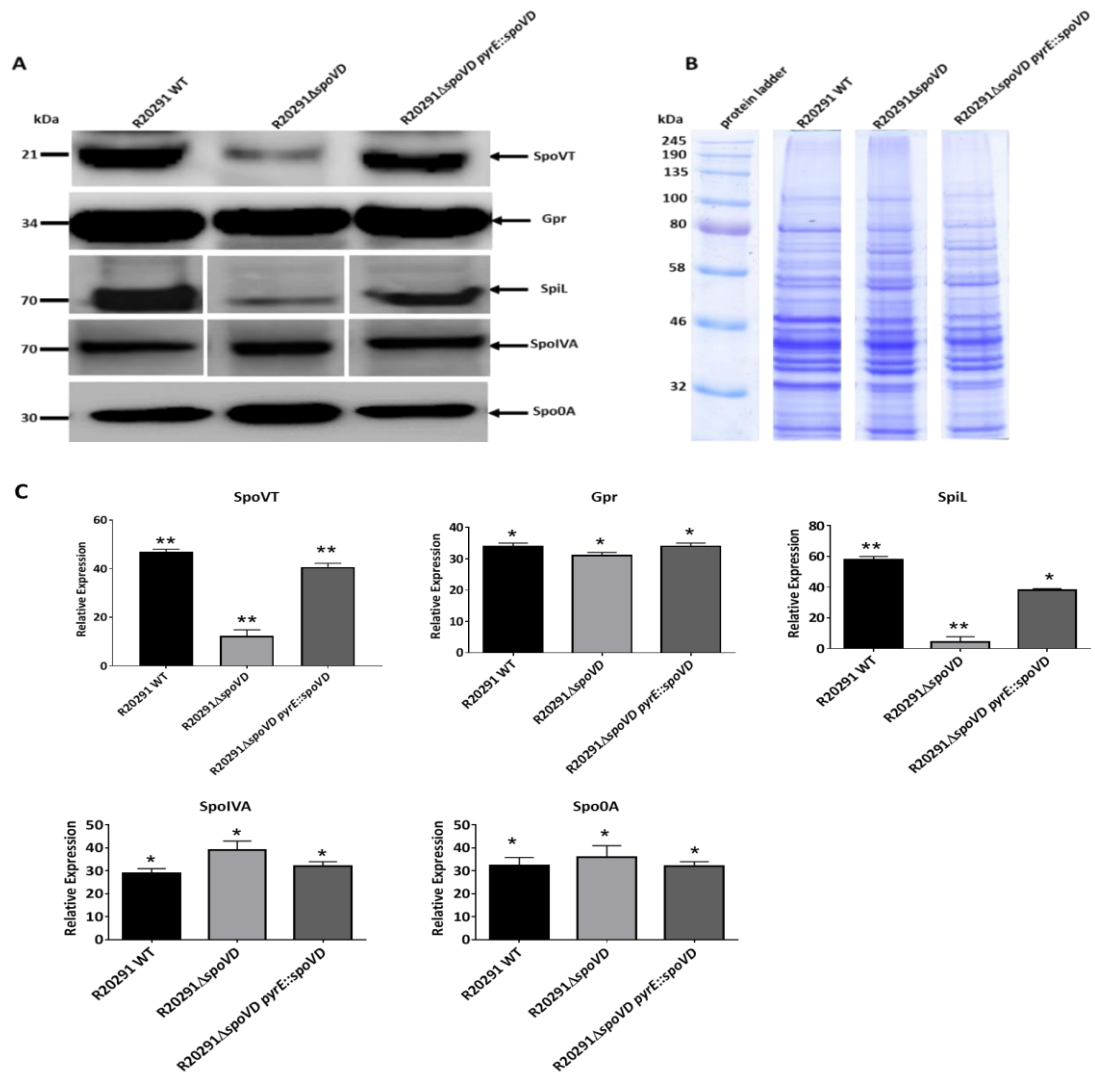


Figure 3.13: Western blot analyses of proteins known to be involved in sporulation. **A:** Western blot analyses of SpoVT, Gpr, SipL, SpoIVA and Spo0A in the three strains (wildtype, $\Delta spoVD$ and complemented). The strains were grown at 37°C in TY broth for 24 h. Each culture was lysed using bacteriophage endolysin and separated by 10%-12% SDS-PAGE. Proteins were detected using specific antisera supplied by Dr. Aimee Shen (Tufts University). **B:** SDS-PAGE analysis of the whole cell lysates. The stained gel was used as control for protein loading. Each sample was resuspended to OD_{600nm} 10 on the SDS-PAGE gel. **C:** Determination of the average intensity of each band in **A** using Image Lab software. Following background subtraction each was expressed as relative intensity. Shown are the mean and standard deviation of at least three biological repeats. p -value was measured using ANOVA statistic, OriginPro 2018 software. **: the population means are significantly different at the 0.01 level. *: the population means are not significantly different at the 0.01 level.

3.7 The impact of *spoVD* mutant on toxin production

In *C. difficile*, the sporulation process is typically started by phosphorylation of the master regulator Spo0A, leading to the sequential expression of four sigma factors (F, E, K and G) (de Hoon *et al.*, 2010). Spo0A in some *C. difficile* strains also regulates toxin production (Mackin *et al.*, 2013). Specifically, the Spo0A in *C. difficile* ribotype 027 negatively controls the expression of both TcdA and TcdB (Pettit *et al.*, 2014). The $\Delta spoVD$ mutant showed increased expression of Spo0A (as described in 3.6). Hence, the expression level of TcdB toxin in the three strains was examined. Western blot analysis of three biological repeats demonstrated that the *spoVD* mutant had a significant decrease in TcdB toxin production in comparison to both the wildtype and the complemented strains in both 48 h and 72 h cultures (Figure 3.14A). The average intensity of the mutant was 8 ± 1 and 6 ± 1 at 48 h and 72 h respectively. The wildtype was 46 ± 2 and 60 ± 5 at 48 h and 72 h respectively, while the complemented strain was 46 ± 3 and 27 ± 6 at 48 h and 72 h respectively (Figure 3.14C). Also, TcdB was visible upon SDS-PAGE analysis of the culture supernatants at the 48 h and 72 h time points for both the wildtype and the complemented strains (Figure 3.14B). None of the strains produced detectable toxin in mid-log or 24 h cultures.

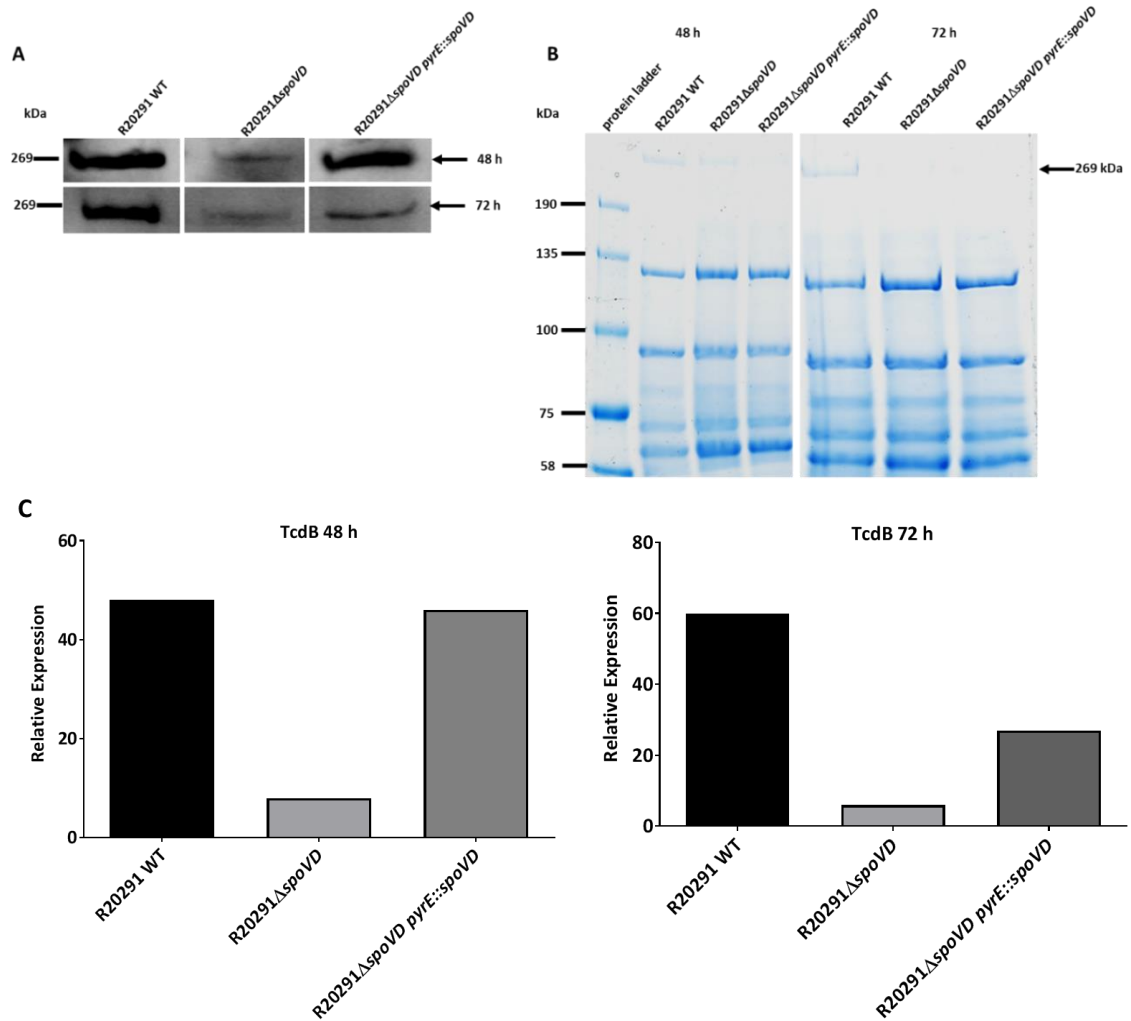


Figure 3.14: TcdB toxin production. **A:** Western blot analyses of TcdB in R20291, R20291ΔspoVD and R20291ΔspoVD pyrE::spoVD. The strains were grown at 37°C in TY broth for 72 h. Each culture supernatant was normalised to an OD_{600nm} of 10, and separated by 6% SDS-PAGE. TcdB was detected using specific antisera for TcdB (Thermo Fisher Scientific, #MAI-74B). **B:** SDS-PAGE analysis of the culture supernatants. The stained gel was used as control for protein loading in panel **A**. **C:** Determination of the average intensity of each band in **A** using Image Lab software. Following background subtraction each was expressed as relative intensity.

3.8 Function analysis of SpoVD domains

SpoVD has three main and conserved domains in both *B. subtilis* and *C. difficile*. These domains are PBP dimer (D), transpeptidase (T) and PASTA (P) (penicillin-binding protein and serine/threonine kinase associated domain). In *Bacillus subtilis*, SpoVD lacking the PASTA domain did not show a dramatic effect on sporulation, while changing Ser294, in the active site for the catalytic activity of the transpeptidase domain, has shown a significant effect on cortex assembly.

In order to identify the role of each domain in both cephalosporin resistance and sporulation efficiency, a series of *spoVD* truncations were cloned under the control of the constitutive promoter (P_{cwp2}). All constructed plasmids included a Clip tag protein fused to the N-terminal of SpoVD (as described in 3.5). The full length *spoVD* was cloned into plasmid pJAK032 between the *Xho*I and *Bam*HI restriction sites under the control of the constitutive promoter P_{cwp2} . Then the plasmid was truncated by inverse PCR, using divergent primers to delete the dimer domain (D) between residues Pro54-Asn241 resulting in pYAA048. Next, a PASTA domain (Tyr593-Asn659) deletion was constructed, also using inverse PCR, resulting in pYAA049. Subsequently, a transpeptidase domain (Asn241-Val584) deletion was constructed, resulting in pYAA050. Finally, a double deletion of both PBP dimer and PASTA domains (Pro54-Asn241 and Tyr593-Asn659 respectively) was constructed, resulting in pYAA051. In addition, Ser 311 was changed to Ala in the full length of *clip-spoVD*, resulting in pYAA063 (Figure 3.15A).

These plasmids were delivered to R20291 Δ *spoVD*, resulting in strains: R20291 Δ *spoVD*+*spoVD*(D.T.P), R20291 Δ *spoVD*+*spoVD*(T.P), R20291 Δ *spoVD*+*spoVD*(D.T), R20291 Δ *spoVD*+*spoVD*(D.P), R20291 Δ *spoVD*+*spoVD*(T) and R20291 Δ *spoVD*+*spoVD*(D.TS311A.P). The sporulation efficiency of these strains was tested to determine which constructs were able to restore cortex synthesis. Strains R20291 Δ *spoVD*+*spoVD*(D.T.P) and R20291 Δ *spoVD*+*spoVD*(D.T) showed formation of heat-resistant spores, sporulating to wildtype levels (Figure 3.16). This result supports the hypothesis that SpoVD is responsible for cortex assembly and the PASTA domain in SpoVD is not essential for cortex synthesis. These results are identical to those shown in *B. subtilis*, which demonstrated that a *spoVD* mutant showed cortex loss and deletion of

the PASTA domain alone (Lys582–Asp646) did not impact on cortex synthesis (Bukowska-Faniband and Hederstedt, 2013; Bukowska-Faniband and Hederstedt, 2015).

In contrast, complementation with transpeptidase and PASTA domains, PBP dimer and PASTA domains and transpeptidase domain alone gave the same sporulation efficiency as the *spoVD* mutant. Strains lacking the PBP dimer or transpeptidase domains did not sporulate at all. SpoVD may use the dimer domain to interact with SpoVE, a membrane protein involved in cell division during the sporulation process (Fay *et al.*, 2010). This interaction recruits SpoVD to the forespore membrane where it assembles the cortex layer. In *B. subtilis*, the SpoVD interaction with SpoVE is crucial for the cortex assembly. SpoVD binds to lipid II in the membrane after the interaction with SpoVE (Fay *et al.*, 2010).

Transmission electron microscopy (TEM) was performed to analyse sporulating cell morphology for all these strains (Figure 3.17). Expression of full length Clip-SpoVD or that lacking the PASTA domain resulted in the formation of morphologically normal spores. In contrast, the other strains showed spores lacking the cortex layer, containing only core and coat, as in the $\Delta spoVD$ strain. Taken together, this proved that the sporulation defect of these strains results from the loss of the cortex layer, resulting in heat-sensitive spores. Likewise, changing the Ser311 in the transpeptidase domain, leading to lose of the catalytic activity, caused misassembly of the spore cortex layer (Figure 3.17).

In addition, the minimum inhibitory concentrations of cephalosporins were determined for these strains. Strains R20291 $\Delta spoVD+spoVD$ (D.T.P), R20291 $\Delta spoVD+spoVD$ (T.P) and R20291 $\Delta spoVD+spoVD$ (D.T) were as resistant to cefoxitin and ceftazidime as the R20291 wild type (128 $\mu\text{g/ml}$ and 256 $\mu\text{g/ml}$ respectively). In contrast, the other strains R20291 $\Delta spoVD+spoVD$ (D.P), R20291 $\Delta spoVD+spoVD$ (T) and R20291 $\Delta spoVD+spoVD$ (D.TS311A.P), were as sensitive to cefoxitin and ceftazidime (32 $\mu\text{g/ml}$ and 64 $\mu\text{g/ml}$ respectively) as the *spoVD* mutant (Table 3.4).

Table 3.4: Minimum inhibitory concentrations against the wild type R20291 and truncation *spoVD* constructs strains ($\mu\text{g/ml}$).

Strains	Cefoxitin	Ceftazidime
R20291 Wild Type	128	256
R20291 Δ <i>spoVD</i>	32	64
R20291 Δ <i>spoVD</i> + <i>spoVD</i> (D.T.P)	128	256
R20291 Δ <i>spoVD</i> + <i>spoVD</i> (T.P)	128	256
R20291 Δ <i>spoVD</i> + <i>spoVD</i> (D.T)	128	256
R20291 Δ <i>spoVD</i> + <i>spoVD</i> (D.P)	32	64
R20291 Δ <i>spoVD</i> + <i>spoVD</i> (T)	32	64
R20291 Δ <i>spoVD</i> + <i>spoVDS311A</i> (D.T.P)	32	64

(D: PBP dimer, T: Transpeptidase, P: PASTA)

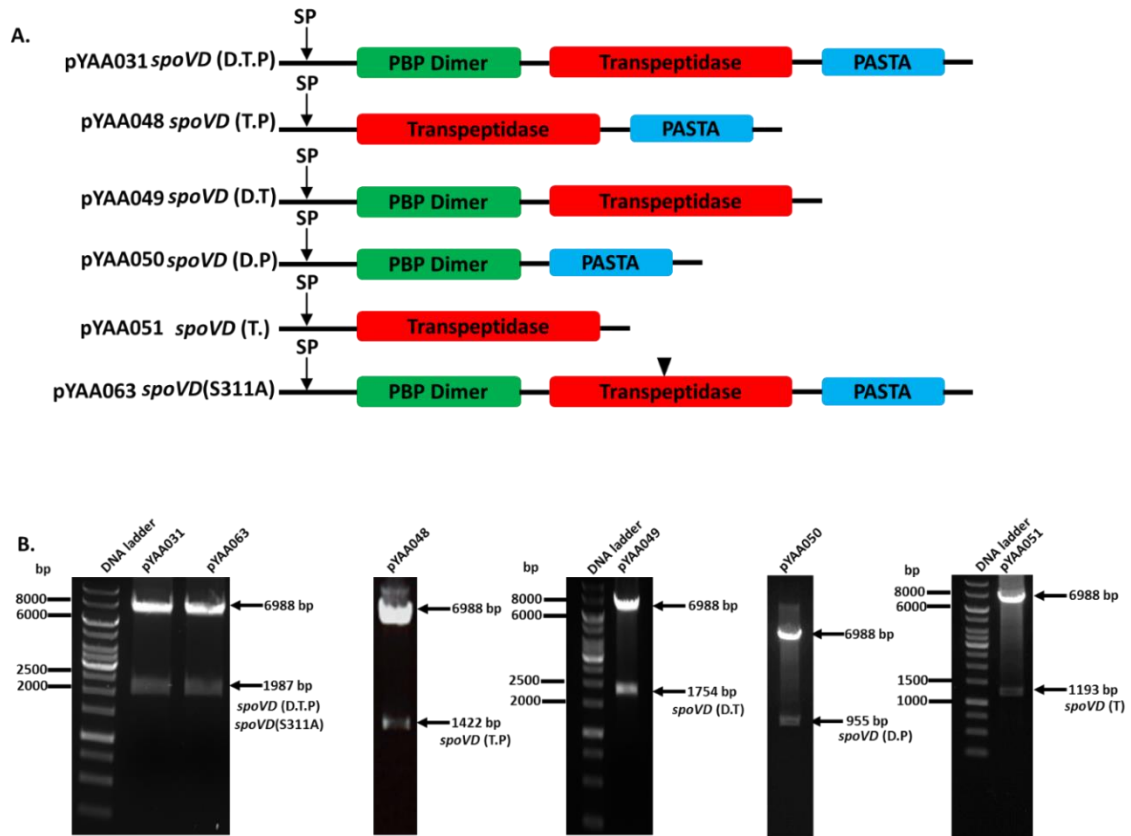


Figure 3.15: Functional analysis of SpoVD domains. **A:** Schematic diagram showing SpoVD truncation to remove PBP Dimer (D), Transpeptidase (T) or PASTA (P) domains. Domains were identified using (<http://pfam.xfam.org/search>), signal peptides (SP) were identified using (<http://www.cbs.dtu.dk/services/LipoP/>). The black triangle indicates the serine 311 to alanine point mutation. **B:** Agarose gel of double digestion for the each constructed plasmids using *Xho*I and *Bam*HI, confirming the successful insertion of *spoVD* (1,987 bp) into pJAK032 plasmid (6,988 bp). Other double digestions show the successful construction of plasmid pYAA031 (Clip-SpoVD(D.T.P)), pYAA063 (Clip-SpoVD (S311A)), pYAA048 (Clip-SpoVD(T.P)), pYAA049 (Clip-SpoVD(D.T)), pYAA050 (Clip-SpoVD(D.P)) and pYAA051 (Clip-SpoVD(T)). The double digestion using *Xho*I and *Bam*HI distinguished the expected product of each truncation of *spoVD*.

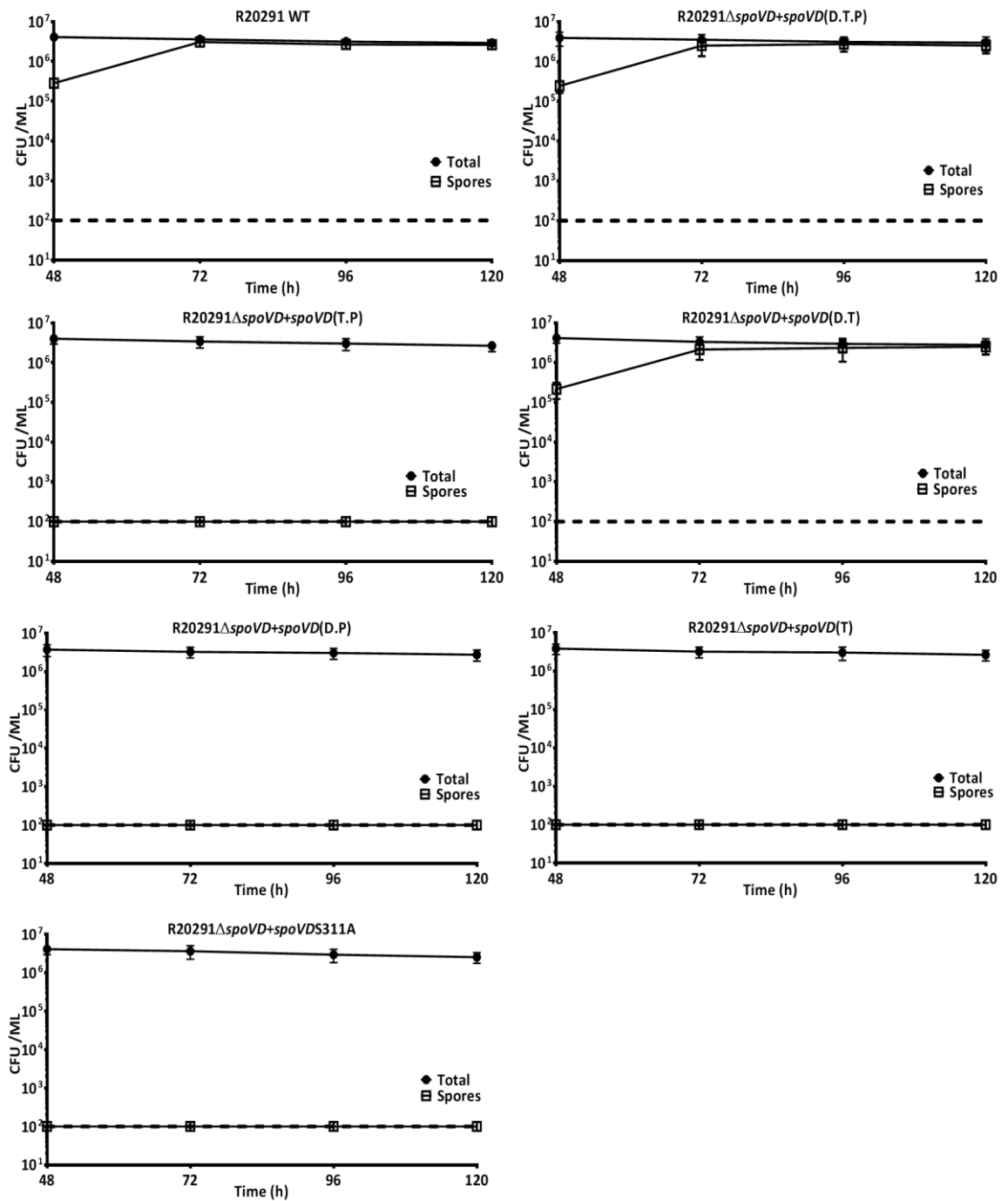
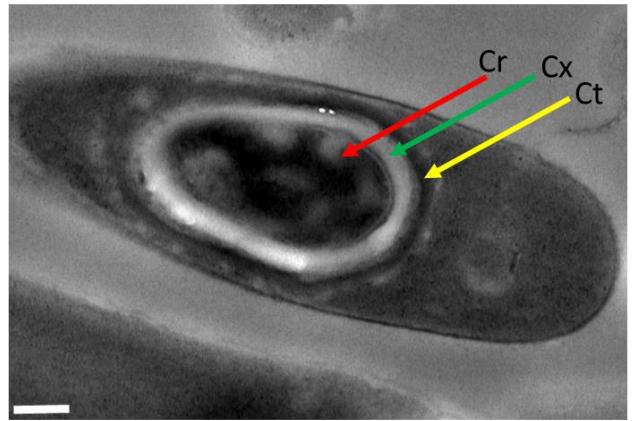
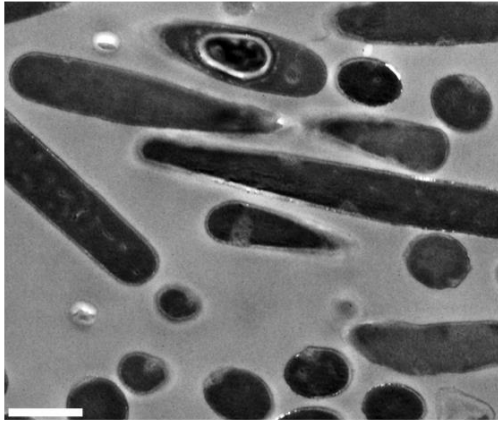
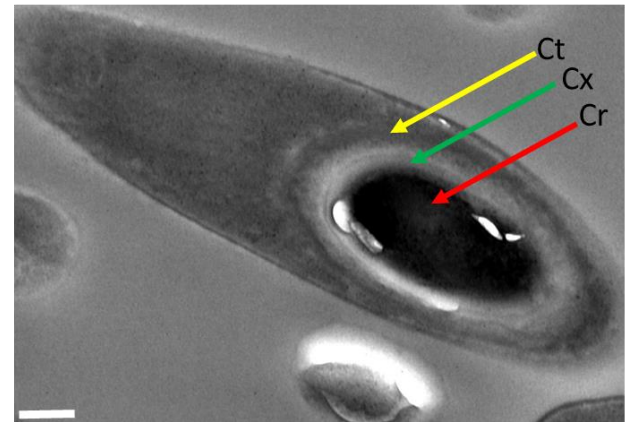
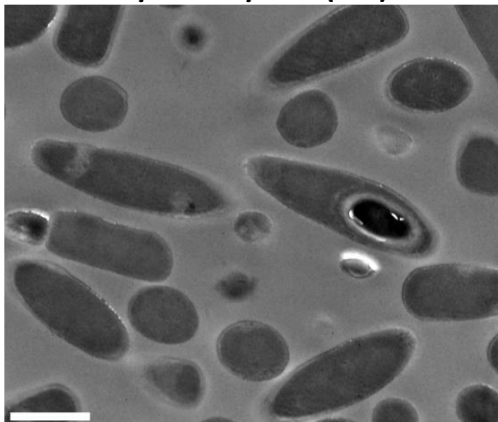


Figure 3.16: Sporulation requires both transpeptidase and PBP dimer domains. The bacterial cultures were incubated anaerobically at 37°C for 5 days in BHI-S broth. Total bacterial and spore counts were counted in each 24 h by CFUs (total) or CFUs (spores) after heat treatment at 65°C for 30 min. The assay was completed in triplicate. Standard deviations are represented by black error bars. The dotted line represents the limit of detection.

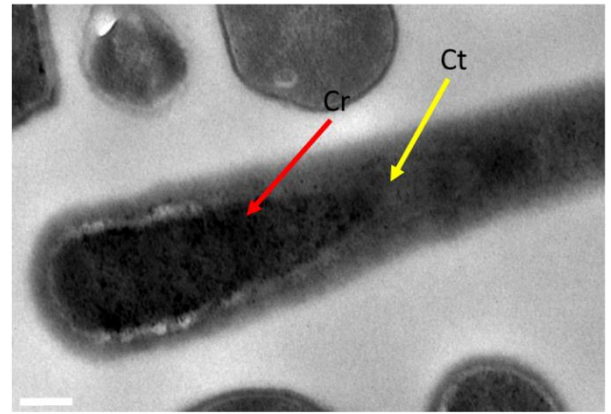
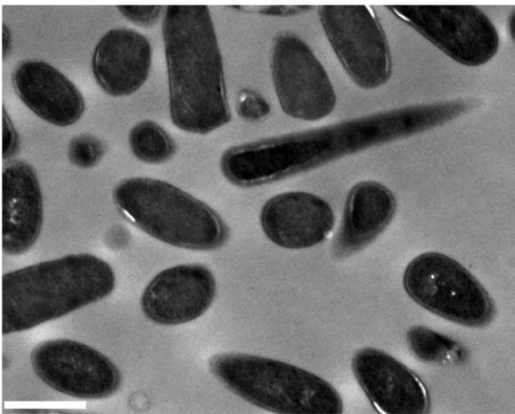
A R20291 Δ spoVD+spoVD(D.T.P)



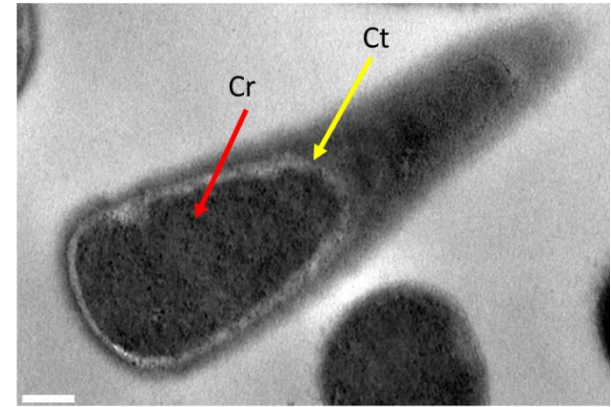
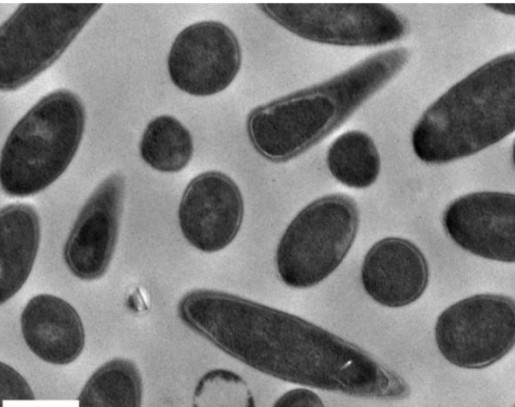
B R20291 Δ spoVD+spoVD(D.T)



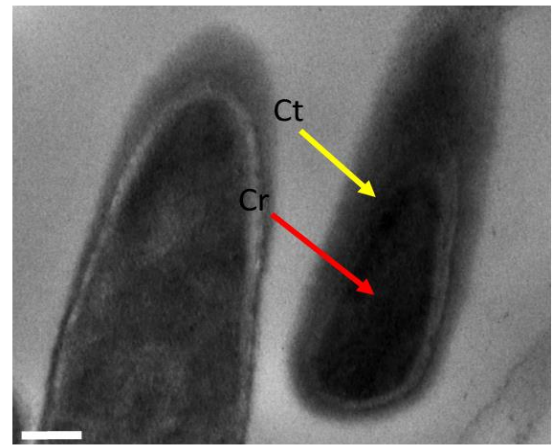
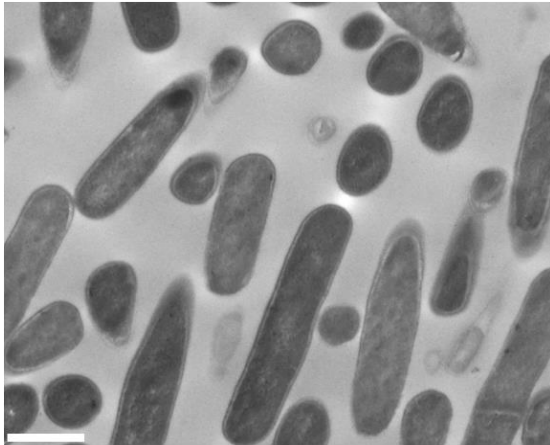
C R20291 Δ spoVD+spoVD(T.P)



D R20291 Δ spoVD+spoVD(D.P)



E R20291 Δ spoVD+spoVD(T)



F R20291 Δ spoVD+spoVD(S311A)

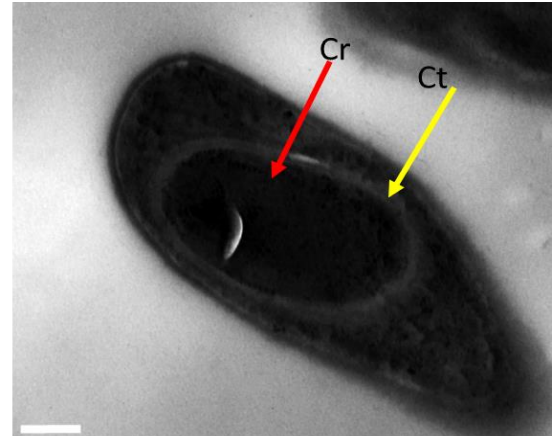
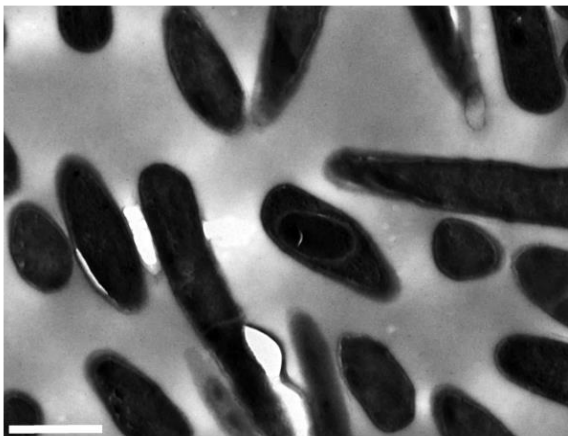


Figure 3.17: TEM analysis of *C. difficile* R20291 Δ spoVD+spoVD (the full-length and truncated spoVD) strain ultrasections. Plasmids carrying *clip-spoVD*(D.T.P) (**A**), *clip-spoVD*(D.T) (**B**), *clip-spoVD*(T.P) (**C**), *clip-spoVD*(D.P) (**D**), *clip-spoVD*(T) (**E**) and *clip-spoVD*(S311A) (**F**) were conjugated into the spoVD mutant strain. Following the conjugation, the strains were grown at 37°C in using TY broth for 24 h. **A** and **B** show the expected three structural layers in developing spores, core (Cr), cortex (Cx) and coat (Ct) as in the wild type. However, **C**, **D**, **E** and **F** show only two structural layers in developing spores, core (Cr) and coat (Ct) as in the mutant strain. Scale bar represents 1 μ m (left) and 0.2 μ m (right).

3.9 Interaction between SpoVD and SpoVE

Our functional analysis of domains of SpoVD showed that the PBP dimer domain deletion caused loss of sporulation efficiency. In *B. subtilis*, SpoVD interaction with SpoVE is crucial for the cortex assembly (Fay *et al.*, 2010). To determine if the same interaction occurs in *C. difficile*, the interaction between the SpoVD and SpoVE was analysed using split Snap and bacterial two-hybrid (BACTH) methods.

The interaction between SpoVD and SpoVE was systematically tested using the BACTH assay. In order to create recombinant plasmids, which can express the hybrid proteins, the T18 fragment of *cyaA* was fused to the N terminal or C terminal of SpoVD, and the T25 fragment of *cyaA* was fused to the N terminal or C terminal of SpoVE (as described in the methods; Karimova *et al.*, 2000).

The *spoVD* gene was cloned into pUT18C between *Bam*HI and *Sac*I, resulting in pYAA083 (T18-SpoVD), and into pUT18 between *Bam*HI and *Sac*I, resulting in pYAA084 (SpoVD-T18). The *spoVE* gene was then cloned into pKT25 between *Bam*HI and *Kpn*I, resulting in pYAA085 plasmid (T25-SpoVE), and into pKNT25 between *Bam*HI and *Kpn*I, resulting in pYAA086 (SpoVE-T25). However, all attempts to clone pYAA086 failed, perhaps due to toxicity in *E. coli*; each cloning produced a stop codon in a different position of the *spoVE* gene. Subsequently, the generated plasmids were co-transformed as pairs into *E. coli cya* DHM1 strain. All empty vectors and constructed plasmids were also transformed into *E. coli* DHM1 *cya* strain individually, as negative controls. The pUT18-zip and pKT25-zip plasmids were co-transformed into *E. coli* DHM1 *cya* strain as positive controls. Those plasmids express both the T18 and T25 fragments fused to the dimerization leucine zipper motifs (Karimova *et al.*, 1998).

The BACTH assay depends on the catalytic activity of CyaA from *Bordetella pertussis*, allowing synthesis of cAMP. cAMP binds to the CAP protein, which is a catabolite activator. The complex (cAMP/CAP) is responsible for regulation of transcription of many genes, including *lac* and *mal*, that are responsible for lactose and maltose utilisation. Therefore, the bacteria are able to utilize the sugars (lactose or maltose) as sole carbon source (Karimova *et al.*, 1998). In addition, the complex cAMP/CAP controls the *lacZ* gene encoding the β -galactosidase enzyme, which can

hydrolyse X-Gal (5-bromo-4-chloro-3-indolyl- β -D-galactopyranoside) in the media. Eventually, once the galactosidase enzyme hydrolyses X-Gal the *E. coli* colonies become blue (Ullmann and Danchin, 1983; Miller,1992).

The strain co-transformed with plasmids expressing T18-SpoVD and T25-SpoVE showed a significant hydrolysis of X-Gal (blue colonies) on LB agar. Subsequently, the efficiency of *cyoA* restoration by T18-SpoVD-T25-SpoVE was determined by direct β -galactosidase quantification using 4-methylumbelliferyl β -D-galactopyranoside (MUG) as a substrate (Figure 3.18).

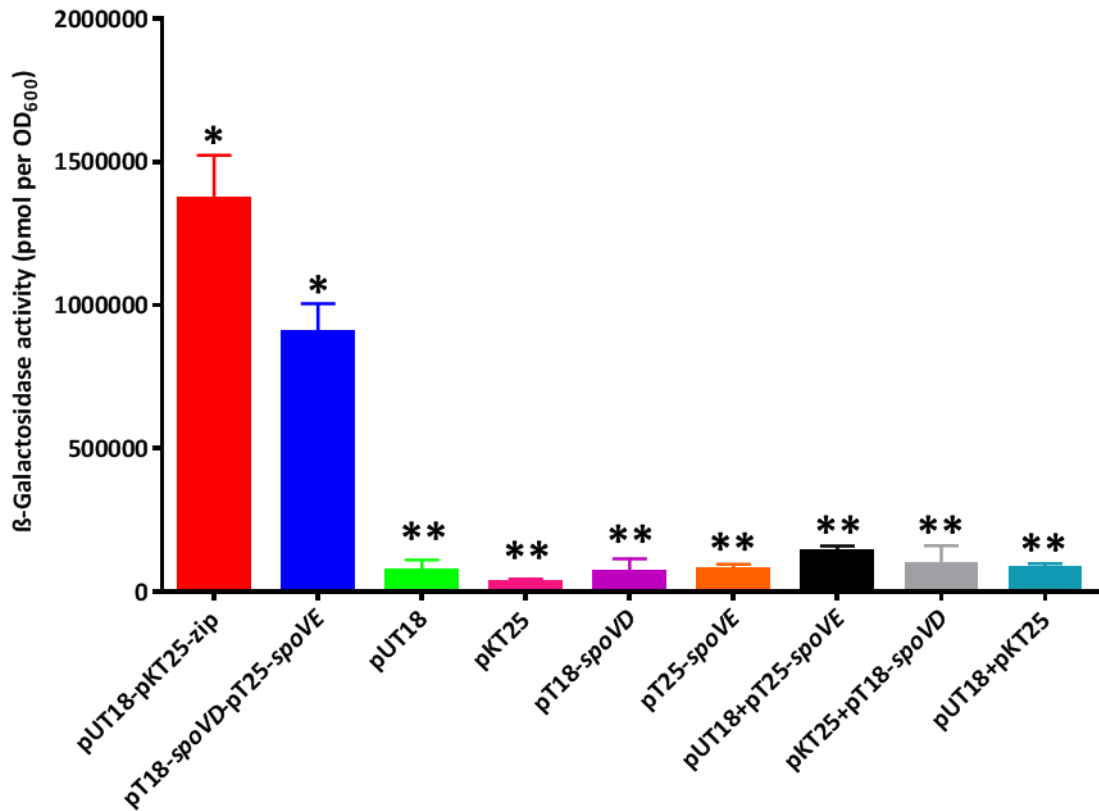


Figure 3.18: β -galactosidase assays showing the interaction between SpoVD and SpoVE. The *E. coli* DHM1 *cya* strain was used as a host for transformation of all the plasmids. pUT18-zip and pKT25-zip were co-transformed and used as positive controls. The strains were induced with 0.5 mM IPTG at 30°C for three hours. The assay was performed in triplicate with three technical repeats. Shown are means of triplicate assays with standard deviations represented by error bars. The enzyme activity was measured and normalised to OD_{600nm}. *p*-value was measured using ANOVA statistic, OriginPro 2018 software. **: the population means are significantly different at the 0.01 level. *: the population means are not significantly different at the 0.01 level.

The interaction between SpoVD and SpoVE was confirmed using the split SNAP tag. The Snap tag is a 20 kDa protein, an O6-alkylguanine-DNA alkyltransferase (hAGT) (Keppler *et al.*, 2003). It is responsible for DNA repair by protection from alkylation. Alkylation process causes DNA damage, attaching an alkyl group to the guanine base. The AGT protein is able to form S-methylcysteine, after O6-alkylguanine converts to the guanine (Fang *et al.*, 2005).

The N-terminal domain of the Snap protein is responsible for enhancing the DNA repair activity, while the C-terminal domain is responsible for the alkyl transfer, containing the acceptor site Cys145. This residue binds O6-alkylguanine to the DNA (Fang *et al.*, 2005). The protein has been crystallised showing those two domains (Wibley *et al.*, 1995). The Snap protein binds covalently to substrates such as TMR-Star, fluorescent derivatives of benzyl purines and benzyl pyrimidines (Keppler *et al.*, 2003). The Snap tag can be split into two parts, as in the BACTH system. The N-terminus, called nSnap, includes residues 1 to 91 and the C-terminus, called cSnap, contains residues 92 to 182. This separation was optimised for restoration of Snap function in the same manner, as in *cyaA* in BACTH (Mie *et al.*, 2012).

The nSnap tag encoding DNA was fused to the 5' end of *spoVD* in the native locus using homologous recombination (Figure 3.18A). The resulting strain was R20291 *nsnap-spoVD*. The fusion insertion was confirmed by PCR using primers flanking the *spoVD* gene (Figure 3.18A), showing the expected product of 2,800 bp for R20291 *nsnap-spoVD*, while the wild type R20291 showed the predicted product of 2,518 bp (Figure 3.18B). Subsequently, the cSnap tag encoding DNA was fused to the 5' end or the 3' end of *spoVE* with expression under the control of the constitutive promoter P_{cwp2} , between *Bam*HI and *Xho*I or *Sac*I and *Xho*I respectively (as described in the methods). The resulting plasmids were pYAA054 and pYAA055 respectively. These plasmids were digested with *Bam*HI and *Xho*I or *Sac*I and *Xho*I, confirming the successful insertion of *csnap-spoVE* and *spoVE-csnap* (Figure 3.18C).

Next, these plasmids were conjugated into strain R20291 *nsnap-spoVD*. The resulting strains were R20291 *nsnap-spoVD+csnap-spoVE* and R20291 *nsnap-spoVD+spoVE-csnap*. The empty plasmid, carrying *csnap* expressed under the control of the constitutive promoter P_{cwp2} was also conjugated into the strain R20291 *nsnap-*

spoVD. The resulting strain was R20291 *nSnap-spoVD+csnap*. The R20291 *nSnap-spoVD+csnap* strain and the original strain R20291 *nSnap-spoVD* were used as negative controls for both labelling and protein-protein interaction.

The strains were labelled with TMR-Star in the exponential phase after 3 h growth, in stationary phase at 24 h and late stationary phase at 48 h. The results showed a positive signal for TMR-Star nSnap-SpoVD-cSnap-SpoVE interaction in mid-log phase, localising to the mother cell compartment. In contrast, in the stationary phase at 24 h and late stationary phase at 48 h, the nSnap-SpoVD-cSnap-SpoVE interaction seems to be confined to the forespore membrane.

The localization of nSnap-SpoVD+SpoVE-cSnap showed similar results, albeit with lower fluorescent signals (data not show). This is similar to that obtained in the BACTH assay. The strains R20291 *nSnap-spoVD* and R20291 *nSnap-spoVD+csnap* were also labelled as negative controls (Figure 3.19). Taken together, this suggests that SpoVD and SpoVE interact. This identical to *B. subtilis*, in which SpoVD and SpoVE localise to the forespore membrane (Fay *et al.*, 2010).

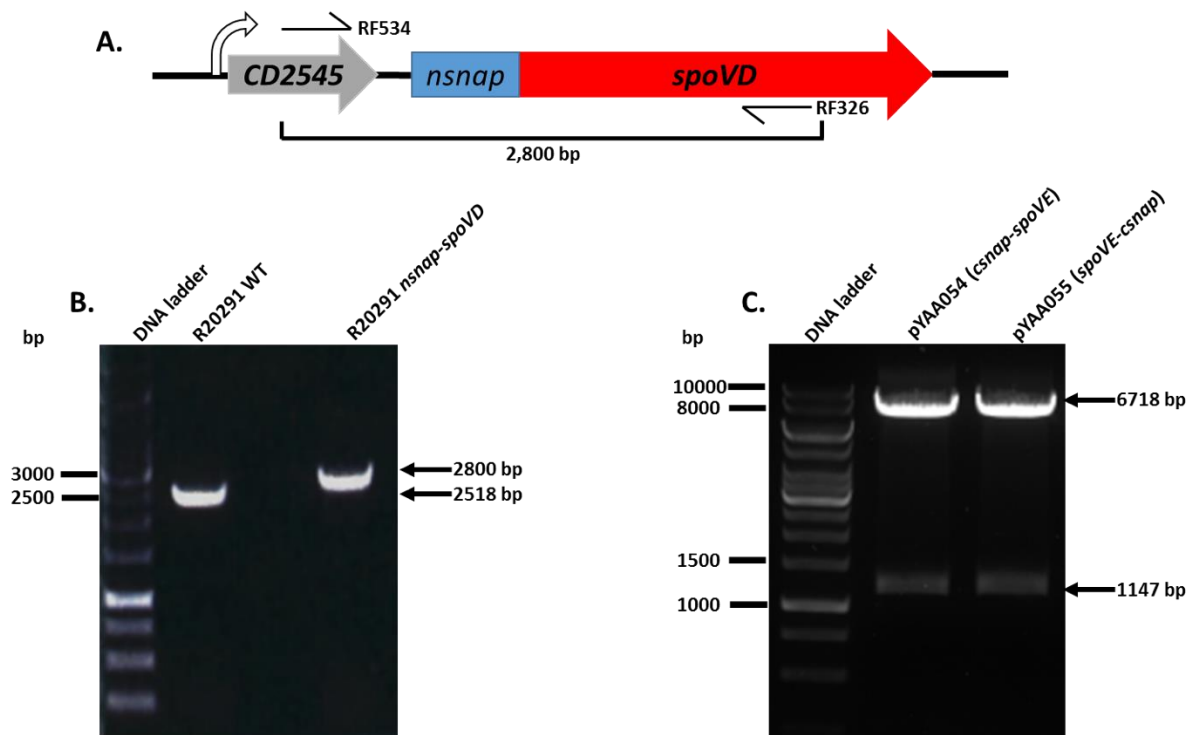
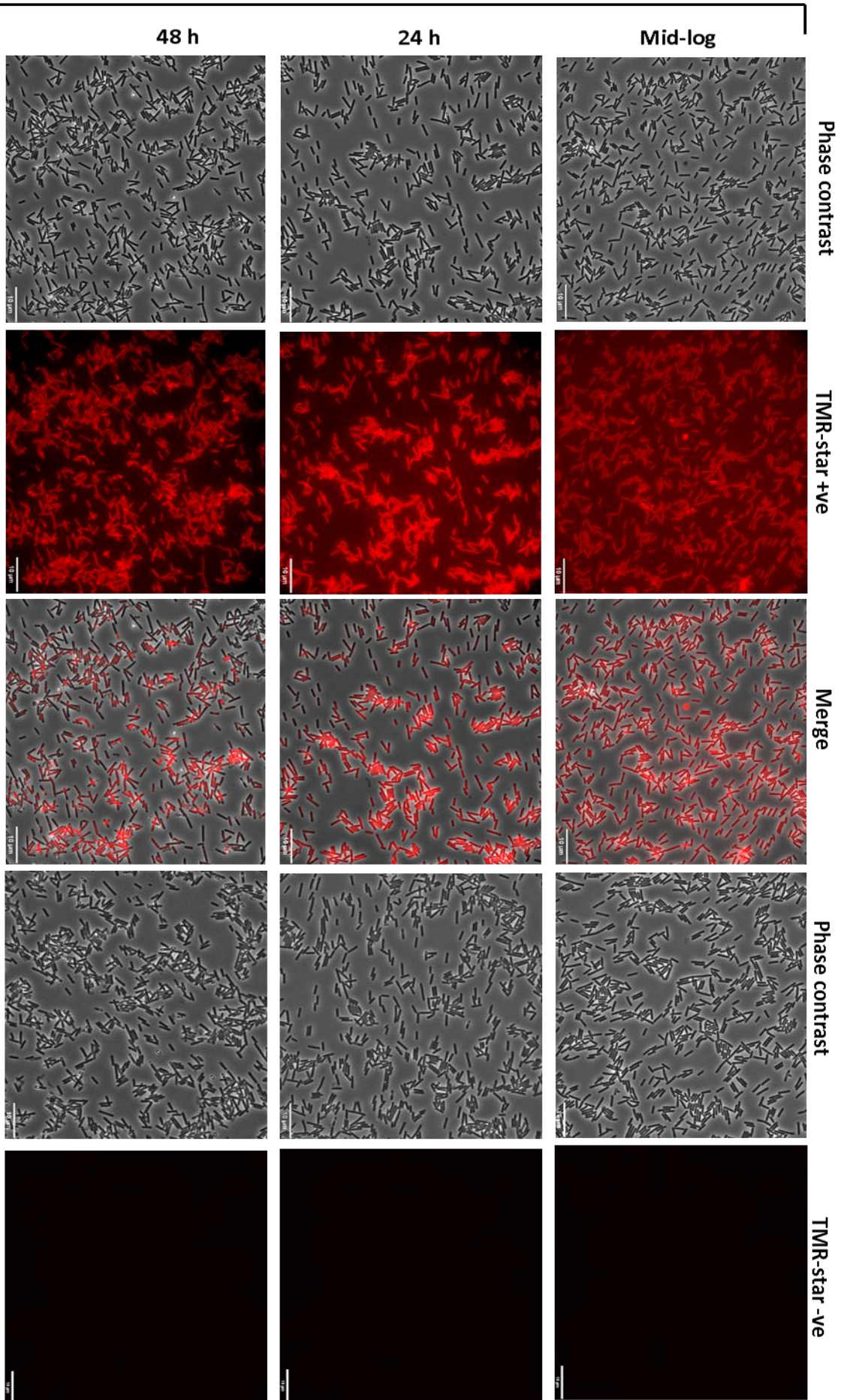


Figure 3.18: The interaction between SpoVD and SpoVE. **A:** Schematic diagram showing the primer design for screening R20291 *nsnap-spoVD*. **B:** Agarose gel showing PCR screen confirming a successful insertion of the nSnap tag in the chromosomal *spoVD* gene, using primers flanking the *spoVD* gene (RF534 and RF326). PCR showed the expected product of 2,800 bp for insertion of the nSnap tag, whereas the wild type R20291 showed the expected product of 2,518 bp. **C:** Agarose gel of double digestion for each constructed plasmid using *Xho*I, *Sac*I or *Bam*HI, *Xho*I, confirming the successful cloning of *spoVE* (1,147 bp) into pAMBL008 and pAMBL009 plasmids respectively (6,718 bp), which yielded pYAA054 (cSnap-SpoVE) and pYAA055 (SpoVE-cSnap). These plasmids were conjugated into strain R20291 *nsnap-spoVD* to demonstrate the interaction between SpoVD and SpoVE proteins using split Snap tag method.

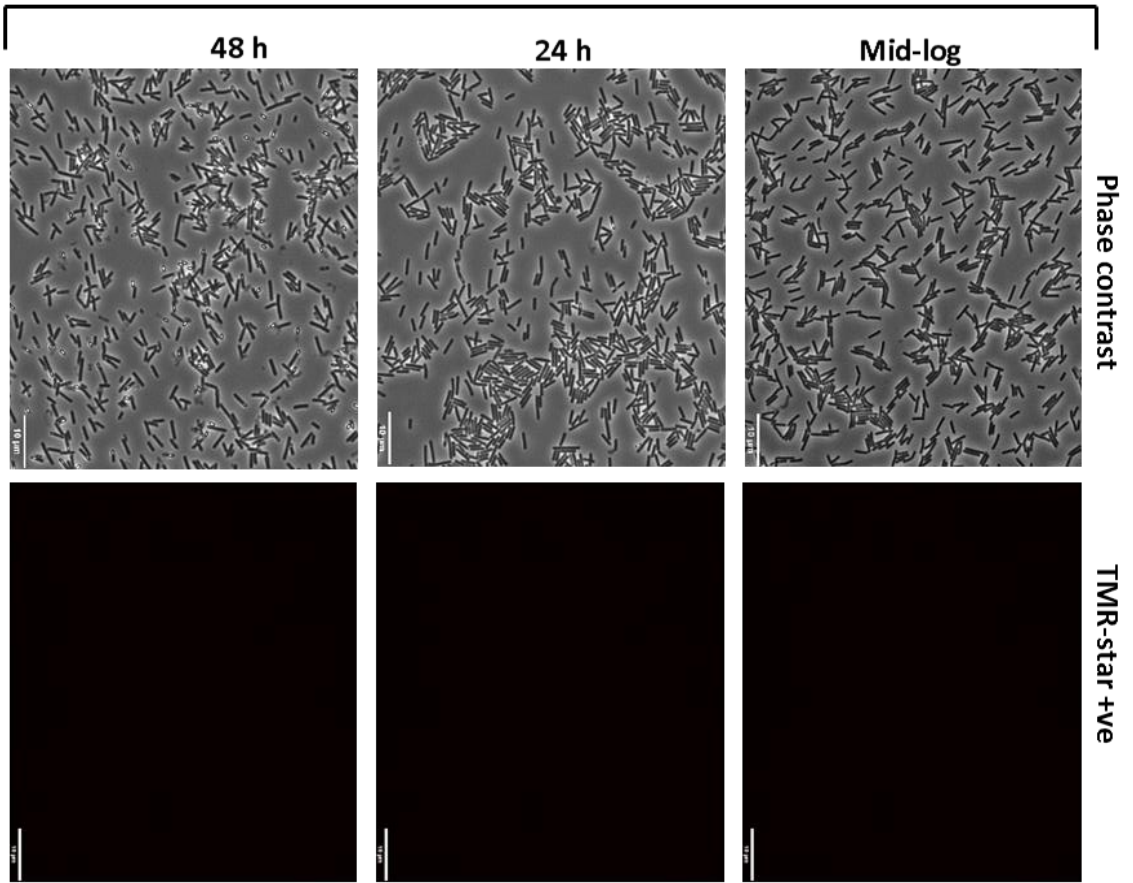
nSnap-SpoVD+cSnap-SpoVE localisation

A



nSnap-SpoVD localisation

B



nSnap-SpoVD+cSnap localisation

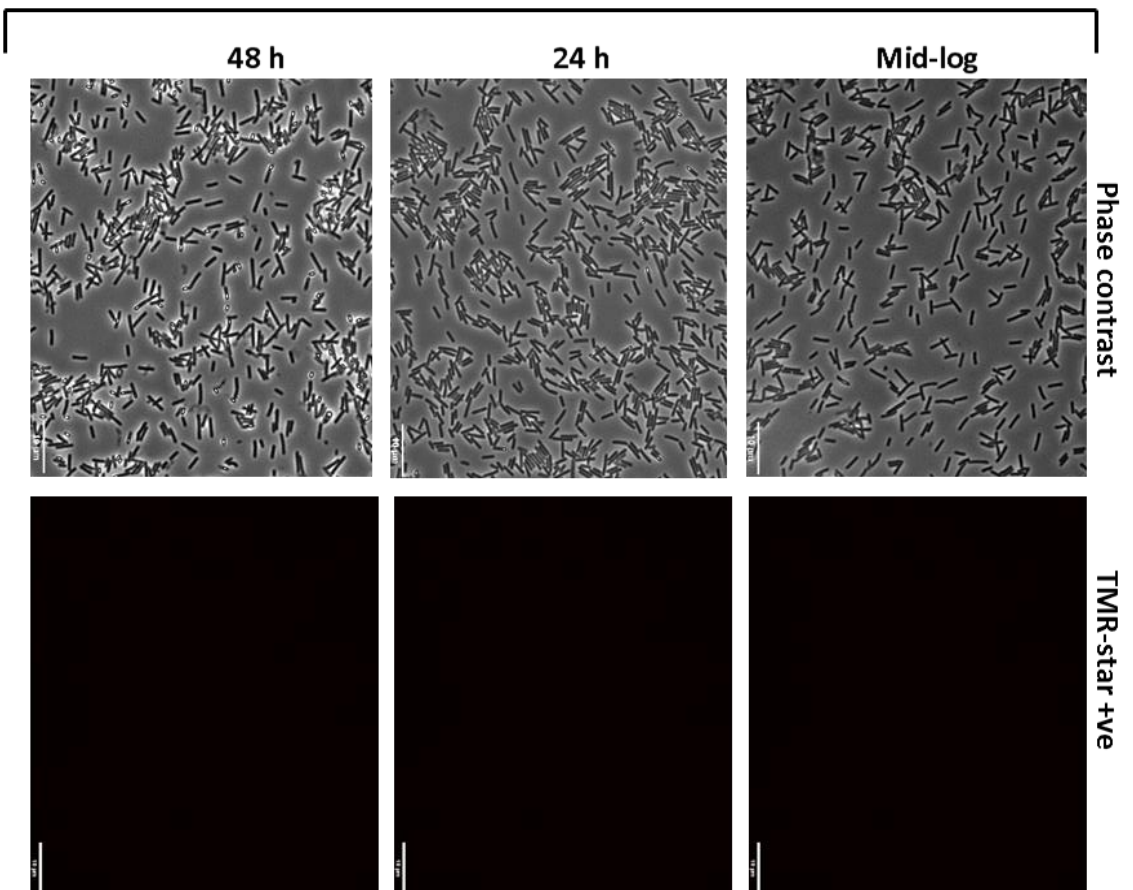


Figure 3.19: The interaction between SpoVD and SpoVE. **A:** The Snap tag was split into nSnap and cSnap. *nsnap* was fused to *spoVD* in the native locus on the chromosome, while *csnap* was cloned with *spoVE* into a plasmid under the control of constitutive promoter P_{cwp2} . The plasmids encoding *csnap-spoVE* and *spoVE-csnap* were conjugated into strain R20291 *nsnap-spoVD*. R20291 *nsnap-spoVD+csnap-spoVE* at 3 h, 24 h, 48 h in TY broth cultures was visualised using phase contrast and fluorescence microscopy. Each culture was labelled with 250 nM TMR-star for 1 h, fixed with 3.7% formaldehyde and dried onto glass slides. Fluorescent microscopy showed that nSnap-SpoVD-cSnap-SpoVE seem to interact in exponential phase and localise to the mother cell. In stationary phase at 24 h and late stationary phase at 48 h, nSnap-SpoVD-cSnap-SpoVE is localised to the forespore membrane. Unlabelled cultures were included as negative controls. Scale bar represents 10 μm . **B:** R20291 *nsnap-spoVD* and R20291 *nsnap+csnap* strains labelled with 250 nM TMR-star for 1 h, as negative control, fixed with 3.7% formaldehyde and dried onto glass slides. The fluorescence microscopy did not show a signal. This suggests the Snap protein has not linked to the substrate. Scale bar represents 10 μm .

3.10 SpoVD is a Class B PBP

In order to confirm that the SpoVD protein has transpeptidase activity, we cloned and purified the protein. His tag encoding DNA was fused to the 5' end of *spoVD* in pET-28a using the restriction enzymes *NheI* and *XhoI*. Following the cloning, the plasmid was transformed into *E. coli* strain Rosetta. Subsequently, protein expression was induced using overnight express instant TB, followed by purification (Figure 3.2A). The molecular weight (MW) of His-SpoVD was confirmed by electrospray ionisation mass spectrometry to 71.38 kDa (Figure 3.20C).

Next, the codon of the active site serine 311 (TCT) was changed to alanine (GCG) by an inverse PCR, to allow identification of the acylation site, which is responsible for the acyl-enzyme mechanism. Subsequently, the SpoVDS311A protein was purified as before (Figure 3.20B). The MW difference was confirmed by electrospray ionisation mass spectrometry to 71.36 kDa (Figure 3.20D). The serine 311 in SpoVD was modified to alanine, after identification of the active motif, containing (Ser-Xaa-Xaa-Lys) residues. These residues were considered as structural, functional and conserved residues in the penicillin binding protein that is typically recognised by class A β -lactamases (Matagne *et al.*, 1999). In *B. subtilis* the substitution of Ser294 to alanine leads to loss of binding with Bocillin-FL substrate. Also, this point mutation forms a heat sensitive spore lacking the cortex layer under the EM (Bukowska-Faniband and Hederstedt, 2013).

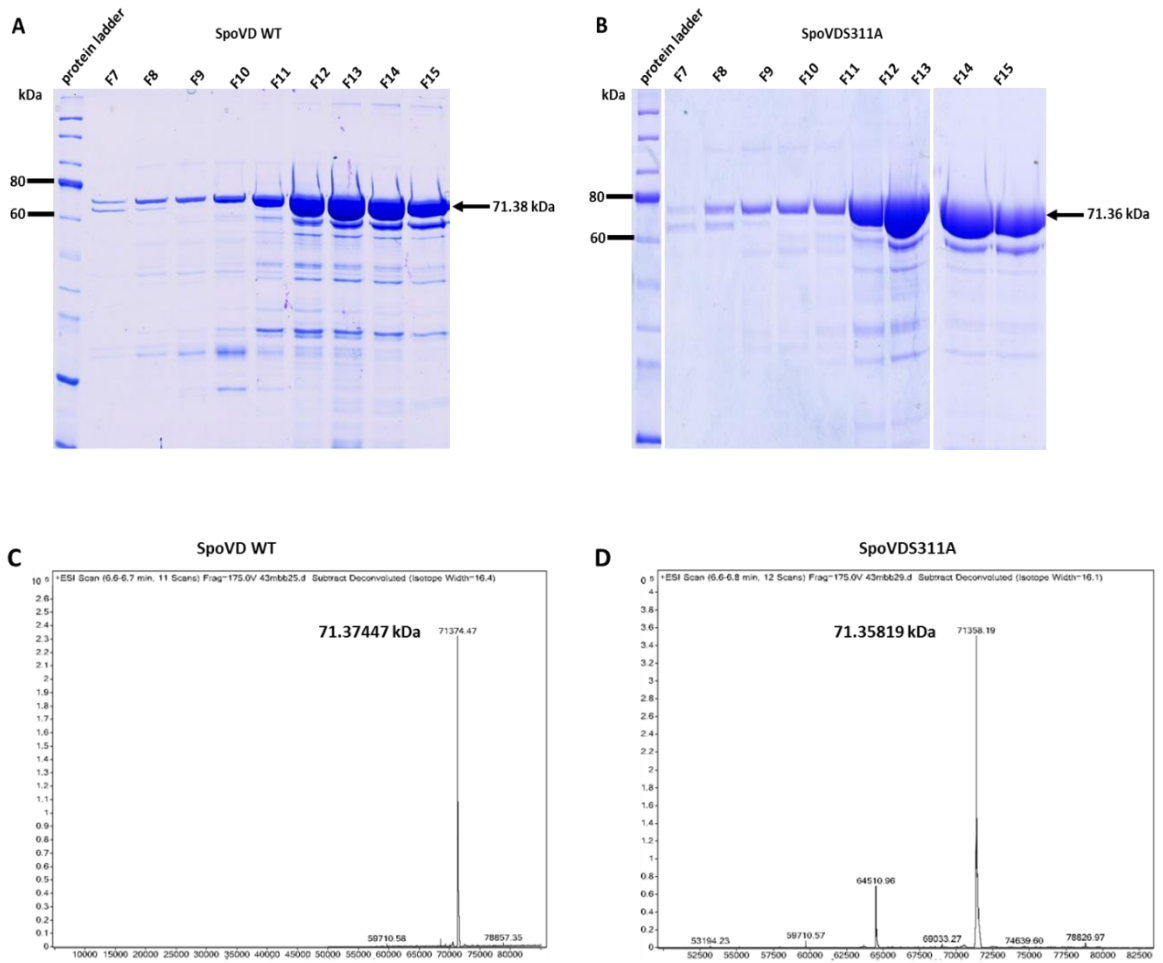


Figure 3.20: Purification of SpoVD and SpoVDS311A. **A** and **B** fractions of His-SpoVD and His-SpoVDS311A eluted from Ni-NTA were analysed by SDS-PAGE stained with Coomassie blue. The fractions with good quality protein were pooled and dialysed against 25 mM Tris, 50 mM NaCl pH 8. **C** and **D** mass spectra of SpoVD and SpoVDS311A, 71.38 kDa and 71.36 kDa respectively.

Subsequently, the transpeptidase activity of both proteins was tested using Bocillin-FL. This is a commercial derivative of penicillin V, bound to a fluorophore by a linker. This substrate binds to and detects PBPs (Zhao *et al.*, 1999). SpoVD bound covalently to the Bocillin-FL substrate (Figure 3.21), whereas the SpoVDS311A failed to bind. This confirmed the disruption of the SpoVD transpeptidase activity by this point mutation (Figure 3.21).

To confirm the acylation mechanism of SpoVD, the protein was preincubated with ceftazidime at different concentrations (14 μM , 28 μM , 56 μM , 112 μM) for 2 h at 37°C to complete the acylation process, followed by addition of Bocillin-FL. Preincubation with ceftazidime blocked labelling with Bocillin-FL (Figure 3.21A). This suggests that the β -lactam ring of the ceftazidime antibiotics binds with the active serine of SpoVD, competing with Bocillin-FL. This is a similar result to that shown in blocking the activity of OXA-1 β -Lactamase from binding with Bocillin-FL, after preincubation OXA-1 with ampicillin (Schneider *et al.*, 2009).

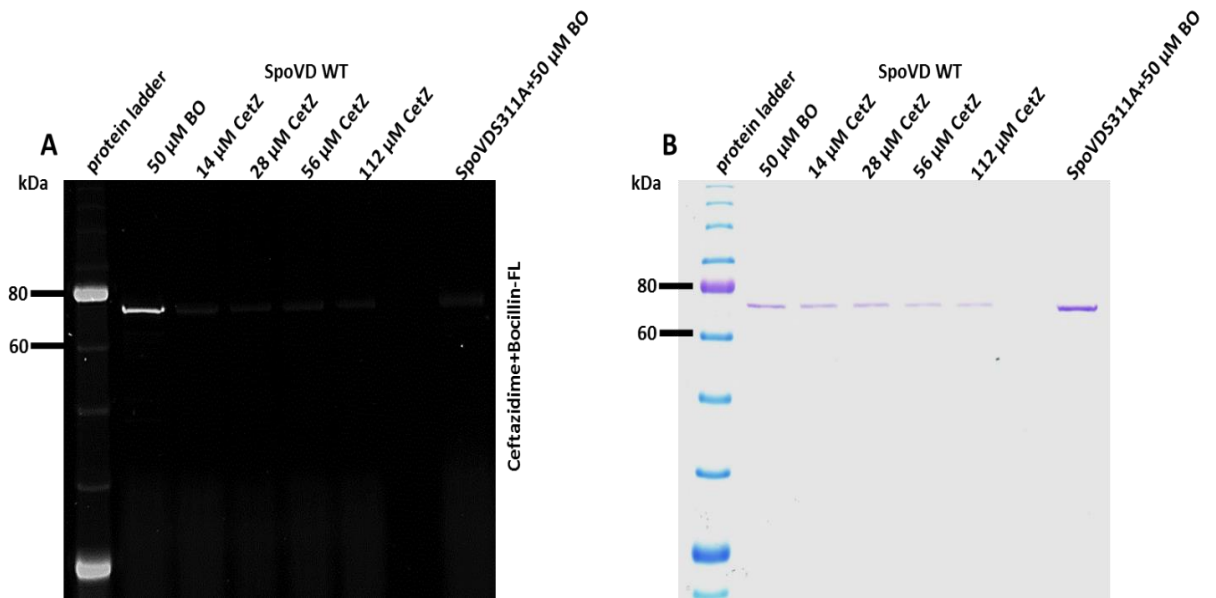


Figure 3.21: Bocillin-FL labelling of SpoVD and SpoVDS311A. **A:** labelling SpoVD with Bocillin-FL substrate at 50 μM for 30 min at 37°C, separated by 10% SDS-PAGE. The protein was also preincubated with ceftazidime for 2 h at different concentration 14 μM, 28 μM, 56 μM, 112 μM, allowing protein binding, followed by Bocillin-FC labelling for 30 min at 37°C. The fluorescent signal detection confirmed the acyl-enzyme intermediates of binding the SpoVD with Bocillin-FL, while the mutant protein SpoVDS311A lost the signal completely. This suggests that the Serine 311 is the active site for binding with the β-lactam ring substrate. The fluorescent gel was imaged using a Cy3 filter. **B:** gel from panel **A** stained with Coomassie blue, resolving both proteins WT and mutant SpoVD. The stained gel was used as control for protein loading. BO: Bocillin-FL, CetZ: ceftazidime.

3.11 Discussion

The aim of the work presented in this chapter was to investigate the role of SpoVD in sporulation and cephalosporin resistance. Spores are completely resistant to many environmental conditions, including chemical and physical agents (Paredes-Sabja *et al.*, 2014). The spores are required to survival in oxygenated or acidic environments, such as outside the host or in the human stomach. The spore germinates to produce a vegetative cell, which proliferates in the anaerobic environment of the gut. Indeed, a deletion of the master regulator *spo0A* prevents persistence and transmission even though *C. difficile* can still cause disease (Deakin *et al.*, 2012).

In *Bacillus subtilis*, the SpoVD protein is classified as a class B PBP (high molecular weight), and it is an essential protein for synthesis of the spore cortex (Daniel *et al.*, 1994; Fay *et al.*, 2010; Liu *et al.*, 2010). In *B. subtilis*, a *spoVD* mutant produced heat sensitive spores, lacking the cortex layer (Bukowska-Faniband and Hederstedt, 2013). The SpoVD protein contains four domains, an N-terminal transmembrane helix (residues 12-31), followed by a domain of unknown function (residues 54-206), the transpeptidase domain (residues 246-557) and a PASTA domain (residues 584-638) (Bukowska-Faniband, 2015). The transpeptidase domain is responsible for the formation of cross-links between the two peptidoglycan precursors in the spore cortex (Liu *et al.*, 2010). The glycan synthesis by SpoVD and the stability of the protein ultimately depend on SpoVE (Fay *et al.*, 2010). This is a membrane protein (lipid II flippase), that protects SpoVD from protease activity (Fay *et al.*, 2010).

In this project, the *spoVD* gene was deleted in *C. difficile* ribotype 027 strain R20291 to elucidate the function of SpoVD during sporulation and cephalosporin resistance. Our results showed that the *spoVD* mutant has a sporulation defect, with phase dark spores completely lacking the cortex. Furthermore, the MIC values of both ceftazidime and cefoxitin were decreased significantly compared to the wild type strain. Complementation restored both sporulation efficiency and cephalosporin resistance, with normal phase bright spores. The complemented strain also showed heat resistant spores, with apparently restored cortex layer. Indeed, previous studies have shown that mutations in *spoIVA*, *sipL*, *spoVT* or sigma factors (*sigF*, *sigE*, *sigK* and *sigG*) also resulted in the production of phase dark spores (Fimlaid *et al.*, 2013; Putnam *et al.*, 2013 and

Saujet *et al.*, 2013). This suggests that SpoVD has two strong phenotypes related to the transpeptidase activity. In *B. subtilis*, the transpeptidase activity of SpoVD has been demonstrated using Bocillin-FL labelling (Bukowska-Faniband and Hederstedt, 2013). The serine residue in the transpeptidase domain is responsible for covalent binding with a β -lactam ring (Goffin and Ghuysen, 1998). The substitution of Ser294 to Ala resulted in loss of Bocillin-FL binding, and the bacteria were unable to produce heat resistant spores (Bukowska-Faniband and Hederstedt, 2013). We have shown that changing Ser311 to Ala in *C. difficile* the transpeptidase domain resulted in heat sensitive spores, lacking the cortex layer. Furthermore, this change also resulted in cephalosporin sensitivity. This clearly shows that Ser311 is the active site serine responsible for binding with the β -lactam ring. This observation also demonstrated that SpoVD is a class B PBP, as in *B. subtilis* (Bukowska-Faniband and Hederstedt, 2013).

One of the most important objectives of this project was localisation of SpoVD. Firstly, we showed that Clip-SpoVD is more functional than SpoVD-Clip in restoration of sporulation efficiency. In contrast, in *B. subtilis*, SpoVD-mCherry fusions are more active than a GFP-SpoVD fusion (Bukowska-Faniband and Hederstedt, 2015). Moreover, our data showed that SpoVD is localised to the mother cell compartment early in the sporulation process. While in the later stage of sporulation the protein is localised to the forespore membrane, as in *B. subtilis* (Bukowska-Faniband and Hederstedt, 2015). Our observation of SpoVD expression during exponential phase is consistent with a role in vegetative cell peptidoglycan synthesis. This has not been previously observed in *Bacillus subtilis* or *C. difficile* and may explain the effect of *spoVD* deletion on cephalosporin resistance.

The next step of this project was the analysis of the impact of $\Delta spoVD$ on SspA, SipI, SpoVT, Gpr and SpoIVA expression and localization. We observed overexpression of SpoIVA (protein coat) and Spo0A (master regulator), and lower expression for Gpr, SpoVT and SipL. Taken together, this suggests that the cortex was lost following *spoVD* deletion, possibly leading to effects on the sigma factor cascade, specifically SigF and SigE. Furthermore, the sporulation defect in $\Delta spoVD$ may be responsible for the observed overexpression of Spo0A and this could influence SpoVT, Gpr and SpiL (low expression level), while also leading to high expression of SpoIVA. Complementation

restored the level of expression, but not for all the genes tested. This could be due to differences in expression of SpoVD from the native locus compared to the *pyrE* locus. These analyses were underpinned by fluorescence labelling of the Snap protein from SspA, SipL and SpoVT promoter reporters. Fluorescence microscopy and in-gel fluorescence also showed lower expression and mislocalization for SpoVT and SipL promoter activity in $\Delta spoVD$, while SspA promoter activity was localised to the forespore compartment, as in the wildtype and complemented strains.

In *B. subtilis*, *sspA* encodes a small acid-soluble protein (SASP) that can protect the DNA from many physical and chemical agents such as UV radiation, peroxides and heat (Moeller *et al.*, 2009). *sspA* transcription is dependent on sigma G (Wang *et al.*, 2006 and Steil *et al.*, 2005) and expression is typically detected after completion of asymmetric cell division, prior to the forespore engulfment (Doan *et al.*, 2009; Camp and Losick, 2009). In *C. difficile* SigG also drives expression of *sspA* in the forespore compartment (Pereira *et al.*, 2013).

In *B. subtilis*, *spoVT* transcription is also dependent on sigma G (Wang *et al.*, 2006). However, in *C. difficile*, *spoVT* is regulated by both SigF and SigG (Fimlaid *et al.*, 2013). In *C. difficile*, a *spoVT* mutant forms a phase dark forespore after completing engulfment (Saujet *et al.*, 2013). It has been suggested that these spores lack or have reduced cortex, leading to production of heat sensitive spores (Saujet *et al.*, 2013). Interestingly a *B. subtilis* *spoVT* mutant showed phase bright spores, with a reduction in sporulation efficiency (Bagyan *et al.*, 1996).

gpr encodes a spore-specific protease that is required for SspA degradation during germination (Nicholson *et al.*, 2000). In *B. subtilis*, *gpr* expression is controlled by both SigF and SigG, while in *C. difficile* it is regulated only by SigF (Pereira *et al.*, 2013). Gpr localises to the forespore and can be detected in the sporulating cell when the asymmetric division is started. The expression of Gpr is also detected in a *sigG* mutant, which suggests that it is not regulated by SigG (Pereira *et al.*, 2013).

In *B. subtilis*, synthesis of both protective envelopes of spore cortex and coat are dependent on SigE (Eichenberger *et al.*, 2003). In *C. difficile* the coat proteins (SpoIVA and SipL) are also regulated by SigE and are orthologues of SpoIVA and SpoVID in *B. subtilis* respectively (Putnam *et al.*, 2013; Paredes-Sabja *et al.*, 2014). These proteins are

typically localised to the putative basement layer of forespores (Putnam *et al.*, 2013; Paredes-Sabja *et al.*, 2014). Expression of these coat proteins is negatively controlled by SpoIIID (Saujet *et al.*, 2013).

Subsequently, the impact of $\Delta spoVD$ on toxin production (TcdB) was also elucidated. The $\Delta spoVD$ showed the highest expression of the master regulator Spo0A possibly due to the sporulation defect and this had an apparent impact on TcdB production. Spo0A has been considered as negative regulator of toxin secretion (TcdA and TcdB) (Pettit *et al.*, 2014). The observation of low toxin production in the $\Delta spoVD$ supports our finding in the important role of SpoVD in sporulation. Taken together, our result suggests that the over expression of Spo0A in $\Delta spoVD$ leads to repression of toxin production.

The next step of this project was SpoVD truncation, in order to identify the importance of each domain in sporulation and cephalosporin resistance. In *C. difficile*, SpoVD has three predicted functional domains: PBP dimer, transpeptidase and PASTA domains (Figure 3.2). Deletion of the PBP dimer domain had a dramatic effect on sporulation. The function of this domains is not known but we hypothesize that it is necessary for the interaction between SpoVD and SpoVE. SpoVE is thought to protect SpoVD from degradation, facilitating the localisation of SpoVD to the forespore membrane (Fay *et al.*, 2010).

Interestingly, the PASTA domain was not essential for spore cortex synthesis. Similar finding in *B. subtilis*, the PASTA domain deletion has not shown an effect on cortex layer assembly (Bukowska-Faniband and Hederstedt, 2015). Surprisingly, both PBP dimer and PASTA domains were necessary for cephalosporin resistance. In both deletions, the cephalosporin MIC was similar to the *spoVD* mutant, suggesting that both of these domains are involved in cephalosporin resistance. Indeed, a previous study has shown the importance of the PASTA domain in transpeptidase domain activity (Maurer *et al.*, 2012). In *S. pneumoniae* a PASTA domain deletion showed a significant decrease (90%) on binding of the transpeptidase domain with the β -lactam ring of Bocillin-FC (Maurer *et al.*, 2012). The PASTA domain also provides stability to the transpeptidase domain binding with the β -lactam ring substrate (Bukowska-Faniband and Hederstedt, 2015). This is consistent with our results and suggests that the PASTA domain deletion

can affect the catalytic activity of the transpeptidase domain. We have shown in chapter five that $\Delta spoVE$ had the same effect on cephalosporin resistance as the $\Delta spoVD$ mutation. Hence, we hypothesize also that the PBP dimer deletion affects not only the SpoVD / SpoVE interaction but that this also leads to an effect on cephalosporin resistance. This suggests that the interaction of SpoVD and SpoVE may have a role in cephalosporin resistance, as we have observed that the proteins interact in the exponential phase, localizing to the mother cell compartment.

The interaction between SpoVD and SpoVE was studied in order to understand how SpoVD is localised. In *B. subtilis*, SpoVD interacts with SpoVE (lipid II flippase), and localises to the forespore membrane (Fay *et al.*, 2010). Localisation of SpoVD to forespores ultimately depends on the interaction with SpoVE (Bukowska-Faniband and Hederstedt, 2015). We have demonstrated SpoVD and SpoVE interaction in two different ways: bacterial two hybrid and Split-Snap. The split Snap experiments showed that the interaction between SpoVD and SpoVE was localised to the mother cell compartment in exponential phase, while in stationary phase the proteins were localised to the forespore membrane, as in *B. subtilis*.

In *B. subtilis*, SpoVD is recruited by SpoVE during the sporulation process. SpoVD is randomly inserted in the mother cell compartment and then diffuses to the forespore membrane (Fay *et al.*, 2010). SpoVE protects SpoVD from protease activity and eliminates the SpoVD from insertion into the mother cell compartment, leading to direct insertion of SpoVD into the forespore membrane (Rudner *et al.*, 2002). The spore cortex assembly is completely dependent on the catalytic activity of the transpeptidase domain of SpoVD and this is clearly demonstrated by SpoVD localisation to the forespore membrane (Bukowska-Faniband and Hederstedt, 2013). Several PBPs are localised to either vegetative or sporulating cells dependent on their transpeptidase activity (Pinho and Errington, 2005; Costa *et al.*, 2008). Another evidence of SpoVD localisation to the forespore membrane, in *B. subtilis*, is a point mutation in the active site serine of the transpeptidase domain (Ser294 to Ala), which showed misassembly of the spore cortex layer. Clearly, this point mutation has an effects the SpoVD localization to the forespore membrane, leading to loss of the spore cortex (Bukowska-Faniband and Hederstedt, 2013). We have shown that changing Ser311 to Ala in the transpeptidase domain, leads

to the same results, as in *B. subtilis*. We have presented clear evidence of SpoVD localisation to the forespore membrane in stationary phase.

Chapter Four

4.1 Introduction

4.1.1: Cwp20

The main point of this project is identification of the gene subsets in *C. difficile* R20291 that are responsible for antibiotic resistance. BLAST analysis (Table 3.1) suggested that Cwp20 is a homologue of the *Bacillus subtilis* 168 PbpE (identity 25%). Functional domain analysis predicted that Cwp20 may have β -lactamase activity. β -lactamases hydrolyse the β -lactam ring in penicillin and cephalosporin antibiotics. The hydrolysis of the four-membered β -lactam ring typically occurs by covalent binding of the active site serine to the β -lactam ring. The chemical processes involved in β -lactam hydrolysis are acylation and deacylation (Harbottle *et al.*, 2006; Stec *et al.*, 2005).

In acylation, the serine in the active site motif SXXK attacks the carbonyl group of the β -lactam ring, with a conducive environment formed by the active site residues. This leads to the formation of a hydrogen bond around the amide bonds of these residues (Massova and Mobashery, 1998; Vakulenko *et al.*, 1999). The active site residues may also form a proton bridge between residues Glu75/Lys48 and the hydroxyl group of Ser45. Class A β -lactamases have a conserved glutamic acid in the omega-loop-like region (Adachi *et al.*, 1991; Nemmara *et al.*, 2011). The acyl enzyme intermediate is able to bind a water molecule to the glutamic acid during the deacylation process. This water molecule helps to release the active serine from the β -lactam ring (Stec *et al.*, 2005). Lastly, the deacylation process ends with a hydrolysed inactivated product (Chen *et al.*, 2006).

Despite the fact that class C β -lactamase enzymes such as AmpC and AmpH hydrolyse β -lactam antibiotics, these enzymes also play a significant role in peptidoglycan remodelling (Vega and Ayala, 2006). Indeed, class C PBPs are responsible for two catalytic activities, DD-carboxypeptidase and DD-endopeptidase. The DD-carboxypeptidase activity works on removing the last D-alanine from the new glycan chain, while the DD-endopeptidase activity works on hydrolysing the linking peptide bridges in the glycan layers (Sauvage *et al.*, 2008).

The *cwp20* gene (CD1218) encodes a putative penicillin-binding protein with predicted β -lactamase activity (Figure 4.1B). Upstream of *cwp20* are two phage genes

CD1319 and CD1320, followed by several ABC transporter genes. Downstream of *cwp20* is CD1317, encoding a putative iron-sulfur protein, also followed by many ABC transporter genes.

SlpA forms the *C. difficile* S-layer and SlpA is cleaved by protease protein Cwp84 into high molecular weight (HMW) and low molecular weight (LMW) S-layer protein (SLP) (Fagan *et al.*, 2009). The HMW SLP contains three cell wall binding motifs (Pfam 04122) and the LMW SLP interacts with the HMW SLP (Fagan *et al.*, 2009). The S-layer proteins (SLPs) and CwpV are translocated by SecA2 (ATPase) via the canonical channel SecYEG (Fagan and Fairweather, 2011) and the proteins are then anchored to the cell wall via an interaction between the CWB2 motifs and the anionic polymer PSII (Willing *et al.*, 2015). This is a new mechanism for protein anchoring to cell wall in Gram-positive bacteria.

The Cwp20 protein (111.800 kDa) has 1013 amino acid residues, containing an N-terminal 29 amino acid signal peptide (<http://www.cbs.dtu.dk/services/SignalP/>), a β -lactamase domain (residues Ala63-Ala401) and three CWB2 motifs (residues Ala718-Ser1005) (<http://pfam.xfam.org/>) (Figure 4.1B).

Research in the Fagan lab focuses on understanding the structure of the S-layer and how the cell wall proteins assemble in this layer. This is critical as part of cell maintenance and interaction between the immune system and *C. difficile* during infection (Fagan and Fairweather, 2014). As Cwp20 has predicted β -lactamase activity, studying this protein in-depth is critical for characterisation of cephalosporin resistance in this organism.

In this chapter, a *cwp20* mutant was created using two different knockout strategies, Clostron insertional mutagenesis and deletion, followed by complementation in the *pyrE* locus using homologous recombination. *cwp20* was found to be a critical gene in cephalosporin resistance. Finally, in an attempt to determine the exact function of Cwp20, the protein was purified, followed by demonstration of the β -lactamase activity *in vitro*. The protein was mutated by changing the active site serine to determine the serine residue that is responsible for the catalytic activity.

Furthermore, the type of the β -lactamase was identified by using clavulanic acid, which showed that Cwp20 is a class A β -lactamase.

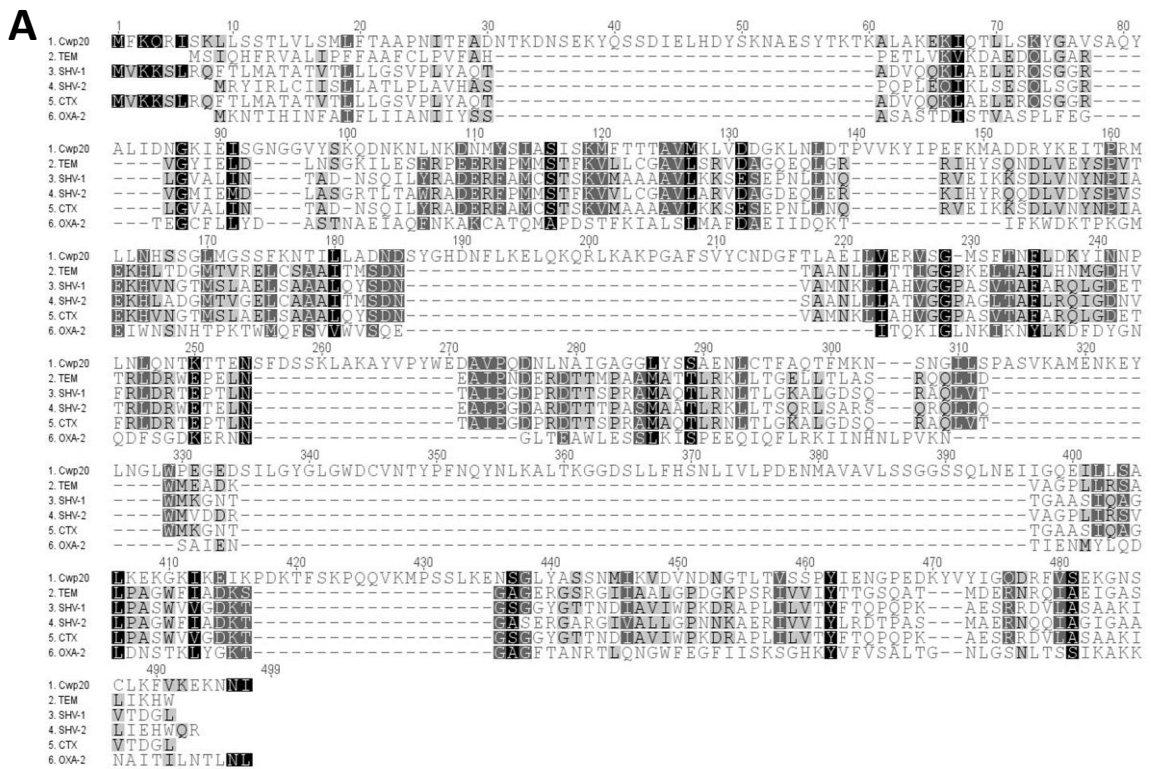


Figure 4.1: General characteristics of Cwp20. **A:** multiple sequence alignment of Cwp20 with other related β -lactamase enzymes, all protein sequences (TEM, SHV1, SHV2, CTX and OXA-2) are from *E. coli*. Alignment produced using Geneious 7.1.7. **B:** Pfam (<http://pfam.xfam.org/>) and signal peptide (<http://www.cbs.dtu.dk/services/SignalP/>) prediction showing the residue numbers of each domain boundary. The signal peptide is shown in red, the β -lactamase domain is in purple and the three CWB2 Pfam O4122 motifs are depicted in blue.

4.2: Results:

4.2.1 Deletion of the *cwp20* gene

The *cwp20* mutant was constructed in *C. difficile* R20291 Δ *pyrE* using a recently developed homologous recombination system (Ng *et al.*, 2013). This system uses the *pyrE* gene as both a positive and negative selectable marker. *pyrE* encodes orotate phosphoribosyltransferase, involved in pyrimidine biosynthesis, that can be used to select for cells carrying the plasmid when grown on minimal media lacking uracil. However, it can also convert 5-fluoro-orotate (FOA) to 5-fluoro-uracil which is toxic for the cell. Hence, FOA can be used for negative selection of the plasmid. The pMTL-YN4 plasmid carrying *pyrE* was used to construct plasmid (pYAA025) with allele exchange cassettes having approximately 650 bp of homology to chromosomal sequence both up- and downstream of the gene to be deleted (Figure 4.2A). This plasmid (pYAA025) was digested with *Bam*HI and *Sac*I to confirm the successful cloning of 1,300 bp insert into pMTL-YN4 (Figure 4.2C).

Plasmids were introduced into *C. difficile* R20291 as described in methods. *C. difficile* transconjugants grew slowly due to the segregational instability of the origin of replication (pBP1 of *Clostridium botulinum*) on plasmid pMTL-YN4. Recombination with the chromosome overcomes the segregational instability and results in faster-growing colonies. The first crossover was confirmed by PCR using a primer specific for the chromosome (RF210) and another on the plasmid pYAA024 (RF143), PCR showed the expected product of 1,416 bp (Figure 4.2D). Double crossovers were then selected for using FOA and successful deletion of *cwp20* was confirmed by PCR using primers flanking the *cwp20* gene (RF210 and RF211). PCR gave the expected product of 1,411 bp for the mutant strain (Figure 4.2E). Following deletion, only 18 bp of the gene remained (Figure 4.2B).

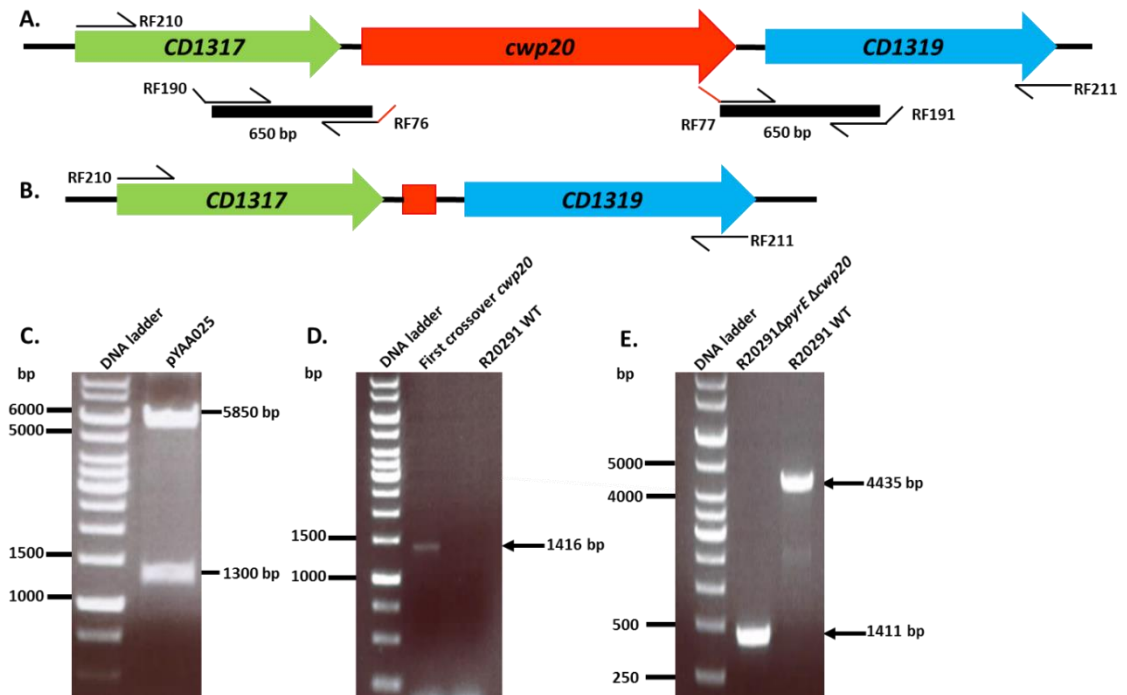


Figure 4.2: Deletion of *cwp20* using homologous recombination. **A:** Schematic diagram showing the primer design to delete the *cwp20* gene. Both internal primers have a short overlap of complementary sequence to downstream and upstream of the gene, whereas the external primers have *Bam*HI and *Sac*I restriction sites. PCR products were joined by SOE PCR and the resulting product was cloned between *Bam*HI and *Sac*I in pMTL-YN4, yielding pYAA025. **B:** Schematic diagram showing the primer design to demonstrate deletion of *cwp20* gene. Following deletion, only 18 bp of the gene remain (shown in red). **C:** Agarose gel of double digestion using *Bam*HI and *Sac*I, confirming the successful cloning of 650 bp downstream and upstream of the *cwp20* gene (1,300 bp) into pMTL-YN4 (5,850 bp). **D:** PCR to demonstrate the first crossover, using a primer specific for the chromosome (RF210) and another on the plasmid pYAA025 (RF143). The PCR amplified a 1,416 bp PCR product as predicted. This confirmed recombination of the plasmid into the chromosome. Wild type R20291Δ*pyrE* was included as a negative control. **E:** PCR to confirm successful deletion of *cwp20*, using primers flanking the *cwp20* gene (RF210 and RF211). PCR amplified the predicted 1,411 bp from the mutant, whereas the wild type R20291Δ*pyrE* gave the predicted 4,435 bp product.

4.2.2 Complementation of the *cwp20* mutant and restoration of the *pyrE* gene

The *cwp20* deletion was created in R20291 Δ *pyrE*, as a result, this mutant strain has two mutations (Δ *pyrE* and Δ *cwp20*). In order to restore the *pyrE*⁺ phenotype, the pMTL-YN2 plasmid, which contains the WT *pyrE* gene was delivered to the mutant strains. Transconjugant colonies were re-streaked onto CDMM agar without uracil to selected for uracil prototrophy, which indicated the successful allele recombination (R20291 Δ *cwp20*) (Figure 4.3A). The restored *pyrE* gene was confirmed by colony PCR using the two primers (RF295/RF297), which anneal in the *pyrE* locus. PCR showed the expected product of 2,000 bp for both the mutant and the wildtype strains (Figure 4.3D). Sanger sequencing was used to confirm the PCR product.

In order to complement the R20291 Δ *cwp20* mutant, it was necessary to clone *cwp20*, along with its native promoter. The complementation was carried out by cloning the WT *cwp20* gene along with the ribosome binding site (RBS) and 204 bp of putative promoter into pMTL-YN2C using *EcoRI* and *BamHI* sites. The promoter region of *cwp20* was predicted using BPROM (SoftBerry). The resulting clone, pYAA028, was digested with *EcoRI* and *BamHI* to confirm the successful cloning of 3,266 bp insert into pMTL-YN2C (6,924 bp) (Figure 4.3C). This plasmid was then delivered into the Δ *cwp20* mutant strain. pMTL-YN2C allows insertion of DNA in the *pyrE* locus at the same time as restoration of the wild type *pyrE* gene.

The entire gene was inserted downstream of the restored *pyrE* gene locus. The complementation and restoration were confirmed by PCR screening using the two primers (RF295/RF297), which annealed to the *pyrE* locus. PCR showed the expected product of 5,520 bp for the complementation strain R20291 Δ *cwp20 pyrE::cwp20*, while the wildtype and the R20291 Δ *cwp20* showed the expected product of 2,000 bp (Figure 4.3D). PCR products were sent for Sanger sequencing to confirm the complementation and *pyrE* restoration.

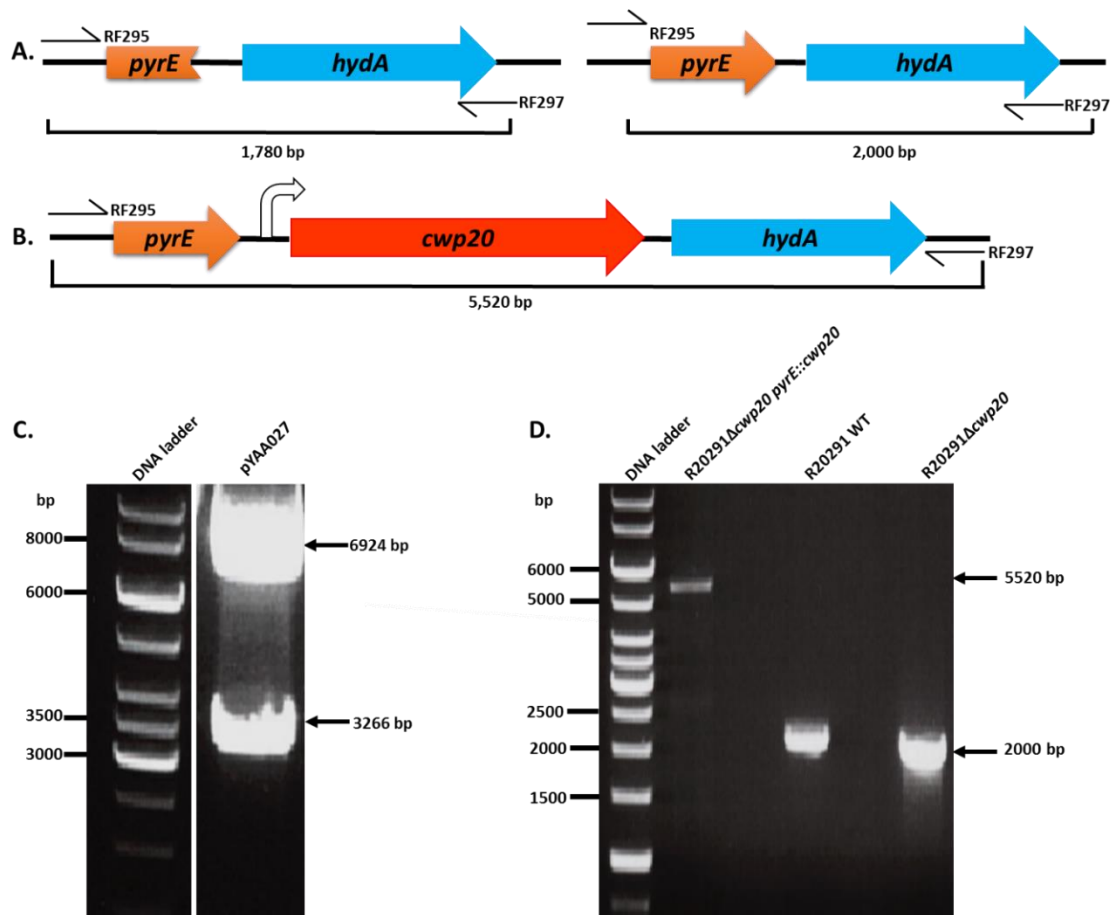
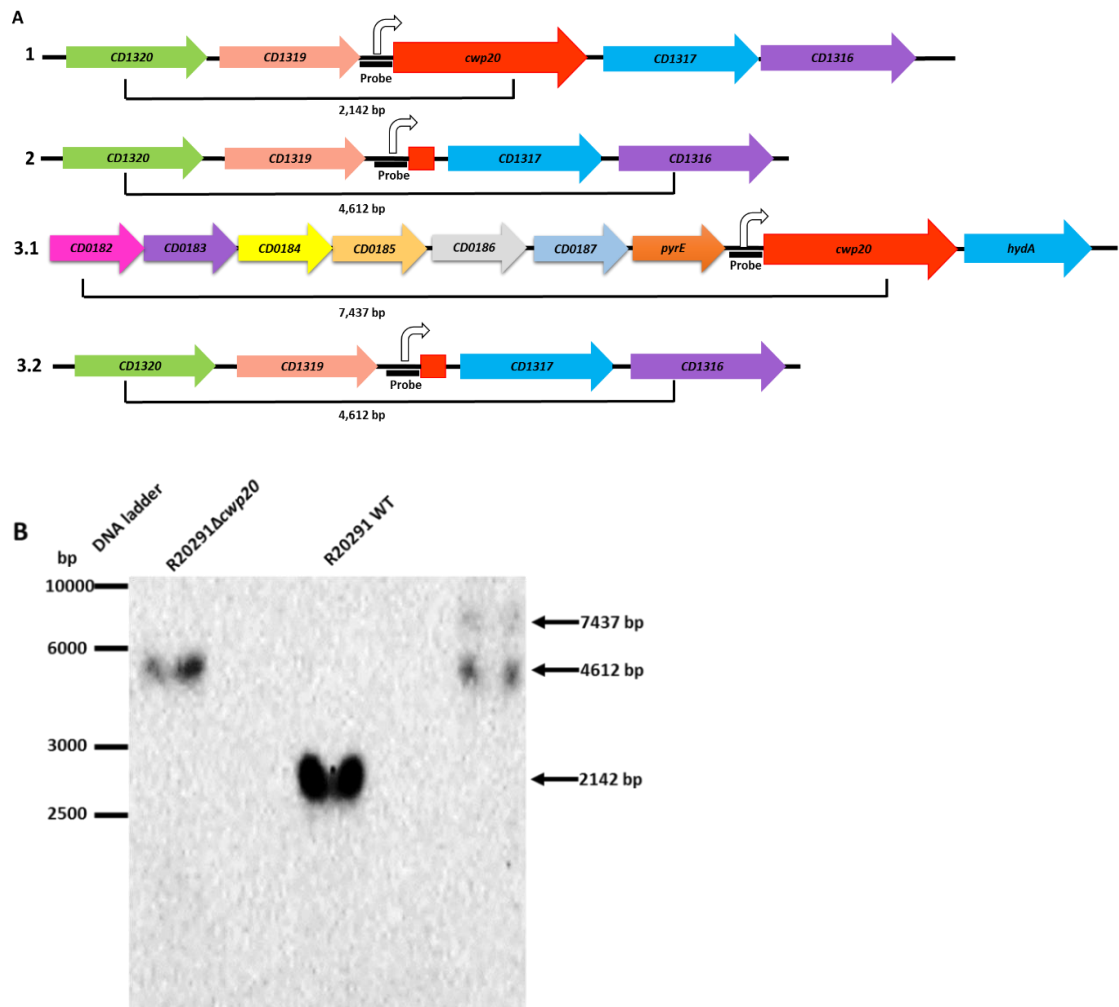


Figure 4.3: Complementation of *cwp20* and restoration of the *pyrE* gene. **A:** Schematic diagram showing the *R20291ΔpyrE* locus and the primer design for PCR screening before and after restoring *pyrE* in the *cwp20* mutant. Using these primers *R20291ΔpyrE* would give a product of 1,780 bp, increasing to 2,000 bp upon restoration of the *pyrE* gene. **B:** Schematic diagram showing the primer design for screening of insertion of *cwp20* into the *pyrE* locus. **C:** Agarose gel of double digestion using *EcoRI* and *BamHI* for plasmid pYAA028. This confirmed the successful cloning of 3,266 bp, including *cwp20*, the ribosome binding site (RBS) of *cwp20* and the 204 bp of the putative promoter into pMTL-YN2C (6,924 bp). **D:** PCR to demonstrate the complementation of *cwp20* and restoration of the *pyrE* gene using a primer flanking the *pyrE* gene locus (RF295, RF297). PCR amplified the predicted 5,520 bp product from the complementation strain, whereas the wild type *R20291* gave the predicted 2,000 bp PCR product. Also, pMTL-YN2 was conjugated into the *cwp20* mutant to fix the *pyrE* gene. The PCR screen gave the expected product of 2,000 bp as the wild type, confirming the restoration of the *pyrE* gene.

4.2.3 Southern blot confirmation of knockout and complementation *cwp20*

In order to confirm the mutant and complementation, the gDNA of three strains, wildtype, *cwp20* mutant and complemented, were extracted, followed by digestion using *Bsr*GI. A 200 bp fragment covering the promoter region of the *cwp20* gene was amplified by PCR and used as probe for DNA detection in a Southern blot. The probe annealed to fragments of the expected sizes: 2,142 bp in wildtype, 4,612 bp in the mutant. The probe identified two bands in the complementation strain, the *cwp20* deletion 4,612 bp, and the entire *cwp20*, along with the native promoter region in the *pyrE* gene locus 7,437 bp (Figure 4.4).



Figures 4.4: Southern blot confirmation of *cwp20* knockout and complementation. **A:** Schematic diagram showing the genomic DNA of **(1)** the wildtype, **(2)** R2921Δ*cwp20* and **(3.1 and 3.2)** R20291Δ*cwp20 pyrE::cwp20*. Below each is an indication of the *P_{cwp20}* fragment size following *BsrGI* digestion. **B:** The gDNA of each strain was digested with *BsrGI*, separated on a 1% agarose gel and transferred to a Biodyne B nylon membrane. The membrane was blotted with a labelled probe specific for the *cwp20* promoter. The probe is illustrated with the thick black line in panel A. The probe visualised the difference between the wild type (2,142 bp) and the mutant strain (4,612 bp). The complementation strain showed two bands, suggesting the successful insertion of the *cwp20* cassette into the *pyrE* gene locus (7,437 bp), along with the mutant locus (4,612 bp).

4.3 Determination of antibiotic MICs

In order to determine the MIC of cephalosporins and ciprofloxacin, the agar dilution method was used following the laboratory standard institute guidelines [Clinical and laboratory standard institute, 2012]. MICs were read after 48 h incubation at 37°C for the three strains (wildtype, $\Delta cwp20$ mutant and complemented). The *C. difficile* R20291 wild type showed the highest MIC for cefoxitin and ceftazidime (128 $\mu\text{g/ml}$ and 256 $\mu\text{g/ml}$ respectively), whereas the *cwp20* mutant strain showed the lowest MICs for cefoxitin and ceftazidime (32 $\mu\text{g/ml}$, 64 $\mu\text{g/ml}$ respectively). Mutation of *cwp20* had no effect on ciprofloxacin resistance as expected. Subsequently, the complemented strain was tested to determine if the wild type MICs were restored. The MIC of ceftazidime, cefoxitin were restored (128 $\mu\text{g/ml}$, 256 $\mu\text{g/ml}$ respectively) (Table 4.1).

Table 4.1. Minimum inhibitory concentrations against the wild type R20291 and *cwp20* mutants and complementation strains ($\mu\text{g/ml}$).

Strains	Cefoxitin	Ceftazidime	Ciprofloxacin
R20291 Wild Type	128	256	512
R20291 $\Delta cwp20$	32	64	512
R20291 $\Delta cwp20$ <i>pyrE::cwp20</i>	128	256	512

4.4 Functional analysis of the β -lactamase domain in Cwp20

In order to confirm that the Cwp20 protein has β -lactamase activity, we cloned and purified the protein. His tag encoding DNA was fused to the 3' end of *cwp20* in pET-28a using the restriction enzymes *NcoI* and *XhoI*. The protein was expressed in *E. coli* Rosetta and purified (Figure 4.5A). The molecular weight (MW) of Cwp20-His was confirmed by electrospray ionisation mass spectrometry (53.72 kDa; Figure 4.5C).

Next, the active site serine motif (Ser-Xaa-Xaa-Lys) (Matagne *et al.*, 1999) was identified and the codon of the putative active site serine 116 (TCT) was changed to alanine (GCG) by an inverse PCR to allow for identification of the acylation site. Subsequently, the Cwp20S116A-His protein was purified as before (Figure 4.5B). The MW difference was confirmed by electrospray ionisation mass spectrometry (53.70 kDa; Figure 4.5D).

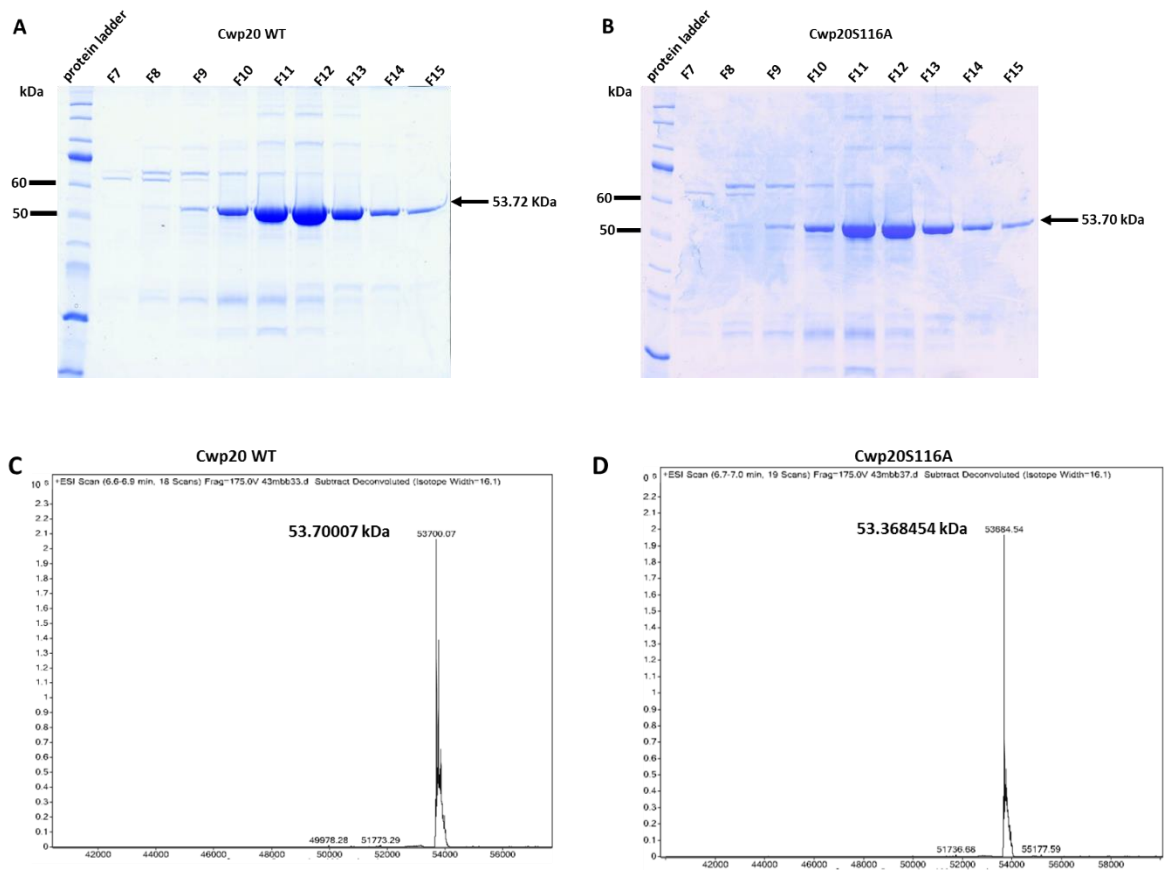


Figure 4.5: Purification of Cwp20 and Cwp20S116A. **A** and **B** fractions of Cwp20-His and Cwp20S116A-His eluted from Ni-NTA were analysed by SDS-PAGE stained with Coomassie blue. The fractions with good quality protein were pooled and dialysed against 25 mM Tris, 50 mM NaCl pH 8. **C** and **D** mass spectra of Cwp20 and Cwp20S116A, 53.72 kDa and 53.70 kDa respectively.

4.5 Cwp20 β -lactamase activity

In order to determine the exact function of Cwp20, the protein was examined for β -lactamase activity *in vitro*.

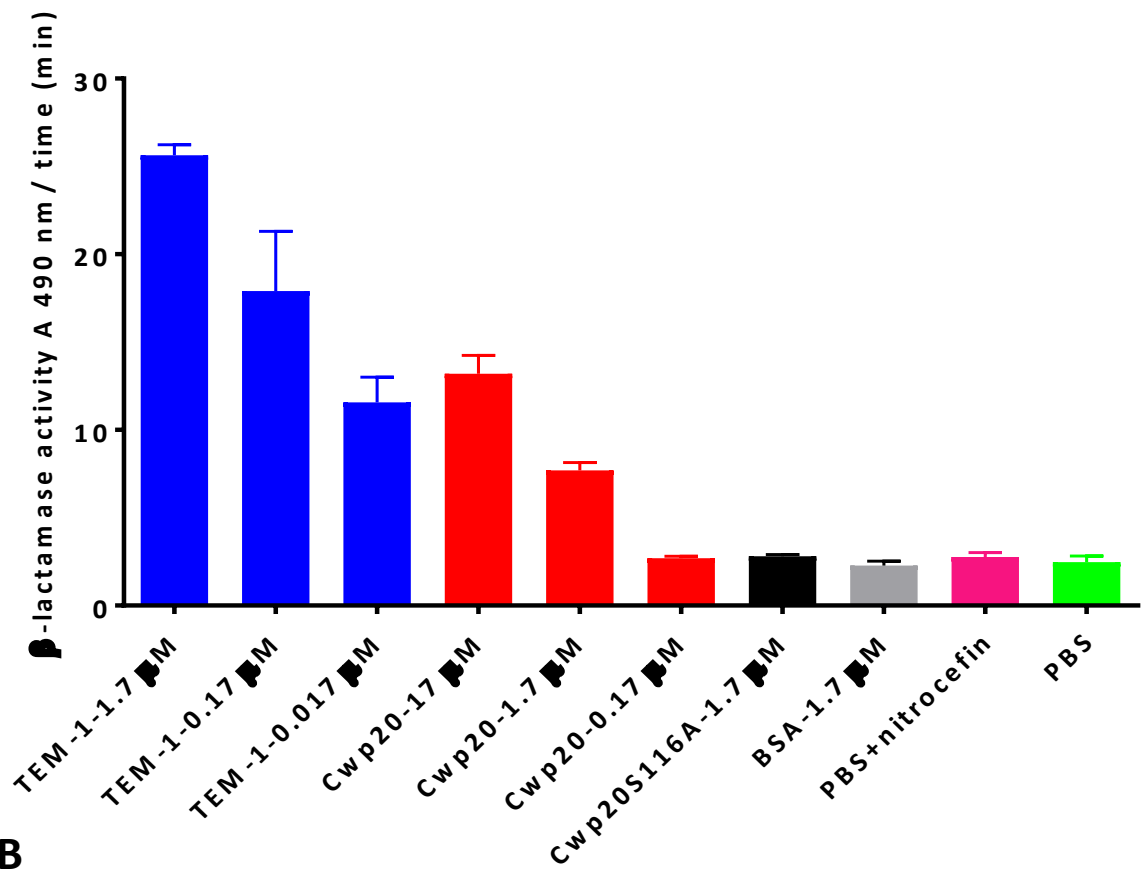
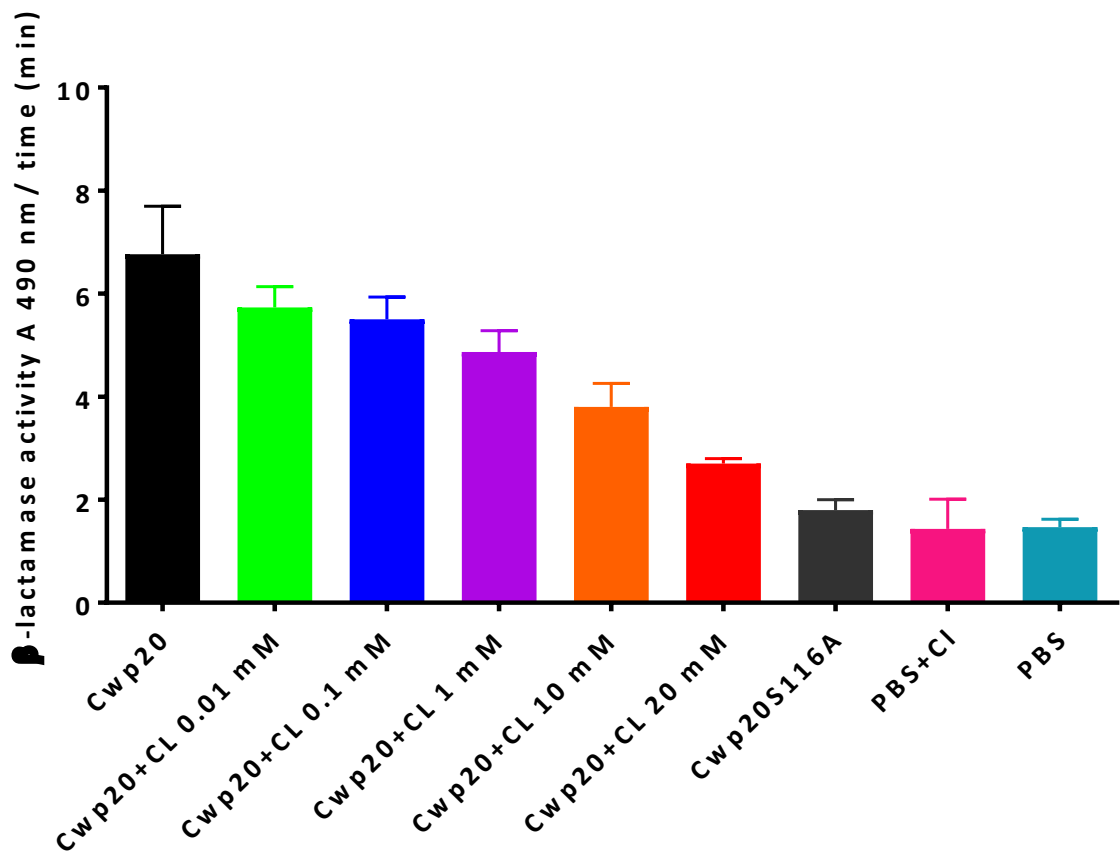
In several bacteria species such as *Neisseria gonorrhoeae*, *Moraxella catarrhalis*, *Haemophilus influenza* and *E. coli*, a colorimetric test has been used to detect different types of β -lactamase, including the extended-spectrum β -lactamases (ESBL) (Livermore and Brown, 2001). β -lactamases (TEM-1, TEM-2, and SHV-1) have been shown to hydrolyse penicillin and cephalosporin antibiotics such as cephaloridine and cephalothin (Matthew, 1979; Roy, *et al.*, 1983). Following purification, β -lactamase assays were carried out on Cwp20 and Cwp20S116A using nitrocefin as the substrate. Nitrocefin is a chromogenic cephalosporin that is hydrolysed by many different types of β -lactamase. Nitrocefin hydrolysis leads to a change in colour from yellow to red, changing the absorbance at 490 nm (O'Callaghan *et al.*, 1972). The TEM-1 enzyme was used as a positive control for class A β -lactamase.

TEM-1 was used in this assay at a range of different concentrations (1.7 μ M, 0.17 μ M and 0.017 μ M), while, the Cwp20 protein was used 17 μ M, 1.7 μ M, 0.17 μ M and 0.017 μ M (Figure 4.6A). Cwp20 showed a clear hydrolysis of nitrocefin, changing the colour of nitrocefin substrate from yellow to red, but at a lower speed than TEM-1. Cwp20S116A failed to hydrolyse the nitrocefin, confirming identification of the active site serine (Ser116) (Figure 4.6A).

To identify the class of β -lactamase, assays were repeated with different inhibitors. The β -lactamase activity of Cwp20 was inhibited by incubation with clavulanic acid (Figure 4.6B). In contrast, EDTA did not show any inhibition of Cwp20 activity (Figure 4.6C). Inhibition with clavulanic acid but not EDTA suggested that Cwp20 is class A β -lactamase. Clavulanic acid and tazobactam completely inhibit class A β -lactamases such as TEM-1, TEM-2, TEM-3, TEM-30, TEM -50, SHV-1, SHV-2, SHV10, CTX-M-15, PER-1, VEB-1, CepA, PSE-1, CARB-3, RTG-4 and PC1, and have a variable effect on class D lactamases such as OXA-1, OXA-10, OXA-11, OXA-15, OXA-23, OXA-48. However, both clavulanic acid and tazobactam do not inhibit class C lactamases such as AmpC, P99, ACT-1, CMY-2, FOX-1, MIR-1, GC1 and CMY-37 (Bush *et al.*, 1995). Furthermore, class A, C and D β -

lactamases hydrolyse the β -lactam ring following covalent binding to the active site serine residue, while class B lactamases require a divalent zinc as co-factor for the hydrolysis process (Bush and Jacoby, 2009). Thus class B lactamases such as IMP-1, VIM-1, CcrA, IND-1, L1, CAU-1, GOB-1, FEZ-1, CphA and Sfh-1 are completely inhibited by EDTA (Bush *et al.*, 1995). Also, changing serine 116 in Cwp20 caused complete loss of protein function, further confirming identification as a class A β -lactamase.

1.7 μ M Cwp20 was the optimum concentration for the β -lactamase assay (Figure 4.6A). 20 mM clavulanic acid was the optimum concentration to inhibit β -lactamase activity (Figure 4.6B). With this optimisation, the kinetics of Cwp20 β -lactamase activity with and without clavulanic acid were determined using different concentrations of nitrocefin (50 μ M-800 μ M). Kinetic values were obtained using the Michaelis-Menten equation. The results showed that Cwp20 had a V_{max} of 39 μ M, K_m 76 μ M, K_{cat} 22.9 min^{-1} and K_{cat}/K_m 0.3 $\mu\text{M}/\text{min}$. While for TEM-1 these values were V_{max} 55 μ M, K_m 1.8 μ M, K_{cat} 32.4 min^{-1} and K_{cat}/K_m 18 $\mu\text{M}/\text{min}$. Values were lowest when incubated with clavulanic acid as an inhibitor, Cwp20: V_{max} 16 μ M, K_m 48 μ M and K_{cat} 9.0 min , TEM-1: V_{max} 51 μ M, K_m 75 μ M and K_{cat} 30 min . In general, Cwp20 showed a lower activity with nitrocefin than TEM-1. Inhibition with clavulanic acid reduced activity to K_{cat}/K_m 0.18 $\mu\text{M}/\text{min}$ and K_{cat}/K_m 0.4 $\mu\text{M}/\text{min}$ for Cwp20 and TEM-1 respectively. In contrast, Cwp20S116A did not show enzymatic activity with nitrocefin, confirming identification of the active site serine (Ser116) (Table 4.2; Figure 4.7).

A**B**

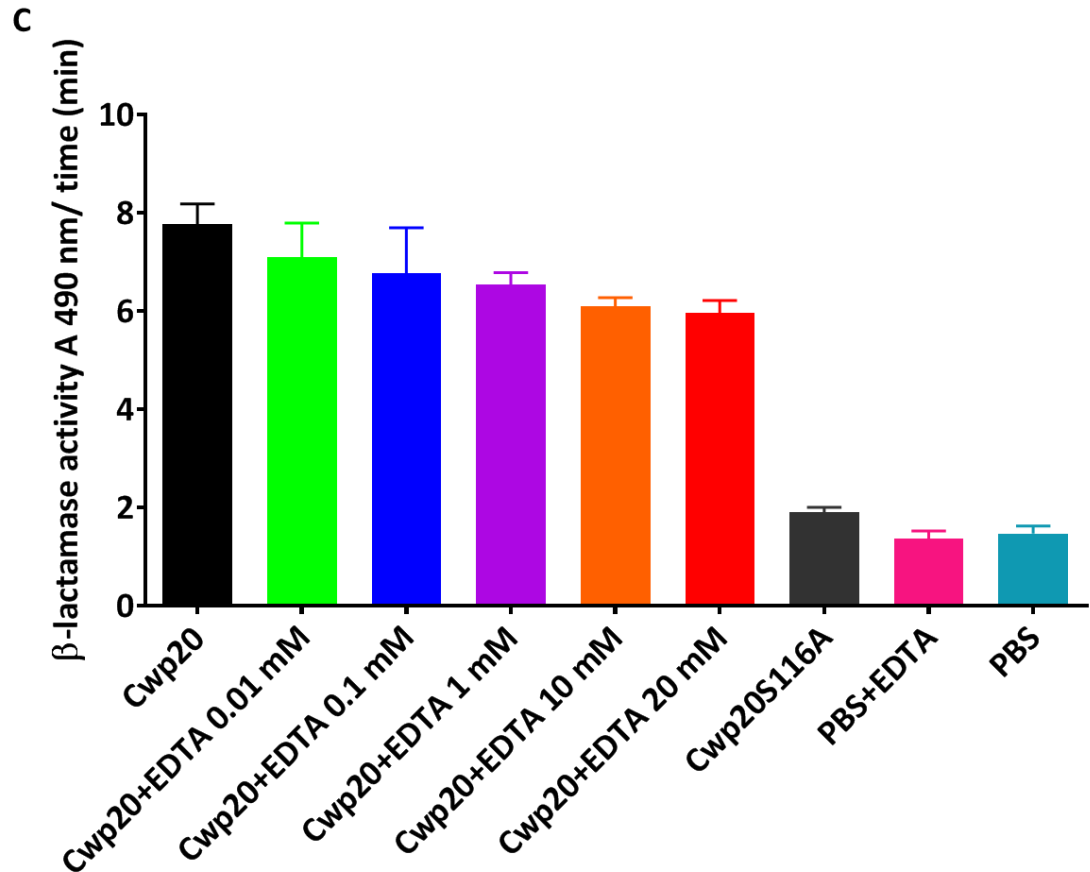


Figure 4.6: β -lactamase activity. **A:** The hydrolysis of nitrocefin substrate by TEM-1 and Cwp20. The proteins were incubated with 100 μ M nitrocefin for 3 h at 25°C, and the absorbance change was measured at 490 nm. Relative activity was calculated by taking the slope of absorbance values at 1, 30, 60, 90, 120, 150 and 180 min and plotted using GraphPad Prism 7 software. **B:** Inhibition of Cwp20 activity by Clavulanic acid. Protein (1.7 μ M) was incubated with different concentrations of clavulanic acid (CL; range 0.01-20 mM) for 30 min at 37°C, then nitrocefin was added (100 μ M), followed by incubation for 3 h at 25°C. The absorbance change and protein activity were measured as in **A**. **C:** Inhibition of Cwp20 activity by EDTA. Protein (1.7 μ M) was incubated with different concentrations of EDTA (range 0.01 -20 mM) for 30 min at 37°C, then nitrocefin was added (100 μ M), followed by incubation for 3 h at 25°C. The absorbance change and protein activity were measured as in **A**. β -lactamase activity = absorbance at 490 nm/time (min).

Table 4.2: Kinetic parameters of TEM-1, Cwp20 and Cwp20S116A.

TEM-1				
Substrate	V _{max} ($\mu\text{M min}^{-1}$)	K _m (μM)	k _{cat} (min^{-1})	k _{cat} /K _m $\mu\text{M}^{-1} \text{min}^{-1}$
Nitrocefin	55	1.8	32.4	18
Clavulanic acid	51	75	30	0.4
Cwp20				
Substrate	V _{max} ($\mu\text{M min}^{-1}$)	K _m (μM)	k _{cat} (min^{-1})	k _{cat} /K _m $\mu\text{M}^{-1} \text{min}^{-1}$
Nitrocefin	39	76	22.9	0.3
Clavulanic acid	16	48	9.0	0.18
Cwp20S116A				
Substrate	V _{max} ($\mu\text{M min}^{-1}$)	K _m (μM)	k _{cat} (min^{-1})	k _{cat} /K _m $\mu\text{M}^{-1} \text{min}^{-1}$
Nitrocefin	0	0	0	0
Clavulanic acid	0	0	0	0

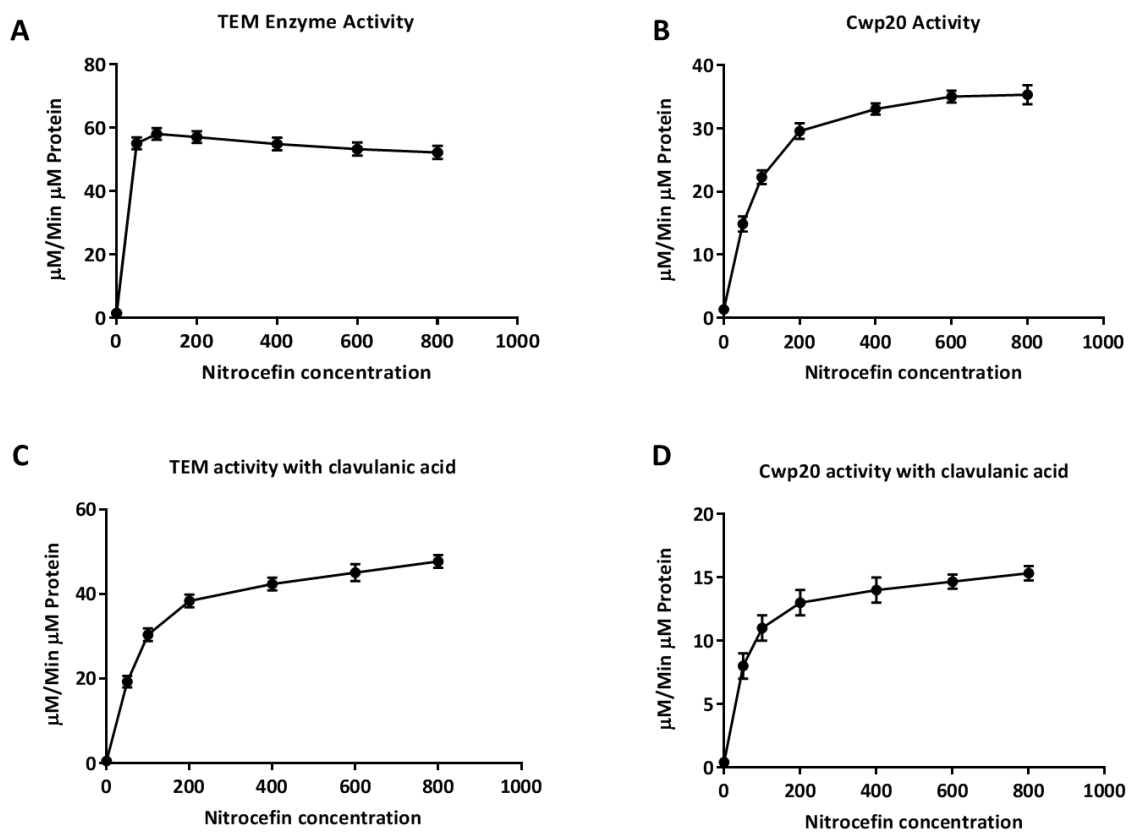


Figure 4.7: Kinetic analysis of Cwp20 and TEM-1 with nitrocefim and clavulanic acid. 1.7 μM of each protein was incubated with different concentrations of nitrocefim (range 50-800 μM) for 3 h at 25°C, and the absorbance change was measured at 490 nm. Kinetics were calculated by taking the slope of absorbance values at 1, 30, 60, 90, 120, 150 and 180 min and fitted to the Michaelis-Menten equation using GraphPad Prism 7 software. The assay was completed in triplicate.

Subsequently, the β -lactamase activity of Cwp20 was confirmed using Bocillin-FL substrate. Cwp20, TEM-1 and Cwp20S116A were incubated with the substrate for 30 min at 37°C (Figure 4.8). Cwp20 showed a faint signal, while TEM-1 did not label with Bocillin-FL at all. This may be due to rapid hydrolysis of the substrate, leading to loss of the fluorescent signal. Cwp20 showed a slow rate of binding with nitrocefin (Figure 4.6A), suggesting that Cwp20 could take more than 30 min to bind with the β -lactam ring, perhaps explaining the weak signal observed with Bocillin-FL. However, Cwp20S116A also failed to bind with Bocillin-FL. This confirmed the disruption of the Cwp20 β -lactamase activity by this point mutation. In this assay, SpoVD was used as a positive control for binding with Bocillin-FC, as described in chapter 3 (Figure 4.8).

Moreover, we confirmed the formation of intermediate products from incubation of Cwp20, followed by electrospray ionization mass spectrometry. We observed an increase in the molecular weight from 53.70007 kDa to 54.65328 kDa (Figure 4.9C). This result confirmed formation of the acyl-enzyme intermediates, and showed that 2 h incubation was not sufficient to complete ceftazidime hydrolysis. In contrast, we did not observe any changes from incubation of Cwp20S116A with ceftazidime, demonstrating complete loss of protein function (Figure 4.9D).

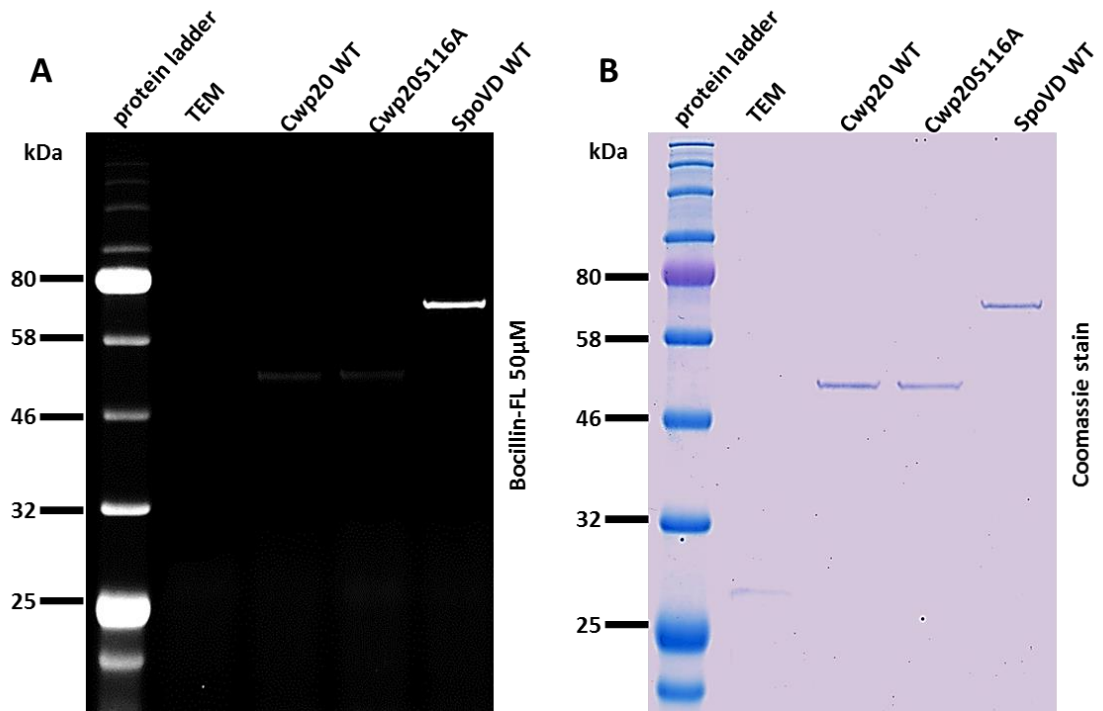


Figure 4.8: Bocillin-FL labelling of Cwp20, Cwp20S116A, TEM-1 and SpoVD. **A:** Cwp20, Cwp20S116A, TEM-1 and SpoVD were incubated with Bocillin-FL (50 μ M) for 30 min at 37°C, followed by 10% SDS-PAGE. Cwp20 showed a faint fluorescence signal, confirming formation of an acyl-enzyme intermediate. Cwp20s116A lost the signal completely. This suggests that serine 116 is the active site for binding with the β -lactam ring. SpoVD was used as positive control for Bocillin-FL labelling. The fluorescent gel was imaged using Bio-Rad imager Cy3 filter. **B:** gel from panel **A** stained with Coomassie blue, resolving all the proteins. The stained gel was used as control for protein loading.

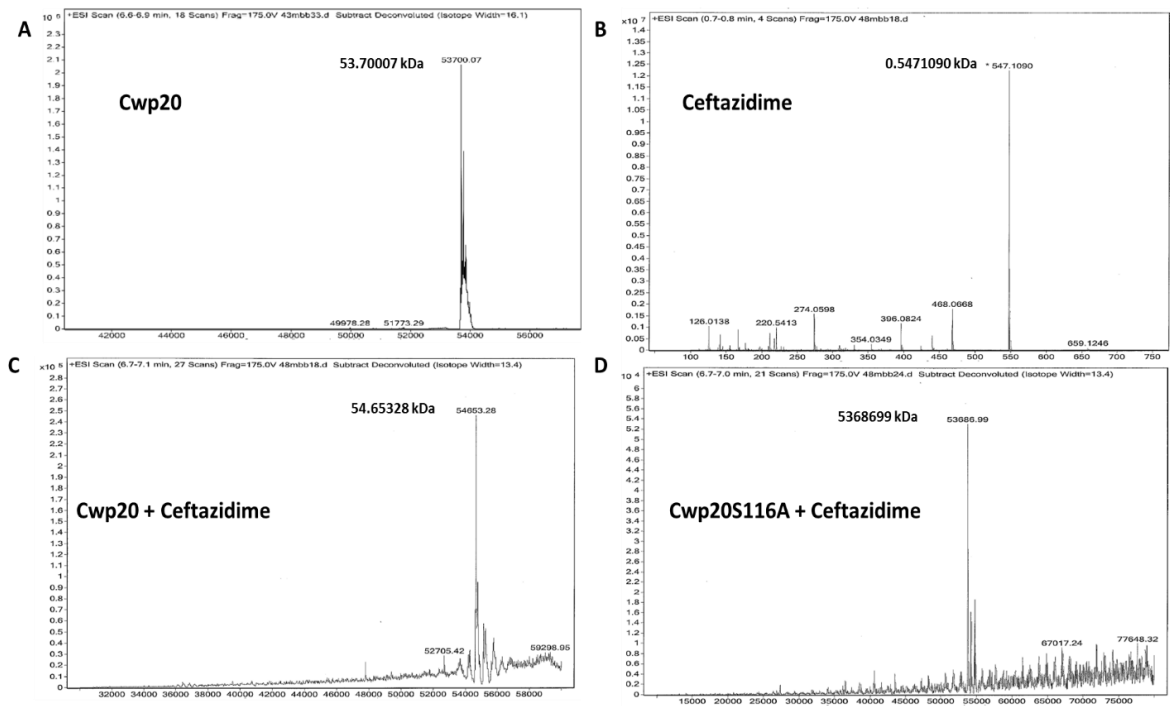


Figure 4.9: Analysis of electrospray ionization mass spectrometry. **A** and **B** mass spectra of Cwp20 and ceftazidime, 53.70007 kDa and 0.547109 kDa respectively. **C** and **D** mass spectra of Cwp20 (40 μ M) and Cwp20S116A (40 μ M) following incubation with ceftazidime (40 mM) at 37C° for 2 h, 54.65328 kDa and 53.68699 kDa respectively.

4.6 The role of the S-layer in cephalosporin resistance

An *slpA* mutant, completely lacking the S-layer, has recently been isolated (Kirk *et al.*, 2017). This mutant (R20291*slpA*) displays several phenotypes, including sensitivity to innate immune effectors and sporulation defects, and restoration of wild type *slpA* (R20291*slpA* revertants) corrects these phenotypes.

Surprisingly, we have also found that this mutation also has a clear effect on cephalosporin resistance (Table 4.3). Therefore, we hypothesise two possibilities, SlpA has a direct role in cephalosporin resistance or a protein in the S-layer that requires the S-layer for function, is responsible for the observed phenotype. To test these hypotheses, we have used Clostron insertional mutagenesis to disrupt *cwp20* in *C. difficile* R20291*slpA* (Heap *et al.*, 2007). This system was used rather than *pyrE* homologous recombination as we do not have a *pyrE* mutation in R20291*slpA*.

Towards this end, a pMTL007C-E5 -based vector carrying a 309 bp *cwp20*-specific intron II targeting region, was synthesised by DNA 2.0 and a *cwp20::ermB* mutant was constructed in R20291*slpA* (Figure 4.10B).

Knockout of *cwp20* in the *slpA* mutant did not make the cephalosporin resistance worse (Table 4.3). This suggests that Cwp20 may be responsible for the *slpA* mutant cephalosporin resistance phenotype. To confirm this the *cwp20* mutant was complemented with plasmid pYAA046 carrying the entire *cwp20* with expression under the control of the constitutive promoter P_{cwp2} . Overexpression of *cwp20* did not increase cephalosporin MICs. This is clear evidence that S-layer loss had an impact on Cwp20 function and Cwp20 relies on functional S-layer.

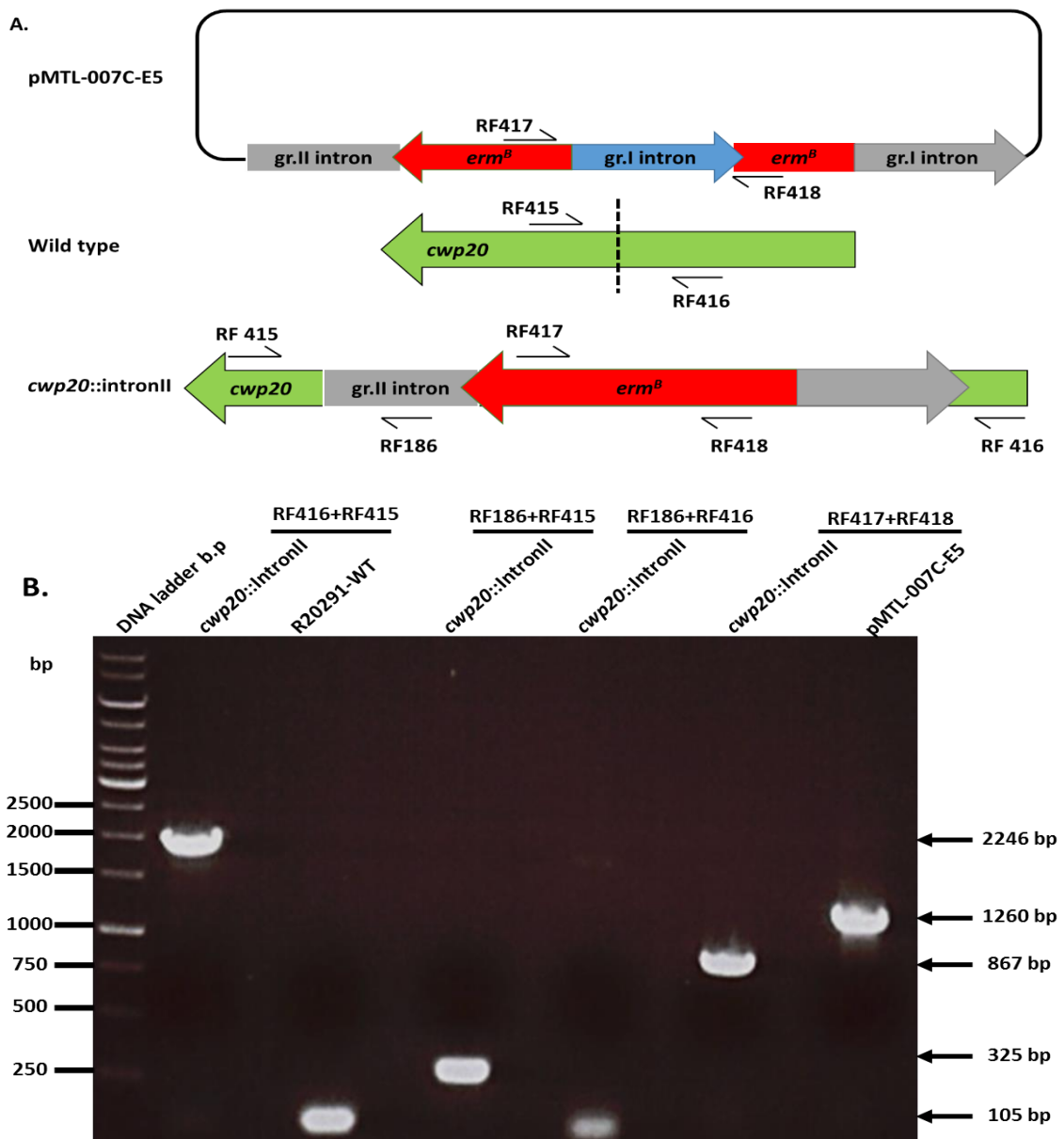


Figure 4.10. Knockout of *cwp20* using Clostron. **A:** Schematic representation of *cwp20* insertional mutagenesis, showing the primer design for PCR screening and indication of the intron II insertion site (dashed line). **B:** Genomic DNA extracted from a putative *cwp20* Clostron mutant was screened by PCR using primers flanking the group II intron insertion site (RF415/RF416) to confirm intron insertion. Primers (RF417/RF418) annealed to the retrotransposon-activated marker (RAM) to confirm the intron I group splicing. To determine the intron II orientation, RF186 an EBS universal primer were used with the *C. difficile* genome primers (RF415/RF416). pMTL007C-E5 plasmid and WT gDNA were used as negative controls.

4.7 Determination of antibiotic MICs

In order to determine the MIC of cephalosporins and ciprofloxacin, the agar dilution method was used following the laboratory standard institute guidelines [Clinical and laboratory standard institute, 2012]. MICs were read after 48 h incubation at 37°C for the these strains (wildtype, R20291*slpA*, R20291*slpA cwp20::ermB*, R20291*slpA cwp20:: ermB/ pYAA046* and R20291*slpA+ pRFP144*).

The *C. difficile* R20291 wild type showed the highest MIC for cefoxitin, ceftazidime and ciprofloxacin (128 µg/ml, 256 µg/ml and 512 µg/ml respectively), whereas both R20291*slpA* and R20291*slpA cwp20::ermB* showed the same MIC for cefoxitin and ceftazidime (32 µg/ml, 64 µg/ml respectively) as R20291Δ*cwp20*. Surprisingly, complementation with *cwp20* did not increase the MICs (32 µg/ml, 64 µg/ml respectively). This suggests that Cwp20 function is reliant on an intact S-layer. All strains retained ciprofloxacin resistance (Table 4.3).

Table 4.3. Minimum inhibitory concentrations of the wild type R20291 and *cwp20* mutants and complementation strains ($\mu\text{g/ml}$).

Strains	Cefoxitin	Ceftazidime	Ciprofloxacin
R20291 Wild Type	128	256	512
R20291 <i>slpA</i>	32	64	512
R20291 <i>slpA</i> revertants	128	256	512
R20291 <i>slpA cwp20::ermB</i>	32	64	512
R20291 <i>slpA cwp20::ermB/ pYAA046</i>	32	64	512
R20291 <i>slpA</i> + pRFP144 (empty vector)	32	64	512

4.8 Discussion

Cephalosporin antibiotic usage has been implicated in *C. difficile* infection since the early 1990s. In particular, ceftazidime, cefotaxime, cefuroxime and ceftriaxone, which are second and third generation cephalosporins, show a significant association with CDI (Bignardi, 1998). The main goal of this chapter was to investigate the role of Cwp20 in cephalosporin resistance.

A *cwp20* mutant showed a significant decrease in resistance to cephalosporins, including cefoxitin and ceftazidime, and complementation restored resistance. This suggests that Cwp20 has a major role in cephalosporin resistance. Domain analysis predicted that Cwp20 has a β -lactamase domain and three CWB2 motifs (Punta *et al.*, 2012). We were keen to understand the precise role of Cwp20 in cephalosporin resistance. The β -lactamase domain of Cwp20 was purified to confirm whether Cwp20 has β -lactamase activity or is a class C PBP.

Nitrocefin assays confirmed that Cwp20 has β -lactamase activity and substitution of serine 116 to alanine, confirmed that this is the active site serine, responsible for the binding of β -lactam ring substrates. The classification of the Cwp20 protein as a class A β -lactamase was confirmed by inhibiting the catalytic activity using clavulanic acid. Based on the Ambler scheme, β -lactamase enzymes classify into four classes (A, B, C and D). The A, C and D classes are dependent on the active site serine for binding with the β -lactam ring, while class B require a metallic co-factor (Ambler, 1980).

Interestingly, a *slpA* mutant completely lacking the S-layer, also showed a clear cephalosporin resistance defect. Indeed, this defect was identical to that observed with R20291 Δ *cwp20*. Mutation of *cwp20* in R20291*slpA* resulted in further loss of cephalosporin resistance and overexpression of *cwp20* did not increase cephalosporin MICs. This suggests that the cephalosporin sensitivity observed in R20291*slpA* was an indirect effect of S-layer loss via Cwp20.

Chapter Five

5.1 Introduction

5.1.1: Transposon mutagenesis

The genetic tools to study the virulence factors of *C. difficile* are critical for gaining an effective understanding. Recently, new gene inactivation methods have been developed using homologous recombination (Cartman *et al.*, 2012, Heap *et al.*, 2012, Ng *et al.*, 2013). In addition, the Clostron system has been used to inactivate genes by insertion of a group II intron (Heap *et al.*, 2010, Heap *et al.*, 2007). These tools allow determination of gene phenotypes, which can be identified experimentally. Although these techniques are useful to study genes with known or suspected functions, they still have limitations. Alternatively, random transposon mutagenesis, followed by a screening experiment, is beneficial to elucidate gene phenotypes without a pre-existing hypothesis (Vidal *et al.*, 2009, Lanckriet *et al.*, 2009).

The main advantage of the mariner-based *Himar1* transposon is that it preferentially inserts into TA target sites using a cut-and-paste mechanism, ensuring random insertion (Lampe *et al.*, 1996, Lampe *et al.*, 1998). This is particularly useful in TA-rich species such as *C. difficile* (Cartman and Minton, 2010). In 2015, a mariner-based transposon was used to create 70,000 unique mutants in *C. difficile* R20291, to identify all essential genes and those required for sporulation and germination (Dembek *et al.*, 2015).

In this chapter, a transposon mutant library was generated and screened for alterations in resistance to cefoxitin, ceftazidime and ciprofloxacin. This was followed by marker rescue analysis for each interesting mutant to identify the transposon insertion site. Identified genes were then characterised further.

5.2: Results:

5.2.1 Construction of transposon mutants in *C. difficile* R20291 and screening for ceftazidime, cefoxitin and ciprofloxacin resistance

Plasmid pRPF215, constructed by Dr Robert Fagan, was used to create a transposon library in *C. difficile*. The advantage of this plasmid is that the expression of the transposase is under the control of an inducible Ptet promoter. This allows control of transposition timing (Dembek *et al.*, 2015). Plasmid pRPF215 was delivered into *C. difficile* R20291, and transposon mutants were selected for on pre-reduced BHI agar supplemented with 20 µg/ml lincomycin and 100 ng/ml anhydrotetracycline (ATC). Subsequently, the mutants were patched on non-selective BHI agar and BHI agar plates supplemented with 100 µg/ml cefoxitin, ceftazidime or ciprofloxacin. The concentration of cefoxitin, ceftazidime or ciprofloxacin was optimised using the wild type strain by determining the minimum concentration that did not kill. This optimisation was very important in order to identify genes that increased antibiotic sensitivity. The following day, the transposon mutants that did not grow under antibiotic selection were isolated and genomic DNA extracted from each. A total of 6,000 transposon mutants were screened for resistance to cefoxitin, ceftazidime, and ciprofloxacin. We isolated 18 mutants that were sensitive to ceftazidime (MICs of 16, 24, 64 and 100 µg/ml compared to the wild type 256 µg/ml), five mutants that were sensitive to cefoxitin (MICs of 32 and 64 µg/ml compared to the wild type 128 µg/ml), and lastly, seven mutants that were sensitive to ciprofloxacin (MICs of 64 and 100 µg/ml compared to the wild type 512 µg/ml) (Table 5.1).

5.3 Identification of the transposon site

In order to identify the transposon insertion site, marker rescue was used. Briefly, genomic DNA was extracted from each transposon mutants and digested with *EcoRV* and *HindIII*. The digested DNA was ligated into pBluescript plasmid cut with the same restriction enzymes, and transformed into *E. coli* NEB with erythromycin selection to ensure recovery of the transposon. The generated plasmids were then sequenced with primers reading out from the inverted repeats of the transposon. The sequencing results were aligned with the R20291 genome using Geneious 7.2.1 (Biomatters). Insertion sites of 10 mutants were successfully identified using this method (Table 5.1).

Table 5.1: MICs of transposon mutants ($\mu\text{g/ml}$).

Ceftazidime strains	MIC	Cefoxitin strains	MIC	Ciprofloxacin strains	MIC
R20291 CD1165::Tn	24	R20291 <i>spoVE</i> ::Tn	32	R20291 CD0622::Tn	64
R20291 CD0398::Tn	16	R20291 CD0018::Tn	64	R20291 CD2904::Tn	100
CetZ-80*	64	R20291 CD3017::Tn	64	R20291 CD1383::Tn	100
CetZ-138*	64	R20291 CD0715::Tn	64	Cip-1*	100
CetZ-140*	64	R2921 CD3432::Tn	64	Cip-2*	100
CetZ-141*	64	R20291 WT	128	Cip-3*	100
CetZ-143*	64			Cip-5*	64
CetZ-148*	64			R20291 WT	512
CetZ-191*	64				
CetZ-202*	64				
CetZ-1*	100				
CetZ-6*	100				
CetZ-35*	100				
CetZ-36*	100				
CetZ-38*	100				
CetZ-39*	100				
CetZ-42*	100				
CetZ-49*	100				
R20291 WT	256				

(*): The transposon insertion sites were not identified in these strains.

Under cefoxitin selection, the first transposon insertion identified was in *CD0018*, encoding a putative membrane protein. However, domain analysis predicted a putative PIN domain, responsible for cleavage of single-stranded RNA, a function of nuclease enzymes (Arcus *et al.*, 2011). The second insertion identified was in *CD3017*, also encoding a putative membrane protein. A BlastP search showed similarity to DUF1877 from *Bacillus cereus* (29% amino acid identity) but there is no known function for this protein. Moreover, Pfam predicted that this protein does not have any identifiable functional domains. However, the gene located immediately downstream, ribonuclease R (*CD3018*), has a catalytic domain for ribonuclease II activity. It is possible that insertion into *CD3017* has a polar effect on expression of this putative ribonuclease. The third gene identified under cefoxitin selection was *CD3432*, encoding a third putative membrane protein. Pfam predicted that this protein has a nitroreductase domain, which is involved in nitrogen reduction and also utilises flavin mononucleotide (FMN) as a cofactor (Hecht *et al.*, 1995; de Oliveira *et al.*, 2007). The fourth transposon insertion was identified in *CD0715*, encoding a putative N-acetylmuramoyl-L-alanine amidase. This enzyme is involved in peptidoglycan hydrolysis by cleavage of the amide bond between N-acetylmuramoyl and the stem peptide L-amino acids (Kuroda *et al.*, 1992). The last transposon insertion was identified in *spoVE*, located upstream of *spoVD*. I previously demonstrated an interaction between SpoVD and SpoVE in chapter 3. This interesting result supports our hypothesis of the involvement of SpoVD in cephalosporin resistance (Figure 5.1A). The *spoVE:Tn* mutant showed the same MIC as $\Delta spoVD$ for both cefoxitin and ceftazidime (32 $\mu\text{g/ml}$ and 64 $\mu\text{g/ml}$ respectively) compared to the wild type (128 $\mu\text{g/ml}$ and 256 $\mu\text{g/ml}$ respectively) (Table 5.2).

Under ceftazidime stress, 18 mutants showing sensitivity were isolated. Using marker rescue, the insertion sites of two were identified. The first was identified in *CD1165*, encoding a DNA translocase. Pfam predicted that this protein has an FtsK domain, which is responsible for coordination of bacterial cell division and chromosome replication (Massey *et al.*, 2006).

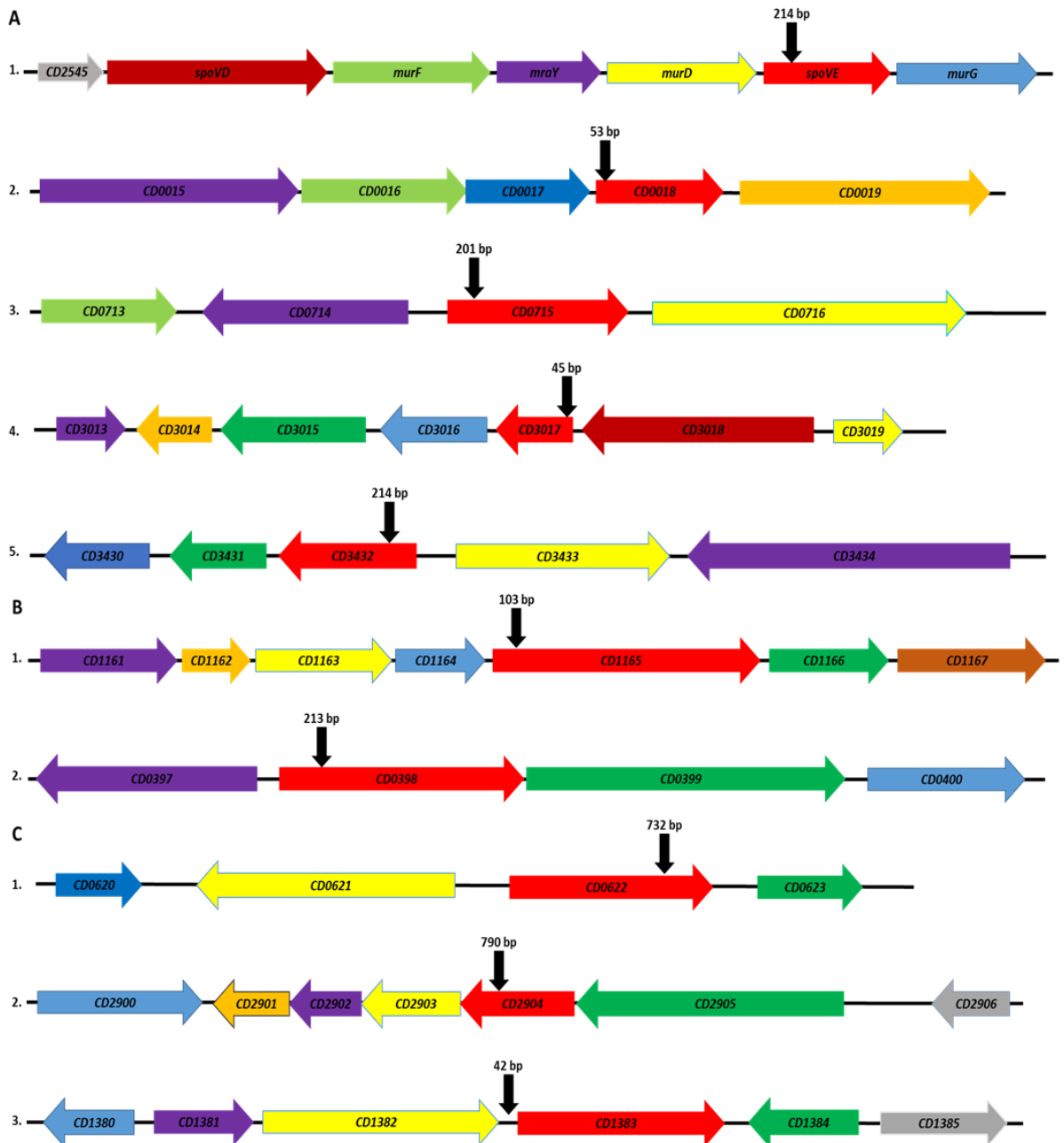


Figure 5.1: Transposon insertion sites. **A:** Cefoxitin sensitive mutants **1:** transposon inserted in *spoVE* 214 bp from the start of the gene, **2:** transposon inserted in *CD0018* 53 bp from the start of the gene, **3:** transposon inserted in *CD0715* 201 bp from the start of the gene, **4:** transposon inserted in *CD3017* 45 bp from the start of the gene and **5:** transposon inserted in *CD3432* 214 bp from the start of the gene. **B:** Ceftazidime sensitive mutants **1:** transposon inserted in *CD1165* 103 bp from the start of the gene and **2:** transposon inserted in *CD0398* 213 bp from the start of the gene. **C:** Ciprofloxacin sensitive mutants **1:** transposon inserted in *CD0622* 732 bp from the start of the gene, **2:** transposon inserted in *CD2904* 790 bp from the start of the gene and **3:** transposon inserted 42 bp before *CD1383*. The black arrow indicates the insertion site.

The second insertion was identified in *CD0398*, encoding a putative membrane protein. This gene is located in an apparent operon with *CD0399*. The promoter region of *CD0398* was identified by BPROM (SoftBerry) (Figure 5.1B). Although *CD0398* is an uncharacterized gene, the *CD0399* annotation suggests a possible β -lactamase activity (Figure 5.1B). Hence, the insertional mutant R20291*CD0398*::Tn was complemented with plasmid pYAA074 carrying *CD0399* with expression under the control of the constitutive promoter P_{cwp2} . R20291*CD0398*::Tn had a low MIC for both cefoxitin and cefazidime (32 $\mu\text{g/ml}$, 16 $\mu\text{g/ml}$ respectively) and these were fully restored to wild type levels by complementation with *CD0399* (128 $\mu\text{g/ml}$, 256 $\mu\text{g/ml}$ respectively) (Table 5.2), suggesting that the transposon insertion in *CD0398* has a polar effect on *CD0399* expression.

Under ciprofloxacin stress, seven mutants, showing sensitivity were isolated and the insertion sites of three were identified. The first transposon insertion was identified in *CD2904*, encoding a PTS system IIc component. PTS systems are typically involved in transport of carbohydrates (Kotrba *et al.*, 2001). The second transposon insertion was identified in *CD1383*, encoding a putative gamma-glutamyltranspeptidase. Gamma-glutamyltransferase is an enzyme that is involved in the glutathione cycle by transferring gamma-glutamyl group from a glutathione molecule to water or a peptide. Furthermore, it plays a significant role in drug or xenobiotic detoxification (Tate and Meister, 1985; Whitfield, 2001; Courtay *et al.*, 1992). The last insertion was identified in *CD0622*, encoding a cation transport protein. Pfam predicted that this protein has a Trk domain that is responsible for sodium uptake during ATP utilisation (Figure 5.1C). R20291*CD0622*::Tn showed the lowest ciprofloxacin MIC (64 $\mu\text{g/ml}$ compared with 512 $\mu\text{g/ml}$ for the WT) (Table 5.2).

Table 5.2: Minimum inhibitory concentrations of the wild type R20291 and deletion and insertional mutant strains ($\mu\text{g/ml}$).

Strains	Cefoxitin	Ceftazidime	Ciprofloxacin
R20291 WT	128	256	512
R20291 <i>spoVE</i> ::Tn	32	64	512
R20291 <i>CD0398</i> ::Tn	32	16	512
R20291 <i>CD0398</i> ::Tn/ pYAA074	128	256	512
R20291 <i>CD0622</i> ::Tn	128	256	64

5.4 Phenotypic analysis

5.4.1 Deletion of *CD0622*

A *CD0622* mutant was constructed in *C. difficile* R20291 using a recently developed homologous recombination system (Cartman *et al.*, 2012). This system uses the *codA* gene as a counterselection marker for genomic manipulation. *codA* encodes cytosine deaminase, which converts cytosine to uracil. *codA* can be toxic to the bacteria due to conversion of 5-fluorocytosine (FC) to 5-fluorouracil (FU) and subsequent misincorporation and fluorination of RNA. Hence, FC can be used to select against the plasmid. The plasmid pMTL-SC7215, carrying *codA*, was used to construct plasmid (pYAA064) with allele exchange arms having approximately 1,200 bp of homology to chromosomal sequence both upstream and downstream of the gene to be deleted (Figure 5.2A). *C. difficile* transconjugants grow slowly due to the segregational instability of the origin of replication (pBP1) on plasmid pMTL-SC7215. Recombination with the chromosome overcomes the segregational instability and results in faster-growing colonies. The first crossover was confirmed by PCR using a primer specific for the chromosome (RF758) and another on the plasmid pMTL-SC7215 (RF21), PCR showed the expected product of 3841 bp (Figure 5.2C). Double crossovers were then selected by using FC and successful deletion of *CD0622* was confirmed by PCR using primers flanking the gene (RF759 and RF760). Following deletion, only 18 bp of the gene remained (Figure 5.2). The resulting mutant, *C. difficile* R20291 Δ *CD0622* was then complemented with plasmid pYAA072 carrying the full length of *CD0622* with expression under the control of the constitutive promoter P_{cwp2} . The resulting strain was R20291 Δ *CD0622*/pYAA072.

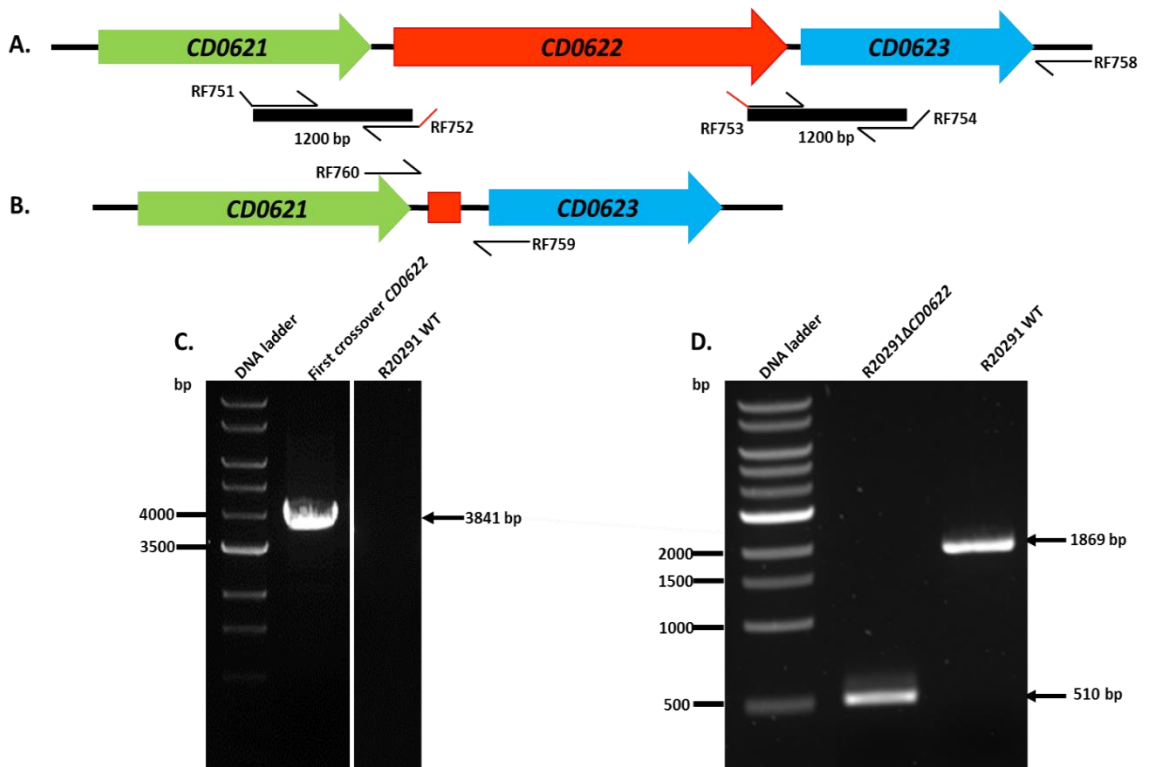


Figure 5.2: Deletion of *CD0622* using homologous recombination. **A:** Schematic diagram showing the primer design to delete *CD0622*. Both internal primers have a short overlap of complementary sequence to downstream and upstream of the gene, whereas the external primers are complementary for the pMTL-SC7215 plasmid. **B:** Schematic diagram showing the primer design to demonstrate deletion of the *CD0622* gene. Following deletion, only 18 bp of the gene remained (shown in red). **C:** PCR to confirm the first crossover, using a primer specific for the chromosome (RF758) and another on the plasmid pYAA064 (RF21). The PCR amplified a 3,841 bp PCR product as expected, wild type R20291 was included as a negative control. This confirmed recombination of the plasmid into the chromosome. **D:** PCR to confirm successful deletion of *CD0622*, using primers flanking the *CD0622* gene (RF759 and RF760). PCR amplified the predicted 510 bp from the mutant, whereas the wild type R20291 gave the predicted 1,869 bp product.

5.4.2 Determination of antibiotic MICs

In order to determine the MIC of ciprofloxacin, the agar dilution method was used following the laboratory standard institute guidelines [Clinical and laboratory standard institute, 2012]. MICs were read after 48 h incubation at 37°C for the four strains (wildtype, $\Delta CD0622$ mutant, R20291 $CD0622::Tn$ and complemented). The *C. difficile* R20291 wild type showed the highest MIC for ciprofloxacin (512 $\mu\text{g/ml}$). The lower R20291 $CD0622::Tn$ MIC was confirmed but this was not fully reproduced in the deletion mutant (64 $\mu\text{g/ml}$, 128 $\mu\text{g/ml}$ respectively). This suggests either that the transposon insertion has an effect on another gene, or there is another insertion in the transposon mutant. However, complementation with $CD0622$ fully restored ciprofloxacin resistance (512 $\mu\text{g/ml}$) (Table 5.3).

Table 5.3. Minimum inhibitory concentrations against the wild type R20291 and $CD0622$ mutants and complementation strains ($\mu\text{g/ml}$).

Strains	Ciprofloxacin
R20291 Wild Type	512
R20291 $CD0622::Tn$	64
R20291 $\Delta CD0622$	128
R20291 $\Delta CD0622$ / pYAA072	512

5.4.3 Synergy between ciprofloxacin and reserpine in *C. difficile* R20291

Recently, increased incidence of fluoroquinolone resistance in *C. difficile* has been observed and this has been attributed to alterations in the targets, DNA gyrase and topoisomerase IV. In particular, fluoroquinolone resistance occurred due to substitution of Thr82 to Ile in *gyrA* and Asn426 to Asp in *gyrB*, leading to loss of the target (Spigaglia *et al.*, 2010).

In other bacteria, over-expression of efflux pumps and membrane impermeability of bacteria have been linked to fluoroquinolone resistance (Ruiz, 2003). Reserpine is an inhibitor of efflux pumps (Markham, 1999; Neyfakh *et al.*, 1993). To test if *C. difficile* ciprofloxacin resistance is dependent on efflux, reserpine was tested against strain R20291. Surprisingly, no effect was observed upon treatment with reserpine alone (data not shown). Subsequently, a series of ciprofloxacin concentrations from 2 µg/ml to 1024 µg/ml, mixed with 100 µg/ml of reserpine (the concentration was optimised), were tested for a synergistic effect. The ciprofloxacin MIC of the wild type was decreased by four fold from 512 µg/ml to 128 µg/ml in the presence of reserpine. However, in both mutant strains (R2091ΔCD0622 and R20291CD0622::Tn), reserpine did not have any further effect on ciprofloxacin resistance (128 µg/ml and 64 µg/ml respectively), consistent with CD0622 being the reserpine target. The combination of reserpine and ciprofloxacin was then tested against a panel of *C. difficile* strains. The MIC of ciprofloxacin was decreased by eight fold in strain M120 (to 4 µg/ml), whereas in the other strains of *C. difficile*, reserpine only reduced the ciprofloxacin MIC by two fold (Table 5.4).

Table 5.4: Minimum inhibitory concentrations of ciprofloxacin in the presence and absence of reserpine ($\mu\text{g/ml}$).

Strains	Ciprofloxacin	Ciprofloxacin + Reserpine 100 $\mu\text{g/ml}$
R20291	512	128
R20291 <i>s/pA</i>	512	128
R20291 Δ CD0622	128	128
R20291 Δ CD0622/ pYAA072	512	128
R20291 CD0622:: <i>Tn</i>	64	64
630	32	16
R7404	32	16
M120	32	4
Ox247	32	16
TL178	32	16
CDKK959	128	64
Liv22	128	64

5.5 CD0399

As described in section 5.3.1, we hypothesized that the resistance phenotype of the *CD0398* transposon mutant was due to a polar effect on the downstream gene *CD0399*, encoding a putative β -lactamase. Consistent with this hypothesis, expression of *CD0399* in *CD0398::Tn* fully restored ceftazidime resistance. This suggested that *CD0399* was involved in cephalosporin resistance, perhaps by β -lactamase activity.

CD0399 is a 36.161 kDa protein consisting of 313 amino acids, and containing a predicted N-terminal membrane-spanning domain. The transmembrane domain (residues 7-24) is predicted to be an α -helix, binding *CD0399* to the cell membrane (<http://www.cbs.dtu.dk/services/TMHMM/>) (Finn, *et al.*, 2014). Residues 47-305 are predicted to be a transpeptidase domain (<http://pfam.xfam.org/>) (Figure 5.3B). In an attempt to determine *CD0399* function, the protein was purified, followed by nitrocefin assays to demonstrate β -lactamase activity. The protein was then mutated by changing the possible active site serines (102 or 108) to determine which residue is responsible for the catalytic activity. Furthermore, the class of β -lactamase enzyme was identified by using clavulanic acid, confirming that *CD0399* is a class A β -lactamase.

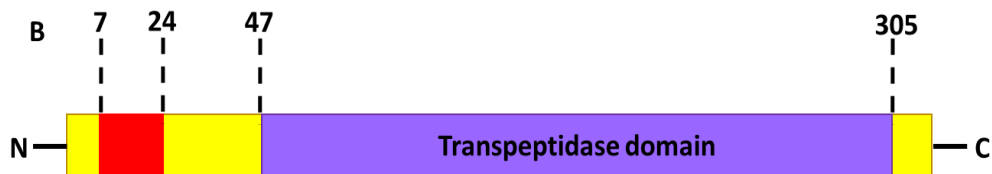
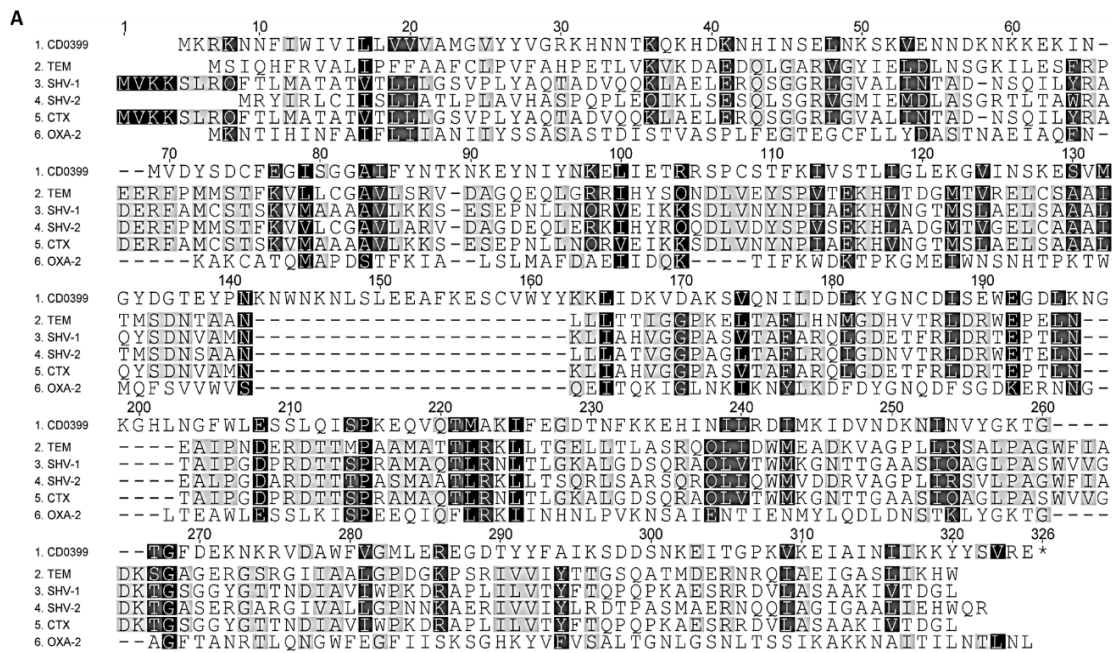


Figure 5.3: General characteristics of CD0399. **A:** Multiple sequence alignment of CD0399 with other related β -lactamase enzymes. All protein sequences (TEM, SHV1, SHV2, CTX and OXA-2) are from *E. coli*. Alignment produced using Geneious 7.1.7. **B:** Pfam (<http://pfam.xfam.org/>) prediction showing the residue numbers of transpeptidase domain, and an N-terminal transmembrane domain (<http://www.cbs.dtu.dk/services/TMHMM/>). The transmembrane domain is shown in red, the transpeptidase domain is in purple.

5.5.1 Functional analysis of the CD0399 β -lactamase domain

In order to confirm that CD0399 has β -lactamase activity, we cloned and purified the protein. His tag encoding DNA was fused to the 3' end of *CD0399* in pET-28a using the restriction enzymes *NcoI* and *XhoI*. The protein was expressed in *E. coli* Rosetta and purified (Figure 5.4A). The molecular weight (MW) of CD0399-His was confirmed by electrospray ionisation mass spectrometry (34.38 kDa; Figure 5.4C). Next, two possible active site serine motifs (Ser-Xaa-Xaa-Lys) (Matagne *et al.*, 1999) were identified and the codon of the putative active site serine 102 (TCT) or 108 (TCA) were changed to alanine (GCG) by an inverse PCR, to allow identification of the acylation site. Subsequently, the CD0399S102A-His protein was purified as before (Figure 5.4B). The MW difference was confirmed by electrospray ionisation mass spectrometry (34.36 kDa; Figure 5.4D).

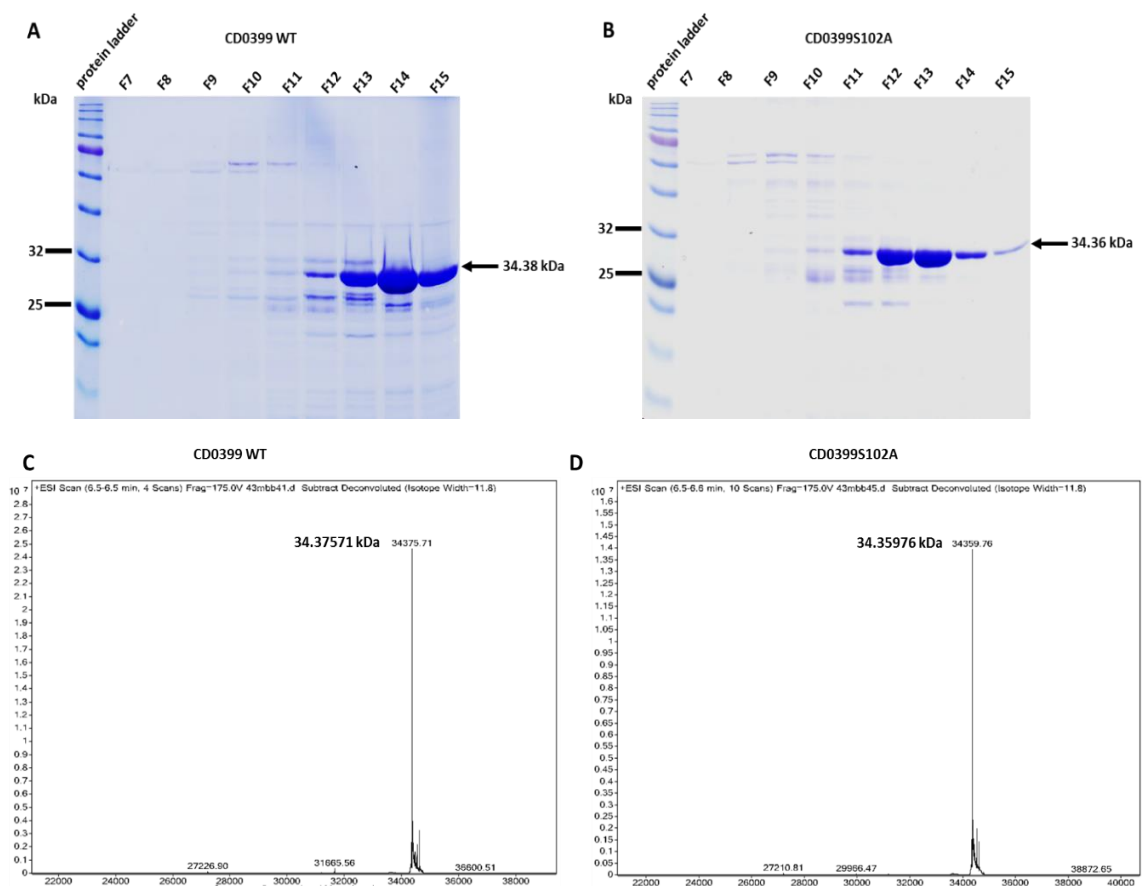
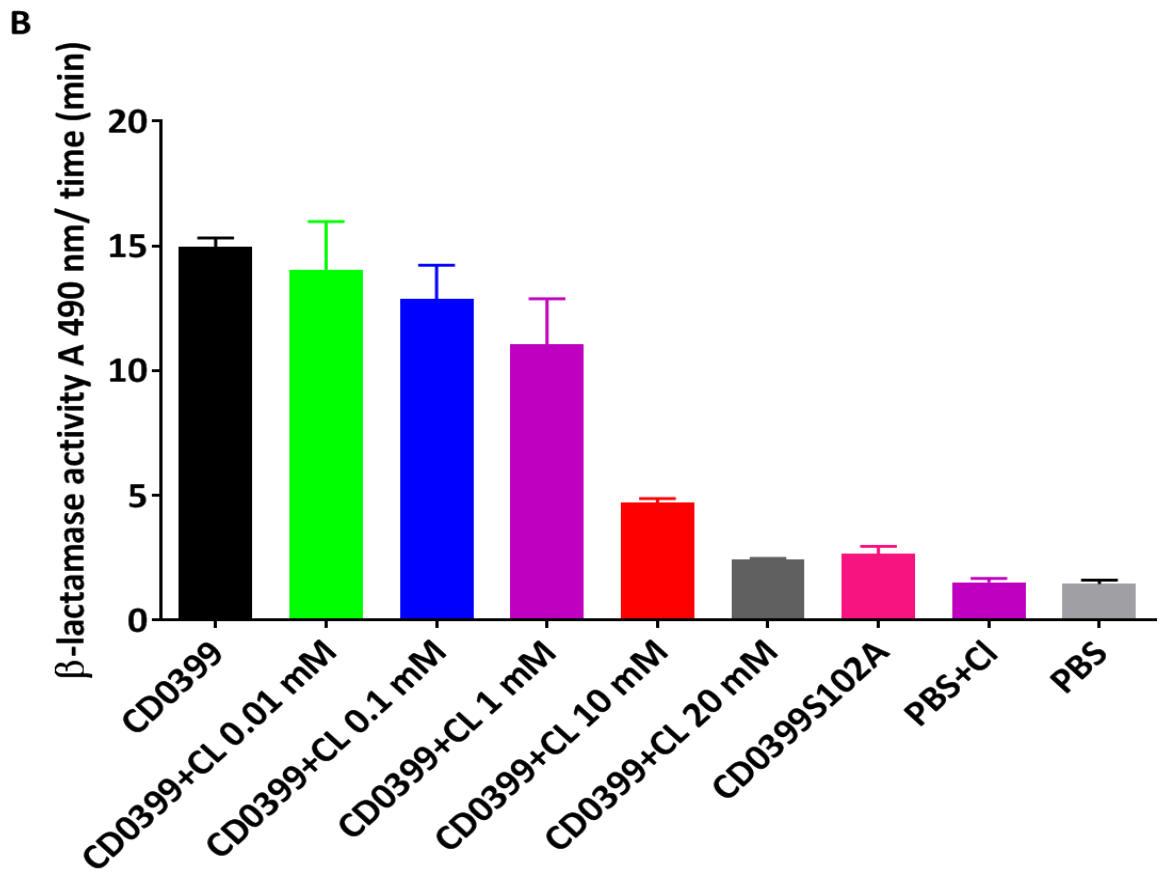
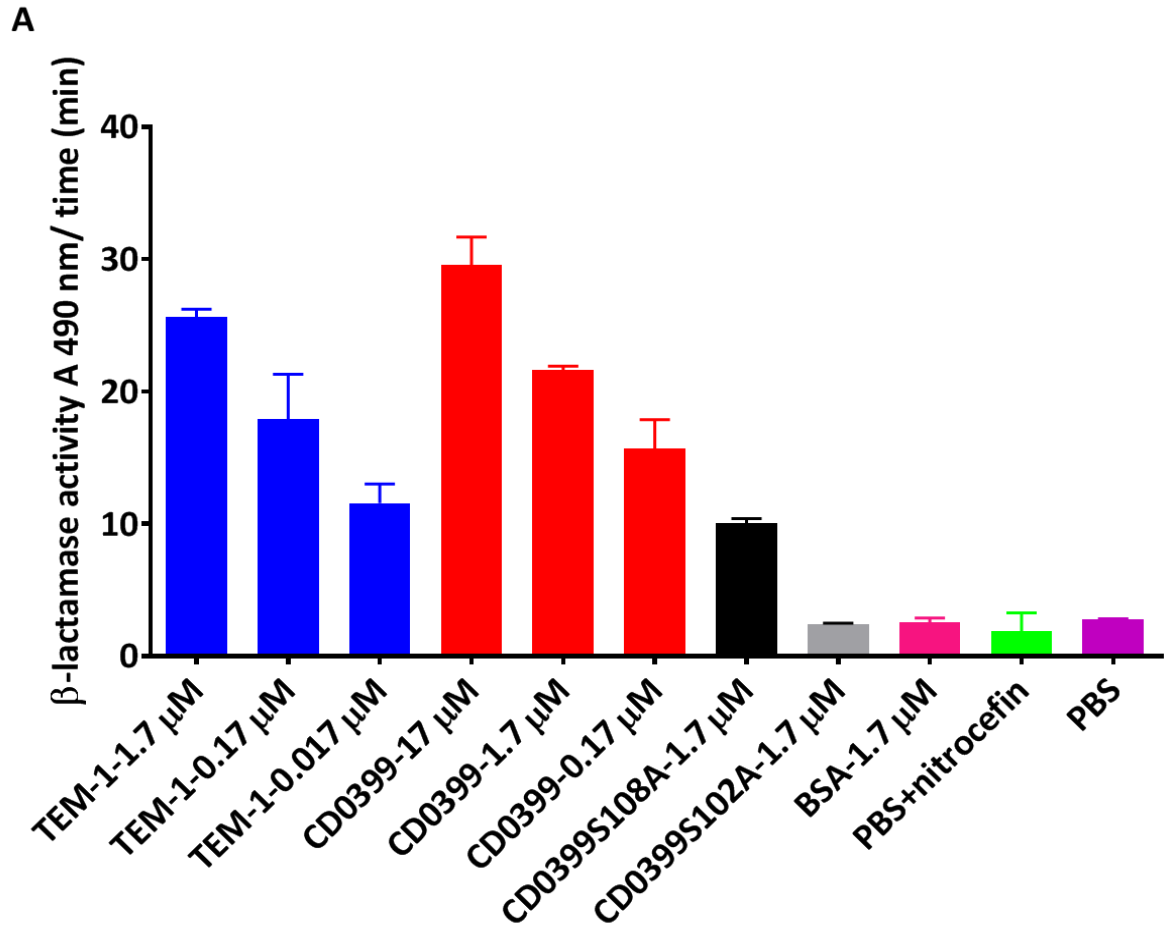


Figure 5.4: Purification of CD0399 and CD0399S120A. **A** and **B** fractions of CD0399-His and CD0399S120A-His eluted from Ni-NTA were analysed by SDS-PAGE stained with Coomassie blue. The fractions with good quality protein were pooled and dialysed against 25 mM Tris, 50 mM NaCl pH 8. **C** and **D** mass spectra of CD0399 and CD0399S120A, 34.38 kDa and 34.36 kDa respectively.

5.5.2 CD0399 β -lactamases activity

In order to determine the exact function of CD0399, the protein was examined for β -lactamase activity *in vitro*. Following purification, β -lactamase assays were carried out on CD0399 and CD0399S102A using nitrocefin as the substrate. TEM-1 (class A β -lactamase) was used as a positive control. CD0399 was used at 17 μ M, 1.7 μ M, 0.17 μ M and 0.017 μ M (Figure 5.5A), and showed clear hydrolysis of nitrocefin, changing the colour of nitrocefin substrate from yellow to red. The rate of nitrocefin hydrolysis of CD0399 was almost the same as TEM-1. CD0399S102A failed to hydrolyse nitrocefin, confirming identification of the active site serine (Ser102) (Figure 5.5A). Changing serine 108 reduced the rate of hydrolysis but did not completely abolish activity (Figure 5.5A).

To identify the class of β -lactamase, assays were repeated with different inhibitors. The activity of CD0399 was inhibited by incubation with clavulanic acid (Figure 5.5B) but not EDTA (Figure 5.5C), suggesting that CD0399 is a class A β -lactamase. Clavulanic acid and tazobactam completely inhibit class A β -lactamases such as TEM-1, TEM-2, TEM-3, TEM-30, TEM-50, SHV-1, SHV-2, SHV10, CTX-M-15, PER-1, VEB-1, CepA, PSE-1, CARB-3, RTG-4 and PC1, and have a variable effect on class D lactamases such as OXA-1, OXA-10, OXA-11, OXA-15, OXA-23, OXA-48. However, both clavulanic acid and tazobactam do not inhibit class C lactamases such as AmpC, P99, ACT-1, CMY-2, FOX-1, MIR-1, GC1 and CMY-37 (Bush *et al.*, 1995). Furthermore, class A, C and D β -lactamases hydrolyse the β -lactam ring following covalent binding to the active site serine residue, while class B lactamases require a divalent zinc as co-factor for the hydrolysis process (Bush and Jacoby, 2009). Thus class B lactamases such as IMP-1, VIM-1, CcrA, IND-1, L1, CAU-1, GOB-1, FEZ-1, CphA and Sfh-1 are completely inhibited by EDTA (Bush *et al.*, 1995). Also, changing serine 102 in CD0399 caused complete loss of protein function, further confirming identification as a class A β -lactamase.



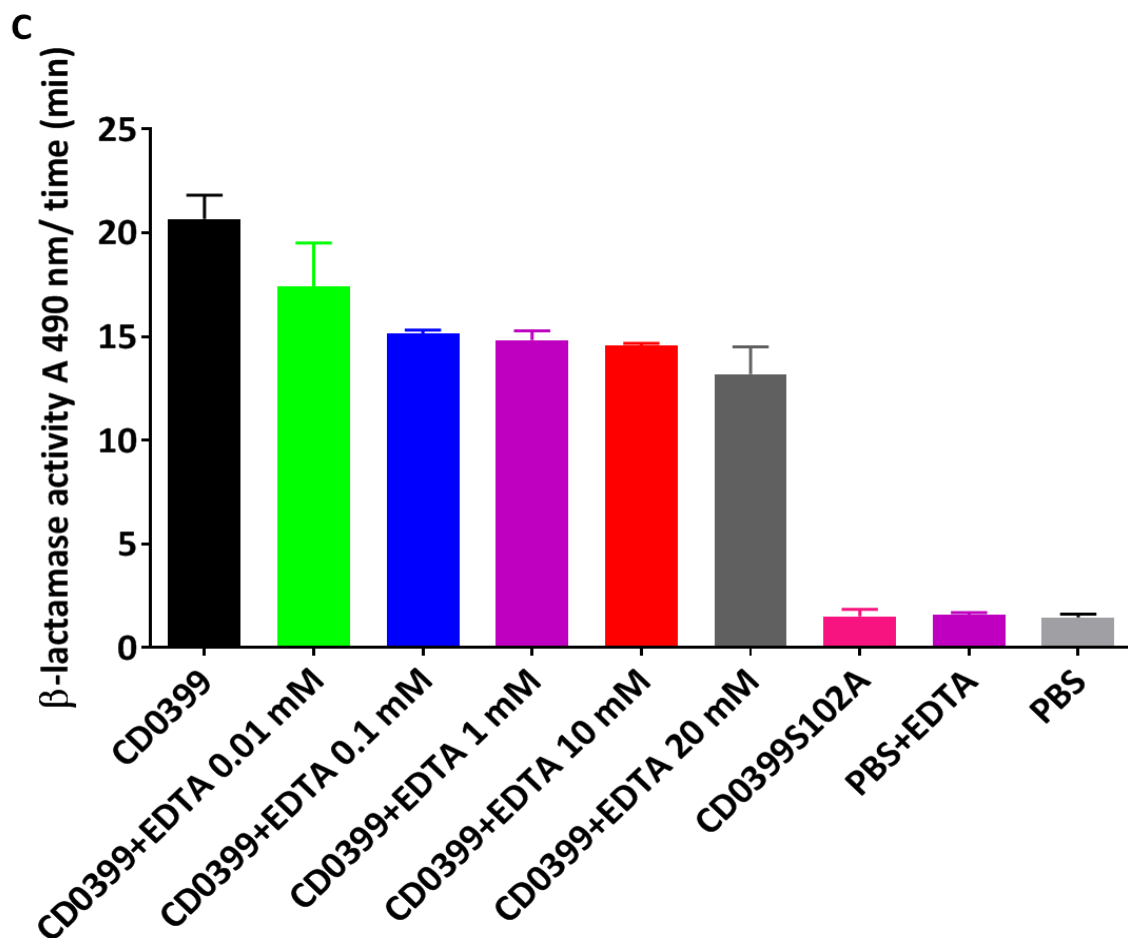


Figure 5.5: β -lactamase activity. **A:** The hydrolysis of nitrocefin substrate by TEM-1 and CD0399. The proteins were incubated with 100 μ M nitrocefin for 3 h at 25°C, and the absorbance change was measured at 490 nm. Protein activity was calculated by taking the slope of absorbance values at 1, 30, 60, 90, 120, 150 and 180 min and plotted using GraphPad Prism 7 software. **B:** Inhibition of CD0399 activity by Clavulanic acid. Protein (1.7 μ M) was incubated with different concentrations of clavulanic acid (CL; range 0.01-20 mM) for 30 min at 37°C, then nitrocefin was added (100 μ M), followed by incubation for 3 h at 25°C. The absorbance change and protein activity were measured as in **A**. **C:** Inhibition of CD0399 activity by EDTA. Protein (1.7 μ M) was incubated with different concentrations of EDTA (range 0.01 -20 mM) for 30 min at 37°C, then nitrocefin was added (100 μ M), followed by incubation for 3 h at 25°C. The absorbance change and protein activity were measured as in **A**. β -lactamase activity = absorbance at 490 nm/time (min).

Moreover, we confirmed the β -lactamase activity of CD0399 from incubation of CD0399 with ceftazidime, followed by electrospray ionization mass spectrometry. We observed a minor peak at 0.4610922 kDa following incubation. This peak confirmed ceftazidime hydrolysis, with loss of the R2 side chain due to the rearrangement of the molecule (Figure 5.6C). This result confirmed the β -lactamase activity, and showed that 2 h incubation was sufficient to complete ceftazidime hydrolysis. In contrast, we did not observe any changes from incubation of CD0399S102A with ceftazidime, demonstrating complete loss of protein function (Figure 5.6D).

In *Burkholderia pseudomallei*, incubation of C69F or PenI β -Lactamase with ceftazidime for 4 h at 37°C, showed two different mechanisms of hydrolysis (Papp-Wallace *et al.*, 2016). The first mechanism of ceftazidime hydrolysis leads to an increase in the molecular weight of ceftazidime by addition of H₂O (Faraci and Pratt 1985). The second mechanism of ceftazidime hydrolysis leads to rearrangement of the product when the R2 group is lost (Citri *et al.*, 1976).

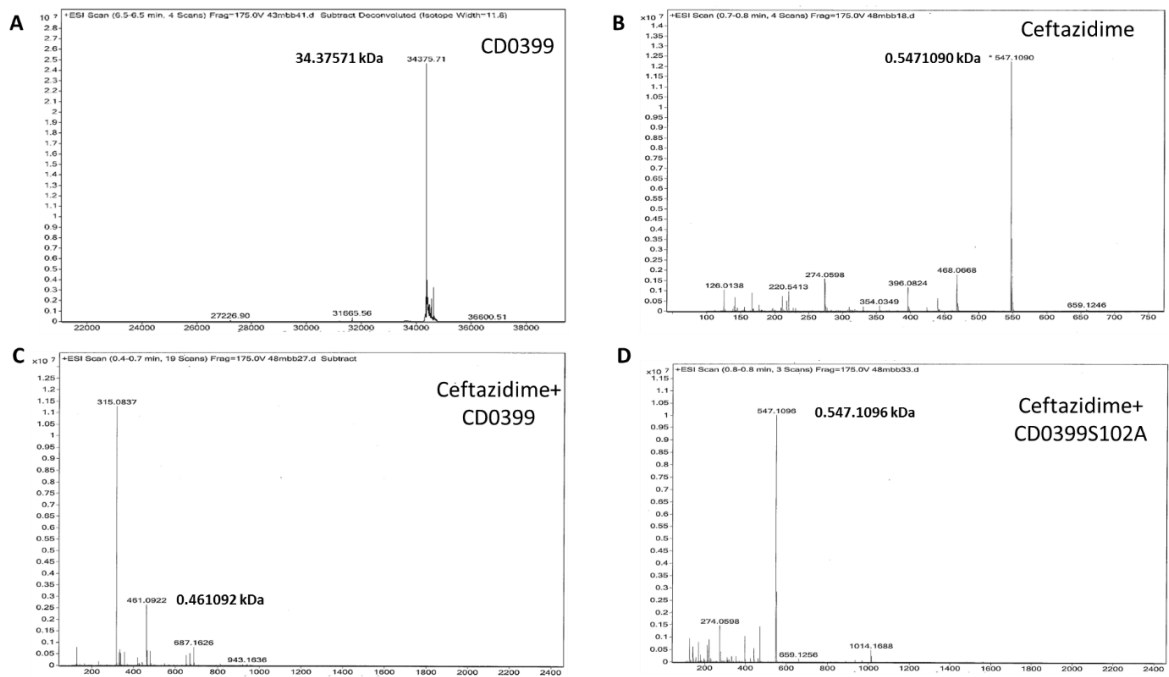


Figure 5.6: Analysis of electrospray ionization mass spectrometry. **A** and **B** mass spectra of CD0399 and ceftazidime, 34.38 kDa and 0.55 kDa respectively. **C** and **D** mass spectra of ceftazidime with CD0399 (40 μ M) and CD0399S102A (40 μ M) following incubation with ceftazidime (40 mM) at 37C° for 2 h, 0.46 kDa and 0.55 kDa respectively.

1.7 μM CD0399 was the optimum concentration for the β -lactamase assay (Figure 5.5A). 20 mM clavulanic acid was the optimum concentration to inhibit β -lactamase activity (Figure 5.5B). With this optimisation, the kinetics of CD0399 β -lactamase activity with and without clavulanic acid were determined using different concentrations of nitrocefin (50 μM -800 μM). Kinetic values were obtained using the Michaelis-Menten equation. The results showed that CD0399 has a V_{max} of 55 μM , K_{m} 10.5 μM , K_{cat} 32.4 min^{-1} and $K_{\text{cat}}/K_{\text{m}}$ 3.1 $\mu\text{M}/\text{min}$. While TEM-1 showed a V_{max} of 55 μM , K_{m} 1.8 μM , K_{cat} 32.4 min^{-1} and $K_{\text{cat}}/K_{\text{m}}$ 18 $\mu\text{M}/\text{min}$. CD0399S108A showed a V_{max} 20 μM , K_{m} 88.4 μM , K_{cat} 11.8 min^{-1} and $K_{\text{cat}}/K_{\text{m}}$ 0.13 $\mu\text{M}/\text{min}$. Values were lowest when incubated with clavulanic acid as an inhibitor, CD0399: V_{max} 44.7 μM , K_{m} 92.6 μM and K_{cat} 26.3 min^{-1} , CD0399S108A showed V_{max} 17.5 μM , K_{m} 91 μM and K_{cat} 10.31 min^{-1} , TEM-1 showed V_{max} 51 μM , K_{m} 75 μM and K_{cat} 30 min (Table 5.5). In general, CD0399 showed the same specificity for nitrocefin as TEM-1 because they have the same rate of nitrocefin hydrolysis. CD0399S108A was considerably less active due to substitution of serine 108. Reaction rates were reduced to $K_{\text{cat}}/K_{\text{m}}$ 0.28 $\mu\text{M}/\text{min}$, $K_{\text{cat}}/K_{\text{m}}$ 0.4 $\mu\text{M}/\text{min}$ and $K_{\text{cat}}/K_{\text{m}}$ 0.11 $\mu\text{M}/\text{min}$ for CD0399, TEM-1 and CD0399S108A respectively, in the presence of clavulanic acid. In contrast, CD0399S102A showed no enzymatic activity with nitrocefin, confirming identification of the active site serine (Ser102) (Table 5.5; Figure 5.7).

Table 5.5: Kinetic parameters of TEM-1, CD0399, CD0399S108A and CD0399S102A.

TEM-1				
Substrate	V _{max} (μM min ⁻¹)	K _m (μM)	k _{cat} (min ⁻¹)	k _{cat} /K _m μM ⁻¹ min ⁻¹
Nitrocefin	55	1.8	32.4	18
Clavulanic acid	51	75	30	0.4
CD0399				
Substrate	V _{max} (μM min ⁻¹)	K _m (μM)	k _{cat} (min ⁻¹)	k _{cat} /K _m μM ⁻¹ min ⁻¹
Nitrocefin	55	10.5	32.4	3.1
Clavulanic acid	44.7	92.6	26.3	0.28
CD0399S108A				
Substrate	V _{max} (μM min ⁻¹)	K _m (μM)	k _{cat} (min ⁻¹)	k _{cat} /K _m μM ⁻¹ min ⁻¹
Nitrocefin	20	88.4	11.8	0.13
Clavulanic acid	17.5	91	10.31	0.11
CD0399S102A				
Substrate	V _{max} (μM min ⁻¹)	K _m (μM)	k _{cat} (min ⁻¹)	k _{cat} /K _m μM ⁻¹ min ⁻¹
Nitrocefin	0	0	0	0
Clavulanic acid	0	0	0	0

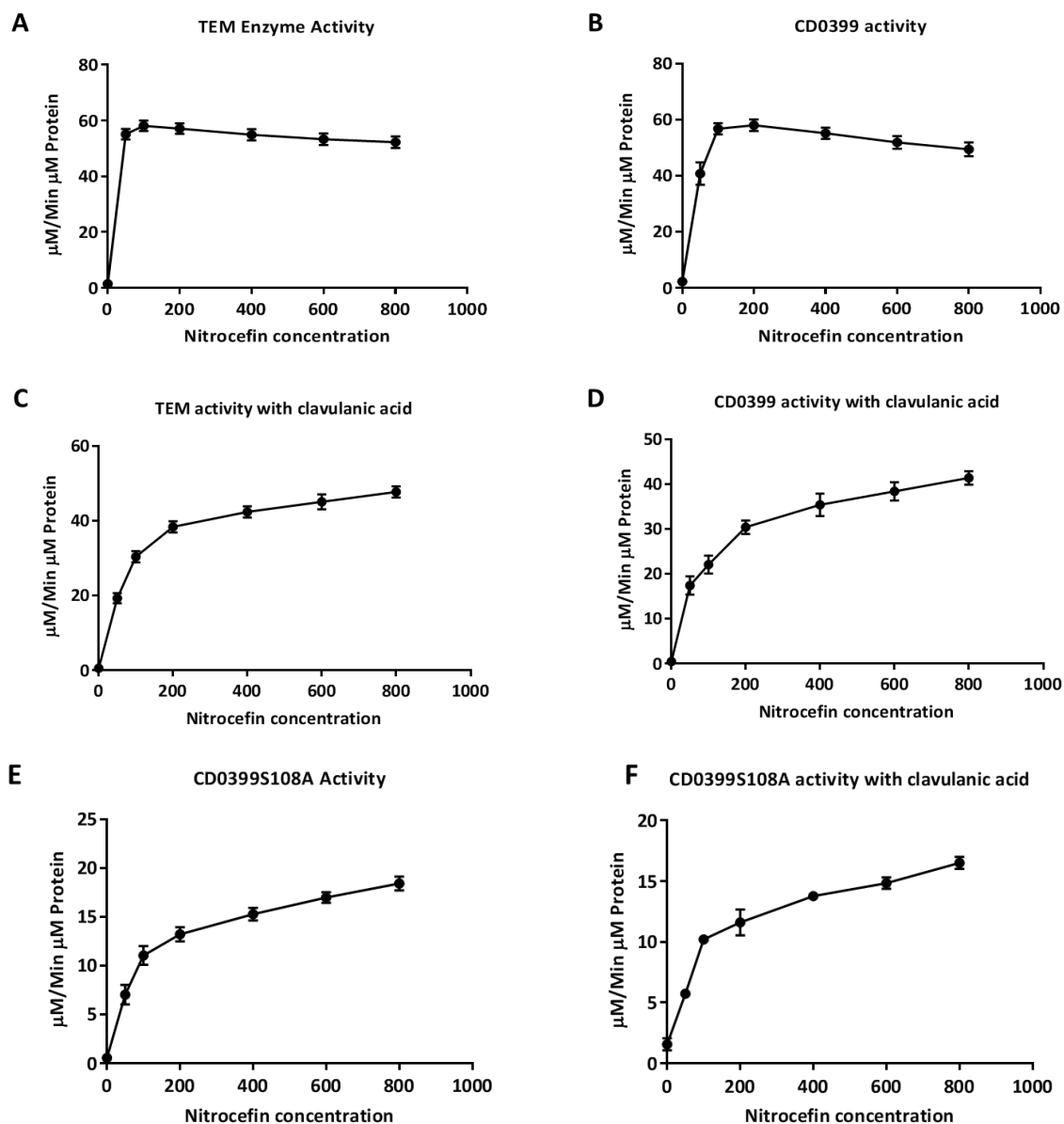


Figure 5.7: Kinetic analysis of CD0399, CD0399S108 and TEM-1 with nitrocefin and clavulanic acid. 1.7 μM of each protein was incubated with different concentrations of nitrocefin (range 50-800 μM) for 3 h at 25°C, and the absorbance change was measured at 490 nm. Kinetics were calculated by taking the slope of absorbance values at 1, 30, 60, 90, 120, 150 and 180 min and fitted to the Michaelis-Menten equation using GraphPad Prism 7 software. The assay was completed in triplicate.

Although, CD0399 showed β -lactamase activity using the nitrocefin assay, domain analysis predicts that this protein has transpeptidase activity which could contribute to peptidoglycan synthesis. This has been previously observed for three β -lactamase enzymes (AmpC, OXA-1 and TEM-1) by labelling with fluorescein-meropenem (June *et al.*, 2014). It was observed that acyl-intermediate products, exhibiting fluorescence, were formed by each enzyme. To test for CD0399 transpeptidase activity, purified protein was labelled with Bocillin-FL. CD0399, TEM-1 and CD0399S102A were incubated with Bocillin-FL substrate for 30 min at 37°C (Figure 5.8A). Surprisingly, CD0399 showed a fluorescent signal, while TEM-1 did not label with Bocillin-FL at all. This may be due to rapid hydrolysis of the substrate by TEM-1, leading to loss of the fluorescent signal. However, CD0399 did not hydrolyse the Bocillin-FL substrate when incubated for 30 min, showing a fluorescent signal consistent with the acyl-enzyme intermediate products. CD0399S102A also failed to bind Bocillin-FL, confirming disruption of the β -lactamase activity by this point mutation. In this assay SpoVD was used as a positive control for binding with Bocillin-FC, as described in chapter 3 (Figure 5.8). Taken together, this suggests that CD0399 can form acyl-enzyme products. To confirm the acylation mechanism of CD0399, the protein was preincubated with ceftazidime at different concentrations (32 μ M, 64 μ M, 128 μ M) for 2 h at 37°C to complete acylation, followed by addition of Bocillin-FL. Preincubation with ceftazidime blocked labelling with Bocillin-FL (Figure 5.9A). This suggests that the β -lactam ring of the ceftazidime binds with the active serine of CD0399, competing with Bocillin-FL. This is similar to results that showed blocking of OXA-1 β -Lactamase binding with Bocillin-FL, after preincubation with ampicillin (Schneider *et al.*, 2009).

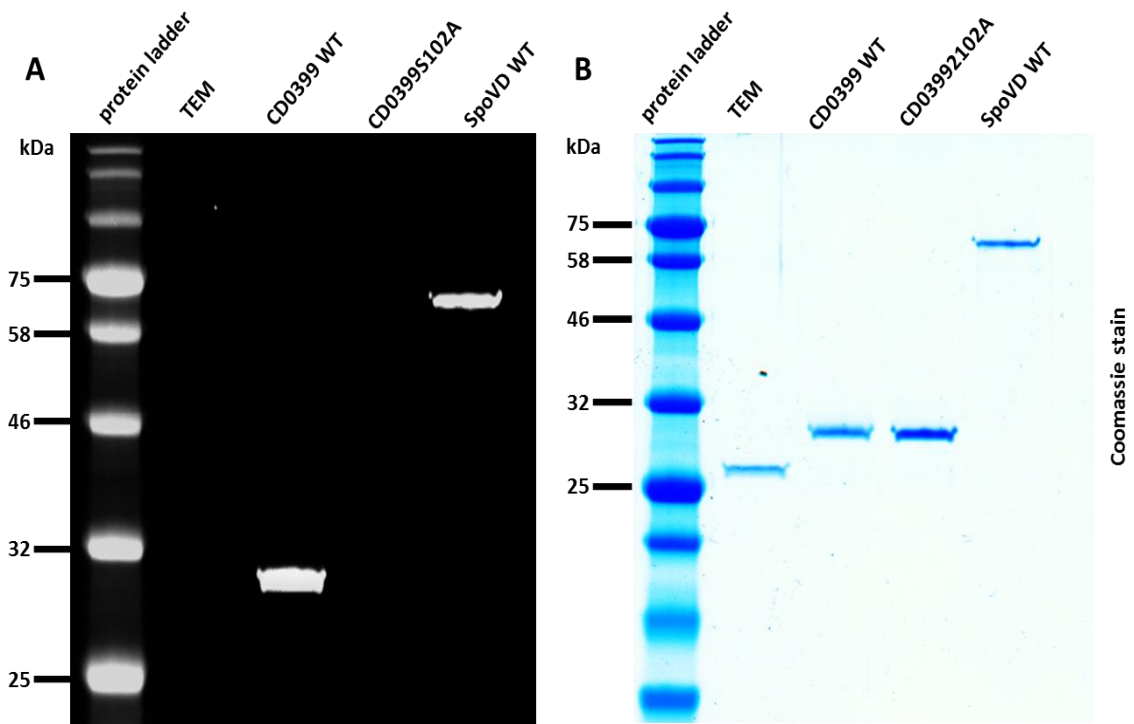


Figure 5.8: Bocillin-FL labelling of CD0399, CD0399S102A, TEM-1 and SpoVD. **A:** CD0399, CD0399S102A, TEM-1 and SpoVD were incubated with Bocillin-FL (50 μ M) for 30 min at 37°C, followed by 12% SDS-PAGE. Detection of fluorescence signal confirmed formation of an acyl-enzyme intermediate. CD0399S102A lost the signal completely. This suggests that serine 102 is the active site for binding with the β -lactam ring. SpoVD was used as positive control for Bocillin-FL labelling. The fluorescent gel was imaged using Bio-Rad imager Cy3 filter. **B:** gel from panel **A** stained with Coomassie blue, resolving all the proteins. The stained gel was used as control for protein loading.

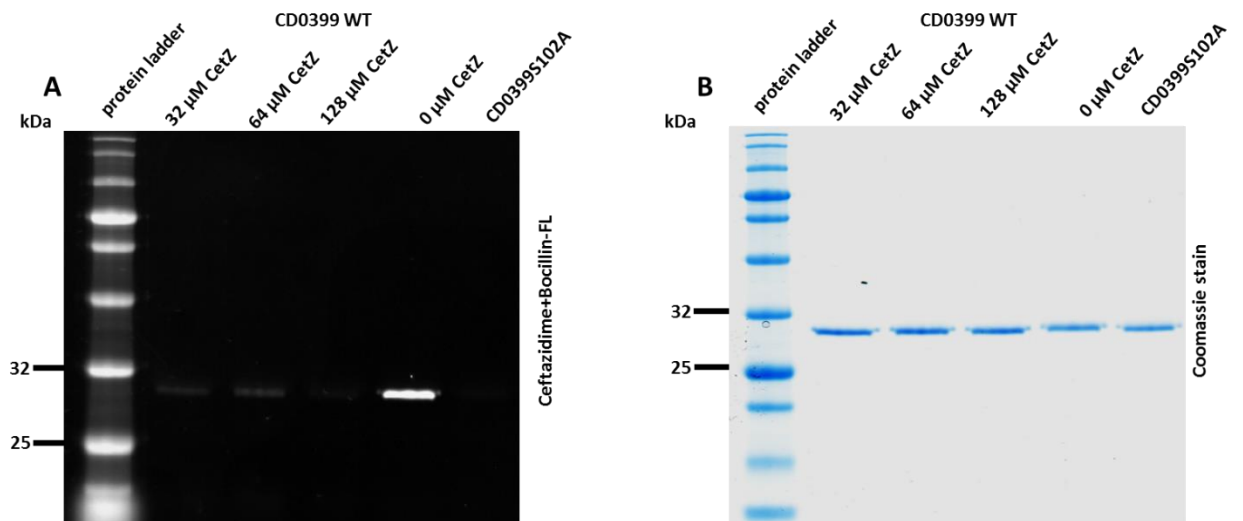


Figure 5.9: Ceftazidime blocks bocillin-FL labelling. **A:** CD0399 was labelled with Bocillin-FL substrate at (50 μ M) for 30 min at 37°C, and separated by 10% SDS-PAGE. The protein was preincubated with ceftazidime for 2 h at different concentrations (0 μ M, 32 μ M, 64 μ M, or 128 μ M), followed by Bocillin-FC labelling for 30 min at 37°C. The fluorescent signal confirmed the acyl-enzyme intermediate formation between CD0399 and Bocillin-FL, while CD0399S102A did not label. This suggests that serine 102 is the active site for binding with the β -lactam ring. The fluorescent gel was imaged using Bio-Rad imager Cy3 filter. **B:** gel from panel **A** stained with Coomassie blue, resolving both proteins. The stained gel was used as control for protein loading. CetZ: ceftazidime.

5.6 Discussion

Transposon mutagenesis has been used previously in *C. difficile* to create large mutant libraries (Dembek *et al.*, 2015). A similar approach was employed in this project to identify genes involved in cephalosporin and fluoroquinolone resistance. A total of 6,000 transposon mutants were screened for sensitivity to cefoxitin, ceftazidime, and ciprofloxacin and the transposon insertion sites of sensitive mutants were identified using marker rescue.

Under cefoxitin selection, we identified insertion sites in five different genes. Most interestingly among these was *spoVE*. This mutant showed the same cefoxitin MIC as $\Delta spoVD$. I have already demonstrated that SpoVD is involved in both sporulation and cephalosporin resistance (chapter 3). In addition, I confirmed that a SpoVD/SpoVE interaction is crucial in both cortex synthesis and cephalosporin resistance. Therefore, this transposon insertion provided further clear evidence for the importance of the interaction on cefoxitin resistance. This interaction has been previously observed in *B. subtilis* and these proteins localise to the forespore compartment (Fay *et al.*, 2010).

Under ceftazidime selection, we identified insertion sites in two genes from over 18 mutants. The most important of those genes was *CD0398*. Upon further analysis we determined that the *CD0398::Tn* phenotype was actually due to a polar effect on *CD0399*, encoding a putative β -lactamase. The β -lactamase activity of CD0399 was confirmed by purification of CD0399, followed by nitrocefin assays. The protein showed a clear hydrolysis of nitrocefin and mutation of serine 102 abolished the catalytic activity. However, CD0399 also showed a fluorescent signal with bocillin-FL, consistent with the formation of acyl-intermediate products. This suggests that CD0399 also has transpeptidase activity.

Under ciprofloxacin selection, we identified insertion sites in three genes from seven mutants. The most important of these genes was *CD0622*, encoding a putative cation transport protein belonging to the Trk superfamily. A *CD0622* deletion showed a similar phenotype, with a decrease in the MIC for ciprofloxacin of four-fold compared to the wild type. The original transposon mutant had a slightly more severe resistance defect, suggesting that the transposon insertion was affecting another gene, perhaps

the downstream *CD0623*, predicted to also encode a cation transport protein. It has been demonstrated that transport proteins can work as efflux pumps with a role in fluoroquinolone resistance (Garvey *et al.*, 2011). In order to confirm an efflux pump mechanism for *CD0622*, reserpine was tested as an inhibitor. A mixture of reserpine and ciprofloxacin led to a decrease in the ciprofloxacin MIC of four-fold in the wild type. This is the same resistance defect observed in the $\Delta CD0622$ mutant. The inclusion of reserpine had no effect on the $\Delta CD0622$ ciprofloxacin MIC, suggesting that *CD0622* is the target. This is identical to previous results from *S. pneumoniae* that demonstrated a synergistic effect of ciprofloxacin and reserpine (Garvey *et al.*, 2011). Moreover, the NorA efflux pump in *Staphylococcus aureus* can also be inhibited with reserpine, leading to a reduction in the MIC of ciprofloxacin, moxifloxacin and sparfloxacin of four-fold (Schmitz *et al.*, 1998).

The experiments carried out in this chapter provide good evidence that transposon mutagenesis can be used to successfully identify new genes contributing to antibiotic resistance.

Chapter Six

Final Discussion

Despite the fact that CDI cases have fallen in recent years in the UK, *C. difficile* is still the main bacterial problem of the healthcare system, causing large problems for hospital workers and care homes. In parallel with increases in the number of CDI cases in the early years of this century, morbidity and mortality also rose due to the emergence of a new epidemic and hypervirulent ribotype 027, called *C. difficile* R20291 (Dubberke and Olsen, 2012; Spigaglia, 2016). This strain caused increased CDI incidence in addition to apparently increased severity and relapse frequency (Spigaglia, 2016).

The primary risk factor for CDI is antibiotic use, leading to shifts in the composition of the microbiota and creating a convenient environment for *C. difficile* infection (Theriot and Young, 2015; Buffie *et al.*, 2015; Theriot *et al.*, 2016). The most important reason behind *C. difficile* antibiotic resistance is the acquisition of a wide range of mobile elements that confer resistance. This has led to the emergence of new epidemic strains that are resistant to many antibiotics, including macrolides, cephalosporins and fluoroquinolones (Spigaglia, 2016). Moreover, a reduction of susceptibility to the effective antibiotics, such as metronidazole, as well as for the antibiotics that are used for CDI recurrences, such as the rifamycins, may result in a weak response to CDI treatment (Spigaglia, 2016).

The most important factors in *C. difficile* pathogenicity and transmission are the spores which germinate *in vivo* to produce vegetative cells. Toxin secretion then leads to diarrhoea in susceptible individuals (Janoir *et al.*, 2007). So prevention of spore germination has a direct impact on CDI (Nerandzic and Donskey, 2010; Nerandzic and Donskey, 2013).

The main aim of this project was to characterise mechanisms of antibiotic resistance in an epidemic and virulent ribotype 027 strain that has been found to produce more spores and toxin than typical *C. difficile* strains (Owens, 2007)

In our preliminary work, a BLAST search was performed against the R20291 genome using PBP protein sequences from *B. subtilis* 168. From the 11 putative PBPs identified, we chose two, one encoding a class B PBP (SpoVD) and a second encoding a

class C PBP (Cwp20), for further study. Deletion of either *spoVD* or *cwp20* was found to have a dramatic effect on cephalosporin resistance.

In addition to a defect in cephalosporin resistance, a Δ *spoVD* mutant also displayed a severe sporulation defect. A recent study has shown that *spoVD* disruption causes loss of spore cortex assembly in *B. subtilis* (Bukowska-Faniband and Hederstedt, 2013). Surprisingly however my data showed *spoVD* expression in growing cells. This is consistent with the observation that SpoVD contributes to cephalosporin resistance. In contrast, *B. subtilis* SpoVD, which is localised to the cell membrane, only appears in the second hour of the sporulation process. The protein is detectable in the mother cell compartment and then localises to the forespore membrane (Bukowska-Faniband and Hederstedt, 2015). This led us to hypothesize that a different sigma factor, perhaps sigma 70, may be responsible for expression of SpoVD in exponential phase. The importance of the sporulation sigma factors (F, E, K and G) in the regulation of sporulation genes in *C. difficile* has been studied by several groups (Fimlaid *et al.*, 2013; Pereira *et al.*, 2013; Saujet *et al.*, 2013). Surprisingly, none of these studies have identified the sigma factor that is responsible for SpoVD expression, while in *B. subtilis* *spoVD* transcription is dependent on σ E and is negatively controlled by SpoIIID (Eichenberger *et al.*, 2003). This points to a novel hypothesis whereby *spoVD* is expressed from two different promoters: one active during vegetative growth phase and involved in cephalosporin resistance, and a second active in sporulation phase that participates in spore cortex assembly. In further experiments I also observed that deletion of *spoVD* caused overexpression of Spo0A, with apparent impacts on the expression of SpoVT, Gpr, SpiL and TcdB (low expression), while also leading to higher expression of SpoIVA.

I have also demonstrated an interaction between SpoVD and SpoVE. In *B. subtilis*, SpoVD interacts with the lipid II flippase SpoVE and the complex localises to the forespore membrane (Fay *et al.*, 2010). However, no study has suggested that this interaction plays a role in cephalosporin resistance or that the PBP dimer may be required for the interaction between SpoVD and SpoVE. My demonstration of the SpoVD-SpoVE interaction in *C. difficile* and SpoVD truncation experiments have demonstrated the role of each domain in cephalosporin resistance, suggesting that the PBP domain may be responsible for the interaction between SpoVD and SpoVE.

The second gene studied was *cwp20*. A *cwp20* mutant showed a clear role for the protein in cephalosporin resistance. Importantly, Cwp20 is a member of the cell wall protein (CWP) family (Fagan *et al.*, 2011), and my bioinformatics analysis predicted β -lactamase activity. A mutation in *slpA* that resulted in a loss of the S-layer (Kirk *et al.*, 2017) also resulted in a massive reduction in cephalosporin resistance. As Cwp20 is located within the S-layer and disruptions to the S-layer have previously been shown to alter cell wall localisation of CWPs (de la Riva *et al.*, 2011), we hypothesised that Cwp20 may be responsible for this observation. A *cwp20* deletion mutant had the same cephalosporin resistance defect, supporting this hypothesis. This was further confirmed by a group intron II insertion in *cwp20* in the S-layer mutant strain, which resulted in no further increase in cephalosporin resistance. I then demonstrated that Cwp20 is a β -lactamase, capable of hydrolysing the β -lactam ring of β -lactam antibiotics.

This activity was confirmed by protein purification and *in vitro* β -lactamase assays. Cwp20's classification as a class A β -lactamase was confirmed by substitution of serine 116 to alanine and inhibition of the catalytic activity using clavulanic acid, as previously shown for MSMEG2433, a class A β -lactamase that relies on an active site serine and is inactivated by clavulanic acid but non EDTA (Bansal *et al.*, 2015).

Finally, by applying transposon mutagenesis combined with marker rescue, we identified further critical genes required for cephalosporin and fluoroquinolone resistance. We identified ten genes contributing to resistance to ciprofloxacin, ceftazidime and cefoxitin, at least three of which had clear resistance phenotypes. R20291*spoVE::Tn* had the same effect on cephalosporin resistance as the Δ *spoVD* mutation, supporting our earlier observation of the SpoVD-SpoVE interaction. An insertion in R20291*CD0398* had a significant impact on ceftazidime resistance. This gene is located upstream of a gene encoding a putative β -lactamase CD0399. We hypothesised that polar effects from the transposon insertion in *CD0398* were responsible for the observed cephalosporin resistance phenotype. To test this, we complemented the *CD0398* with *CD0399*, *in trans*, and this fully restored the resistance level to wild type. I demonstrated that CD0399 is also a β -lactamase and this was confirmed by β -lactamase assays on the pure protein. Furthermore, CD0399

classification as a class A β -lactamase was confirmed by substitution of serine 102 to alanine and inhibition of the catalytic activity using clavulanic acid. Lastly, insertion in R20291CD0622::Tn had a significant effect on ciprofloxacin resistance. This was confirmed with a clean deletion, R20291 Δ CD0622. CD0622 appears to be a membrane efflux pump which may be involved in antibiotic export to prevent accumulation inside the cell. This demonstrates how useful transposon mutagenesis is to understand and identify new mechanisms of antibiotic resistance in *C. difficile*.

Further work

- 1- Studying *spoVD* expression in growing cells, using QRT-PCR and microarray.
- 2- Identification of the sigma factor that is responsible for regulation SpoVD in the exponential phase and stationary phase, and protein that is responsible for down regulation of SpoVD.
- 3- Using QRT-PCR and microarray to confirm that *spoVD* knockout is effect on other sporulation genes such as Spo0A, SspA, SipL, SpoIVA, SpoVT, Gpr, and TcdB.
- 4- Determination of the PBP dimer of SpoVD is responsible for the interaction between SpoVD and SpoVE using bacterial two-hybrid or co-affinity purifications of His-SpoVD with either SpoVE or HA-SpoVE.
- 5- Studying *cwp20* expression during cephalosporin effect using QRT-PCR.
- 6- Examination of Cwp20 composition into *slpA* mutant, completely lacking the S-layer and followed by sub-cellular localisation of Cwp20.
- 7- Examination of Cwp20 secretion using fluorescent D-amino acid HADA labelling.
- 8- Structural study for Cwp20 confirmation of how Cwp20 binds and then hydrolyses β -lactam antibiotics
- 9- Studying CD0399 in details such as expression and localisation as an important protein for β -lactamase activity.
- 10- Studying CD0622 in details such as expression and localisation as an important protein for efflux pumps mechanism.

7. References

- Abraham, E.P., 1991. A retrospective view of beta-lactamases. *J Chemother* 3, 67-74.
- Abraham, E.P., Chain, E., 1940. An enzyme from bacteria able to destroy penicillin. *Nature* 146, 837-837.
- Abraham, E.P., Gardner, A.D., Chain, E., Heatley, N.G., Fletcher, C.M., Jennings, M.A., 1941. Further observations on penicillin. *Lancet* 2, 177-189.
- Adachi, H., Ohta, T., Matsuzawa, H., 1991. Site-directed mutants, at position 166, of RTEM-1 beta-lactamase that form a stable acyl-enzyme intermediate with penicillin. *The Journal of biological chemistry* 266, 3186-3191.
- Adams, C.M., Eckenroth, B.E., Putnam, E.E., Doublet, S., Shen, A., 2013. Structural and functional analysis of the CspB protease required for *Clostridium* spore germination. *PLoS pathogens* 9.
- Adler, A., Miller-Roll, T., Bradenstein, R., Block, C., Mendelson, B., Parizade, M., Paitan, Y., Schwartz, D., Peled, N., Carmeli, Y., Schwaber, M.J., 2015. A national survey of the molecular epidemiology of *Clostridium difficile* in Israel: the dissemination of the ribotype 027 strain with reduced susceptibility to vancomycin and metronidazole. *Diagnostic Microbiology and Infectious Disease* 83, 21-24.
- Aktories, K., Just, I., 2005. Clostridial Rho-inhibiting protein toxins. *Bacterial Virulence Factors and Rho Gtpases* 291, 113-145.
- Alekshun, M.N., Levy, S.B., 2007. Molecular mechanisms of antibacterial multidrug resistance. *Cell* 128, 1037-1050.
- Al-Hinai, M.A., Jones, S.W., Papoutsakis, E.T., 2014. σ K of *Clostridium acetobutylicum* is the first known sporulation-specific sigma factor with two developmentally separated roles, one early and one late in sporulation. *Journal of bacteriology* 196, 287-299.
- Ambler, R.P., 1980. The structure of beta-lactamases. *Philosophical transactions of the Royal Society of London. Series B, Biological sciences* 289, 321-331.
- Amimoto, K., Noro, T., Oishi, E., Shimizu, M., 2007. A novel toxin homologous to large clostridial cytotoxins found in culture supernatant of *Clostridium*

perfringens type Microbiology Society Journals - Microbiology Society 153, 1198-1206.

- Arcus, V.L., McKenzie, J.L., Robson, J., Cook, G.M., 2011. The PIN-domain ribonucleases and the prokaryotic VapBC toxin-antitoxin array. *Protein Engineering, Design and Selection* 24, 33-40.
- Autret, N., Dubail, I., Trieu-Cuot, P., Berche, P., Charbit, A., 2001. Identification of new genes involved in the virulence of *Listeria monocytogenes* by signature-tagged transposon mutagenesis. *Infection and Immunity* 69, 2054-2065.
- Bacci, S., Molbak, K., Kjeldsen, M.K., Olsen, K.E., 2011. Binary toxin and death after *Clostridium difficile* infection. *Emerging infectious diseases* 17, 976-982.
- Bagyan, I., Hobot, J., Cutting, S., 1996. A compartmentalized regulator of developmental gene expression in *Bacillus subtilis*. *Journal of bacteriology* 178, 4500-4507.
- Bahl, H., Dürre. P., 2001. *Clostridia: Biotechnology and Medical Applications*, Wiley-VCH, Weinheim, p. 279.
- Bansal, A., Kar, D., Murugan, R.A., Mallick, S., Dutta, M., Pandey, S.D., Chowdhury, C., Ghosh, A.S., 2015. A putative low-molecular-mass penicillin-binding protein (PBP) of *Mycobacterium smegmatis* exhibits prominent physiological characteristics of DD-carboxypeptidase and beta-lactamase. *Microbiology* 161, 1081-1091.
- Barbut, F., Decre, D., Lalande, V., Burghoffer, B., Noussair, L., Gigandon, A., Espinasse, F., Raskine, L., Robert, J., Mangeol, A., Branger, C., Petit, J.C., 2005. Clinical features of *Clostridium difficile*-associated diarrhoea due to binary toxin (actin-specific ADP-ribosyltransferase) producing strains. *Journal of medical microbiology* 54, 181-185.
- Barquist, L., Boinett, C.J., Cain, A.K., 2013. Approaches to querying bacterial genomes with transposon-insertion sequencing. *RNA Biology* 10, 1161-1169.
- Barra-Carrasco, J., Olguin-Araneda, V., Plaza-Garrido, A., Miranda-Cardenas, C., Cofre-Araneda, G., Pizarro-Guajardo, M., Sarker, M.R., Paredes-Sabja, D., 2013. The *Clostridium difficile* exosporium cysteine (CdeC) rich protein is required for

exosporium morphogenesis and coat assembly. *Journal of bacteriology* 195, 3863-3875.

- Barreteau, H., Kovac, A., Boniface, A., Sova, M., Gobec, S., Blanot, D., 2008. Cytoplasmic steps of peptidoglycan biosynthesis. *FEMS microbiology reviews* 32, 168-207.
- Bartlett, J.G., 2002. *Clostridium difficile*-associated enteric disease. *Current infectious disease reports* 4, 477-483.
- Bauer, M.P., Kuijper, E.J., van Dissel, J.T., European Society of Clinical, M., Infectious, D., 2009. European Society of Clinical Microbiology and Infectious Diseases (ESCMID): treatment guidance document for *Clostridium difficile* infection (CDI). *Clinical Microbiology and Infection* 15, 1067-1079.
- Bauer, M.P., Notermans, D.W., van Benthem, B.H., Brazier, J.S., Wilcox, M.H., Rupnik, M., Monnet, D.L., van Dissel, J.T., Kuijper, E.J., Group, E.S., 2011. *Clostridium difficile* infection in Europe: a hospital-based survey. *Lancet* 377, 63-73.
- Bauvois, C., Ibuka, A.S., Celso, A., Alba, J., Ishii, Y., Frere, J.M., Galleni, M., 2005. Kinetic properties of four plasmid-mediated AmpC beta-lactamases. *Antimicrobial Agents and Chemotherapy* 49, 4240-4246.
- Baxter, R., Ray, G.T., Fireman, B.H., 2008. Case-control study of antibiotic use and subsequent *Clostridium difficile*- associated diarrhea in hospitalized patients. *Infection control and hospital epidemiology* 29, 44-50.
- Bayles, K.W., 2000. The bactericidal action of penicillin: new clues to an unsolved mystery. *Trends in microbiology* 8, 274-278.
- Beadle, B.M., Nicholas, R.A., Shoichet, B.K., 2001. Interaction energies between beta-lactam antibiotics and *E. coli* penicillin-binding protein 5 by reversible thermal denaturation. *Protein Science* 10, 1254-1259.
- Ben-Yehuda, S., Rudner, D.Z., Losick, R., 2003. RacA, a bacterial protein that anchors chromosomes to the cell poles. *Science* 299, 532-536.
- Bignardi, G.E., 1998. Risk factors for *Clostridium difficile* infection. *The Journal of hospital infection* 40, 1-15.

- Blanco, P., Hernando-Amado, S., Reales-Calderon, J.A., Corona, F., Lira, F., Alcalde-Rico, M., Bernardini, A., Sanchez, M.B., Martinez, J.L., 2016. Bacterial multidrug efflux pumps: much more than antibiotic resistance determinants. *Microorganisms* 4.
- Bouhss, A., Trunkfield, A.E., Bugg, T.D., Mengin-Lecreux, D., 2008. The biosynthesis of peptidoglycan lipid-linked intermediates. *FEMS microbiology reviews* 32, 208-233.
- Bradford, M.M., 1976. A rapid and sensitive method for the quantitation of microgram quantities of protein utilizing the principle of protein-dye binding. *Analytical Biochemistry* 72, 248-254.
- Bradford, P.A., 2001. Extended-spectrum beta-lactamases in the 21st century: characterization, epidemiology, and detection of this important resistance threat. *Clinical Microbiology Reviews* 14, 933-951, table of contents.
- Brazier, J.S., Raybould, R., Patel, B., Duckworth, G., Pearson, A., Charlett, A., Duerden, B.I., Network, H.P.A.R.M., 2008. Distribution and antimicrobial susceptibility patterns of *Clostridium difficile* PCR ribotypes in English hospitals, 2007-08. *Euro surveillance: bulletin Europeen sur les maladies transmissibles, European communicable disease bulletin* 13.
- Broder, D.H., Pogliano, K., 2006. Forespore engulfment mediated by a ratchet-like mechanism. *Cell* 126, 917-928.
- Brotzu, G., 1948. *Lav. Ist. Ig. Cagliari*.
- Buffie, C.G., Bucci, V., Stein, R.R., McKenney, P.T., Ling, L., Gobourne, A., No, D., Liu, H., Kinnebrew, M., Viale, A., Littmann, E., van den Brink, M.R., Jenq, R.R., Taur, Y., Sander, C., Cross, J.R., Toussaint, N.C., Xavier, J.B., Pamer, E.G., 2015. Precision microbiome reconstitution restores bile acid mediated resistance to *Clostridium difficile*. *Nature* 517, 205-208.
- Bukowska-Faniband, E., 2015. On the role of penicillin-binding protein SpoVD in endospore cortex assembly. Department of Biology, Lund University.
- Bukowska-Faniband, E., Hederstedt, L., 2013. Cortex synthesis during *Bacillus subtilis* sporulation depends on the transpeptidase activity of SpoVD. *FEMS microbiology letters* 346, 65-72.

- Bukowska-Faniband, E., Hederstedt, L., 2015. The PASTA domain of penicillin-binding protein SpoVD is dispensable for endospore cortex peptidoglycan assembly in *Bacillus subtilis*. *Microbiology - Microbiology Society* 161, 330-340.
- Burbulys, D., Trach, K.A., Hoch, J.A., 1991. Initiation of sporulation in *Bacillus subtilis* is controlled by a multicomponent phosphorelay. *Cell* 64, 545-552.
- Burkholder, W.F., Kurtser, I., Grossman, A.D., 2001. Replication initiation proteins regulate a developmental checkpoint in *Bacillus subtilis*. *Cell* 104, 269-279.
- Burns, D.A., Heap, J.T., Minton, N.P., 2010. SleC is essential for germination of *Clostridium difficile* spores in nutrient-rich medium supplemented with the bile salt taurocholate. *Journal of bacteriology* 192, 657-664.
- Burton, H.S., Abraham, E.P., 1951. Isolation of antibiotics from a species of cephalosporium; cephalosporins P1, P2, P3, P4, and P5. *Biochem J* 50, 168-174.
- Bush, K., Bradford, P.A., 2016. Beta-Lactams and beta-lactamase inhibitors: an overview. *Cold Spring Harbor Perspectives in Medicine* 6.
- Bush, K., Jacoby, G.A., 2009. Updated functional classification of beta-lactamases. *Antimicrob Agents Chemother* 54, 969-976.
- Bush, K., Jacoby, G.A., Medeiros, A.A., 1995. A functional classification scheme for beta-lactamases and its correlation with molecular structure. *Antimicrobial agents chemotherapy* 39, 1211-1233.
- Cabrera-Hernandez, A., Setlow, P., 2000. Analysis of the regulation and function of five genes encoding small, acid-soluble spore proteins of *Bacillus subtilis*. *Gene* 248, 169-181.
- Calabi, E., Fairweather, N., 2002. Patterns of sequence conservation in the S-layer proteins and related sequences in *Clostridium difficile*. *Journal of bacteriology* 184, 3886-3897.
- Camp, A.H., Losick, R., 2009. A feeding tube model for activation of a cell-specific transcription factor during sporulation in *Bacillus subtilis*. *Genes & development* 23, 1014-1024.
- Carter, G.P., Douce, G.R., Govind, R., Howarth, P.M., Mackin, K.E., Spencer, J., Buckley, A.M., Antunes, A., Kotsanas, D., Jenkin, G.A., Dupuy, B., Rood, J.I., Lyras,

- D., 2011. The anti-sigma factor TcdC modulates hypervirulence in an epidemic BI/NAP1/027 clinical isolate of *Clostridium difficile*. PLoS pathogens 7, e1002317.
- Carter, G.P., Lyras, D., Allen, D.L., Mackin, K.E., Howarth, P.M., O'Connor, J.R., Rood, J.I., 2007. Binary toxin production in *Clostridium difficile* is regulated by CdtR, a LytTR family response regulator. Journal of bacteriology 189, 7290-7301.
 - Cartman, S.T., Kelly, M.L., Heeg, D., Heap, J.T., Minton, N.P., 2012. Precise manipulation of the *Clostridium difficile* chromosome reveals a lack of association between the *tcdC* genotype and toxin production. Applied and environmental microbiology 78, 4683-4690.
 - Cartman, S.T., Minton, N.P., 2010. A mariner-based transposon system for *in Vivo* random mutagenesis of *Clostridium difficile*. Applied and environmental microbiology 76, 1103-1109.
 - Cato, E. P., George, W. L., Finegold, S. M., 1986. Genus *Clostridium* Prazmowski 1880, In P. H. A. Sneath, N. S. Mair, M. E. Sharpe, and J. G. Holt (ed.), Bergey's manual of systematic bacteriology, vol. 1. The Williams & Wilkins Co., Baltimore 23 AL, p. 1141-1200.
 - Chastanet, A., Losick, R., 2007. Engulfment during sporulation in *Bacillus subtilis* is governed by a multi-protein complex containing tandemly acting autolysins. Molecular Microbiology 64, 139-152.
 - Chen, Y., Minasov, G., Roth, T.A., Prati, F., Shoichet, B.K., 2006. The deacylation mechanism of AmpC beta-lactamase at ultrahigh resolution. Journal of the American Chemical Society 128, 2970-2976.
 - Chesnel, L., Pernot, L., Lemaire, D., Champelovier, D., Croize, J., Dideberg, O., Vernet, T., Zapun, A., 2003. The structural modifications induced by the M339F substitution in PBP2x from *Streptococcus pneumoniae* further decreases the susceptibility to beta-lactams of resistant strains. Journal of Biological Chemistry 278, 44448-44456.
 - Chesnokova, O.N., McPherson, S.A., Steichen, C.T., Turnbough, C.L., Jr., 2009. The spore-specific alanine racemase of *Bacillus anthracis* and its role in suppressing germination during spore development. Journal of bacteriology 191, 1303-1310.

- Chirakkal, H., O'Rourke, M., Atrih, A., Foster, S.J., Moir, A., 2002. Analysis of spore cortex lytic enzymes and related proteins in *Bacillus subtilis* endospore germination. *Microbiology-Microbiology Society* 148, 2383-2392.
- Chung, Y.J., Saier, M.H., Jr., 2001. SMR-type multidrug resistance pumps. *Current Opinion in Drug Discovery & Development* 4, 237-245.
- Citri, N., Samuni, A., Zyk, N., 1976. Acquisition of substrate-specific parameters during the catalytic reaction of penicillinase. *Proceedings of the National Academy of Sciences of the United States of America* 73, 1048-1052.
- Clements, A.C., Magalhaes, R.J., Tatem, A.J., Paterson, D.L., Riley, T.V., 2010. *Clostridium difficile* PCR ribotype 027: assessing the risks of further worldwide spread. *The Lancet Infectious Diseases* 10, 395-404.
- Clinical and laboratory standard institute. Performance standards for antimicrobial susceptibility testing; The Clinical & Laboratory Standards Institute. Jan 2012; M100-S22.
- Cohen, S.H., Gerding, D.N., Johnson, S., Kelly, C.P., Loo, V.G., McDonald, L.C., Pepin, J., Wilcox, M.H., Society for Healthcare Epidemiology of, A., Infectious Diseases Society of, A., 2010. Clinical practice guidelines for *Clostridium difficile* infection in adults: 2010 update by the society for healthcare epidemiology of America (SHEA) and the infectious diseases society of America (IDSA). *Infection control and hospital epidemiology* 31, 431-455.
- Cohn F., 1877. Untersuchungen über bacterien. IV. Beiträge zur biologie der Bacillen. *Beiträge zur biologie der Pflanzen*. 1877; 7:249–276.
- Coley, J., Duckworth, M., Baddiley, J., 1975. Extraction and purification of lipoteichoic acids from Gram-positive bacteria. *Carbohydrate Research* 40, 41-52.
- Costa, T., Priyadarshini, R., Jacobs-Wagner, C., 2008. Localization of PBP3 in *caulobacter crescentus* is highly dynamic and largely relies on its functional transpeptidase domain. *Molecular Microbiology* 70, 634-651.
- Courtay, C., Oster, T., Michelet, F., Visvikis, A., Diederich, M., Wellman, M., Siest, G., 1992. Gamma-glutamyltransferase: nucleotide sequence of the human

- pancreatic cDNA. Evidence for a ubiquitous gamma-glutamyltransferase polypeptide in human tissues. *Biochemical Pharmacology* 43, 2527-2533.
- Cowan, A.E., Olivastro, E.M., Koppel, D.E., Loshon, C.A., Setlow, B., Setlow, P., 2004. Lipids in the inner membrane of dormant spores of *Bacillus* species are largely immobile. *Proceedings of the National Academy of Sciences of the United States of America* 101, 7733-7738.
 - Creagh, H., 2008. Number of deaths involving *C. difficile* rose by 72% in a year. *BMJ* 336, 529-529.
 - Crowfoot, D., Bunn, C. W., Rogers-Low, B.W., Turner-Jones, A., 1949. X-ray crystallographic investigation of the structure of penicillin. In *Chemistry of penicillin* (ed. H. T. Clarke, J.R. Johnson & R. Robinson), Princeton University Press, pp. 310-67.
 - Daniel, R.A., Drake, S., Buchanan, C.E., Scholle, R., Errington, J., 1994. The *Bacillus subtilis spoVD* gene encodes a mother-cell-specific penicillin-binding protein required for spore morphogenesis. *Journal of molecular biology* 235, 209-220.
 - Daniel, R.A., Errington, J., 1993. DNA sequence of the *murE-murD* region of *Bacillus subtilis* 168. *General Microbiology* 139, 361-370.
 - de Hoon, M.J.L., Eichenberger, P., Vitkup, D., 2010. Hierarchical evolution of the bacterial sporulation network. *Current Biology* 20, R735-R745.
 - de la Riva, L., Willing, S.E., Tate, E.W., Fairweather, N.F., 2011. Roles of cysteine proteases Cwp84 and Cwp13 in biogenesis of the cell wall of *Clostridium difficile*. *Journal of bacteriology* 193, 3276-3285.
 - de Oliveira, I.M., Henriques, J.A., Bonatto, D., 2007. In *silico* identification of a new group of specific bacterial and fungal nitroreductases-like proteins. *Biochemical and Biophysical Research Communications* 355, 919-925.
 - de Pedro, M.A., Holtje, J.V., Schwarz, H., 2002. Fast lysis of *Escherichia coli* filament cells requires differentiation of potential division sites. *Microbiology-Microbiology Society* 148, 79-86.
 - Deakin, L.J., Clare, S., Fagan, R.P., Dawson, L.F., Pickard, D.J., West, M.R., Wren, B.W., Fairweather, N.F., Dougan, G., Lawley, T.D., 2012. The *Clostridium difficile*

spo0A gene is a persistence and transmission factor. *Infection and Immunity* 80, 2704-2711.

- Dembek, M., 2014. Whole-genome analysis of sporulation and germination in *Clostridium difficile*.
- Dembek, M., Barquist, L., Boinett, C.J., Cain, A.K., Mayho, M., Lawley, T.D., Fairweather, N.F., Fagan, R.P., 2015. High-throughput analysis of gene essentiality and sporulation in *Clostridium difficile*. *MBio* 6, e02383.
- Dembek, M., Reynolds, C.B., Fairweather, N.F., 2012. *Clostridium difficile* cell wall protein CwpV undergoes enzyme-independent intramolecular autoprolysis. *Journal of Biological Chemistry* 287, 1538-1544.
- Deneve, C., Janoir, C., Poilane, I., Fantinato, C., Collignon, A., 2009. New trends in *Clostridium difficile* virulence and pathogenesis. *International journal of antimicrobial agents* 33 Suppl 1, S24-28.
- Depestel, D.D., Aronoff, D.M., 2013. Epidemiology of *Clostridium difficile* infection. *Journal of pharmacy practice* 26, 464-475.
- Dessen, A., Mouz, N., Gordon, E., Hopkins, J., Dideberg, O., 2001. Crystal structure of PBP2x from a highly penicillin-resistant *Streptococcus pneumoniae* clinical isolate: A mosaic framework containing 83 mutations. *Journal of Biological Chemistry* 276, 45106-45112.
- Dineen, S.S., Villapakkam, A.C., Nordman, J.T., Sonenshein, A.L., 2007. Repression of *Clostridium difficile* toxin gene expression by CodY. *Molecular Microbiology* 66, 206-219.
- Doan, T., Morlot, C., Meisner, J., Serrano, M., Henriques, A.O., Moran, C.P., Rudner, D.Z., 2009. Novel secretion apparatus maintains spore integrity and developmental gene expression in *Bacillus subtilis*. *PLoS genetics* 5.
- Driks, A., 2002. Proteins of the spore core and coat, *Bacillus subtilis* and its closest relatives. *American Society of Microbiology*, pp. 527-535.
- Dubberke, E.R., Olsen, M.A., 2012. Burden of *Clostridium difficile* on the healthcare system. *Clinical Infectious Diseases* 55 Suppl 2, S88-92.
- Dubberke, E.R., Reske, K.A., Noble-Wang, J., Thompson, A., Killgore, G., Mayfield, J., Camins, B., Woeltje, K., McDonald, J.R., McDonald, L.C., Fraser, V.J., 2007.

Prevalence of *Clostridium difficile* environmental contamination and strain variability in multiple health care facilities. *American journal of infection control* 35, 315-318.

- Dubberke, E.R., Wertheimer, A.I., 2009. Review of current literature on the economic burden of *Clostridium difficile* infection. *Infection control and hospital epidemiology* 30, 57-66.
- Dupuy, B., Govind, R., Antunes, A., Matamouros, S., 2008. *Clostridium difficile* toxin synthesis is negatively regulated by TcdC. *Journal of medical microbiology* 57, 685-689.
- Egerer, M., Giesemann, T., Jank, T., Satchell, K.J.F., Aktories, K., 2007. Auto-catalytic cleavage of *Clostridium difficile* toxins A and B depends on cysteine protease activity. *Journal of Biological Chemistry* 282, 25314-25321.
- Eichenberger, P., Jensen, S.T., Conlon, E.M., van Ooij, C., Silvaggi, J., Gonzalez-Pastor, J.E., Fujita, M., Ben-Yehuda, S., Stragier, P., Liu, J.S., Losick, R., 2003. The sigma E regulon and the identification of additional sporulation genes in *Bacillus subtilis*. *Journal of molecular biology* 327, 945-972.
- Emerson, J., Fairweather, N.F., 2009a. Surface structures of *Clostridium difficile* and other clostridia. In: Bruggemann, H. & Gottschalk, G. (eds.) *Clostridia - Molecular Biology in the Post-Genomic Era*. Norfolk, UK: Caister Academic Press.
- Emerson, J.E., Reynolds, C.B., Fagan, R.P., Shaw, H.A., Goulding, D., Fairweather, N.F., 2009b. A novel genetic switch controls phase variable expression of CwpV, a *Clostridium difficile* cell wall protein. *Molecular Microbiology* 74, 541-556.
- Errington, J., 2003. Regulation of endospore formation in *Bacillus subtilis*. *Nature Reviews Microbiology* 1, 117-126.
- Eyre, D.W., Cule, M.L., Wilson, D.J., Griffiths, D., Vaughan, A., O'Connor, L., Ip, C.L., Golubchik, T., Batty, E.M., Finney, J.M., Wyllie, D.H., Didelot, X., Piazza, P., Bowden, R., Dingle, K.E., Harding, R.M., Crook, D.W., Wilcox, M.H., Peto, T.E., Walker, A.S., 2013. Diverse sources of *C. difficile* infection identified on whole-genome sequencing. *The New England journal of medicine* 369, 1195-1205.

- Fagan, R.P., Albesa-Jove, D., Qazi, O., Svergun, D.I., Brown, K.A., Fairweather, N.F., 2009. Structural insights into the molecular organization of the S-layer from *Clostridium difficile*. *Molecular Microbiology* 71, 1308-1322.
- Fagan, R.P., Fairweather, N.F., 2011. *Clostridium difficile* has two parallel and essential Sec secretion systems. *Journal of Biological Chemistry* 286, 27483-27493.
- Fagan, R.P., Fairweather, N.F., 2014. Biogenesis and functions of bacterial S-layers. *Nature reviews. Microbiology - Microbiology Society* 12, 211-222.
- Fagan, R.P., Janoir, C., Collignon, A., Mastrantonio, P., Poxton, I.R., Fairweather, N.F., 2011. A proposed nomenclature for cell wall proteins of *Clostridium difficile*. *Journal of medical microbiology* 60, 1225-1228.
- Fang, Q., Kanugula, S., Pegg, A.E., 2005. Function of domains of human O6-alkylguanine-DNA alkyltransferase. *Biochemistry* 44, 15396-15405.
- Faraci, W.S., Pratt, R.F., 1985. Mechanism of inhibition of the Pc1 beta-lactamase of *Staphylococcus aureus* by cephalosporins - Importance of the 3'-Leaving Group. *Biochemistry-U.S.* 24, 903-910.
- Fay, A., Meyer, P., Dworkin, J., 2010. Interactions between late acting proteins required for peptidoglycan synthesis during sporulation. *Journal of molecular biology* 399, 547-561.
- Fernandes, R., Amador, P., Prudencio, C., 2013. Beta-lactams: chemical structure, mode of action and mechanisms of resistance. *Clinical Microbiology Reviews* 24, 7-17.
- Fimlaid, K.A., Bond, J.P., Schutz, K.C., Putnam, E.E., Leung, J.M., Lawley, T.D., Shen, A., 2013. Global analysis of the sporulation pathway of *Clostridium difficile*. *PLoS genetics* 9.
- Fimlaid, K.A., Jensen, O., Donnelly, M.L., Siegrist, M.S., Shen, A.M., 2015. Regulation of *Clostridium difficile* Spore formation by the SpoIIQ and SpoIIIA proteins. *PLoS genetics* 11.
- Finn, R.D., Bateman, A., Clements, J., Coghill, P., Eberhardt, R.Y., Eddy, S.R., Heger, A., Hetherington, K., Holm, L., Mistry, J., Sonnhammer, E.L.L., Tate, J.,

- Punta, M., 2014. Pfam: the protein families database, *Nucleic Acids Research*, vol. 42, pp. D222-230.
- Fischetti, V.A., 2005. Bacteriophage lytic enzymes: novel anti-infectives. *Trends in microbiology* 13, 491-496.
 - Fleming, A., 1929. On the antibacterial action of cultures of a penicillium, with special reference to their use in the isolation of *B. Influenzae*. *British Journal of Experimental Pathology journal* 10, 226-236.
 - Fleming, A., 1943. *Streptococcal meningitis* treated with penicillin - measurement of bacteriostatic power of blood and cerebrospinal fluid. *Lancet* 2, 434-438.
 - Francis, M.B., Allen, C.A., Shrestha, R., Sorg, J.A., 2013. Bile acid recognition by the *Clostridium difficile* germinant receptor, CspC, is important for establishing infection. *PLoS pathogens* 9.
 - Freeman, J., Vernon, J., Morris, K., Nicholson, S., Todhunter, S., Longshaw, C., Wilcox, M.H., Surveill, P.-E.L., 2015. Pan-European longitudinal surveillance of antibiotic resistance among prevalent *Clostridium difficile* ribotypes. *Clinical Microbiology and Infection* 21.
 - Fujita, M., Losick, R., 2005. Evidence that entry into sporulation in *Bacillus subtilis* is governed by a gradual increase in the level and activity of the master regulator Spo0A. *Genes & Development* 19, 2236-2244.
 - Galperin, M.Y., Mekhedov, S.L., Puigbo, P., Smirnov, S., Wolf, Y.I., Rigden, D.J., 2012. Genomic determinants of sporulation in *Bacilli* and *Clostridia*: towards the minimal set of sporulation-specific genes. *Environmental microbiology* 14, 2870-2890.
 - Gan, L., Chen, S., Jensen, G.J., 2008. Molecular organization of Gram-negative peptidoglycan. *Proceedings of the National Academy of Sciences of the United States of America* 105, 18953-18957.
 - Garvey, M.I., Baylay, A.J., Wong, R.L., Piddock, L.J.V., 2011. Overexpression of *patA* and *patB*, which encode ABC transporters, is associated with fluoroquinolone resistance in clinical isolates of *Streptococcus pneumoniae*. *Antimicrobial Agents and Chemotherapy* 55, 190-196.

- Genth, H., Dreger, S.C., Huelsenbeck, J., Just, I., 2008. *Clostridium difficile* toxins: more than mere inhibitors of Rho proteins. *The International Journal of Biochemistry & Cell Biology* 40, 592-597.
- Gerding, D.N., Muto, C.A., Owens, R.C., Jr., 2008. Measures to control and prevent *Clostridium difficile* infection. *Clinical infectious diseases: an official publication of the Infectious Diseases Society of America* 46 Suppl 1, S43-49.
- Giesemann, T., Jank, T., Gerhard, R., Maier, E., Just, I., Benz, R., Aktories, K., 2006. Cholesterol-dependent pore formation of *Clostridium difficile* toxin A. *Journal of Biological Chemistry* 281, 10808-10815.
- Goffin, C., Ghuysen, J.M., 1998. Multimodular penicillin-binding proteins: an enigmatic family of orthologs and paralogs. *Microbiology and Molecular Biology Reviews* 62, 1079-1093.
- Goffin, C., Ghuysen, J.M., 2002. Biochemistry and comparative genomics of SxxK superfamily acyltransferases offer a clue to the mycobacterial paradox: presence of penicillin-susceptible target proteins versus lack of efficiency of penicillin as therapeutic agent. *Microbiology and Molecular Biology Reviews* 66, 702-+.
- Gonzalez-Pastor, J.E., Hobbs, E.C., Losick, R., 2003. Cannibalism by sporulating bacteria. *Science* 301, 510-513.
- Goorhuis, A., Van der Kooi, T., Vaessen, N., Dekker, F.W., Van den Berg, R., Harmanus, C., van den Hof, S., Notermans, D.W., Kuijper, E.J., 2007. Spread and epidemiology of *Clostridium difficile* polymerase chain reaction ribotype 027/toxinotype III in The Netherlands. *Clinical infectious diseases: an official publication of the Infectious Diseases Society of America* 45, 695-703.
- Goudarzi, M., Goudarzi, H., Alebouyeh, M., Azimi Rad, M., Shayegan Mehr, F.S., Zali, M.R., Aslani, M.M., 2013. Antimicrobial susceptibility of *Clostridium difficile* clinical isolates in Iran. *Iranian Red Crescent Medical Journal*. 15, 704-711.
- Govind, R., Dupuy, B., 2012. Secretion of *Clostridium difficile* toxins A and B requires the holin-like protein TcdE. *PLoS pathogens* 8, e1002727.
- Greco, A., Ho, J.G.S., Lin, S.J., Palcic, M.M., Rupnik, M., Ng, K.K.S., 2006. Carbohydrate recognition by *Clostridium difficile* toxin A. *Nature Structural & Molecular Biology* 13, 460-461.

- Gutelius, D., Hokeness, K., Logan, S.M., Reid, C.W., 2014. Functional analysis of SleC from *Clostridium difficile*: an essential lytic transglycosylase involved in spore germination. *Microbiology - Microbiology Society* 160, 209-216.
- Hall, I.C., O'Toole, E., 1935. Intestinal flora in newborn infants: with a description of a new pathogenic anaerobe, *Bacillus difficilis*. *American Journal of Diseases of Children* 49, 390-402.
- Hamon, M.A., Lazazzera, B.A., 2001. The sporulation transcription factor Spo0A is required for biofilm development in *Bacillus subtilis*. *Molecular Microbiology* 42, 1199-1209.
- Hancock, I., Baddiley, J., 1976. *In vitro* synthesis of the unit that links teichoic acid to peptidoglycan. *Journal of bacteriology* 125, 880-886.
- Handke, L.D., Shivers, R.P., Sonenshein, A.L., 2008. Interaction of *Bacillus subtilis* CodY with GTP. *Journal of bacteriology* 190, 798-806.
- Haraldsen, J.D., Sonenshein, A.L., 2003. Efficient sporulation in *Clostridium difficile* requires disruption of the *sigmaK* gene. *Molecular Microbiology* 48, 811-821.
- Harbottle, H., Thakur, S., Zhao, S., White, D.G., 2006. Genetics of antimicrobial resistance. *Animal Biotechnology* 17, 111-124.
- Harry, K.H., Zhou, R., Kroos, L., Melville, S.B., 2009. Sporulation and enterotoxin (CPE) synthesis are controlled by the sporulation-specific sigma factors SigE and SigK in *Clostridium perfringens*. *Journal of bacteriology* 191, 2728-2742.
- He, M., Miyajima, F., Roberts, P., Ellison, L., Pickard, D.J., Martin, M.J., Connor, T.R., Harris, S.R., Fairley, D., Bamford, K.B., D'Arc, S., Brazier, J., Brown, D., Coia, J.E., Douce, G., Gerding, D., Kim, H.J., Koh, T.H., Kato, H., Senoh, M., Louie, T., Mitchell, S., Butt, E., Peacock, S.J., Brown, N.M., Riley, T., Songer, G., Wilcox, M., Pirmohamed, M., Kuijper, E., Hawkey, P., Wren, B.W., Dougan, G., Parkhill, J., Lawley, T.D., 2013. Emergence and global spread of epidemic healthcare-associated *Clostridium difficile*. *Nature genetics* 45, 109-113.
- He, M., Sebaihia, M., Lawley, T.D., Stabler, R.A., Dawson, L.F., Martin, M.J., Holt, K.E., Seth-Smith, H.M., Quail, M.A., Rance, R., Brooks, K., Churcher, C., Harris, D., Bentley, S.D., Burrows, C., Clark, L., Corton, C., Murray, V., Rose, G., Thurston, S.,

- van Tonder, A., Walker, D., Wren, B.W., Dougan, G., Parkhill, J., 2010. Evolutionary dynamics of *Clostridium difficile* over short and long time scales. Proceedings of the National Academy of Sciences of the United States of America 107, 7527-7532.
- Health Protection Agency. Outbreak of *Clostridium difficile* infection in a hospital in south east England. Commun Dis Rep Wkly 2005: 15(25): 23/06/2005 (<http://www.hpa.org.uk/cdr/archives/archive05/News/news2405.htm#cdiff>).
 - Heap, J.T., Ehsaan, M., Cooksley, C.M., Ng, Y.K., Cartman, S.T., Winzer, K., Minton, N.P., 2012. Integration of DNA into bacterial chromosomes from plasmids without a counter-selection marker. Nucleic Acids Research 40.
 - Heap, J.T., Kuehne, S.A., Ehsaan, M., Cartman, S.T., Cooksley, C.M., Scott, J.C., Minton, N.P., 2010. The Clostron: Mutagenesis in *Clostridium* refined and streamlined. The Journal of Microbiological Methods 80, 49-55.
 - Heap, J.T., Pennington, O.J., Cartman, S.T., Carter, G.P., Minton, N.P., 2007. The Clostron: a universal gene knock-out system for the genus *Clostridium*. The Journal of Microbiological Methods 70, 452-464.
 - Heap, J.T., Pennington, O.J., Cartman, S.T., Minton, N.P., 2009. A modular system for *Clostridium* shuttle plasmids. The Journal of Microbiological Methods 78, 79-85.
 - Hecht, H.J., Erdmann, H., Park, H.J., Sprinzl, M., Schmid, R.D., 1995. Crystal structure of NADH oxidase from *Thermus thermophilus*. Nature Structural & Molecular Biology 2, 1109-1114.
 - Heidelberger, C., Danenberg, P.V., Moran, R.G., 1983. Fluorinated pyrimidines and their nucleosides. Advances in enzymology and related areas of molecular biology 54, 57-119.
 - Henderson, J.W., 1997. The yellow brick road to penicillin: a story of serendipity. Mayo Clinic proceedings 72, 683-687.
 - Henriques, A.O., Moran, C.P., 2007. Structure, assembly, and function of the spore surface layers. Annual review of microbiology 61, 555-588.

- Hensel, M., Shea, J.E., Gleeson, C., Jones, M.D., Dalton, E., Holden, D.W., 1995. Simultaneous identification of bacterial virulence genes by negative selection. *Science* 269, 400-403.
- Higgins, D., Dworkin, J., 2012. Recent progress in *Bacillus subtilis* sporulation. *FEMS microbiology reviews* 36, 131-148.
- Hirschhorn, L.R., Trnka, Y., Onderdonk, A., Lee, M.L., Platt, R., 1994. Epidemiology of community-acquired *Clostridium difficile*-associated diarrhea. *The Journal of infectious diseases* 169, 127-133.
- Howerton, A., Patra, M., Abel-Santos, E., 2013. A new strategy for the prevention of *Clostridium difficile* infection. *The Journal of infectious diseases* 207, 1498-1504.
- Howerton, A., Ramirez, N., Abel-Santos, E., 2011. Mapping interactions between germinants and *Clostridium difficile* spores. *Journal of bacteriology* 193, 274-282.
- Hullo, M.F., Moszer, I., Danchin, A., Martin-Verstraete, I., 2001. CotA of *Bacillus subtilis* is a copper-dependent laccase. *Journal of bacteriology* 183, 5426-5430.
- Hundsberger, T., Braun, V., Weidmann, M., Leukel, P., Sauerborn, M., von Eichel-Streiber, C., 1997. Transcription analysis of the genes *tcdA-E* of the pathogenicity locus of *Clostridium difficile*. *European journal of biochemistry* 244, 735-742.
- Jank, T., Gieseemann, T., Aktories, K., 2007. Rho-glucosylating *Clostridium difficile* toxins A and B: new insights into structure and function. *Glycobiology* 17, 15R-22R.
- Janoir, C., Pechine, S., Grosdidier, C., Collignon, A., 2007. Cwp84, a surface-associated protein of *Clostridium difficile*, is a cysteine protease with degrading activity on extracellular matrix proteins. *Journal of bacteriology* 189, 7174-7180.
- Jarvis, W.R., 2001. Infection control and changing health-care delivery systems. *Emerging infectious diseases* 7, 170-173.
- Jiang, M., Shao, W.L., Perego, M., Hoch, J.A., 2000. Multiple histidine kinases regulate entry into stationary phase and sporulation in *Bacillus subtilis*. *Molecular Microbiology* 38, 535-542.
- Johnson, S., Samore, M.H., Farrow, K.A., Killgore, G.E., Tenover, F.C., Lyras, D., Rood, J.I., DeGirolami, P., Baltch, A.L., Rafferty, M.E., Pear, S.M., Gerding, D.N.,

1999. Epidemics of diarrhea caused by a clindamycin-resistant strain of *Clostridium difficile* in four hospitals. *The New England journal of medicine* 341, 1645-1651.
- Jones, A.L., Knoll, K.M., Rubens, C.E., 2000. Identification of *Streptococcus agalactiae* virulence genes in the neonatal rat sepsis model using signature-tagged mutagenesis. *Molecular Microbiology* 37, 1444-1455.
 - June, C.M., Vaughan, R.M., Ulberg, L.S., Bonomo, R.A., Witucki, L.A., Leonard, D.A., 2014. A fluorescent carbapenem for structure function studies of penicillin-binding proteins, beta-lactamases, and beta-lactam sensors. *Analytical Biochemistry* 463, 70-74.
 - Just, I., Gerhard, R., 2004. Large clostridial cytotoxins. *Reviews of Physiology, Biochemistry and Pharmacology* 152, 23-47.
 - Just, I., Selzer, J., Wilm, M., von Eichel-Streiber, C., Mann, M., Aktories, K., 1995. Glucosylation of Rho proteins by *Clostridium difficile* toxin B. *Nature* 375, 500-503.
 - Karasawa, T., Ikoma, S., Yamakawa, K., Nakamura, S., 1995. A defined growth medium for *Clostridium difficile*. *Microbiology - Microbiology Society* 141 (Pt 2), 371-375.
 - Karimova, G., Pidoux, J., Ullmann, A., Ladant, D., 1998. A bacterial two-hybrid system based on a reconstituted signal transduction pathway. *Proceedings of the National Academy of Sciences of the United States of America* 95, 5752-5756.
 - Karimova, G., Ullmann, A., Ladant, D., 2000. A bacterial two-hybrid system that exploits a cAMP signaling cascade in *Escherichia coli*. *Methods in enzymology* 328, 59-73.
 - Keppler, A., Gendreizig, S., Gronemeyer, T., Pick, H., Vogel, H., Johnsson, K., 2003. A general method for the covalent labeling of fusion proteins with small molecules *in vivo*. *Nature biotechnology* 21, 86-89.
 - Kidwell, M.G., Lisch, D.R., 2001. Perspective: Transposable elements, parasitic DNA, and genome evolution. *Evolution* 55, 1-24.
 - Kim, J., Smathers, S.A., Prasad, P., Leckerman, K.H., Coffin, S., Zaoutis, T., 2008. Epidemiological features of *Clostridium difficile*-associated disease among

inpatients at children's hospitals in the United States, 2001-2006. *Pediatrics* 122, 1266-1270.

- Kirby, J.M., Ahern, H., Roberts, A.K., Kumar, V., Freeman, Z., Acharya, K.R., Shone, C.C., 2009. Cwp84, a surface-associated cysteine protease, plays a role in the maturation of the surface layer of *Clostridium difficile*. *Journal of Biological Chemistry* 284, 34666-34673.
- Kirk, J.A., Fagan, R.P., 2016. Heat shock increases conjugation efficiency in *Clostridium difficile*. *Anaerobe* 42, 1-5.
- Kirk, J.A., Gebhart, D., Buckley, A.M., Lok, S., Scholl, D., Douce, G.R., Govoni, G.R., Fagan, R.P., 2017. New class of precision antimicrobials redefines role of *Clostridium difficile* S-layer in virulence and viability. *Science Translational Medicine* 9.
- Klobutcher, L.A., Ragkousi, K., Setlow, P., 2006. The *Bacillus subtilis* spore coat provides eat resistance during phagocytic predation by the protozoan *Tetrahymena thermophila*. *Proceedings of the National Academy of Sciences of the United States of America* 103, 165-170.
- Knecht, H., Neulinger, S.C., Heinsen, F.A., Knecht, C., Schilhabel, A., Schmitz, R.A., Zimmermann, A., dos Santos, V.M., Ferrer, M., Rosenstiel, P.C., Schreiber, S., Friedrichs, A.K., Ott, S.J., 2014. Effects of beta-lactam antibiotics and fluoroquinolones on human gut microbiota in relation to *Clostridium difficile* associated diarrhea. *PloS one* 9, e89417.
- Knothe, H., Shah, P., Krcmery, V., Antal, M., Mitsuhashi, S., 1983. Transferable resistance to cefotaxime, ceftiofex, cefamandole and cefuroxime in clinical isolates of *Klebsiella pneumoniae* and *Serratia marcescens*. *Infection* 11, 315-317.
- Kotnik, M., Anderluh, P.S., Prezelj, A., 2007. Development of novel inhibitors targeting intracellular steps of peptidoglycan biosynthesis. *Current Pharmaceutical Design* 13, 2283-2309.
- Kotrba, P., Inui, M., Yukawa, H., 2001. Bacterial phosphotransferase system (PTS) in carbohydrate uptake and control of carbon metabolism. *The Journal of Bioscience and Bioengineering* 92, 502-517.

- Krutova, M., Matejkova, J., Tkadlec, J., Nyc, O., 2015. Antibiotic profiling of *Clostridium difficile* ribotype 176--A multidrug resistant relative to *C. difficile* ribotype 027. *Anaerobe* 36, 88-90.
- Kuehne, S.A., Cartman, S.T., Heap, J.T., Kelly, M.L., Cockayne, A., Minton, N.P., 2010. The role of toxin A and toxin B in *Clostridium difficile* infection. *Nature* 467, 711-U797.
- Kuijper, E.J., Debast, S.B., Van Kregten, E., Vaessen, N., Notermans, D.W., van den Broek, P.J., 2005. [*Clostridium difficile* ribotype 027, toxinotype III in The Netherlands]. *Nederlands tijdschrift voor geneeskunde* 149, 2087-2089.
- Kuijper, E.J., van den Berg, R.J., Debast, S., Visser, C.E., Veenendaal, D., Troelstra, A., van der Kooi, T., van den Hof, S., Notermans, D.W., 2006. *Clostridium difficile* ribotype 027, toxinotype III, the Netherlands. *Emerging infectious diseases* 12, 827-830.
- Kuipers, E.J., Surawicz, C.M., 2008. *Clostridium difficile* infection. *Lancet* 371, 1486-1488.
- Kuroda, A., Sugimoto, Y., Funahashi, T., Sekiguchi, J., 1992. Genetic structure, isolation and characterization of a *Bacillus licheniformis* cell wall hydrolase. *Molecular and General Genetics* 234, 129-137.
- Kuroda, T., Tsuchiya, T., 2009. Multidrug efflux transporters in the MATE family. *Biochim Biophys Acta* 1794, 763-768.
- Laaberki, M.H., Dworkin, J., 2008. Role of spore coat proteins in the resistance of *Bacillus subtilis* spores to *Caenorhabditis elegans* predation. *Journal of bacteriology* 190, 6197-6203.
- Lachowicz, D., Pituch, H., Obuch-Woszczatynski, P., 2015. Antimicrobial susceptibility patterns of *Clostridium difficile* strains belonging to different polymerase chain reaction ribotypes isolated in Poland in 2012. *Anaerobe* 31, 37-41.
- Laemmli, U.K., 1970. Cleavage of structural proteins during the assembly of the head of bacteriophage T4. *Nature* 227, 680-685.
- Lambert, P.A., Hancock, I.C., Baddiley, J., 1977. Occurrence and function of membrane teichoic acids. *Biochim Biophys Acta* 472, 1-12.

- Lamontagne, F., Labbe, A.C., Haeck, O., Lesur, O., Lalancette, M., Patino, C., Leblanc, M., Laverdiere, M., Pepin, J., 2007. Impact of emergency colectomy on survival of patients with fulminant *Clostridium difficile* colitis during an epidemic caused by a hypervirulent strain. *Annals of Surgery* 245, 267-272.
- Lampe, D.J., Akerley, B.J., Rubin, E.J., Mekalanos, J.J., Robertson, H.M., 1999. Hyperactive transposase mutants of the *Himar1* mariner transposon. *Proceedings of the National Academy of Sciences of the United States of America* 96, 11428-11433.
- Lampe, D.J., Churchill, M.E.A., Robertson, H.M., 1996. Purified mariner transposase is sufficient to mediate transposition *in vitro*. *EMBO J* 15, 5470-5479.
- Lampe, D.J., Grant, T.E., Robertson, H.M., 1998. Factors affecting transposition of the *Himar1* mariner transposon *in vitro*. *Genetics* 149, 179-187.
- Lanckriet, A., Timbermont, L., Happonen, L.J., Pajunen, M.I., Pasmans, F., Haesebrouck, F., Ducatelle, R., Savilahti, H., Van Immerseel, F., 2009. Generation of single-copy transposon insertions in *Clostridium perfringens* by electroporation of phage Mu DNA transposition complexes. *Applied and Environmental Microbiology* 75, 2638-2642.
- Langridge, G.C., Phan, M.D., Turner, D.J., Perkins, T.T., Parts, L., Haase, J., Charles, I., Maskell, D.J., Peters, S.E., Dougan, G., Wain, J., Parkhill, J., Turner, A.K., 2009. Simultaneous assay of every *Salmonella Typhi* gene using one million transposon mutants. *Genome Research* 19, 2308-2316.
- Law, C.J., Maloney, P.C., Wang, D.N., 2008. Ins and outs of major facilitator superfamily antiporters. *Annual review of microbiology* 62, 289-305.
- Lawley, T.D., Clare, S., Walker, A.W., Goulding, D., Stabler, R.A., Croucher, N., Mastroeni, P., Scott, P., Raisen, C., Mottram, L., Fairweather, N.F., Wren, B.W., Parkhill, J., Dougan, G., 2009a. Antibiotic treatment of *Clostridium difficile* carrier mice triggers a supershedder state, spore-mediated transmission, and severe disease in immunocompromised hosts. *Infection and Immunity* 77, 3661-3669.
- Lawley, T.D., Croucher, N.J., Yu, L., Clare, S., Sebahia, M., Goulding, D., Pickard, D.J., Parkhill, J., Choudhary, J., Dougan, G., 2009b. Proteomic and genomic

characterization of highly infectious *Clostridium difficile* 630 spores. Journal of bacteriology 191, 5377-5386.

- Lewis, J.C., Snell, N.S., Burr, H.K., 1960. Water permeability of bacterial spores and the concept of a contractile cortex. Science 132, 544-545.
- Ligon, B.L., 2004. Sir Howard Walter Florey--the force behind the development of penicillin. Seminars in pediatric infectious diseases 15, 109-114.
- Lim, D., Strynadka, N.C.J., 2002. Structural basis for the beta-lactam resistance of PBP2a from methicillin-resistant *Staphylococcus aureus*. Nature Structural Biology 9, 870-876.
- Liu, Y.M., Moller, M.C., Petersen, L., Soderberg, C.A.G., Hederstedt, L., 2010. Penicillin-binding protein SpoVD disulphide is a target for StoA in *Bacillus subtilis* forespores. Molecular Microbiology 75, 46-60.
- Livermore, D.M., Brown, D.F., 2001. Detection of β -lactamase-mediated resistance. Journal of Antimicrobial Chemotherapy 48, 59-64.
- Llinas, A., Ahmed, N., Cordaro, M., Laws, A.P., Frere, J.M., Delmarcelle, M., Silvaggi, N.R., Kelly, J.A., Page, M.I., 2005. Inactivation of bacterial DD-peptidase by beta-sultams. Biochemistry-U.S. 44, 7738-7746.
- Loessner, M.J., 2005. Bacteriophage endolysins--current state of research and applications. Current Opinion in Microbiology 8, 480-487.
- Longley, D.B., Harkin, D.P., Johnston, P.G., 2003. 5-fluorouracil: mechanisms of action and clinical strategies. Nature Reviews Cancer 3, 330-338.
- Lorca, G.L., Barabote, R.D., Zlotopolski, V., Tran, C., Winnen, B., Hvorup, R.N., Stonestrom, A.J., Nguyen, E., Huang, L.W., Kim, D.S., Saier, M.H., Jr., 2007. Transport capabilities of eleven Gram-positive bacteria: comparative genomic analyses. Biochim Biophys Acta 1768, 1342-1366.
- Louie, T.J., Miller, M.A., Mullane, K.M., Weiss, K., Lentnek, A., Golan, Y., Gorbach, S., Sears, P., Shue, Y.K., Group, O.P.T.C.S., 2011. Fidaxomicin versus vancomycin for *Clostridium difficile* infection. The New England journal of medicine 364, 422-431.

- Lubelski, J., Konings, W.N., Driessen, A.J., 2007. Distribution and physiology of ABC-type transporters contributing to multidrug resistance in bacteria. *Microbiology and Molecular Biology Reviews* 71, 463-476.
- Lyras, D., O'Connor, J.R., Howarth, P.M., Sambol, S.P., Carter, G.P., Phumoonna, T., Poon, R., Adams, V., Vedantam, G., Johnson, S., Gerding, D.N., Rood, J.I., 2009. Toxin B is essential for virulence of *Clostridium difficile*. *Nature* 458, 1176-1179.
- Macheboeuf, P., Contreras-Martel, C., Job, V., Dideberg, O., Dessen, A., 2006. Penicillin binding proteins: key players in bacterial cell cycle and drug resistance processes. *FEMS microbiology reviews* 30, 673-691.
- Macheboeuf, P., Di Guilmi, A.M., Job, V., Vernet, T., Dideberg, O., Dessen, A., 2005. Active site restructuring regulates ligand recognition in class A penicillin-binding proteins. *Proceedings of the National Academy of Sciences of the United States of America* 102, 577-582.
- Mackin, K.E., Carter, G.P., Howarth, P., Rood, J.I., Lyras, D., 2013. Spo0A differentially regulates toxin production in evolutionarily diverse strains of *Clostridium difficile*. *Plos One* 8.
- Makino, S., Moriyama, R., 2002. Hydrolysis of cortex peptidoglycan during bacterial spore germination. *Medical Science Monitor* 8, RA119-127.
- Mani, N., Dupuy, B., 2001. Regulation of toxin synthesis in *Clostridium difficile* by an alternative RNA polymerase sigma factor. *Proceedings of the National Academy of Sciences of the United States of America* 98, 5844-5849.
- Markham, P.N., 1999. Inhibition of the emergence of ciprofloxacin resistance in *Streptococcus pneumoniae* by the multidrug efflux inhibitor reserpine. *Antimicrob Agents Chemother* 43, 988-989.
- Mascher, T., Heintz, M., Zahner, D., Merai, M., Hakenbeck, R., 2006. The CiaRH system of *Streptococcus pneumoniae* prevents lysis during stress induced by treatment with cell wall inhibitors and by mutations in *pbp2x* involved in beta-lactam resistance. *Journal of bacteriology* 188, 1959-1968.
- Massey, T.H., Mercogliano, C.P., Yates, J., Sherratt, D.J., Lowe, J., 2006. Double-stranded DNA translocation: structure and mechanism of hexameric FtsK. *Molecular Cell* 23, 457-469.

- Massova, I., Mobashery, S., 1998. Kinship and diversification of bacterial penicillin-binding proteins and beta-lactamases. *Antimicrobial Agents and Chemotherapy* 42, 1-17.
- Matagne, A., Dubus, A., Galleni, M., Frere, J.M., 1999. The beta-lactamase cycle: a tale of selective pressure and bacterial ingenuity. *Natural product reports* 16, 1-19.
- Matamouros, S., England, P., Dupuy, B., 2007. *Clostridium difficile* toxin expression is inhibited by the novel regulator TcdC. *Mol Microbiol* 64, 1274-1288.
- Matthew, M., 1979. Plasmid-mediated beta-lactamases of Gram-negative bacteria: properties and distribution. *The Journal of antimicrobial chemotherapy* 5, 349-358.
- Maurer, P., Todorova, K., Sauerbier, J., Hakenbeck, R., 2012. Mutations in *Streptococcus pneumoniae* penicillin-binding protein 2x: importance of the C-terminal penicillin-binding protein and serine/threonine kinase-associated domains for beta-lactam binding. *Microbial drug resistance* 18, 314-321.
- Mayer, M.J., Narbad, A., Gasson, M.J., 2008. Molecular characterization of a *Clostridium difficile* bacteriophage and its cloned biologically active endolysin. *Journal of bacteriology* 190, 6734-6740.
- McClintock, B., 1950. The origin and behavior of mutable loci in Maize. *Proceedings of the National Academy of Sciences of the United States of America* 36, 344-355.
- McDonald, L.C., Killgore, G.E., Thompson, A., Owens, R.C., Jr., Kazakova, S.V., Sambol, S.P., Johnson, S., Gerding, D.N., 2005. An epidemic, toxin gene-variant strain of *Clostridium difficile*. *The New England journal of medicine* 353, 2433-2441.
- McFarland, L.V., 2005. Alternative treatments for *Clostridium difficile* disease: what really works? *Journal of medical microbiology* 54, 101-111.
- McFarland, L.V., 2008. Antibiotic-associated diarrhea: epidemiology, trends and treatment. *Future microbiology* 3, 563-578.

- McFarland, L.V., Brandmarker, S.A., Guandalini, S., 2000. Pediatric *Clostridium difficile*: a phantom menace or clinical reality? *Journal of pediatric gastroenterology and nutrition* 31, 220-231.
- McGlone, S.M., Bailey, R.R., Zimmer, S.M., Popovich, M.J., Tian, Y., Ufberg, P., Muder, R.R., Lee, B.Y., 2012. The economic burden of *Clostridium difficile*. *Clinical Microbiology and Infection* 18, 282-289.
- McKenney, P.T., Driks, A., Eichenberger, P., 2013. The *Bacillus subtilis* endospore: assembly and functions of the multilayered coat. *Nature Reviews Microbiology* 11, 33-
- McKenney, P.T., Driks, A., Eskandarian, H.A., Grabowski, P., Guberman, J., Wang, K.H., Gitai, Z., Eichenberger, P., 2010. A Distance-weighted interaction map reveals a previously uncharacterized layer of the *Bacillus subtilis* spore coat. *Current Biology* 20, 934-938.
- McMurry, L., Petrucci, R.E., Jr., Levy, S.B., 1980. Active efflux of tetracycline encoded by four genetically different tetracycline resistance determinants in *Escherichia coli*. *Proceedings of the National Academy of Sciences of the United States of America* 77, 3974-3977.
- Meberg, B.M., Paulson, A.L., Priyadarshini, R., Young, K.D., 2004. Endopeptidase penicillin-binding proteins 4 and 7 play auxiliary roles in determining uniform morphology of *Escherichia coli*. *Journal of bacteriology* 186, 8326-8336.
- Mei, J.M., Nourbakhsh, F., Ford, C.W., Holden, D.W., 1997. Identification of *Staphylococcus aureus* virulence genes in a murine model of bacteraemia using signature-tagged mutagenesis. *Molecular Microbiology* 26, 399-407.
- Meyer, P., Gutierrez, J., Pogliano, K., Dworkin, J., 2010. Cell wall synthesis is necessary for membrane dynamics during sporulation of *Bacillus subtilis*. *Molecular Microbiology* 76, 956-+.
- Mie, M., Naoki, T., Uchida, K., Kobatake, E., 2012. Development of a split SNAP-tag protein complementation assay for visualization of protein-protein interactions in living cells. *The Analyst* 137, 4760-4765.
- Miller, J. H., 1992. *A short course in bacterial genetics*. Cold Spring Harbor Laboratory Press, Cold Spring Harbor, New York.

- Moeller, R., Setlow, P., Reitz, G., Nicholson, W.L., 2009. Roles of small, acid-soluble spore proteins and core water content in survival of *Bacillus subtilis* spores exposed to environmental solar UV radiation. *Applied and environmental microbiology* 75, 5202-5208.
- Mohr, G., Smith, D., Belfort, M., Lambowitz, A.M., 2000. Rules for DNA target-site recognition by a lactococcal group II intron enable retargeting of the intron to specific DNA sequences. *Genes & Development* 14, 559-573.
- Moura, I., Spigaglia, P., Barbanti, F., Mastrantonio, P., 2013. Analysis of metronidazole susceptibility in different *Clostridium difficile* PCR ribotypes. *The Journal of antimicrobial chemotherapy* 68, 362-365.
- Mullane, K., 2014. Fidaxomicin in *Clostridium difficile* infection: latest evidence and clinical guidance. *Therapeutic Advances in Chronic Disease* 5, 69-84.
- Mullane, K.M., Miller, M.A., Weiss, K., Lentnek, A., Golan, Y., Sears, P.S., Shue, Y.K., Louie, T.J., Gorbach, S.L., 2011. Efficacy of fidaxomicin versus vancomycin as therapy for *Clostridium difficile* infection in individuals taking concomitant antibiotics for other concurrent infections. *Clinical infectious diseases: an official publication of the Infectious Diseases Society of America* 53, 440-447.
- Mullany, P., Wilks, M., Puckey, L., Tabaqchali, S., 1994. Gene cloning in *Clostridium difficile* using Tn916 as a shuttle conjugative transposon. *Plasmid* 31, 320-323.
- Mullany, P., Wilks, M., Tabaqchali, S., 1991. Transfer of Tn916 and Tn916-Delta-E into *Clostridium difficile* demonstration of a hot-spot for these elements in the *Clostridium difficile* genome. *FEMS Microbiology Letters* 79, 191-194.
- Murrell, W.G., 1967. The biochemistry of the bacterial endospore. *Advances in Microbial Physiology* 1, 133-251.
- Nelson, D.E., Young, K.D., 2001. Contributions of PBP 5 and DD-carboxypeptidase penicillin binding proteins to maintenance of cell shape in *Escherichia coli*. *Journal of bacteriology* 183, 3055-3064.
- Nemmara, V.V., Dzhekueva, L., Sarkar, K.S., Adediran, S.A., Duez, C., Nicholas, R.A., Pratt, R.F., 2011. Substrate specificity of low-molecular mass bacterial DD-peptidases. *Biochemistry* 50, 10091-10101.

- Nerandzic, M.M., Donskey, C.J., 2010. Triggering germination represents a novel strategy to enhance killing of *Clostridium difficile* spores. PLoS One 5, e12285.
- Nerandzic, M.M., Donskey, C.J., 2013. Activate to eradicate: inhibition of *Clostridium difficile* spore outgrowth by the synergistic effects of osmotic activation and nisin. PLoS One 8, e54740.
- Neyfakh, A.A., Borsch, C.M., Kaatz, G.W., 1993. Fluoroquinolone resistance protein NorA of *Staphylococcus aureus* is a multidrug efflux transporter. Antimicrobial Agents and Chemotherapy 37, 128-129.
- Ng, Y.K., Ehsaan, M., Philip, S., Collery, M.M., Janoir, C., Collignon, A., Cartman, S.T., Minton, N.P., 2013. Expanding the repertoire of gene tools for precise manipulation of the *Clostridium difficile* genome: Allelic Exchange Using pyrE Alleles. PLoS one 8.
- Nicholson, W.L., Munakata, N., Horneck, G., Melosh, H.J., Setlow, P., 2000. Resistance of *Bacillus* endospores to extreme terrestrial and extraterrestrial environments. Microbiology and Molecular Biology Reviews 64, 548-+.
- Nikaido, H., 2009. Multidrug resistance in bacteria. Annual Review of Biochemistry 78, 119-146.
- Nikaido, H., 2011. Structure and mechanism of RND-type multidrug efflux pumps. Advances in enzymology and related areas of molecular biology 77, 1-60.
- Nikaido, H., Takatsuka, Y., 2009. Mechanisms of RND multidrug efflux pumps. Biochim Biophys Acta 1794, 769-781.
- Obuch-Woszczatynski, P., Lachowicz, D., Schneider, A., Mol, A., Pawlowska, J., Ozdzenska-Milke, E., Pruszczyk, P., Wultanska, D., Mlynarczyk, G., Harmanus, C., Kuijper, E.J., van Belkum, A., Pituch, H., 2014. Occurrence of *Clostridium difficile* PCR-ribotype 027 and it's closely related PCR-ribotype 176 in hospitals in Poland in 2008-2010. Anaerobe 28, 13-17.
- O'Callaghan, C.H., Morris, A., Kirby, S.M., Shingler, A.H., 1972. Novel method for detection of beta-lactamases by using a chromogenic cephalosporin substrate. Antimicrobial Agents and Chemotherapy 1, 283-288.

- O'Connor, J.R., Lyras, D., Farrow, K.A., Adams, V., Powell, D.R., Hinds, J., Cheung, J.K., Rood, J.I., 2006. Construction and analysis of chromosomal *Clostridium difficile* mutants. *Molecular Microbiology* 61, 1335-1351.
- Oliva, M., Dideberg, O., Field, M.J., 2003. Understanding the acylation mechanisms of active-site serine penicillin-recognizing proteins: A molecular dynamics simulation study. *Proteins* 53, 88-100.
- Owens, R.C., 2007. *Clostridium difficile*-associated disease: changing epidemiology and implications for management. *Drugs* 67, 487-502.
- Panessa-Warren, B.J., Tortora, G.T., Warren, J.B., 2007. High resolution FESEM and TEM reveal bacterial spore attachment. *Microscopy and Microanalysis* 13, 251-266.
- Papp-Wallace, K.M., Becka, S.A., Taracila, M.A., Winkler, M.L., Gatta, J.A., Rholl, D.A., Schweizer, H.P., Bonomo, R.A., 2016. exposing a beta-Lactamase "twist": the mechanistic basis for the high level of ceftazidime resistance in the C69F variant of the *Burkholderia pseudomallei* PenI beta-Lactamase. *Antimicrobial Agents and Chemotherapy* 60, 777-788.
- Paredes, C.J., Alsaker, K.V., Papoutsakis, E.T., 2005. A comparative genomic view of clostridial sporulation and physiology. *Nature reviews. Microbiology* 3, 969-978.
- Paredes-Sabja, D., Setlow, P., Sarker, M.R., 2009a. The protease CspB is essential for initiation of cortex hydrolysis and dipicolinic acid (DPA) release during germination of spores of *Clostridium perfringens* type A food poisoning isolates. *Microbiology - Microbiology Society* 155, 3464-3472.
- Paredes-Sabja, D., Setlow, P., Sarker, M.R., 2009b. SleC is essential for cortex peptidoglycan hydrolysis during germination of spores of the pathogenic bacterium *Clostridium perfringens*. *Journal of bacteriology* 191, 2711-2720.
- Paredes-Sabja, D., Setlow, P., Sarker, M.R., 2011. Germination of spores of *Bacillales* and *Clostridiales* species: mechanisms and proteins involved. *Trends in microbiology* 19, 85-94.

- Paredes-Sabja, D., Shen, A., Sorg, J.A., 2014. *Clostridium difficile* spore biology: sporulation, germination, and spore structural proteins. Trends in microbiology 22, 406-416.
- Paterson, D.L., Bonomo, R.A., 2005. Extended-spectrum beta-lactamases: a clinical update. Clinical Microbiology Reviews 18, 657-686.
- Pelaez, T., Alcalá, L., Alonso, R., Rodríguez-Creixems, M., García-Lechuz, J.M., Bouza, E., 2002. Reassessment of *Clostridium difficile* susceptibility to metronidazole and vancomycin. Antimicrobial agents and chemotherapy 46, 1647-1650.
- Peltier, J., Courtin, P., El Meouche, I., Lemee, L., Chapot-Chartier, M.P., Pons, J.L., 2011. *Clostridium difficile* has an original peptidoglycan structure with a high level of N-Acetylglucosamine deacetylation and mainly 3-3 cross-links. Journal of Biological Chemistry 286, 29053-29062.
- Peltier, J., Shaw, H.A., Couchman, E.C., Dawson, L.F., Yu, L., Choudhary, J.S., Kaeber, V., Wren, B.W., Fairweather, N.F., 2015. Cyclic diGMP regulates production of sortase substrates of *Clostridium difficile* and their surface exposure through Zmpl protease-mediated cleavage. Journal of Biological Chemistry 290, 24453-24469.
- Pepin, J., Saheb, N., Coulombe, M.A., Alary, M.E., Corriveau, M.P., Authier, S., Leblanc, M., Rivard, G., Bettez, M., Primeau, V., Nguyen, M., Jacob, C.E., Lanthier, L., 2005. Emergence of fluoroquinolones as the predominant risk factor for *Clostridium difficile*-associated diarrhea: a cohort study during an epidemic in Quebec. Clinical infectious diseases: an official publication of the Infectious Diseases Society of America 41, 1254-1260.
- Pepin, J., Valiquette, L., Gagnon, S., Routhier, S., Brazeau, I., 2007. Outcomes of *Clostridium difficile*-associated disease treated with metronidazole or vancomycin before and after the emergence of NAP1/027. Am J Gastroenterol 102, 2781-2788.
- Perego, M., Hanstein, C., Welsh, K.M., Djavakhishvili, T., Glaser, P., Hoch, J.A., 1994. Multiple protein aspartate phosphatases provide a mechanism for the

integration of diverse signals in the control of development in *Bacillus subtilis*. *Cell* 79, 1047-1055.

- Perego, M., Spiegelman, G.B., Hoch, J.A., 1988. Structure of the gene for the transition-state regulator, Abrb - regulator synthesis is controlled by the Spo0A sporulation gene in *Bacillus subtilis*. *Molecular Microbiology* 2, 689-699.
- Pereira, F.C., Saujet, L., Tome, A.R., Serrano, M., Monot, M., Couture-Tosi, E., Martin-Verstraete, I., Dupuy, B., Henriques, A.O., 2013. The spore differentiation pathway in the enteric pathogen *Clostridium difficile*. *PLoS genetics* 9.
- Perelle, S., Gibert, M., Bourlioux, P., Corthier, G., Popoff, M.R., 1997. Production of a complete binary toxin (actin-specific ADP-ribosyltransferase) by *Clostridium difficile* CD196. *Infection and Immunity* 65, 1402-1407.
- Permpoonpattana, P., Tolls, E.H., Nadem, R., Tan, S., Brisson, A., Cutting, S.M., 2011. Surface layers of *Clostridium difficile* endospores. *Journal of bacteriology* 193, 6461-6470.
- Pettit, L.J., Browne, H.P., Yu, L., Smits, W.K., Fagan, R.P., Barquist, L., Martin, M.J., Goulding, D., Duncan, S.H., Flint, H.J., Dougan, G., Choudhary, J.S., Lawley, T.D., 2014. Functional genomics reveals that *Clostridium difficile* Spo0A coordinates sporulation, virulence and metabolism. *BMC genomics* 15, 160.
- Pinho, M.G., Errington, J., 2005. Recruitment of penicillin-binding protein PBP2 to the division site of *Staphylococcus aureus* is dependent on its transpeptidation substrates. *Molecular Microbiology* 55, 799-807.
- Pizarro-Guajardo, M., Olguin-Araneda, V., Barra-Carrasco, J., Brito-Silva, C., Sarker, M.R., Paredes-Sabja, D., 2014. Characterization of the collagen-like exosporium protein, BclA1, of *Clostridium difficile* spores. *Anaerobe* 25, 18-30.
- Polissi, A., Pontiggia, A., Feger, G., Altieri, M., Mottl, H., Ferrari, L., Simon, D., 1998. Large-scale identification of virulence genes from *Streptococcus pneumoniae*. *Infection and Immunity* 66, 5620-5629.
- Popham, D.L., Helin, J., Costello, C.E., Setlow, P., 1996. Muramic lactam in peptidoglycan of *Bacillus subtilis* spores is required for spore outgrowth but not for spore dehydration or heat resistance. *Proceedings of the National Academy of Sciences of the United States of America* 93, 15405-15410.

- Pottathil, M., Lazazzera, B.A., 2003. The extracellular Phr peptide-Rap phosphatase signaling circuit of *Bacillus subtilis*. *Frontiers in Bioscience* 8, d32-45.
- Price, A.B., Davies, D.R., 1977. Pseudomembranous colitis. *Journal of clinical pathology* 30, 1-12.
- Priyadarshini, R., Popham, D.L., Young, K.D., 2006. Daughter cell separation by penicillin-binding proteins and peptidoglycan amidases in *Escherichia coli*. *Journal of bacteriology* 188, 5345-5355.
- Punta, M., Coghill, P.C., Eberhardt, R.Y., Mistry, J., Tate, J., Boursnell, C., Pang, N., Forslund, K., Ceric, G., Clements, J., Heger, A., Holm, L., Sonnhammer, E.L., Eddy, S.R., Bateman, A., Finn, R.D., 2012. The Pfam protein families database. *Nucleic acids research* 40, D290-301.
- Purdy, D., O'Keeffe, T.A.T., Elmore, M., Herbert, M., McLeod, A., Bokori-Brown, M., Ostrowski, A., Minton, N.P., 2002. Conjugative transfer of clostridial shuttle vectors from *Escherichia coli* to *Clostridium difficile* through circumvention of the restriction barrier. *Molecular Microbiology* 46, 439-452.
- Putnam, E.E., Nock, A.M., Lawley, T.D., Shen, A., 2013. SpoIVA and SipL are *Clostridium difficile* spore morphogenetic proteins. *Journal of bacteriology* 195, 1214-1225.
- Rahn-Lee, L., Gorbatyuk, B., Skovgaard, O., Losick, R., 2009. The conserved sporulation protein YneE inhibits DNA replication in *Bacillus subtilis*. *Journal of bacteriology* 191, 3736-3739.
- Rammelkamp, C.H., Keefer, C.S., 1943. The absorption, excretion, and distribution of penicillin. *Journal of Clinical Investigation* 22, 425-437.
- Ratnayake-Lecamwasam, M., Serror, P., Wong, K.W., Sonenshein, A.L., 2001. *Bacillus subtilis* CodY represses early-stationary-phase genes by sensing GTP levels. *Genes & Development* 15, 1093-1103.
- Reineke, J., Tenzer, S., Rupnik, M., Koschinski, A., Hasselmayer, O., Schratzenholz, A., Schild, H., von Eichel-Streiber, C., 2007. Autocatalytic cleavage of *Clostridium difficile* toxin B. *Nature* 446, 415-419.

- Reineke, K., Mathys, A., Heinz, V., Knorr, D., 2013. Mechanisms of endospore inactivation under high pressure. *Trends in microbiology* 21, 296-304.
- Reinert, D.J., Jank, T., Aktories, K., Schulz, G.E., 2005. Structural basis for the function of *Clostridium difficile* toxin B. *Journal of Molecular Biology* 351, 973-981.
- Reynolds, C.B., Emerson, J.E., de la Riva, L., Fagan, R.P., Fairweather, N.F., 2011. The *Clostridium difficile* cell wall protein CwpV is antigenically variable between strains, but exhibits conserved aggregation-promoting function. *PLoS pathogens* 7.
- Riegler, M., Sedivy, R., Pothoulakis, C., Hamilton, G., Zacherl, J., Bischof, G., Cosentini, E., Feil, W., Schiessel, R., LaMont, J.T., et al., 1995. *Clostridium difficile* toxin B is more potent than toxin A in damaging human colonic epithelium *in vitro*. *Journal of Clinical Investigation* 95, 2004-2011.
- Riesenman, P.J., Nicholson, W.L., 2000. Role of the spore coat layers in *Bacillus subtilis* spore resistance to hydrogen peroxide, artificial UV-C, UV-B, and solar UV radiation. *Applied and environmental microbiology* 66, 620-626.
- Riggs, M.M., Sethi, A.K., Zabarsky, T.F., Eckstein, E.C., Jump, R.L., Donskey, C.J., 2007. Asymptomatic carriers are a potential source for transmission of epidemic and nonepidemic *Clostridium difficile* strains among long-term care facility residents. *Clinical infectious diseases: an official publication of the Infectious Diseases Society of America* 45, 992-998.
- Roberts, J. M., 1952. *Mycologia* 44, 292.
- Roupael, N.G., O'Donnell, J.A., Bhatnagar, J., Lewis, F., Polgreen, P.M., Beekmann, S., Guarner, J., Killgore, G.E., Coffman, B., Campbell, J., Zaki, S.R., McDonald, L.C., 2008. *Clostridium difficile*-associated diarrhea: an emerging threat to pregnant women. *American journal of obstetrics and gynecology* 198, 635 e631-636.
- Roy, C., Foz, A., Segura, C., Tirado, M., Fuster, C., Reig, R., 1983. Plasmid-determined beta-lactamases identified in a group of 204 ampicillin-resistant *Enterobacteriaceae*. *The Journal of antimicrobial chemotherapy* 12, 507-510.

- Rudner, D.Z., Pan, Q., Losick, R.M., 2002. Evidence that subcellular localization of a bacterial membrane protein is achieved by diffusion and capture. *Proceedings of the National Academy of Sciences of the United States of America* 99, 8701-8706.
- Ruiz, J., 2003. Mechanisms of resistance to quinolones: target alterations, decreased accumulation and DNA gyrase protection. *Journal of Antimicrobial Chemotherapy* 51, 1109-1117.
- Rupnik, M., 2008. Heterogeneity of large clostridial toxins: importance of *Clostridium difficile* toxinotypes. *FEMS microbiology reviews* 32, 541-555.
- Rupnik, M., Just, I., 2006. In the comprehensive sourcebook of bacterial protein toxins 3rd edn (eds Alouf, J. A. & Popoff, M. R.). Academic Press, Burlington, Massachusetts, USA, 409–429.
- Rupnik, M., Wilcox, M.H., Gerding, D.N., 2009. *Clostridium difficile* infection: new developments in epidemiology and pathogenesis. *Nature reviews. Microbiology* 7, 526-536.
- Sakakibara, J., Nagano, K., Murakami, Y., Higuchi, N., Nakamura, H., Shimozato, K., Yoshimura, F., 2007. Loss of adherence ability to human gingival epithelial cells in S-layer protein-deficient mutants of *Tannerella forsythensis*. *Microbiology - Microbiology Society* 153, 866-876.
- Saujet, L., Monot, M., Dupuy, B., Soutourina, O., Martin-Verstraete, I., 2011. The key sigma factor of transition phase, SigH, controls sporulation, metabolism, and virulence factor expression in *Clostridium difficile*. *Journal of bacteriology* 193, 3186-3196.
- Saujet, L., Pereira, F.C., Serrano, M., Soutourina, O., Monot, M., Shelyakin, P.V., Gelfand, M.S., Dupuy, B., Henriques, A.O., Martin-Verstraete, I., 2013. Genome-wide analysis of cell type-specific gene transcription during spore formation in *Clostridium difficile*. *PLoS genetics* 9.
- Sauvage, E., Kerff, F., Fonze, E., Herman, R., Schoot, B., Marquette, J.P., Taburet, Y., Prevost, D., Dumas, J., Leonard, G., Stefanic, P., Coyette, J., Charlier, P., 2002. The 2.4-Å crystal structure of the penicillin-resistant penicillin-binding protein

PBP5fm from *Enterococcus faecium* in complex with benzylpenicillin. Cellular and Molecular Life Sciences 59, 1223-1232.

- Sauvage, E., Kerff, F., Terrak, M., Ayala, J.A., Charlier, P., 2008. The penicillin-binding proteins: structure and role in peptidoglycan biosynthesis. FEMS microbiology reviews 32, 234-258.
- Sauvage, E., Terrak, M., 2016. Glycosyltransferases and transpeptidases/penicillin-binding proteins: valuable targets for new antibacterials. Antibiotics (Basel) 5.
- Saxton, K., Baines, S.D., Freeman, J., O'Connor, R., Wilcox, M.H., 2009. Effects of exposure of *Clostridium difficile* PCR ribotypes 027 and 001 to fluoroquinolones in a human gut model. Antimicrobial agents and chemotherapy 53, 412-420.
- Schaeffer, P., Millet, J., Aubert, J.P., 1965. Catabolic repression of bacterial sporulation. Proceedings of the National Academy of Sciences of the United States of America 54, 704-+.
- Schaffer, C., Messner, P., 2005. The structure of secondary cell wall polymers: how Gram-positive bacteria stick their cell walls together. Microbiology - Microbiology Society 151, 643-651.
- Schmitz, F.J., Fluit, A.C., Luckefahr, M., Engler, B., Hofmann, B., Verhoef, J., Heinz, H.P., Hadding, U., Jones, M.E., 1998. The effect of reserpine, an inhibitor of multidrug efflux pumps, on the *in-vitro* activities of ciprofloxacin, sparfloxacin and moxifloxacin against clinical isolates of *Staphylococcus aureus*. Journal of Antimicrobial Chemotherapy 42, 807-810.
- Schneider, K.D., Bethel, C.R., Distler, A.M., Hujer, A.M., Bonomo, R.A., Leonard, D.A., 2009. Mutation of the active site carboxy-lysine (K70) of OXA-1 beta-lactamase results in a deacylation-deficient enzyme. Biochemistry 48, 6136-6145.
- Schwan, C., Stecher, B., Tzivelekidis, T., van Ham, M., Rohde, M., Hardt, W.D., Wehland, J., Aktories, K., 2009. *Clostridium difficile* toxin CDT induces formation of microtubule-based protrusions and increases adherence of bacteria. PLoS pathogens 5, e1000626.

- Sebaihia, M., Wren, B.W., Mullany, P., Fairweather, N.F., Minton, N., Stabler, R., Thomson, N.R., Roberts, A.P., Cerdeno-Tarraga, A.M., Wang, H.W., Holden, M.T.G., Wright, A., Churcher, C., Quail, M.A., Baker, S., Bason, N., Brooks, K., Chillingworth, T., Cronin, A., Davis, P., Dowd, L., Fraser, A., Feltwell, T., Hance, Z., Holroyd, S., Jagels, K., Moule, S., Mungall, K., Price, C., Rabinowitsch, E., Sharp, S., Simmonds, M., Stevens, K., Unwin, L., Whithead, S., Dupuy, B., Dougan, G., Barrell, B., Parkhill, J., 2006. The multidrug-resistant human pathogen *Clostridium difficile* has a highly mobile, mosaic genome. *Nature genetics* 38, 779-786.
- Sekiguchi, J., Akeo, K., Yamamoto, H., Khasanov, F.K., Alonso, J.C., Kuroda, A., 1995. Nucleotide-sequence and regulation of a new putative cell-wall hydrolase gene, Cwld, which affects germination in *Bacillus subtilis*. *Journal of bacteriology* 177, 5582-5589.
- Setlow, P., 1994. Mechanisms which contribute to the long-term survival of spores of *Bacillus* Species. *Journal of Applied Bacteriology* 76, S49-S60.
- Setlow, P., 2006. Spores of *Bacillus subtilis*: their resistance to and killing by radiation, heat and chemicals. *Journal of applied microbiology* 101, 514-525.
- Setlow, P., 2007. I will survive: DNA protection in bacterial spores. *Trends in microbiology* 15, 172-180.
- Shaughnessy, M.K., Amundson, W.H., Kuskowski, M.A., DeCarolis, D.D., Johnson, J.R., Drekonja, D.M., 2013. Unnecessary antimicrobial use in patients with current or recent *Clostridium difficile* infection. *Infection control and hospital epidemiology* 34, 109-116.
- Silhavy, T.J., Kahne, D., Walker, S., 2010. The bacterial cell envelope. *Cold Spring Harbor Perspectives in Biology* 2, a000414.
- Silvaggi, N.R., Josephine, H.R., Kuzin, A.P., Nagarajan, R., Pratt, R.F., Kelly, J.A., 2005. Crystal structures of complexes between the R61 DD-peptidase and peptidoglycan-mimetic beta-lactams: A non-covalent complex with a "perfect penicillin". *Journal of Molecular Biology* 345, 521-533.

- Siranosian, K.J., Grossman, A.D., 1994. Activation of Spo0A transcription by sigma H is necessary for sporulation but not for competence in *Bacillus-Subtilis*. Journal of bacteriology 176, 3812-3815.
- Slimings, C., Riley, T.V., 2013. Antibiotics and hospital-acquired *Clostridium difficile* infection: update of systematic review and meta-analysis. The Journal of antimicrobial chemotherapy 69, 881-891.
- Sonenshein, A.L., 2000. Control of sporulation initiation in *Bacillus subtilis*. Current Opinion in Microbiology 3, 561-566.
- Sorg, J.A., Sonenshein, A.L., 2008. Bile salts and glycine as cogerminants for *Clostridium difficile* spores. Journal of bacteriology 190, 2505-2512.
- Sorg, J.A., Sonenshein, A.L., 2009. Chenodeoxycholate is an inhibitor of *Clostridium difficile* spore germination. Journal of bacteriology 191, 1115-1117.
- Spigaglia, P., 2016. Recent advances in the understanding of antibiotic resistance in *Clostridium difficile* infection. Therapeutic advances in infectious disease 3, 23-42.
- Spigaglia, P., Barbanti, F., Dionisi, A.M., Mastrantonio, P., 2010. *Clostridium difficile* isolates resistant to fluoroquinolones in Italy: emergence of PCR ribotype 018. Journal of clinical microbiology 48, 2892-2896.
- Spigaglia, P., Barbanti, F., Mastrantonio, P., Brazier, J.S., Barbut, F., Delmee, M., Kuijper, E., Poxton, I.R., Dif, E.S.G.C., 2008. Fluoroquinolone resistance in *Clostridium difficile* isolates from a prospective study of *C. difficile* infections in Europe. Journal of medical microbiology 57, 784-789.
- Spigaglia, P., Barbanti, F., Morandi, M., Moro, M.L., Mastrantonio, P., 2016. Diagnostic testing for *Clostridium difficile* in Italian microbiological laboratories. Anaerobe 37, 29-33.
- Spigaglia, P., Carattoli, A., Barbanti, F., Mastrantonio, P., 2010. Detection of *gyrA* and *gyrB* mutations in *Clostridium difficile* isolates by real-time PCR. Molecular and Cellular Probes 24, 61-67.
- Stabler, R.A., He, M., Dawson, L., Martin, M., Valiente, E., Corton, C., Lawley, T.D., Sebahia, M., Quail, M.A., Rose, G., Gerding, D.N., Gibert, M., Popoff, M.R., Parkhill, J., Dougan, G., Wren, B.W., 2009. Comparative genome and phenotypic

analysis of *Clostridium difficile* 027 strains provides insight into the evolution of a hypervirulent bacterium. *Genome Biology* 10, R102.

- Stec, B., Holtz, K.M., Wojciechowski, C.L., Kantrowitz, E.R., 2005. Structure of the wild-type TEM-1 beta-lactamase at 1.55 Å and the mutant enzyme Ser70Ala at 2.1 Å suggest the mode of noncovalent catalysis for the mutant enzyme. *Acta crystallographica. Section D, Biological crystallography* 61, 1072-1079.
- Steil, L., Serrano, M., Henriques, A.O., Volker, U., 2005. Genome-wide analysis of temporally regulated and compartment-specific gene expression in sporulating cells of *Bacillus subtilis*. *Microbiology - Microbiology Society* 151, 399-420.
- Steiner, E., Dago, A.E., Young, D.I., Heap, J.T., Minton, N.P., Hoch, J.A., Young, M., 2011. Multiple orphan histidine kinases interact directly with Spo0A to control the initiation of endospore formation in *Clostridium acetobutylicum*. *Molecular Microbiology* 80, 641-654.
- Stubbs, S., Rupnik, M., Gibert, M., Brazier, J., Duerden, B., Popoff, M., 2000. Production of actin-specific ADP-ribosyltransferase (binary toxin) by strains of *Clostridium difficile*. *FEMS Microbiology Letters* 186, 307-312.
- Sumner, H.W., Tedesco, F.J., 1975. Rectal biopsy in clindamycin-associated colitis. An analysis of 23 cases. *Archives of pathology* 99, 237-241.
- Tate, S.S., Meister, A., 1985. Gamma-glutamyl transpeptidase from kidney. *Methods Enzymol* 113, 400-419.
- Tedesco, F.J., Barton, R.W., Alpers, D.H., 1974. Clindamycin-associated colitis. A prospective study. *Annals of internal medicine* 81, 429-433.
- Teichert, M., Tatge, H., Schoentaube, J., Just, I., Gerhard, R., 2006. Application of mutated *Clostridium difficile* toxin A for determination of glucosyltransferase-dependent effects. *Infection and Immunity* 74, 6006-6010.
- Tenover, F.C., Tickler, I.A., Persing, D.H., 2012. Antimicrobial-resistant strains of *Clostridium difficile* from North America. *Antimicrobial agents and chemotherapy* 56, 2929-2932.
- Thelestam, M., Chaves-Olarte, E., 2000. Cytotoxic effects of the *Clostridium difficile* toxins. *Current topics in microbiology and immunology* 250, 85-96.

- Theriot, C.M., Bowman, A.A., Young, V.B., 2016. Antibiotic-induced alterations of the gut microbiota alter secondary bile acid production and allow for *Clostridium difficile* spore germination and outgrowth in the large intestine. *mSphere* 1.
- Theriot, C.M., Young, V.B., 2015. Interactions between the gastrointestinal microbiome and *Clostridium difficile*. *Annual review of microbiology* 69, 445-461.
- Thomas, C., Stevenson, M., Riley, T.V., 2003. Antibiotics and hospital-acquired *Clostridium difficile*-associated diarrhoea: a systematic review. *Journal of Antimicrobial Chemotherapy* 51, 1339-1350.
- Tipper, D.J., Linnett, P.E., 1976. Distribution of peptidoglycan synthetase activities between sporangia and forespores in sporulating cells of *Bacillus sphaericus*. *Journal of bacteriology* 126, 213-221.
- Tseng, T.T., Gratwick, K.S., Kollman, J., Park, D., Nies, D.H., Goffeau, A., Saier, M.H., Jr., 1999. The RND permease superfamily: an ancient, ubiquitous and diverse family that includes human disease and development proteins. *Journal of Molecular Microbiology and Biotechnology*. 1, 107-125.
- Ubukata, K., Itoh-Yamashita, N., Konno, M., 1989. Cloning and expression of the *norA* gene for fluoroquinolone resistance in *Staphylococcus aureus*. *Antimicrobial agents and chemotherapy* 33, 1535-1539.
- Ullmann, A., Danchin, A., 1983. Role of cyclic Amp in bacteria. Greengard and G. A. Robinson (Ed.), *Advances in Cyclic Nucleotide Research*. Raven Press, New York. P. 1-44. in P.
- Vaishnavi, C., 2010. Clinical spectrum & pathogenesis of *Clostridium difficile* associated diseases. *The Indian journal of medical research* 131, 487-499.
- Vakulenko, S.B., Taibi-Tronche, P., Toth, M., Massova, I., Lerner, S.A., Mobashery, S., 1999. Effects on substrate profile by mutational substitutions at positions 164 and 179 of the class A TEM (pUC19) beta-lactamase from *Escherichia coli*. *The Journal of biological chemistry* 274, 23052-23060.
- Varma, A., Young, K.D., 2004. FtsZ collaborates with penicillin binding proteins to generate bacterial cell shape in *Escherichia coli*. *Journal of bacteriology* 186, 6768-6774.

- Varshney, J.B., Very, K.J., Williams, J.L., Hegarty, J.P., Stewart, D.B., Lumadue, J., Venkitanarayanan, K., Jayarao, B.M., 2014. Characterization of *Clostridium difficile* isolates from human fecal samples and retail meat from Pennsylvania. *Foodborne Pathogens Disease* 11, 822-829.
- Vasudevan, P., Weaver, A., Reichert, E.D., Linnstaedt, S.D., Popham, D.L., 2007. Spore cortex formation in *Bacillus subtilis* is regulated by accumulation of peptidoglycan precursors under the control of sigma K. *Molecular Microbiology* 65, 1582-1594.
- Vega, D., Ayala, J.A., 2006. The DD-carboxypeptidase activity encoded by *pbp4B* is not essential for the cell growth of *Escherichia coli*. *Archives of microbiology* 185, 23-27.
- Vidal, J.E., Chen, J.M., Li, J.H., McClane, B.A., 2009. Use of an EZ-Tn5-based random mutagenesis system to identify a novel toxin regulatory locus in *Clostridium perfringens* Strain 13. *PloS one* 4.
- Vollmer, W., 2008. Structural variation in the glycan strands of bacterial peptidoglycan. *FEMS microbiology reviews* 32, 287-306.
- von Eichel-Streiber, C., Boquet, P., Sauerborn, M., Thelestam, M., 1996. Large clostridial cytotoxins--a family of glycosyltransferases modifying small GTP-binding proteins. *Trends in microbiology* 4, 375-382.
- Wagner, J.K., Marquis, K.A., Rudner, D.Z., 2009. SirA enforces diploidy by inhibiting the replication initiator DnaA during spore formation in *Bacillus subtilis*. *Molecular Microbiology* 73, 963-974.
- Walbrown, M.A., Aspinall, S.L., Bayliss, N.K., Stone, R.A., Cunningham, F., Squier, C.L., Good, C.B., 2008. Evaluation of *Clostridium difficile*-associated diarrhea with a drug formulary change in preferred fluoroquinolones. *Journal of managed care pharmacy: JMCP* 14, 34-40.
- Waligora, A.J., Hennequin, C., Mullany, P., Bourlioux, P., Collignon, A., Karjalainen, T., 2001. Characterization of a cell surface protein of *Clostridium difficile* with adhesive properties. *Infection and Immunity* 69, 2144-2153.
- Walsh, C., 2000. Molecular mechanisms that confer antibacterial drug resistance. *Nature* 406, 775-781.

- Walsh, C., 2003. Antibiotics: actions, origins and resistance. Washington, District of Columbia: ASM Press- American Society for Microbiology.
- Wang, K.H., Isidro, A.L., Domingues, L., Eskandarian, H.A., McKenney, P.T., Drew, K., Grabowski, P., Chua, M.H., Barry, S.N., Guan, M., Bonneau, R., Henriques, A.O., Eichenberger, P., 2009. The coat morphogenetic protein SpoVID is necessary for spore encasement in *Bacillus subtilis*. *Molecular Microbiology* 74, 634-649.
- Wang, Q.M., Peery, R.B., Johnson, R.B., Alborn, W.E., Yeh, W.K., Skatrud, P.L., 2001. Identification and characterization of a monofunctional glycosyltransferase from *Staphylococcus aureus*. *Journal of bacteriology* 183, 4779-4785.
- Wang, S.T., Setlow, B., Conlon, E.M., Lyon, J.L., Imamura, D., Sato, T., Setlow, P., Losick, R., Eichenberger, P., 2006. The forespore line of gene expression in *Bacillus subtilis*. *Journal of molecular biology* 358, 16-37.
- Warth, A.D., Strominger, J.L., 1969. Structure of the peptidoglycan of bacterial spores: occurrence of the lactam of muramic acid. *Proceedings of the National Academy of Sciences of the United States of America* 64, 528-535.
- Warth, A.D., Strominger, J.L., 1972. Structure of the peptidoglycan from spores of *Bacillus subtilis*. *Biochemistry-Us* 11, 1389-1396.
- Wei, Y., McPherson, D.C., Popham, D.L., 2004. A mother cell-specific class B penicillin-binding protein, PBP4b, in *Bacillus subtilis*. *Journal of bacteriology* 186, 258-261.
- Weidenmaier, C., Peschel, A., 2008. Teichoic acids and related cell-wall glycopolymers in Gram-positive physiology and host interactions. *Nature reviews. Microbiology* 6, 276-287.
- Whitfield, J.B., 2001. Gamma glutamyl transferase. *Critical Reviews in Clinical Laboratory Sciences* 38, 263-355.
- Wibley, J.E., McKie, J.H., Embrey, K., Marks, D.S., Douglas, K.T., Moore, M.H., Moody, P.C., 1995. A homology model of the three-dimensional structure of human O6-alkylguanine-DNA alkyltransferase based on the crystal structure of

the C-terminal domain of the Ada protein from *Escherichia coli*. Anti-cancer drug design 10, 75-95.

- Wilke, M.S., Lovering, A.L., Strynadka, N.C.J., 2005. beta-lactam antibiotic resistance: a current structural perspective. *Current Opinion in Microbiology* 8, 525-533.
- Willing, S.E., Candela, T., Shaw, H.A., Seager, Z., Mesnage, S., Fagan, R.P., Fairweather, N.F., 2015. *Clostridium difficile* surface proteins are anchored to the cell wall using CWB2 motifs that recognise the anionic polymer PSII. *Molecular Microbiology* 96, 596-608.
- Wright, A., Wait, R., Begum, S., Crossett, B., Nagy, J., Brown, K., Fairweather, N., 2005. Proteomic analysis of cell surface proteins from *Clostridium difficile*. *Proteomics* 5, 2443-2452.
- Wu, L.J., Errington, J., 1994. *Bacillus subtilis* SpoIIIE protein required for DNA segregation during asymmetric cell-division. *Science* 264, 572-575.
- Yanouri, A., Daniel, R.A., Errington, J., Buchanan, C.E., 1993. Cloning and sequencing of the cell-division gene PbpB, which encodes penicillin-binding protein 2B in *Bacillus subtilis*. *Journal of bacteriology* 175, 7604-7616.
- Yassin, S. F. 2009. Pseudomembranous Colitis, Surgical Treatment. *eMedicine General Surgery*.
- Yeats, C., Finn, R.D., Bateman, A., 2002. The PASTA domain: a beta-lactam-binding domain. *Trends in Biochemical Sci* 27, 438.
- Zapun, A., Contreras-Martel, C., Vernet, T., 2008. Penicillin-binding proteins and beta-lactam resistance. *FEMS microbiology reviews* 32, 361-385.
- Zhang, B., Daniel, R.A., Errington, J., Kroos, L., 1997. *Bacillus subtilis* SpoIIID protein binds to two sites in the *spoVD* promoter and represses transcription by sigma E RNA polymerase. *Journal of bacteriology* 179, 972-975.
- Zhao, G., Meier, T.I., Kahl, S.D., Gee, K.R., Blaszczyk, L.C., 1999. BOCILLIN FL, a sensitive and commercially available reagent for detection of penicillin-binding proteins, *Antimicrobial agents and chemotherapy*, vol. 43, pp. 1124-1128.
- Zhong, J., Karberg, M., Lambowitz, A.M., 2003. Targeted and random bacterial gene disruption using a group II intron (targetron) vector containing a

retrotransposition-activated selectable marker. *Nucleic Acids Research* 31, 1656-1664.

Appendix A

Table A1. Primers used in this study.

Name	Orientation	Sequence (5' to 3')	Restriction site	Description
RF13	F	AAACTTAGGGTAACAAAAACA CCG		For inverse PCR to linearise pMTL-SC7215 or 7315
RF20	R	AAACTCCTTTTTGATAATCTCAT GACC		For inverse PCR to linearise pMTL-SC7215 or 7315
RF21	F	GGATTTACATTTGCCGTTTTGT AAAC		Screening for the insertion into pMTL-SC7215
RF22	R	GATCTTTTCTACGGGGTCTGAC		Screening for the insertion into pMTL-SC7215
RF67	F	gtttttgttacctaagtttGTTCTTTA TTAGATTAATAAAGTCAATG		Gibson assembly: to delete <i>CD2544</i> (<i>spoVD</i>) via pMTL-SC7215
RF68	R	tttgagaaaaGAAACTAAAAAGT AACAGATAATTAACATATAC		
RF69	F	tacttttagttttcTTTTCTCAAATCT ATTCCCCC		
RF70	R	gattatcaaaaaggagtttCTTAGGA ATCAGAGAGTAGATAG		
RF71	F	gtttttgttacctaagtttTTCTTTAA CTCAAAGATTTATGTATG		Gibson assembly: to delete <i>CD1067</i> (via pMTL-SC7215)
RF72	R	aatttattttatTTTTGACATGAAAT CACCC		
RF73	F	catgtcaaaaATAAAATAAATTAT GTAATAAAAATTAAGGATAT ATC		
RF74	R	gattatcaaaaaggagtttAGAAATT AAAGATTCAATTAAGACAGTAA AAAATAG		Gibson assembly: to delete <i>CD1318</i> (<i>cwp20</i>) via pMTL-SC7215
RF75	F	gtttttgttacctaagtttCTGTGAA GCAATGGTAGC		
RF76	R	tatgtttaagATAGCTTAACATAAC TAAAAAAGGC		
RF77	F	gttaagctatCTTAAACATATTACA TTACCTCTTCC		
RF78	R	gattatcaaaaaggagtttATATTTAC TACAAAACTGTCATAGAAAA AG		
RF139	F	GTCA <u>GAGCTC</u> GTT CTT TAT TTA GAT TAA ATA AAG TCA ATG	<i>SacI</i>	To clone <i>spoVD</i> into pMTL-YN4
RF143	R	CCA AGC TTG CAT GTC TGC AG		Screening for the insertion between <i>BamHI</i> and <i>SacI</i> into pMTL-YN4
RF186	R	CGAAATTAGAACTTGC GTTCA GTAAC		Clostron EBS universal primer
RF187	R	GTCA <u>GGATCC</u> CTT AGG AAT CAG AGA GTA GAT AG	<i>BamHI</i>	To clone <i>spoVD</i> into pMTL-YN4

RF190	F	GTCA <u>GAGCTC</u> CTG TGA AGC AAT GGT AGC	<i>SacI</i>	To clone <i>cwp20</i> into pMTL-YN4
RF191	R	GTCA <u>GGATCC</u> ATA TTT ACT ACA AAA ACT GTC ATA GAA AAA AG	<i>Bam</i> HI	To clone <i>cwp20</i> into pMTL-YN4
RF210	F	GAAAATGTTAGGAAAGGGGTT ACG		screening for single crossovers of pYAA025- <i>cwp20</i> deletion
RF211	R	CTA AGT TCA TAT TAA AAG GTA GTA GCT A		screening for single crossovers of pYAA025- <i>cwp20</i> deletion
RF212	F	CATATATTA ACTTCCCATTAGTT GCAAG		screening for double crossovers of <i>spoVD</i> deletion
RF213	R	GCT AAA GGC TAA GGA ATT GCT C		screening for double crossovers of <i>spoVD</i> deletion
RF214	F	GCT TGA ACC AGC TAA AAA GAT TTT AGC		screening for double crossovers of <i>cwp20</i> deletion
RF215	R	GCT AAT TAT AAA TTA TTA AAA AGG GAA AGA GG		screening for double crossovers of <i>cwp20</i> deletion
RF220	F	CCA GAC ATA CCC ATC TCT ATT AC		screening for single crossovers of pYAA024- <i>spoVD</i> deletion
RF221	R	GAT ATA GAT GGT ATT AAG TAA TAT AAT GGA G		screening for single crossovers of pYAA024- <i>spoVD</i> deletion
RF295	F	GGAATAAAAAGTTTAGACGAA ATAAGAGG		Primer flank the <i>pyrE</i> gene locus
RF297	R	CAA AAG CAG CAA CTA TTT TCA TTG AAG AG		Primer flank the <i>pyrE</i> gene locus
RF298	F	GTCA GGATCC TTAAGCTATTTCTTTTATTTGCTT AAATGAG	<i>Bam</i> HI	To clone <i>cwp20</i> into pMTL-YN2C
RF299	R	GTCA GAATTC GTC TAA AAT TCC TCC ATT TTA TTT ATA TAT TAC C	<i>Eco</i> RI	To clone <i>cwp20</i> into pMTL-YN2C
RF300	F	CCGCTGTATCCATATGACCATG		Screening for the insertion between <i>Bam</i> HI and <i>Sac</i> I into pMTL-YN2C
RF307	F	GCAGCTACTGCAGCAGTAAAG		Primer annealed to <i>snap</i> tag
RF323	F	GTCA <u>GGATCC</u> GTTTATGGGTATATGTTAATTAT CTGTTAC	<i>Sac</i> I	To clone <i>spoVD</i> into pMTL-YN2C
RF324	R	GTCA <u>GAGCTC</u> CTT AGG AAT CAG AGA GTA GAT AG	<i>Bam</i> HI	To clone <i>spoVD</i> into pMTL-YN2C
RF325	F	CAGGTATAGATTTACCAGGAGA AGC		To sequence the whole <i>spoVD</i>
RF326	R	GTA TTG GAG TTA CTG ATA TAG ATT GAC C		To sequence the whole <i>spoVD</i>
RF327	F	GATTATAAAGATATTTACGCTTT AATAAGC		To sequence the whole <i>spoVD</i>

RF328	R	CCA CTT AAT TTA GCA TCT CTT ATT TGA C		To sequence the whole <i>spoVD</i>
RF372	F	GTCA <u>GAGCTC</u> GGG GAA TAG ATT TGA GAA AAG TAA AG	<i>SacI</i>	To clone <i>spoVD</i> into pJAK033 (<i>P_{cwp2}/spoVD-clip</i>)
RF373	R	GATC <u>CTCGAG</u> GTTTTCAAATATAGGGTTATA CTTGAGTC	<i>XhoI</i>	To clone <i>spoVD</i> into pJAK033 (<i>P_{cwp2}/spoVD-clip</i>)
RF374	F	GATC <u>CTCGAG</u> AGA AAA GTA AAG AGG ATA AGT AAG AAA AGG	<i>XhoI</i>	To clone <i>spoVD</i> into pJAK032 (<i>P_{cwp2}/clip-spoVD</i>)
RF375	R	GTCA <u>GGATCC</u> TTAGTTTTCAAATATAGGGTT ATACTTGAG	<i>BamHI</i>	To clone <i>spoVD</i> into pJAK032 (<i>P_{cwp2}/clip-spoVD</i>)
RF407	R	CCT TTA CTG CAG GAG CTC AGA TCT G		To clone inducible promoter Ptet into pMTL-YN2C
RF408	F	GATC <u>GCGGCCGC</u> GCA TCA AGC TAG CAT AAA AAT AAG AAG	<i>NotI</i>	To clone inducible promoter Ptet into pMTL-YN2C
RF415	F	GGT GGA GAC TCT TTA TTA TTC CAC AG		Screening for <i>cwp20</i> ClosTron mutants
RF416	R	CTT GTC CAA TTA TTT CGT TAA GTT GAC TAC		Screening for <i>cwp20</i> ClosTron mutants
RF417	F	CGACTCATAGAATTATTTCTCC CGTTAAATAATAG		Screening for RAM amplification ClosTron mutants
RF418	R	GGA ACT TCT ATA TTG ATA AAA ATA ATA ATA GTG G		Screening for RAM amplification ClosTron mutants
RF458	F	CTTAAACATATTACATTACCTCT TTCC		<i>cwp20</i> (<i>CD1318</i>) amplification for Southern blot (200 bp product)
RF459	R	GTCTAAAATTCCTCCATTTTATT TATATATTACC		<i>cwp20</i> (<i>CD1318</i>) amplification for Southern blot (200 bp product)
RF460	F	CTCAAATCTATTCCCCCTAGTTA TCC		<i>spoVD</i> (<i>CD1318</i>) amplification for Southern blot (200 bp product)
RF461	R	GAA TCT ATG TGG TTA TTC AAA AAT CTC G		<i>spoVD</i> (<i>CD1318</i>) amplification for Southern blot (200 bp product)
RF490	F	GATC <u>CCATGG</u> ATAATTCCGAAAAATATCAAAG TTCTGATATAG	<i>NcoI</i>	To clone <i>cwp20-his</i> into pET- 28a
RF506	F	TAATACGACTCACTATAGGG		Screening for the insertion into pET-28a
RF507	R	GCTAGTTATTGCTCAGCGGT		Screening for the insertion into pET-28a
RF512	F	GATC <u>GTCGAC</u> AAA GAG GTA ATG TAA TAT GTT TAA GCA AAG G	<i>SalI</i>	To clone <i>P_{cwp2}/cwp20</i> into pRPF144

RF513	R	GATC <u>GGATCC</u> TTA AGC TAT TTC TTT TAT TTG CTT AAA TGA GTT TTC	<i>Bam</i> HI	To clone P _{cwp2} / <i>cwp20</i> into pRPF144
RF524	R	GCA CTA TCA ACA CAC TCT TAA GTT TGC		To sequence out from the transposon insertion
RF528	F	aaatacgggtgtttttgttacccaagttt AAGCTAGAATAGATGGACC		Gibson assembly: to insert <i>snap-spoVD</i> via pMTL-SC7215
RF529	R	acaatctttatccatATCTATTCCCC TAGTTATCC		
RF530	F	ctagggggaatagatATGGATAAAG ATTGTGAAATGAAGAGAACCAC		
RF531	R	cctctttacttttctAGCAGCTGCCCC AAGTCC		
RF532	F	cttggggcagctgctAGAAAAGTAA AGAGGATAAGTAAGAAAAG		
RF533	R	tttggcatgagattatcaaaaaggagtt tTAAATCTATACCTGTCTTATCC ATAAG		
RF534	F	CAGGAAAATTAGTAGATATAAT TAAAAAAGCTATCC		screening for single crossovers of pYAA047- <i>snap-spoVD</i> or <i>nsnap-spoVD</i> insertion
RF582	R	TAT ATC TCT TGT TTG TTG TTC TAG TGC TTT TG		To delete PBP dimer domain of <i>SpoVD</i> by inverse PCR of pYAA031
RF583	F	GCAAAAAAGGTTACTGCAATAG CTATG		To delete PBP dimer domain of <i>spoVD</i> by inverse PCR of pYAA031
RF584	R	GGT TTA ACT CCC AAA TAT TTT AAA GAG TCA TTC		To delete PASTA domain of <i>spoVD</i> by inverse PCR of pYAA031
RF585	F	TAAGGATCCACTAGTAACGGCC		To delete PASTA domain of <i>spoVD</i> by inverse PCR of pYAA031
RF586	F	AGTATATAAAGAAGAAGAAAA AGCTGAGTATG		To delete transpeptidase domain of <i>spoVD</i> by inverse PCR of pYAA031
RF587	R	ATT ATT TAA CTC ATA AGC TTT CTG TAC TGC		To delete transpeptidase domain of <i>spoVD</i> by inverse PCR of pYAA031
RF594	F	GAGTATTTTCCAATATACGAAG ATGAAAGG		screening for single crossovers of pYAA05- <i>CD1067</i> deletion
RF595	R	GAA AGG TCC AAC AAT ATA AGT TCA AGA AC		screening for single crossovers of pYAA05- <i>CD1067</i> deletion
RF600	F	CTATCAGTAAAAGTTGGTAAAG ATTATATGC		screening for double crossovers of <i>CD1067</i> deletion

RF601	R	CTT GTT CAA GAA AGT TAA TAC TAT ATT TTA AAA GG		screening for double crossovers of <i>CD1067</i> deletion
RF602	F	GATC GCTAGC AAGGGAAATTGGTTGAGTACA AAAGC	<i>NheI</i>	To clone <i>his-spoVD</i> into pET- 28a
RF603	R	GATC CTCGAG TTA GTT TTC AAA ATA TAG GGT TAT ACT TGA GTC	<i>XhoI</i>	To clone <i>his-spoVD</i> into pET- 28a
RF615	R	TAA TCC AGG GAC ATC ATC ATA AGA GC		Inverse PCR to clone <i>cwp20- his</i> into pET-28a
RF616	F	CTCGAGCACCACCACCAC	<i>XhoI</i>	Inverse PCR to clone <i>cwp20- his</i> into pET-28a
RF670	F	GCA GCT GCT AGA AAA GTA AAG AGG		To delete <i>csnap</i> of <i>snap- spoVD</i> by inverse PCR of pYAA047
RF671	R	TTG TTG AAA TAC AGG ATG GTG AAG AG		To delete <i>csnap</i> of <i>snap- spoVD</i> by inverse PCR of pYAA047
RF672	F	GATC <u>CTCGAG</u> CCT AAA GAA AAT TTG AAA AAA CAA ATT GAC ATA A	<i>XhoI</i>	To clone <i>spoVE</i> into pAMBL009
RF673	R	GATC <u>GGATCC</u> TTA ATT AAT TTT GAC ATG CTT TGA GAT GTT TAA C	<i>BamHI</i>	To clone <i>spoVE</i> into pAMBL009
RF674	F	GATC <u>GAGCTC</u> GGAGGTAGATTAGTTGGATGC CT	<i>SacI</i>	To clone <i>spoVE</i> into pAMBL008
RF675	R	GATC <u>CTCGAG</u> ATT AAT TTT GAC ATG CTT TGA GAT GTT TAA C	<i>XhoI</i>	To clone <i>spoVE</i> into pAMBL008
RF676	F	GTACCACTTCTCGTAGTTCCAG		To sequence the whole <i>spoVE</i>
RF677	R	CCA GCA ACA AAT ATC ATT ACA AAA GTA AC		To sequence the whole <i>spoVE</i>
RF678	F	<u>GCGACATTTAAGCTTATTACATC</u> TTCCAGTGC		To change serine 311 to alanine of <i>SpoVD</i> by inverse PCR of pYAA052
RF679	R	ACC TGG TTC ATA TGT ATC ACT TAC TG		To change serine 311 to alanine of <i>SpoVD</i> by inverse PCR of pYAA052
RF680	F	<u>GCGATCAGTAAAATGTTTACTA</u> CAACAGCTGTTA		To change serine 116 to alanine of <i>Cwp20</i> by inverse PCR of pYAA053
RF681	R	TGC GAT ACT ATA CAT ATT ATC CTT ATT TAA GTT		To change serine 116 to alanine of <i>Cwp20</i> by inverse PCR of pYAA053
RF747	F	GTA AAT TTG GAA AGT TAC ACG TTA CTA A		To sequence out from the transposon insertion

RF751	F	aaatacgggtgtttttgttacctaagttt CAGTTCTTGTCTGTATAAGTTCT AAG		Gibson assembly: to delete <i>CD0622</i> via pMTL-SC7215
RF752	R	ggtaacttaaccaacAGGACGCATT CCATCTGC		
RF753	F	gatggaatgcgtcctGTTGGTTAAGT TACCAAGG		
RF754	R	tttggtcatgagattatcaaaaaggagtt tTGTTTATATTTGTAATCATTTTA TCTAAATGC		
RF757	F	CTA TAT AAT TCT TAA ATC CTT GCT TAC TTG C		screening for single crossovers of pYAA064- <i>CD0622</i> deletion
RF758	R	GCT CTT GTA TAC TTT AAC TTT TCA TTA TCC		screening for single crossovers of pYAA064- <i>CD0622</i> deletion
RF759	F	CCAAACAGAAATTATAAAAATT ACTATCATTGTC		screening for double crossovers of <i>CD0622</i> deletion
RF760	R	CTT CCT CCC TAA TAC ACA ATT TAT ATA ATA TC		screening for double crossovers of <i>CD0622</i> deletion
RF782	F	GATC <u>GAGCTC</u> ACT TAT TCT CTA CGC AGA TGG AAT G	<i>SacI</i>	To clone <i>CD0622</i> into pRPF144
RF783	R	GATC <u>GGATCC</u> TTA ACC AAC CAT AAT TTT ACC TTC TGC	<i>Bam</i> HI	To clone <i>CD0622</i> into pRPF144
RF784	F	GCTTGGAGGGCTAGGATTCC		To sequence the whole <i>CD0622</i>
RF785	R	ACC CAC AAA AAT AAG TGT AGC AGT TG		To sequence the whole <i>CD0622</i>
RF786	F	GATC <u>GAGCTC</u> TGTAGAGGAGATGGTATAAAG TATGAAA	<i>SacI</i>	To clone <i>CD0399</i> into pRPF144
RF787	R	GATC <u>GGATCC</u> TTATCCCTTACACTATAATATT TCTTAATTATATT	<i>Bam</i> HI	To clone <i>CD0399</i> into pRPF144
RF788	F	GCATTTAAGGAGTCTTGTGTTT GG		To sequence the whole <i>CD0399</i>
RF814	F	GATC CCATGG GAA GAA AGC ATA ACA ACA CAA AAC AAA AAC	<i>Nco</i> I	To clone <i>CD0399-his</i> into pET-28a
RF817	R	GATC <u>CTCGAG</u> TTC CCT TAC ACT ATA ATA TTT CTT AAT TAT ATT AAT TGC	<i>Xho</i> I	To clone <i>CD0399-his</i> into pET-28a
RF818	F	<u>GCG</u> ACT TTT AAA ATA GTT TCA ACT TTA ATT GGT TTA GAA AAA G		To change serine 102 to alanine of <i>CD0399</i> by inverse PCR of pYAA080

RF819	R	ACA TGG TGA CCT TCT TGT TTC AAT TAA TTC		To change serine 102 to alanine of CD0399 by inverse PCR of pYAA080
RF820	F	<u>GCG</u> ACTTTAATTGGTTTAGAAAAAG GGGTAATAAAC		To change serine 108 to alanine of CD0399 by inverse PCR of pYAA080
RF821	R	AAC TAT TTT AAA AGT AGA ACA TGG TGA CCT TC		To change serine 108 to alanine of CD0399 by inverse PCR of pYAA080
RF827	F	GATC <u>GGATCC</u> CAGAAAAGTAAAGAGGATAAG TAAGAAAAGG	<i>Bam</i> HI	To clone <i>spoVD</i> into pUT18C
RF828	R	GATC <u>GAGCTC</u> TTA GTT TTC AAA ATA TAG GGT TAT ACT TGA GTC	<i>Sac</i> I	To clone <i>spoVD</i> into pUT18C
RF829	R	GATC <u>GAGCTC</u> GGG TTT TCA AAA TAT AGG GTT ATA CTT GAG	<i>Sac</i> I	To clone <i>spoVD</i> into pUT18
RF830	F	GATC <u>GGATCC</u> TAA AGA AAA TTT GAA AAA ACA AAT TGA CAT AAG GA	<i>Bam</i> HI	To clone <i>spoVE</i> into pKT25
RF831	R	GATC <u>GGTACC</u> TTA ATT AAT TTT GAC ATG CTT TGA GAT GTT TAA C	<i>Kpn</i> I	To clone <i>spoVE</i> into pKT25
RF832	R	GATC <u>GGTACC</u> CGA TTA ATT TTG ACA TGC TTT GAG ATG TT	<i>Kpn</i> I	To clone <i>spoVE</i> into pKNT25

Table A2. Plasmids used in this project

Official name	Descriptive name	Description and comments
pYAA005	pMTL-SC7215- Δ CD1067	To delete <i>CD1067</i> , only 18 bp of the gene remains, using <i>codA</i> system.
pYAA024	pMTL-YN4- Δ <i>spoVD</i> (<i>SacI/BamHI</i>)	To delete <i>spoVD</i> , only 18 bp of the gene remains, using Δ <i>pyrE</i> system.
pYAA025	pMTL-YN4- Δ CWP20 (<i>SacI/BamHI</i>)	To delete <i>cwp20</i> , only 18 bp of the gene remains, using Δ <i>pyrE</i> system.
pYAA027	pMTL-YN2C- <i>spoVD</i> (<i>SacI/BamHI</i>)	<i>spoVD</i> complementation using Δ <i>pyrE</i> system.
pYAA028	pMTL-YN2C- <i>cwp20</i> (<i>EcoRI/BamHI</i>)	<i>cwp20</i> complementation using Δ <i>pyrE</i> system.
pYAA030	pJAK033- <i>spoVD-clip</i> (<i>SacI/XhoI</i>)	Cloning <i>spoVD-clip</i> into pJAK033 under the control of the constitutive promoter (P_{cwp2}).
pYAA031	pJAK032- <i>clip-spoVD</i> (<i>XhoI/BamHI</i>)	Cloning <i>clip-spoVD</i> into pJAK032 under the control of the constitutive promoter (P_{cwp2}).
pYAA036	pMTL-YN2C- Ptet (<i>NotI/SacI</i>)	Cloning inducible tetR promoter into pMTL-YN2C.
pYAA039	pMTL007C-E5- <i>cwp20</i>	Intron II targeting <i>cwp20</i> .
pYAA046	pRPF144- <i>cwp20</i> (<i>SacI/BamHI</i>)	<i>cwp20</i> complementation under the control of the constitutive promoter (P_{cwp2}).
pYAA047	pMTL-SC7215- <i>snap-spoVD</i>	Snap tag encoding DNA was added to 5' end on <i>spoVD</i> in the native locus using <i>codA</i> system.
pYAA048	pYAA031- <i>clip-spoVD</i> -trunc	$P_{cwp2}/clip-spoVD$ with deletion of PBP dimer domain.
pYAA049	pYAA031- <i>clip-spoVD</i> -trunc	$P_{cwp2}/clip-spoVD$ with deletion of PASTA domain.
pYAA050	pYAA031- <i>clip-spoVD</i> -trunc	$P_{cwp2}/clip-spoVD$ with deletion of transpeptidase domain.
pYAA051	pYAA031- <i>clip-spoVD</i> -trunc	$P_{cwp2}/clip-spoVD$ with deletion of PBP dimer and PASTA domains.
pYAA052	pET-28a- <i>his-spoVD</i> (<i>NheI/XhoI</i>)	His tag encoding DNA was fused to the 5' end of <i>spoVD</i> in pET-28a.
pYAA053	pET-28a- <i>cwp20-his</i> (<i>NcoI/XhoI</i>)	His tag encoding DNA was fused to the 3' end of <i>cwp20</i> in pET-28a.
pYAA054	pAMBL008- <i>csnap-spoVE</i> (<i>XhoI/BamHI</i>)	cSnap tag encoding DNA was fused to the 5' end of <i>spoVE</i> with expression under the control of the constitutive promoter (P_{cwp2}).
pYAA055	pAMBL009- <i>spoVE-csnap</i> (<i>XhoI/BamHI</i>)	cSnap tag encoding DNA was fused to the 3' end of <i>spoVE</i> with expression under the control of the constitutive promoter (P_{cwp2}).
pYAA056	pMTL-SC7215- <i>nsnap-spoVD</i>	nSnap tag encoding DNA was added to 5' end on <i>spoVD</i> in the native locus using <i>codA</i> system.
pYAA060	pET-28a- <i>his-spoVDS311A</i> (<i>NheI/XhoI</i>)	Changing the active site serine 311 to alanine of <i>spoVD</i> on pYAA052.
pYAA061	pET-28a- <i>cwp20S116A-his</i> (<i>NcoI/XhoI</i>)	Changing the active site serine 116 to alanine of <i>cwp20</i> on pYAA053.

pYAA063	pYAA031- <i>clip-spoVD</i> (XhoI/BamHI)	Changing the active site serine 311 to alanine of <i>spoVD</i> on pYAA031.
pYAA064	pMTL-SC7215- Δ CD0622	To delete <i>CD0622</i> , only 18 bp of the gene remains, using <i>codA</i> system.
pYAA065	pBlueskript- <i>CD0018</i> ::Tn	Identification of transposon insertion site in <i>CD0018</i> , using marker rescue.
pYAA066	pBlueskript- <i>spoVE</i> ::Tn	Identification of transposon insertion site in <i>spoVE</i> , using marker rescue.
pYAA067	pBlueskript- <i>CD3017</i> ::Tn	Identification of transposon insertion site in <i>CD3017</i> , using marker rescue.
pYAA068	pBlueskript- <i>CD0715</i> ::Tn	Identification of transposon insertion site in <i>CD0715</i> , using marker rescue.
pYAA069	pBlueskript- <i>CD3432</i> ::Tn	Identification of transposon insertion site in <i>CD3432</i> , using marker rescue.
pYAA070	pBlueskript- <i>CD0622</i> ::Tn	Identification of transposon insertion site in <i>CD0622</i> , using marker rescue.
pYAA071	pBlueskript- <i>CD0398</i> ::Tn	Identification of transposon insertion site in <i>CD0398</i> , using marker rescue.
pYAA072	pRPF144- <i>CD0622</i> (<i>SacI</i> /BamHI)	<i>CD0622</i> complementation under the control of the constitutive promoter (P_{cwp2}).
pYAA074	pRPF144- <i>CD0399</i> (<i>SacI</i> /BamHI)	<i>CD0398</i> complementation, carrying the full length of <i>CD0399</i> with expression under the control of the constitutive promoter (P_{cwp2}).
pYAA075	pBlueskript- <i>CD1165</i> ::Tn	Identification of transposon insertion site in <i>CD1165</i> , using marker rescue.
pYAA076	pBlueskript- <i>CD2904</i> ::Tn	Identification of transposon insertion site in <i>CD2904</i> , using marker rescue.
pYAA077	pBlueskript- <i>CD1383</i> ::Tn	Identification of transposon insertion site in <i>CD1383</i> , using marker rescue.
pYAA080	pET-28a- <i>CD0399-his</i> (<i>NcoI</i> /XhoI)	His tag encoding DNA was fused to the 3' end of <i>CD0399</i> in pET-28a.
pYAA081	pET-28a- <i>CD0399S102A-his</i> (<i>NcoI</i> /XhoI)	Changing the active site serine 102 to alanine of <i>CD0399</i> on pYAA080.
pYAA082	pET-28a- <i>CD0399S108A-his</i> (<i>NcoI</i> /XhoI)	Changing the active site serine 108 to alanine of <i>CD0399</i> on pYAA080.
pYAA083	pUT18C- <i>T18-spoVD</i> (<i>SacI</i> /BamHI)	Determination of the interaction between SpoVD and SpoVE, using bacterial two-hybrid.
pYAA084	pUT18- <i>spoVD-T18</i> (<i>SacI</i> /BamHI)	Determination of the interaction between SpoVD and SpoVE, using bacterial two-hybrid.
pYAA085	pKT25- <i>T25-spoVE</i> (<i>SacI</i> /KpnI)	Determination of the interaction between SpoVD and SpoVE, using bacterial two-hybrid.
pYAA088	pRPF144- <i>csnap</i> (<i>SacI</i> /BamHI)	<i>csnap</i> expression under the control of the constitutive promoter (P_{cwp2}).

Table A3. Antibodies used in this project

Primary antibody	Conjugate	Dilution for Western blotting	Species	Source
anti-SpoVT	N/A	1:1000 or 1:2000	rabbit	Dr. Aimee Shen (Tufts University)
anti-SpoIVA	N/A	1:2000 or 1:5000	rabbit	Dr. Aimee Shen (Tufts University)
anti-SpoOA	N/A	1:2000 or 1:5000	rabbit	Dr. Aimee Shen (Tufts University)
anti-SipL	N/A	1:2000 or 1:5000	rabbit	Dr. Aimee Shen (Tufts University)
anti-GPR	N/A	1:1000 or 1:2000	rabbit	Dr. Aimee Shen (Tufts University)
Anti-TcdB	N/A	1:1000	rabbit	Thermo Fisher Scientific
Secondary antibody	Conjugate	Dilution for Western blotting	Species	Source
anti-rabbit IgG-HRP	horse radish peroxidase	1:1000	goat	Sigma

Appendix B

Table: Permissions summary

Page no.	Type of work	Reference	License Number
5	Reproduced figure	Rupnik, M., Wilcox, M.H., Gerding, D.N., 2009. <i>Clostridium difficile</i> infection: new developments in epidemiology and pathogenesis. Nature reviews. Microbiology 7, 526-536.	4170261237771
8	Reproduced figure	Deneve, C., Janoir, C., Poilane, I., Fantinato, C., Collignon, A., 2009. New trends in <i>Clostridium difficile</i> virulence and pathogenesis. International journal of antimicrobial agents 33 Suppl 1, S24-28.	4170770349499
10	Reproduced figure	Rupnik, M., Wilcox, M.H., Gerding, D.N., 2009. <i>Clostridium difficile</i> infection: new developments in epidemiology and pathogenesis. Nature reviews. Microbiology 7, 526-536.	4170261237771
14	Reproduced figure	Fagan, R.P., Janoir, C., Collignon, A., Mastrantonio, P., Poxton, I.R., Fairweather, N.F., 2011. A proposed nomenclature for cell wall proteins of <i>Clostridium difficile</i> . Journal of medical microbiology 60, 1225-1228.	4171460734857
19	Reproduced figure	Sauvage, E., Terrak, M., 2016. Glycosyltransferases and Transpeptidases/Penicillin-Binding Proteins: Valuable Targets for New Antibacterials. Antibiotics (Basel) 5.	The Creative Commons Attribution License (CC BY 4.0).
20	Reproduced figure	Barreteau, H., Kovac, A., Boniface, A., Sova, M., Gobec, S., Blanot, D., 2008. Cytoplasmic steps of peptidoglycan biosynthesis. FEMS microbiology reviews 32, 168-207.	4171330176454
22	Reproduced figure	Macheboeuf, P., Contreras-Martel, C., Job, V., Dideberg, O., Dessen, A., 2006. Penicillin binding proteins: key players in bacterial cell cycle and drug resistance processes. FEMS microbiology reviews 30, 673-691.	4171331109691

26	Reproduced figure	Beadle, B.M., Nicholas, R.A., Shoichet, B.K., 2001. Interaction energies between beta-lactam antibiotics and <i>E-coli</i> penicillin-binding protein 5 by reversible thermal denaturation. <i>Protein Sci</i> 10, 1254-1259.	4171390489967
29	Reproduced figure	McKenney, P.T., Driks, A., Eichenberger, P., 2013. The <i>Bacillus subtilis</i> endospore: assembly and functions of the multilayered coat. <i>Nature Reviews Microbiology</i> 11, 33-	4171890832781
33	Reproduced figure	Paredes-Sabja, D., Shen, A., Sorg, J.A., 2014. <i>Clostridium difficile</i> spore biology: sporulation, germination, and spore structural proteins. <i>Trends in microbiology</i> 22, 406-416.	4171351458039
35	Reproduced figure	Reineke, K., Mathys, A., Heinz, V., Knorr, D., 2013. Mechanisms of endospore inactivation under high pressure. <i>Trends in microbiology</i> 21, 296-304.	4183201416307
37	Reproduced figure	Popham, D.L., Helin, J., Costello, C.E., Setlow, P., 1996. Muramic lactam in peptidoglycan of <i>Bacillus subtilis</i> spores is required for spore outgrowth but not for spore dehydration or heat resistance. <i>P Natl Acad Sci USA</i> 93, 15405-15410.	Copyright (1996) from National Academy of Sciences, U.S.A
40	Reproduced figure	Paredes-Sabja, D., Shen, A., Sorg, J.A., 2014. <i>Clostridium difficile</i> spore biology: sporulation, germination, and spore structural proteins. <i>Trends in microbiology</i> 22, 406-416.	4171351458039